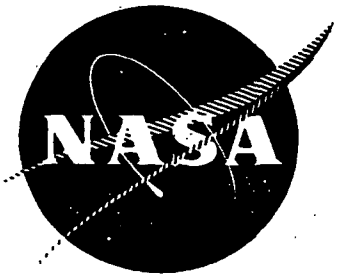

ENRICHED ALUMINIDE COATINGS FOR DISPERSION STRENGTHENED NICKEL MATERIALS

by

M.A. Levinstein

GENERAL ELECTRIC COMPANY

prepared for

NATIONAL AERONAUTICS AND SPACE ADMINISTRATION

NASA-Lewis Research Center
Contract NAS3-14314
J. Smialek, Project Manager

Requests for copies of this report should be referred to:

National Aeronautics and Space Administration
Office of Scientific and Technical Information
Attention: AFSS-A
Washington, D.C. 20546

1. Report No.	2. Government Accession No.	3. Recipient's Catalog No.
121250	--	--

4. Title and Subtitle	5. Report Date
ENRICHED ALUMINIDE COATINGS FOR DISPERSION STRENGTHENED NICKEL MATERIALS	August 1973
	6. Performing Organization Code: --

7. Author(s)	8. Performing Organization Report No.
MOSES A. LEVINSTEIN	--
	10. Work Unit No.: --

9. Performing Organization Name and Address	11. Contract or Grant No.
GENERAL ELECTRIC CO. AIRCRAFT ENGINE GROUP 1 JIMSON ROAD CINCINNATI, OHIO 45215	NAS3-14314
	13. Type of Report and Period Covered: Contractor Report

12. Sponsoring Agency Name and Address	14. Sponsoring Agency Code
NATIONAL AERONAUTICS AND SPACE ADMINISTRATION LEWIS RESEARCH CENTER CLEVELAND, OHIO	--

15. Supplementary Notes

Project Manager, James Smialek, NASA Lewis Research Center

16. Abstract

Improved aluminide/barrier coating combinations for dispersion-strengthened nickel materials were investigated. The barrier materials involved alloys with refractory metal content to limit interdiffusion between the coating and the substrate, thereby minimizing void formation. Improved aluminide coatings involved the dispersion of aluminum-rich compounds. Coatings were tested in argon at 1533°K (2300°F) for 100 hours and in cyclic oxidation at 1422°K (2100°F). Two coatings on TDNiCr completed 300 hours of oxidation testing, none on TDNi.

Selected coating combinations were evaluated in Mach 1 burner rig testing using JP-4 fuel and air at 1422°K (2100°F) and 1477°K (2200°F) for 350 and 100 hours, respectively. Static oxidation in 1-hour cycles was conducted at 1533°K (2300°F) for 100 hours. For comparison purposes a physical vapor deposition (PVD) NiCrAlY coating was tested concurrently. Only the NiCrAlY coating survived the 1477°K (2200°F)/100-hour burner rig test and 275 hours of the 350-hour 1422°K (2100°F) test. Elevated temperature exposure reduced room temperature tensile properties but had little effect on elevated temperature properties.

17. Key Words (Suggested by Author(s))	18. Distribution Statement
TD Nickel TD Nichrome Oxidation Resistant Coatings Aluminide Coatings Barrier Layer Mach 1 Burner Rig Testing	UNCLASSIFIED

19. Security Classif. (of this report)	20. Security Classif. (of this page)	21. No. of Pages	22. Price*
UNCLASSIFIED	UNCLASSIFIED	190	3.00

* For sale by the National Technical Information Service, Springfield, Virginia 22151

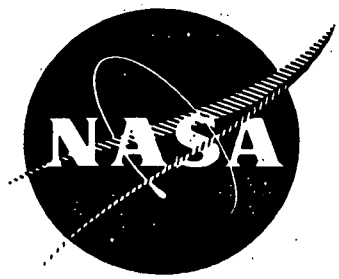

ENRICHED ALUMINIDE COATINGS FOR DISPERSION STRENGTHENED NICKEL MATERIALS

by

M.A. Levinstein

GENERAL ELECTRIC COMPANY

prepared for

NATIONAL AERONAUTICS AND SPACE ADMINISTRATION

NASA-Lewis Research Center
Contract NAS3-14314
J. Smialek, Project Manager

FOREWORD

This report was prepared by the Material and Process Technology Laboratories of the General Electric Company under NASA-Lewis Research Contract NAS33-14314. The program was conducted to evaluate improved aluminide/barrier layer coating combinations for dispersion-strengthened nickel materials for jet engine hot component applications.

Technical direction was under the cognizance of J. Smialek, Project Manager, NASA-Lewis Research Center. Salvatore J. Grisaffe served as technical advisor. General Electric personnel who contributed to the program were Moses A. Levinstein, principal investigator, and D. B. Arnold and W. H. Chang, consultants. Mr. W. Foster, of General Electric's Thompson Laboratory in Lynn, Massachusetts was responsible for the Mach 1 burner rig tests.

Special recognition is made of T. R. Berding and T. W. Kline, technicians who carried out a major share of the tests and of V. Poynter, Metallography Supervisor who was responsible for the electron microprobe analysis and metallographic work.

TABLE OF CONTENTS

TABLE OF CONTENTS (Concluded)

LIST OF TABLES

LIST OF TABLES

LIST OF ILLUSTRATIONS

LIST OF ILLUSTRATIONS (Continued)

LIST OF ILLUSTRATIONS (Continued)

LIST OF ILLUSTRATIONS (Continued)

LIST OF ILLUSTRATIONS (Continued)

LIST OF ILLUSTRATIONS (Concluded)

ABSTRACT

Improved aluminide/barrier coating combinations for dispersion-strengthened nickel materials were investigated. The barrier materials involved alloys with refractory metal content to limit interdiffusion between the coating and the substrate, thereby minimizing void formation. Improved aluminide coatings involved the dispersion of aluminum-rich compounds. Coatings were tested in argon at 1533°K (2300°F) for 100 hours and in cyclic oxidation at 1422°K (2100°F). Two coatings on TDNiCr completed 300 hours of oxidation testing, none on TDNi.

Selected coating combinations were evaluated in Mach 1 burner rig testing using JP-4 fuel and air at 1422° K (2100°F) and 1477° K (2200°F) for 350 and 100 hours, respectively. Static oxidation in 1-hour cycles was conducted at 1533° K (2300°F) for 100 hours. For comparison purposes a physical vapor deposition (PVD) NiCrAlY coating was tested concurrently. Only the NiCrAlY coating survived the 1477°K (2200°F)/100-hour burner rig test and 275 hours of the 350-hour 1422° K (2100° F) test. Elevated temperature exposure reduced room temperature tensile properties but had little effect on elevated temperature properties.

1.0 SUMMARY

The overall goal of this program was to identify coatings for TDNi and TDNiCr for jet engine hot component applications with 1477°K (2200°F)/500-hour and 1422°K (2100°F)/1000-hour operational capability. To achieve this goal the program objectives were twofold: (1) to identify barrier layer materials which would limit interdiffusion between coatings and the two dispersion-strengthened nickel substrates, thereby minimizing void formation, and (2) to improve aluminide type covercoats through the dispersion of aluminum-rich compounds in the form of very fine particles which would act as aluminum reservoirs for any aluminum depleted during exposure. Four barrier layer materials with an improved aluminide covercoat, NC11-A (developed under another NASA contract), were evaluated under Task I by exposure in argon at 1533°K (2300°F) for 100 hours. Then, under Task II, selected barrier/substrate combinations were aluminide coated incorporating the aluminum-rich compounds as dispersoids. These were tested in cyclic oxidation at 1422°K (2100°F) for 300 hours, cycling once per hour. The oxidation testing was conducted in a low velocity flame tunnel. Specimens were in the form of sheet tensile coupons which were tested at room temperature and at 1422°K (2100°F) in the as-processed and after exposure conditions. From these tests coatings were selected for advanced testing in a Mach 1 velocity burner rig under Task III.

The barrier layers consisted of three add-on coatings applied by plasma spraying: A cobalt-base alloy, X40 and two modifications of Hastelloy C (C-1 and C-2) in which the molybdenum and tungsten contents were varied. Another diffusion barrier was produced by a duplex chromizing/carburizing process. The latter barrier was applied only to TDNiCr; the other three barriers were applied to both TDNi and TDNiCr. Of the three materials evaluated on TDNi in the 1533°K (2300°F)/100 hour argon exposure, both of the Hastelloy C modifications showed no evidence of void formation whereas the X40 barrier coating produced excessive voids at the barrier/substrate interface. On the other hand, all three add-on barriers were compatible with TDNiCr, but the chromized/carburized layer approach proved unsatisfactory.

During the exposure in argon at 1533°K (2300°F), some degradation of the NC11-A covercoat occurred - in part due to aluminum volatization at the elevated temperature, and partially to oxidation from residual oxygen in the argon gas. However, there was little diffusion of aluminum into either substrate as revealed by microprobe analysis, Figure A. In this regard, the X40 barrier appeared to be most effective on TDNiCr, (Figure A, top, left), and the Hastelloy C-2 barrier on TDNi, (Figure A, bottom, right). Microprobe analysis also revealed the extent of diffusion of barrier layer constituents into the aluminide covercoat and substrate during processing and after exposure at 1533°K (2300°F) for 100 hours, Figures B and C. Figure B illustrates the diffusion effects for the X40 barrier, as-processed and after exposure, and Figure C, the diffusion effects of the Hastelloy C-1 constituents on TDNi and TDNiCr and the Hastelloy C-2 constituents on TDNi after 1533°K (2300°F) exposure only. Both molybdenum and tungsten diffused readily into the substrates. This elemental diffusion was reflected in hardness changes in the substrates. The elevated temperature exposure also resulted in

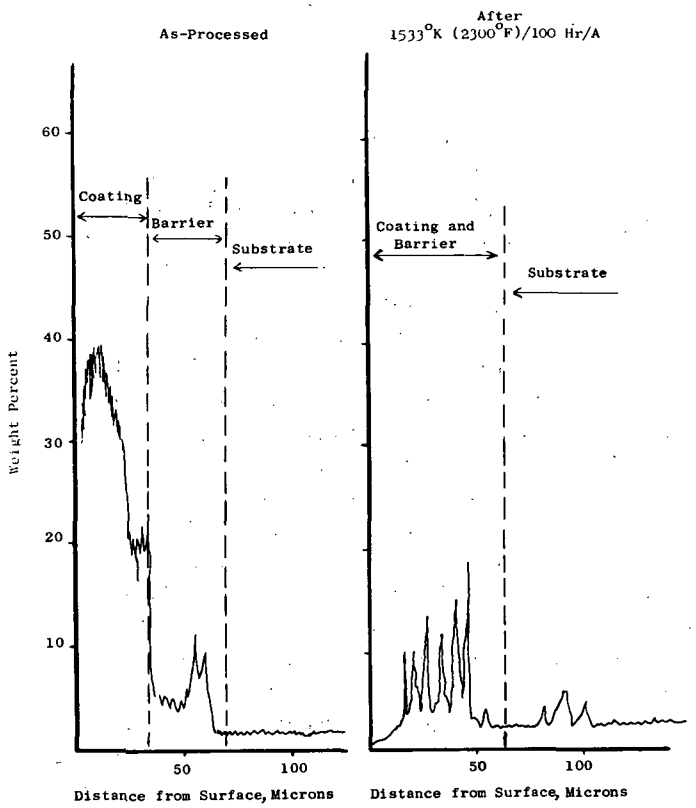

Electron Microprobe Traces for Al. X40 Barrier Layer on TDNiCr (AVCO Gun).

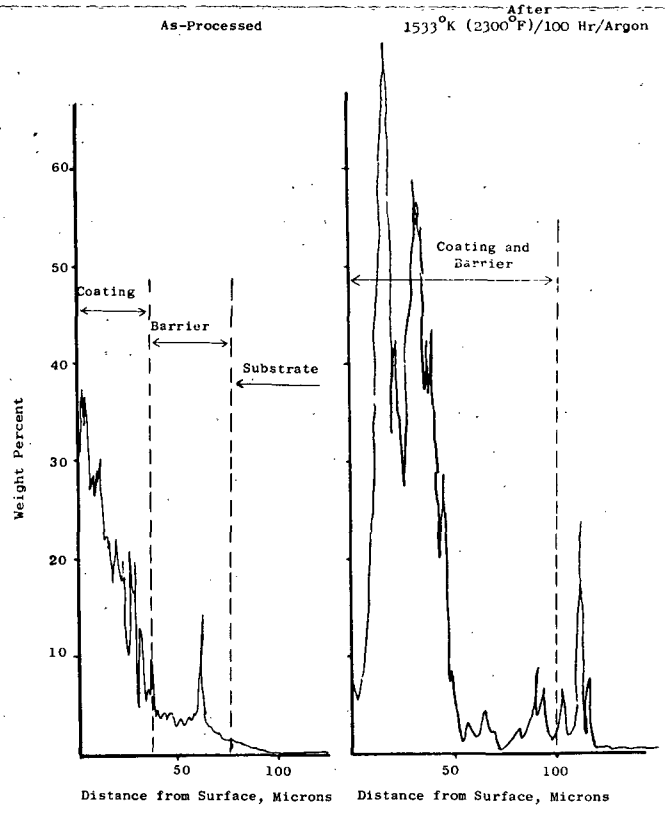

Electron Microprobe Traces for Al. Hastelloy C-1 Barrier Layer on TDNi (AVCO Gun).

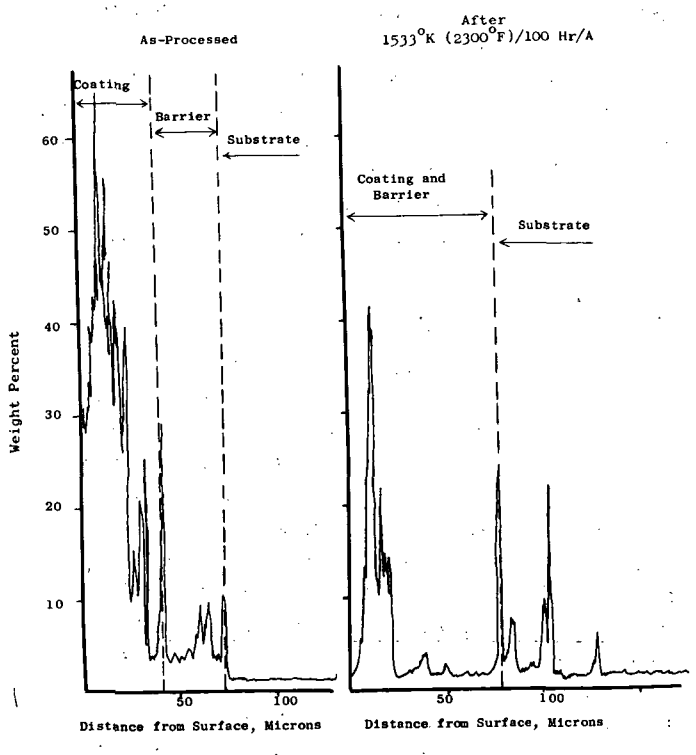

Electron Microprobe Traces for Al. Hastelloy C-1 Barrier Layer on TDNiCr (Metco Gun).

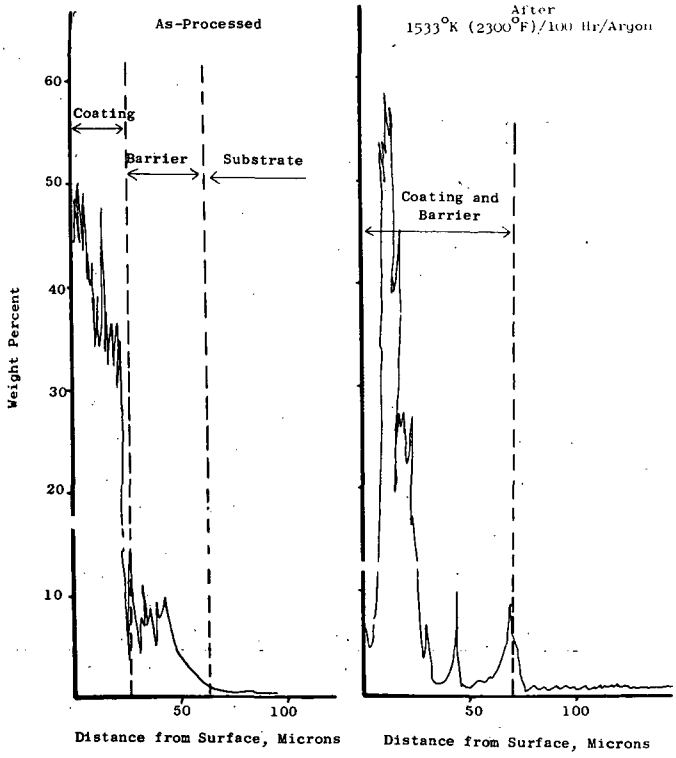

Electron Microprobe Traces for Al. Hastelloy C-2 Barrier Layer on TDNi (AVCO Gun).

Figure A Aluminum Diffusion As-Processed and After 1533°K (2300°F)/100-Hour/Argon

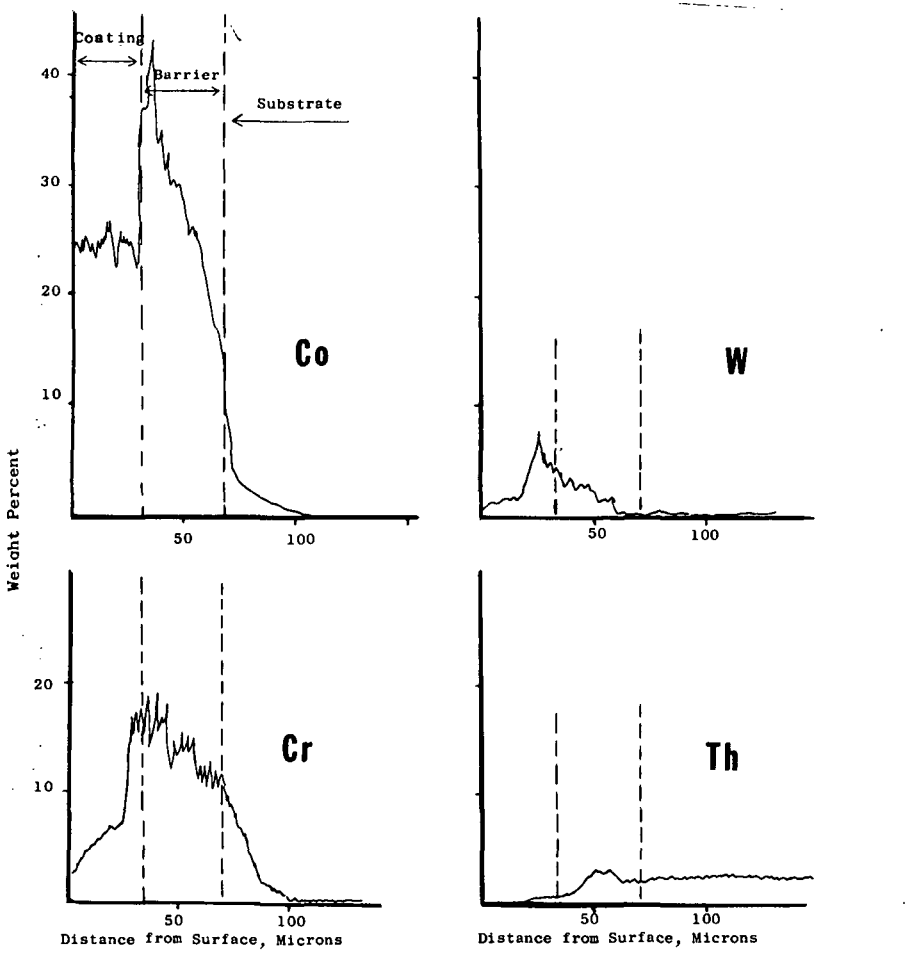

Electron Microprobe Elemental Traces for X40 Barrier Layer on TDNi, As-Processed (AVCO Gun).

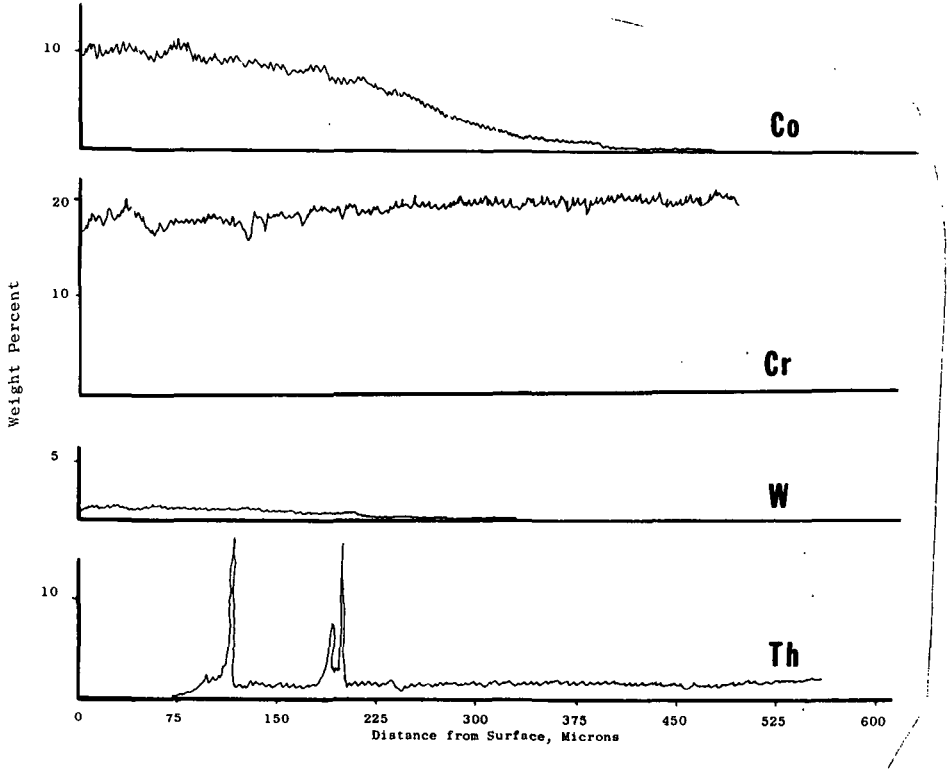

Electron Microprobe Elemental Traces for X40 Barrier Layer on TDNiCr After 1533°K (2300°F)/100 Hr/A Exposure (AVCO Gun).

Figure B X40 Barrier Layer Constitutent Diffusion, As-Processed and After 1533°K (2300°F)/100-Hr/Argon

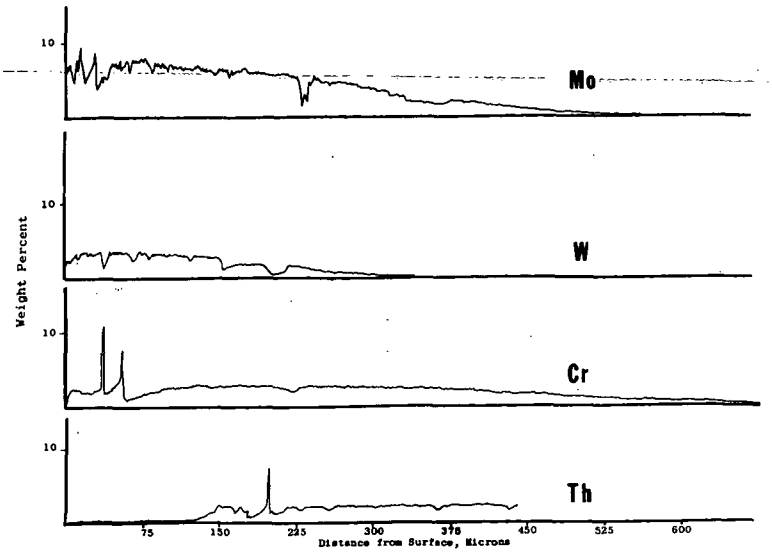

Electron Microprobe Traces for Hastelloy C-1 Barrier Layer on TDNi After 1533°K (2300°F)/100 Hr/A Exposure (AVCO Gun).

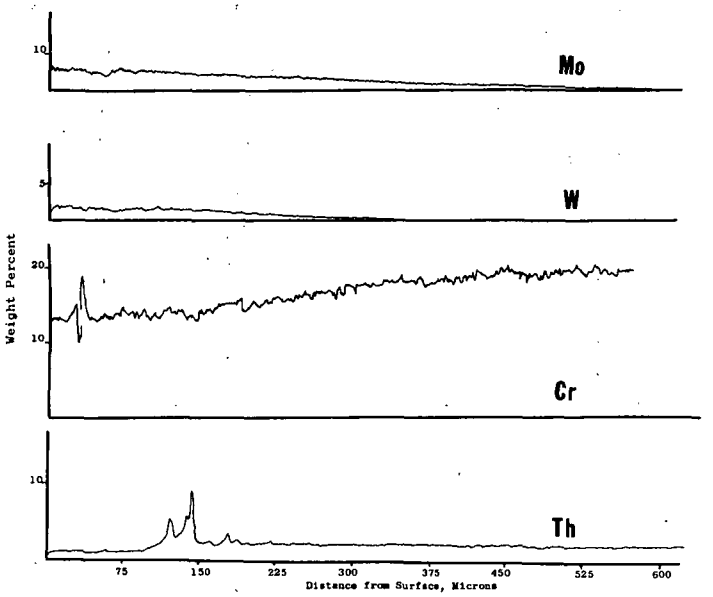

Electron Microprobe Traces for Hastelloy C-1 Barrier Layer on TDNiCr After 1533°K (2300°F)/100 Hr/A Exposure (AVCO Gun).

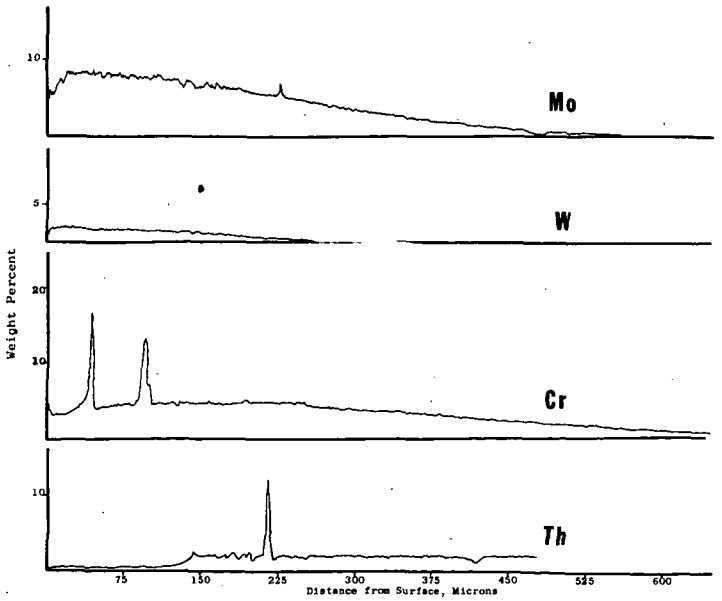

Electron Microprobe Elemental Traces for Hastelloy C-2 Barrier Layer on TDNi After 1533°K (2300°F)/100 Hr/A Exposure (Metco Gun).

Figure C Hastelloy C-1 and C-2 Barrier Layer Constituent Diffusion After 1533°K (2300°F)/100-Hr/Argon

the formation of a band of recrystallized grains in the substrate just below the barrier layer. This recrystallized band corresponds to the two thorium peaks shown in Figure B, right. Each barrier/substrate combination shows this tendency for thorium concentration, Figure C, indicating physical movement of the thoria particles in the substrates. Examination of the recrystallized grains at high magnification indicated that the grains themselves were devoid of thoria particles, but that the thoria was concentrated in the grain boundaries. The basis for this grain recrystallization and growth and thoria movement could not be determined.

Under Task II, the X40 and Hastelloy C-1 barriers were applied to TDNiCr tensile specimens,and, both Hastelloy C modifications were applied to TDNi tensile specimens. The three aluminum-rich dispersoids in the aluminide covercoats were Al_2O_3 (NC11-A), Cr_5Al_8, and CoAl. A fourth dispersoid, $MoAl_2$, was eliminated because of poor oxidation behavior in preliminary evaluation. Testing was conducted at 1422°K (2100°F) under cyclic conditions for a projected period of 300 hours. The results of these tests are compiled in Table A. The only combinations that completed the 300 hours were the Al_2O_3 and Cr_5Al_8 dispersoids over the X40 barrier layer on TDNiCr. Next best were the same dispersoids over the Hastelloy C-1 barrier layer, also on TDNiCr. Coating performance on TDNi was marginal at best. Microprobe analysis indicated a lesser degree of diffusion of barrier layer constituents into the substrates in 300 hours at 1422°K (2100°F) than in 100 hours at 1533°K (2300°F). This would be expected considering the differences in diffusion rates at these two temperature levels. The recrystallized layer observed after the 1533°K (2300°F) exposure was also observed after the 1422°K (2100°F) exposure.

A significant difference occurred in the behavior of the Hastelloy C-1 and C-2 barrier layer on both TDNi and TDNiCr in the cyclic oxidation test at 1422°K (2100°F) compared with the static exposure at 1533°K (2300°F) in argon. In the latter test neither barrier showed void formation whereas in the cyclic test,voids were formed with both substrates. Void formation could be attributed to three possible causes, (1) pull-out due to the sensitivity of the recrystallized layer to polishing technique, (2) residual voids from the plasma spraying operation, and (3) stresses induced during cycling due to differences in expansion coefficients of the barrier and substrate materials.

Coatings both as-processed and after the 1422°K (2100°F) exposure showed some effect on mechanical properties, though the sample "number" was too small to draw firm conclusions. Room temperature ductility was generally lowered, and strength was either unaffected or increased slightly. The least effect on strength was experienced with the two coating combinations that completed the 1422°K (2100°F)/300-hour test. Ductility at the 1422°K (2100°F) test temperature was not appreciably affected by the coatings.

It would appear that the formation of the recrystallized layer had little effect on mechanical properties.

Before proceeding to the advanced testing of selected coatings under Task III, consideration was given to improving the quality of the barrier

Table A. Performance of Coated Tensile Specimens In $1422^{\circ}K$ ($2100^{\circ}F$) Oxidation Tests

Specimen	Substrate	Barrier	Covercoat	Test Results
C	TDNiCr	Hastelloy C-1	Cr_5Al_8	Edge Spalling - 200 hrs
E	TDNiCr	Hastelloy C-1	Cr_5Al_8	Edge Spalling - 200 hrs
F	TDNiCr	Hastelloy C-1	CoAl	Coating Failed - 50 hrs
G	TDNiCr	Hastelloy C-1	CoAl	Coating Failed - 158 hrs
I	TDNiCr	Hastelloy C-1	NCl1-A	Edge Spalling - 200 hrs
D	TDNiCr	Hastelloy C-1	NCl1-A	Spalling - 200 hrs
2	TDNi	Hastelloy C-1	Cr_5Al_8	Intact - 45 hrs
4	TDNi	Hastelloy C-1	Cr_5Al_8	Edge Spalling - 145 hrs
5	TDNi	Hastelloy C-1	Cr_5Al_8	Edge Spalling - 145 hrs
8	TDNi	Hastelloy C-1	CoAl	Coating Failed - 145 hrs
11	TDNi	Hastelloy C-1	CoAl	Coating Failed - 100 hrs
12	TDNi	Hastelloy C-1	NCl1-A	Blistering - 45 hrs
15	TDNi	Hastelloy C-1	NCl1-A	Blistering - 100 hrs
16	TDNi	Hastelloy C-1	NCl1-A	Blistering - 100 hrs
N	TDNiCr	X40	Cr_5Al_8	Completed 300 hrs
R	TDNiCr	X40	Cr_5Al_8	Completed 300 hrs
S	TDNiCr	X40	NCl1-A	Completed 300 hrs
T	TDNiCr	X40	NCl1-A	Completed 300 hrs
19	TDNi	Hastelloy C-2	Cr_5Al_8	Edge Spalling - 150 hrs
20	TDNi	Hastelloy C-2	NCl1-A	Edge Spalling - 175 hrs

layer by other means of deposition. With advancements that had been made in physical vapor deposition, applying the barrier layers by this method offered promise of denser and more uniform coatings than that obtained by plasma deposition. However, in actual practice the method did not prove to be feasible due to failure to transfer tungsten and molybdenum during deposition. Consequently it was necessary to revert to thermal spray methods for barrier application on Task III. Improvement was made in the application of the X40 barrier by using the detonation-gun process, and the application of the Hastelloy C-2 barrier was improved using a high velocity plasma technique. Three coating combinations were selected for evaluation under Task III:

Coating	Substrate
Detonation-gun Deposited X40 Barrier + NC11-A Aluminide	TDNiCr
High Velocity Plasma Deposited Hastelloy C-1 Barrier + NC11-A Aluminide	TDNiCr
High Velocity Plasma Deposited Hastelloy C-1 Barrier + NC11-A Aluminide	TDNi

In addition, an in-house developed physical vapor deposited NiCrAlY coating which had demonstrated good performance on TDNiCr was included for comparison purposes.

Test Specimens were of two types: (1) sheet tensile to determine the effect of elevated temperature on mechanical properties and, (2) oxidation/erosion wedges to determine coating performance in a Mach 1 burner rig. The tensile specimens were exposed statically at 1533° K (2300°F) for up to 100 hours, cycling to room temperature once per hour. Only a few specimens survived the 1533° K (2300° F)/100-hour test with the coating visually intact: the X40 barrier/aluminide on TDNiCr and the NiCrAlY on TDNiCr (Figure D). The modified Hastelloy C barrier/aluminide coatings on both TDNiCr and TDNi failed very early. Subsequently, as-coated and exposed specimens were tested in tension at room temperature, 1422°K (2100°F), and 1533° K (2300° F). The 1533° K (2300° F) exposure resulted in: (1) a moderate lowering of room temperature strength and a severe reduction in elongation, (2) a minor increase in both strength and ductility at 1422° K (2100°F), and (3) strength and ductility values at 1533° K (2300° F) that fall within the projected 1533° K (2300°F) range[11, 12]. The results of the 1422° K (2100° F) testing correlate closely with the Task II values obtained after 1422°K (2100° F) exposure.

Testing in the Mach 1 burner rig was scheduled for 500 hours at 1422° K (2100° F) and 100 hours at 1477° K (2200° F), cycling once per hour to approximately 366° K (200° F). None of the coatings survived more than about 300 hours at 1422° K (2100° F), Figure E. The test was terminated after 350 hours due to simultaneous specimen failure in fatigue and coating failure. The longest-lived coating was the NiCrAlY with a life of approximately 275 hours.

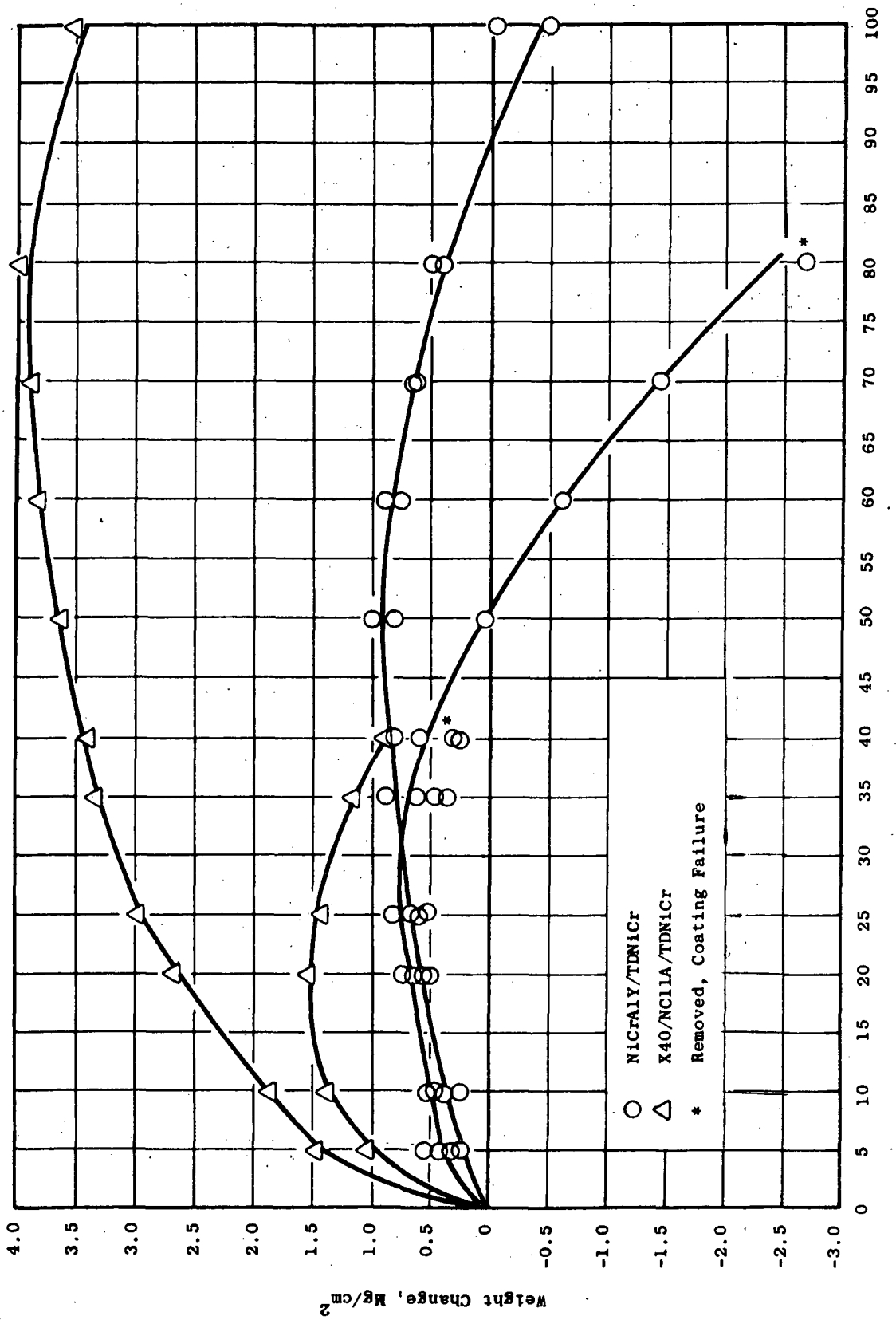

Figure D. 1533° K (2300° F) Static Oxidation Test, Cumulative Weight Change for X40/NC11A and NiCrAlY Coated TDNiCr.

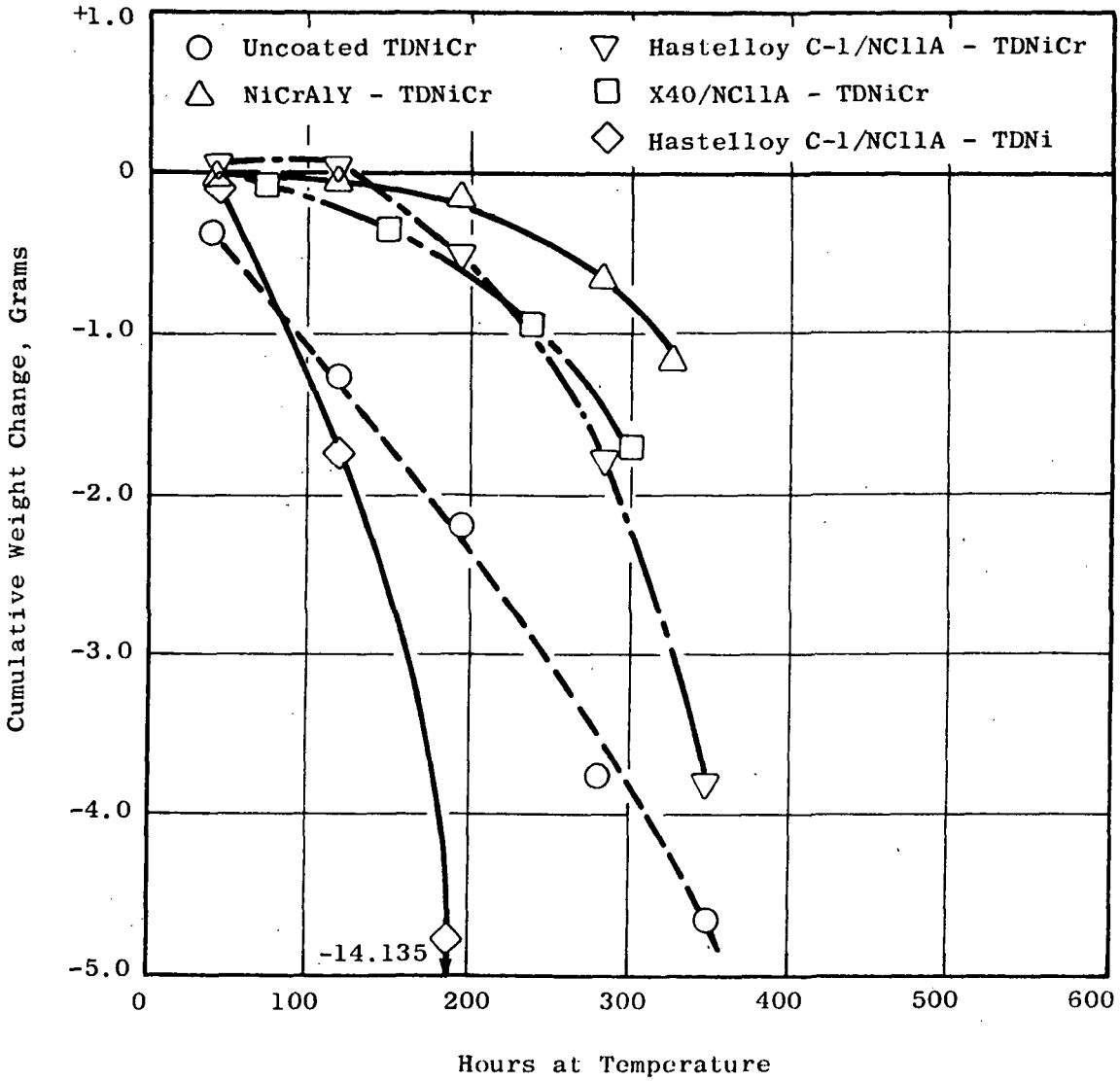

Figure E. Cumulative Weight Change, 1422° K (2100° F) Mach 1 Burner Rig Test. 1-Hour Cycles.

At the 1477° K (2200° F) testing temperature, only the vapor-deposited NiCrAlY coating survived the 100-hour test. Aside from coating failures, some specimens were lost due to fatigue failure in the slotted area where the specimen was clamped in the holding fixture. Based on the results obtained in the burner rig test, the goal of a coating with a potential life of 1477° K (2200° F)/500-hour and 1422° K (2100° F)/1000-hour operational life on jet engine hot components was not attained for Mach 1 conditions.

2.0 INTRODUCTION

Among the more attractive materials for hot-part turbine components are the thoria dispersion-strengthened nickel-base alloys, TD nickel and TD nichrome. Their exceptional mechanical properties at temperatures above 1366°K (2000°F) make them leading candidates for turbine vanes, combustion cans, and afterburner liners. Other desirable features are: (1) high melting point, (2) good thermal conductivity, (3) excellent thermal shock resistance, and (4) exceptional thermal stability. Unfortunately, their resistance to oxidation falls short at the temperatures which the above components will experience in advanced engine environments. Although the oxidation resistance of TD nichrome is significantly better than that of TD nickel, it is still inadequate for long operating life in the dynamic environment to which hot-part turbine components are exposed (and, more specifically, to temperatures above 1366° K (2000° F) and for operating times in excess of 1000 hours). Consequently, protective coatings are a necessity for the successful utilization of these materials in advanced engine applications.

Early coating development efforts on TDNi, circa 1963, were initiated by the Air Force and resulted in a two-step coating of chromium enrichment followed by aluminum enrichment. In cyclic oxidation/erosion tests, a coating life of 120 hours at 1477° K (2200° F) was reported by Du Pont[1]. Under cyclic sulfidation/erosion conditions, coating life was lowered to 70 hours at 1477°K (2200° F). TRW[2] concluded that their vacuum-pack and slurry-applied duplex chromium-aluminum coating on TDNi demonstrated cyclic oxidation life exceeding 200 hours at 1589° K (2400° F), 500 hours at 1477° K (2200° F), and 700 hours at 1366° K (2000° F). However, in several in-house coating evaluation programs by General Electric, test specimens with these coatings have consistently fallen far short of reported lives.

NASA has sponsored several coating efforts on both TDNi and TDNiCr. Under one program[3] modified NiCrAl- and FeCrAl-type cladding alloys were developed with some improved oxidation resistance to 1533° K (2300° F). However, interdiffusion between coating and substrate occurred leading to void formation in both the cladding and substrate after only 100 hours at 1533° K (2300° F). After 300 hours, nearly-complete homogenization had occurred of all substrate cladding combinations needed.

In another program[4], based on the application of fused-slurry NiCrAl-type coatings, 1533° K (2300° F) protection for several hundred hours was achieved in static oxidation; but, diffusional voids again occurred in both the coating and substrate.

High-velocity (Mach 1) oxidation testing at NASA[5] of coated specimens from both of these programs and other coating developments produced imminent oxidation failure after only 100 hours at 1422° K (2100° F). This demonstrated that coatings developed prior to 1970 offered only limited protection in high-velocity combustion environments at 1422° K (2100° F), whereas the substrate materials have useful strengths to at least 1477° K (2200° F). In addition,

the persistent void formation which occurs at 1422° K (2100° F) and above is a significant problem in retaining intact coatings. Thus, in order to utilize the 1477° K (2200° F) mechanical and physical properties of these materials, coatings with improved oxidation and diffusional stability are needed which produce no degradation of these properties over the desired service life.

To achieve these improvements, several approaches were investigated in this program. Under Task I, methods to promote diffusional stability were considered for minimizing void formation. In these studies the basic concept involved the introduction of a barrier layer between the substrate and the coating which would reduce the inward diffusion of coating constituents and the outward diffusion of substrate constituents. The compositions of the barrier layers were derived from an analysis of the performance of aluminide-type coatings on the two thoria-dispersion-strengthened materials and on other nickel- and cobalt-base superalloys, and from the behavior of alloys designed for brazing these thoria-dispersion-strengthened alloys.

When TDNi is given a nominal aluminiding treatment and then exposed under cyclic conditions at elevated temperatures, void formation becomes pronounced in less than 100 hours. Where chromium is present, as in TDNiCr, void formation is retarded and does not reach the degree obtained with TDNi under equivalent test conditions. This retardation is due to the reduced mobility of nickel in the presence of chromium. The presence of chromium also serves to inhibit the inward diffusion of aluminum. In studies of aluminide-type coatings on nickel superalloys, it has been observed that increasing amounts of certain refractory elements promote oxidation resistance. Thus, General Electric alloy SEL-15, coated with an in-house CODEP coating, is much more oxidation resistant than René 100 with the same coating. Compositionally these two alloys differ basically in the percent of refractory metals, 6.5% Mo and 1.5% W for the SEL-15, versus only 3.7% Mo and no tungsten for the René 100. Exceptional oxidation resistance has been obtained with an aluminide coating[6] on NASA-VIA alloy which has a very high refractory element content (9.0% Ta, 5.5% W, 6.0% Cr, 2.0% Mo, and 0.5% each of Rh, Hf, and Cb). Microprobe analysis revealed little evidence of inward diffusion of aluminum.

The effect of high refractory element content is also evident from brazing studies[7,8]. Successful General-Electric-developed braze alloys were modifications of Hastelloy C, TD-6 with 16% Cr, 17% Mo, and 5% W, and TD-20 with 16% Cr, 25% Mo, and 5% W. 100-hour exposures of brazing joints at 1477° K 2200° F) produced only minor pinpoint void formation, whereas a Hastelloy X modification, TD-5, with 22% Cr and only 9% Mo yielded significantly more and larger voids. The performance of the TD-6 and TD-20 in minimizing void formation made them attractive candidates as barrier layer materials. However, as brazing alloys they also contain 4% Si to lower the melting point for brazing. Since the lower melting point was not desired and there was evidence pointing to silicon as a factor in void formation, modifications of these alloys were made by reducing the silicon level to below 1% and raising the tungsten content of the TD-6 alloy to 10%, so that its refractory element content would be equivalent to TD-20 on a weight-percent basis. These compositional modifications were designed Hastelloy C-1 and C-2, respectively.

A similar study of cobalt-base alloys reveals the outstanding performance of an in-house aluminide coating on X40, which is attributed to the exceptional scale-forming characteristics of CoAl, the low diffusion coefficient of Al in cobalt, and the formation of a continuous $M_{23}C_6$ carbide (CoCrC) at the coating/base-metal interface. This carbide acts as a most effective diffusion barrier to inward diffusion of aluminum or outward diffusion of cobalt. Consequently, this alloy was selected as one of the barrier layer materials to be investigated.

Another approach to barrier layer formation was derived from the $M_{23}C_6$ carbide formation noted above and the observation that a number of nickel-base alloys, when aluminided, form inner diffusion zones that tend to act as barrier layers. Neither TDNi nor TDNiCr tend to form inner diffusion zones of this nature. It was hypothesized that, by diffusing carbon into the surface layer of TDNiCr, massive chromium carbides would form and would act as diffusion barriers.

For each of the above cases the barrier layer would serve two functions: (1) provide a barrier layer for the substrate, and (2) provide a new surface for the formation of a protective aluminide-type coating. With a sufficiently thick barrier layer, only a part would be converted to coating. The second consideration then was the improvement of the aluminide coating to meet the high exposure temperature required in the program. This study was conducted as Task II of the program.

The degradation mechanism of aluminide coatings is primarily an aluminum-depletion phenomenon due to successive Al_2O_3 film formation and spallation under cyclic exposure conditions. Under a recent NASA contract[6], improvement in oxidation resistance was shown through the incorporation of a dispersion of very fine Al_2O_3 particles in an aluminum-enriched outer coating layer. These particles (which tend to concentrate in the surface layer) form an intermittent oxide layer, thereby requiring less aluminum to maintain a continuous oxide film. The particles, it is believed, also tend to serve as anchorage for the oxide film and inhibit spallation. Thus, a combination of particle embedment and aluminum enrichment offered a promising approach for an improved aluminide coating system, and the NC11-A coating from that program was selected as one of the approaches to be used. A second approach was to obtain aluminum enrichment by providing aluminum reservoirs within the coating. This was to be achieved by the incorporation of intermetallic compound particles of high aluminum content in the outer coating layer, similar to the oxide-particle embedment mentioned above. Thus, as the coating matrix was depleted of aluminum, aluminum would be drawn from the reservoirs. In selecting such reservoir materials, consideration was given to base metals that would also retard diffusion (e.g., molybdenum, chromium, and cobalt). The intermetallic compounds selected were Cr_5Al_8, $MoAl_2$, and CoAl.

Under Task I of the program, the different barrier approaches were screened by exposure in an inert atmosphere at 1533° K (2300° F). Evaluation of the results was made by metallography, electron microprobe, and X-ray diffraction. Hardness surveys were made before and after exposure. Coefficients of expansion

were measured for the modified Hastelloy C barrier materials. Based on these results, the best barrier layer was selected for further investigation under Task II. A flow diagram describing Task I is presented in Figure 1.

In Task II, the several aluminum-rich intermetallic compounds were melted and attrited to ultrafine particles, 1-3 M. Studies were conducted for incorporation of the particles as dispersions in the outer coating layer. Tensile specimens were coated and tested in the as-processed condition and after cyclic low velocity burner rig testing at 1422°K (2100° F) for up to 300 hours. Tensile testing was at room temperature and 1422° K (2100° F). After tensile testing, the coatings were evaluated by metallographic, electron microprobe, and X-ray diffraction techniques. A flow diagram describing Task II is presented in Figure 2.

Based on the demonstration of a successful coating/substrate combination(s) under Task II, more advanced oxidation testing was conducted under Task III. This involved high-velocity burner rig testing at 1422° K (2100° F) and 1477°K (2200° F), and tensile testing after air exposures at 1533° K (2300° F).

This report summarizes the work conducted under Task I, II and III.

3.0 INVESTIGATION

3.1 Barrier Layer Diffusion Studies - Task I

3.1.1 Materials

3.1.1.1 Test Specimens

Test specimens were 2.54- x 10.16-cm panels (1- x 4-inch) made from the following materials:

a. 0.016-cm (0.065-inch) TDNi - HT No. 3092 - Fansteel Inc., Chicago, Ill., General Electric Specification B50T97

b. 0.016-cm (0.063-inch) TDNiCr - HT No. 2992-2 - Fansteel Inc., Chicago, Ill., General Electric Specification - B50TF46

3.1.1.2 Barrier Layer Materials

a. Stellite No. 31 powder (X40), lot No. 2546 particle size -325 mesh/20 M and -20 M.

Element	Weight Percent
Cr	25.3
W	7.67
Ni	9.84
C	0.52
Fe	0.24
Mn	0.47
Si	0.50
Co	Balance

b. Hastelloy C modifications - Alloy Metals Inc., Troy, Michigan, Lot No. 682 - Hastelloy C-1.

Chemistry	Actual $^{W}/_{o}$	Designed $^{W}/_{o}$, Nominal
Ni	55.44	57
Cr	16.96	16
Mo	17.61	17
W	10.57	10
Si	0.43	--

Particle Size Distribution

Size, Mesh	Weight %
-230, +325	24.37
-325, +20 μM	47.3
-20 μM	28.4

Lot No. 683 - Hastelloy C-2

Chemistry	% Actual	% Designed
Ni	50.38	52 - 54
Cr	17.01	16 - 18
Mo	27.46	25
W	4.78	5
Si	0.36	---

3.1.1.3 Processing Materials

Pack Carburizing Materials

Wood Charcoal	500 gms
Ba CO_3	35 gms
Na_2 CO_3	15 gms

Pack Chromizing Materials

Chromium Powder	400 gms
Al_2O_3 Powder	600 gms - G.E. Spec A50TF100
$CrCl_3$ - Activator	10 gms

Pack Mixture for Vapophase Coating Process

CODEP "B" powder	400 gms - G.E. Spec B50TF93 - Class I
Al_2O_3 Powder	600 gms - G.E. Spec A50TF100
NH_4F Activator	0.1% - G.E. Spec A50TF101

3.1.1.4 Processing and Test Facilities

Plasma Spray Equipment

The three barrier layer materials (X40, Hastelloy C-1, and Hastelloy C-2) were deposited with plasma-spray equipment: (1) a Metco 3MB unit, and (2) an AVCO PG100.

Heat Treat Facility

Diffusion heat treating of the plasma-sprayed barrier material was conducted under a hydrogen atmosphere in a sand-sealed retort in a Lindberg atmosphere furnace. Retort temperature was monitored with a Pt, Pt-Rh thermocouple placed in a thermocouple well in the retort lid.

1533° K (2300° F) Argon Test Facility

Test specimens were mounted in racks in a retort provided with an inlet tube to introduce an argon atmosphere. The retort was placed in a Hevi-Duty Lindberg furnace with a muffle designed to maintain an argon atmosphere. A T-joint was connected to the argon line so that the argon flow was divided between the retort and the furnace muffle. Retort temperature was monitored with a Pt, Pt-Rh thermocouple positioned in a thermocouple well in the retort lid.

Carburizing and Chromizing

The carburizing and chemistry operations were carried out in a sand-sealed retort in the Lindberg atmosphere furnace.

3.1.2 Barrier Layer Composite Coatings

3.1.2.1 Barrier Layers by Plasma Deposition

The barrier layer materials selected for investigation are compiled in Table I. For feasibility studies of these materials, plasma deposition was selected as the method of application. Coatings of 90-95 percent theoretical density can be obtained by this method, and further densification was achieved by diffusion heat treatment in hydrogen at elevated temperature. Plasma deposition has the disadvantage of producing some oxidation of the powder particles during deposition, thereby yielding deposits with entrapped oxides. Also, there is a greater loss of the more oxidizable and more volatile elements, which results in some change in the chemistry of the deposit in comparison with that of the original powders. However, elemental losses can be minimized by the proper selection of spraying parameters and the utilization of special cooling techniques.

In the plasma spraying of these powders, it was highly desirable to obtain as smooth a deposit as possible, thereby reducing the amount of subsequent grinding to a minimum. The goal was the deposition of a 125-150 μM coating

which would clean up at 75-100 μM. The trend in plasma spraying has been toward finer and finer powders which are capable of producing high-density coatings with as-sprayed finishes under 100 RMS. Therefore, powders in the -325 mesh/+20 μM and -20 μM ranges were prepared. Spraying was conducted with two types of plasma equipment: a Metco 3MB unit manufactured by Metco, Inc., Long Island, New York, and an AVCO PG100, manufactured by Bay State Abrasives Division, AVCO Corporation, Westboro, Mass.

Initial studies were carried out using the manufacturers recommended spraying parameters for X40 (Stellite No. 31). These results were compared with those obtained at higher-power settings, different design nozzles, and various powder flow rates. From these studies the following spray parameters were established:

Parameter	AVCO Gun	Metco Gun
Nozzle	High-Velocity	GE
Argon-Primary Gas Pressure/Flow	5.6 kg/cm^2/3.1 M^3/H (80 psi/90 CFH)	5.6 Kg/cm^2/3.4 M^3/H (80 psi/100 CFH)
Hydrogen-Secondary Gas Pressure/Flow	3.5 Kg/cm^2/0.24 M^3/H (50 psi/7 CFH)	3.5 Kg/cm^2/0.13 M^3/H (50 psi/4 CFH)
Amperes	400	400
Volts	50	50
Kilowatts	20	20
Spray Distance	7.7-10.1 cm (3-4 inches)	7.7-10.1 cm (3-4 inches)
Powder Flow Rate	2.73-3.2 Kg/hr (6-7 lb/hr)	2.7-3.2 Kg/hr (6-7 lb/hr)

3.1.2.2 Diffusion Heat Treatment

Diffusion heat treatment of the spray deposits was conducted both in hydrogen and vacuum at 1477° K (2200° F) for two hours. Typical structures of the X40 coating deposited with the AVCO gun following the above treatment are shown in Figures 3 and 4, respectively. Note the excellent diffusion bond between the coating and the substrate. The hydrogen-heat-treated coating, Figure 3, is significantly cleaner than the vacuum-heat-treated coating, the result of the reduction of oxides in the hydrogen atmosphere. Also, there appears to be greater consolidation of the coating under the hydrogen treatment. The combined beneficial effects of the hydrogen treatment resulted in its selection for the diffusion heat treatment of all the plasma-sprayed barrier materials. Following the diffusion heat treatment, the barrier layers were to receive the NC11-A coating developed under NASA Contract NAS3-11160.

3.1.2.3 Specimen Preparation for 1533° K (2300° F)/100-Hour Argon Exposure

In all, 18 barrier layer/NC11-A coating combinations were prepared for the 1533° K (2300° F)/100-hour exposure in argon, Table II. The X40 (Stellite No.

31) barrier was applied with the AVCO gun. Both guns were used for the Hastelloy C-1 and C-2 barriers. Two powder-size ranges were investigated, -325 mesh/ +20 M and a 50-50 mixture of -325 mesh/+20 and -20 , to determine the better powder-size distribution for coating density and surface finish.

Two panels each, 2.54 x 10.1 cm (1 inch x 4 inches), of TDNi and TDNiCr were prepared by grit blast with 120 M Al_2O_3 grit at a pressure of 60 psi (3.0 Kg/cm^2) to a surface roughness of 100 M RMS. The panels were fixtured on a mandrel which was mounted in a lathe and rotated during the spraying operation to assure uniformity of deposition. The gun itself was operated manually. Spraying was confined to one side of the panel. This was one method of determining coefficient of expansion compatibility with the substrate in subsequent exposure at 1533° K (2300° F), since significant expansion differences would result in panel distortion.

Following the spray operation, the panels were diffusion heat treated in three groups in dry hydrogen 229° K (-80°F) dew point at 1422° - 1477° K (2100° - 2200° F) at a hydrogen flow rate of 0.86 M^3/H (25 CFH). Processing times were as follows:

Group	Panels	Processing Time
1	16a, 16b, 17a, 17b, 18a, 19a, 20a, 21a, 22a, 23a, 24a, 25a,	Above 1422° K (2100°F) - 2.5 hr At 1455° K (2160°F) - 1.5 hr
2	18b, 19b, 20b, 21b, 22b, 23b, 24b, 25b, 26a, 26b, 27a	Above 1422° K (2100° F) - 2.75 hr At 1455° K (2160° F) - 2.25 hr
3	27b, 28a, 28b, 29a, 29b, 30a, 30b, 31a, 31b, 32a, 32b, 33a, 33b	Above 1422° K (2100° F) - 2.4 hr At 1477° K (2200° F) - 1.4 hr

After the diffusion heat treatment, both panels of each coating combination were partially hand ground on the coated surface preparatory to the application of the NC11-A coating. From 3.8 to $5.1X10^{-3}$ cm (1.5 to 2.0 mils) of carrier material were removed in the hand grinding operation, leaving approximately $7.6X10^{-3}$ cm (3 mils) of carrier material as a base for the subsequent coating operation. A section from one of the panels of each combination was taken for metallographic examination. These diffusion-heat-treated structures are shown in Figures 5 through 8. In most cases the structures shown are after hand grinding. In a few instances the fully-sprayed structure is depicted. Since the X40 barrier was deposited only with the AVCO gun using a single particle size range of powder, a comparison of the effect of plasma gun type and powder particle size was made only with the Hastelloy C-1 and C-2 powder. Examination of Figures 5 through 8 reveals that the deposits sprayed with the Metco gun contain relatively fewer oxides and are somewhat more dense than the AVCO gun deposits. With both guns, more uniform deposits containing fewer

oxides and voids are produced with the -325 mesh/+20 μM powders than with the 50-50 mixture of -325 mesh/+20 μM and -20 μM.

Aluminide Coating Application

The NC11-A coating application involved several steps. A pack mixture was prepared consisting of 40% aluminiding powder, 60% aluminum oxide filler, and an ammonium fluoride activator (see Section 3.1.1.3). The aluminiding powder is a ternary alloy of titanium, aluminum, and carbon of high aluminum activity. The pack ingredients were thoroughly mixed prior to filling the bottom of a coating box to a depth of approximately 2.54 cm (1 inch). Processing of the test specimens was conducted in Inconel coating boxes, 15.24X 15.2X12.7 cm (6X6X5 inches). A thermocouple tube, sealed at the end which extends into the center of the box, provided for monitoring the internal temperature throughout the coating cycle. In the NC11-A coating process, very fine Al_2O_3 particles, 2 μM in size, are embedded in the outer coating layer. Introduction of the oxide particles is accomplished by a relatively simple method. A slurry is prepared consisting of the aluminum oxide powder, a binder, and a solvent in approximately the following amounts:

Al_2O_3 powder	200 grams
Nicrobraze cement	50 cc
Acetone	50 cc

The ingredients are mixed in a high-speed blender with a rotating cutter for a period of 5 minutes (minimum) and then transferred to the spray can of a DeVilbiss paint spray gun. Prior to the application of the slurry, the specimens are degreased, liquid honed, and rinsed with acetone. Using the air-operated DeVilbiss spray gun at a line pressure of 2.8-3.5 Kg/cm^2 (40-50 psi), a smooth, opaque, adherent coating is applied free of wrinkles, blisters, or other surface discontinuities. Slurry coating thickness varies from 25 to $38X10^{-3}$ cm (10-15 mils). After spraying, the slurry coating is allowed to dry in air for a minimum of 30 minutes.

The slurry-coated panels were then suspended above the pack mixture along with René 41 control panels to monitor the activity of the pack mixture. After positioning the specimens, the box was covered with a lid and inserted into the forward section of an atmosphere-controlled retort (Figure 9) and set in a Harper furnace (Figure 10). The processing cycle was four hours at 1366° K (2000° F) under a flowing hydrogen atmosphere. The panels were coated in four separate coating runs. Weight gains on the René 41 control panels were quite consistent.

Run No.	Weight Gain, mg/cm^2
EF	5.23, 5.47, 5.60, 5.67
FF	4.62, 4.84, 4.79, 4.87
GF	4.67, 4.76, 4.45, 4.64
HG	5.43, 5.39, 5.27, 5.33

3.1.3 Carburized Barrier Layer

Originally, this barrier concept involved carburizing TDNiCr prior to aluminiding, to promote the formation of a layer of chromium carbide which would serve as a barrier to the interdiffusion of aluminum and nickel. In the preliminary studies, the chromium level proved to be too low to produce a significant amount of carbide in the inner diffusion zone. Consequently, a prior chromizing step was introduced to build up the chromium level in the surface layer.

3.1.3.1 Preliminary Test

TDNiCr panels were pack chromized under hydrogen at 1411° K (2100° F) for five hours. The pack consisted of electrolytic chromium powder, (10% by weight) in an Al_2O_3 filler (90% by weight). One percent $CrCl_3$ activator was added to the pack mixture. Weight gains averaged 3.0 mg/cm^2.

Prior to preparing the pack carburizing mixture (see Section 3.1.1.3) the charcoal was heated in hydrogen at 1366°K (2000°F) for one hour to drive off any residual oils, tars, or other substances used to bind the charcoal into briquets. Then two carburizing runs were made in a sand-sealed retort at 1366° K (2000° F) for one hour and the other for four hours. A hydrogen atmosphere was maintained in the retort by slowly bleeding in hydrogen through an inlet tube. Weight gains of approximately 2 mg/cm^2 were obtained in the one-hour process and 5.5 mg/cm^2 in four hours.

Aluminiding was conducted in a high-aluminum-activity pack using a NH_4F activator and an Al_2O_3 filler. Weight gains in each case averaged 8 mg/cm^2.

The combined chromizing and carburizing steps produced a distinct inner diffusion zone, Figure 11. Total coating thickness in both cases was 45 μM of which approximately half was inner diffusion zone. The outer coating layers differ slightly, the specimen with the four-hour carburizing treatment showing a dispersed secondary phase (Figure 11, bottom).

Specimens representing each carburizing treatment were exposed in argon at 1477° K (2200° F) for 100 hours to determine interdiffusion effects. Metallographic examination revealed that a significant amount of void formation and separation had occurred in the inner diffusion zone. Void formation was more pronounced on the samples that had the longer carburizing treatment.

3.1.3.2 Specimen Preparation for the 1533° K (2300° F) Argon Exposure

In the preparation of specimens for the 1533° K (2300° F) argon exposure, chromizing time and temperature were increased. Two groups of TDNiCr were chromized, one at 1477° K (2200° F) for 5 hours and the other for 20 hours. Weight gains averaged 5 mg/cm^2 for the 5-hour treatment and 11 mg/cm^2 for the 20-hour treatment. Both groups were carburized at 1366°K (2000° F) for one hour.

The NC11-A aluminiding process, as described in the previous section, followed. These specimens were processed along with the sprayed barrier layer specimen in run No. HF, see Section 3.1.2.3.

3.1.4 1533° K (2300° F)/100-hour Argon Exposure

Panels with the 20-barrier layer/NC11-A coating considerations described in Sections 3.2.3 and 3.3.3 were mounted on racks in the retort described in Section 3.1.1.4 and placed in the furnace described in the same section. Argon flow rate was set at 0.85 M^3/ hour (25 CFH) with half of the argon flowing into the retort and half into the furnace muffle. During the initial 20 hours of exposure, the temperature increased overnight to 1544° K (2320° F), and that temperature was maintained for approximately 10 hours. Adjustments were made and the temperature was held at 1533° K (2300° F) for the remaining 80 hours of test time.

In spite of the argon atmosphere in the furnace, the exterior of the retort was severely oxidized in some areas. There was some evidence of oxidation on the inside of the box and on the panels. Minor internal oxidation could be expected from the slight amount of oxygen (about 100 ppm) in the argon. During the test, over 34 M^3 (1000 cubic feet) of the gas passed through the retort.

3.1.4.1 Metallographic Examination

Both the as-processed and exposed panels of all coating systems were sectioned and examined metallographically. Of particular interest were (1) the outer coating layer and barrier layer/coating interface, and (2) interdiffusion effects between the barrier layer and the substrate. The results of the more successful combinations are presented in the following sections. In all cases these were the spray deposits of the -325 mesh/+20 μM powders which were more uniform and contained fewer voids and oxides than those powders containing half -20 μM particles.

X40 Barrier Layer

With the X40 (AVCO gun) plasma-sprayed barrier layer, there was a marked difference in results between the TDNi and TDNiCr substrates, Figures 12 and 13. Outer coating thickness on the TDNi, as processed, was 35 μM Figure 12, top, compared with 20 μM on the TDNiCr, Figure 13, top. The barrier layer of the former was somewhat denser, showing few oxides and only isolated voids. The Al_2O_3 particle distribution in the outer coating layer was about the same for both systems.

The 1533° K (2300°F) /100-hour exposure in argon produced major changes in the TDNi specimen, Figure 12, bottom. Considerable apparent void formation occurred in the outer layer, within the barrier layer, and in a 75 μM zone in the substrate below the barrier/substrate interface. Much of the outer coating layer was gone due either to spalling or volatilization of aluminum at 1533° K (2300° F). The voids in the substrate were columnar in shape and appeared to coincide with recrystallized grains.

On the other hand, the TDNiCr specimen showed little change due to the 1533° K (2300° F)/100-hour argon exposure. There were some apparent voids in the outer coating layer (Figure 13, bottom) but no gross void formation in the barrier layer or in the substrate. Closer examination revealed recrystallized grains in the substrate which are outlined by segregated thoria. As a barrier material, X40 appeared to be compatible with TDNiCr.

Hastelloy C-1a Barrier Layer

The influence of the Hastelloy C-1a barrier on TDNi is shown in Figure 14 for the deposits sprayed with the Metco gun. A very thick NC11-A coating was produced consisting of 37 μM outer layer and 50 μM inner diffusion zone Figure 14, top. After the 1533° K (2300° F)/100-hour exposure, little residual outer coating layer remained; and, minor void formation occurred in the barrier layer, Figure 14, bottom. However, no void formation was evident in the substrate in the 75 μM zone below the barrier/substrate interface. Grain recrystallization also was apparent as evidenced by thoria segregation.

The Hastelloy C-1a barrier on TDNiCr deposited with the AVCO equipment is shown in Figure 15. Note that these photomicrographs are at 250X magnification and represent the etched condition. Total NC11-A coating thickness varied from 75 to 90 μM with an outer layer of 37 μM and a residual barrier layer of about 50 μM. The 1533° K (2300° F)/100-hour exposure produced some void formation in the outer coating layer and loss of coating probably due to aluminum volatilization. These was evidence of substrate grain recrystallization and growth in the 75 μM zone below the barrier/substrate interface. This barrier material does not appear to promote void formation in either TDNi or TDNiCr.

Hastelloy C-2a Barrier Layer

In Figure 16, the plasma-sprayed (Metco gun) Hastelloy C-2a barrier on TDNi with the NC11-A covercoat is shown at 500X. Total coating, as processed, was only 37 μM, with an outer layer 25 μM thick (Figure 16, top). The barrier layer thickness was very dense with a residue of scattered oxide particles from the spraying operation. As with the other barrier systems, the 1533° K (2300° F)/100-hour exposure produced considerable void formation and loss of outer coating (Figure 16, bottom). However, the barrier material appeared to be compatible with the TDNi substrate. Though there was evidence of grain recrystallization and growth, the apparent void formation observed with the X40 barrier was not present.

The plasma-sprayed (Metco gun) Hastelloy C-2a barrier on TDNiCr with the NC11-A covercoat is presented in Figures 17 and 18. Figure 17, top, shows the as-processed coating to be very similar in thickness and structure to the one on TDNi, Figure 16, bottom. Figure 18 depicts the results after the 1533° K (2300° F)/100-hour exposure. The latter figure is at 250X magnification and in the etched condition. Though there had been some void formation in the outer coating layer, the inner diffusion zone was fully intact and appeared to form a continuous barrier. There also appeared to be less grain recrystallization and growth in the substrate, Figure 18. The Hastelloy C-2a barrier material apparently was compatible with both substrates.

Overall, of the coating systems involving the Hastelloy C-1a and Hastelloy C-2 barrier, the deposits sprayed with the Metco gun generally contained fewer oxides and were denser than the deposits sprayed with the AVCO gun. On this basis, the Metco gun and spray parameters were selected for the barrier layer application in Task II.

Chromized/Carburized Barrier on TDNiCr

In the preliminary evaluation of this approach, a significant amount of void formation occurred when the coatings were exposed in argon at only 1477° K (2200° F) for 100 hours. Increasing the amount of chromium through a longer chromizing time (20 hours) and a higher temperature [1477° K (2200° F)] did show some improvement in the test conducted at 1533° K (2300° F). The higher chromium level in the surface layer resulted in thicker (75 μM) coatings and a correspondingly heavier inner diffusion zone (Figure 19, top).

However, for both chromizing treatments, the extent of void formation from the 1533° K (2300° F) exposure was still considerable (Figure 19, bottom). Consequently, the chromized/carburized approach was considered inadequate as a barrier layer for TDNiCr, and this avenue was not pursued further.

Artifacts in TDNi/TDNiCr

In the preparation of coated TDNi and TDNiCr specimens for metallographic examination, the polishing procedure is very critical. Certain polishing methods and the use of etchants in intermediate steps can produce artifacts that give a false metallographic structure. This is shown in Figure 20, top, where excessive polishing combined with intermediate etchants produced "pullout" of grains in the recrystallization zone and in the barrier layer, in contrast to a correctly polished specimen, Figure 20, bottom. Because of the criticality in the amount of polishing and the effect of etchants, most of the specimens were prepared in the unetched condition. The TDNi appeared to be more sensitive in this regard than the TDNiCr which is shown in the etched condition in Figures 15 and 18.

3.1.4.2 X-Ray Diffraction Analysis

The results of the x-ray diffraction analyses are presented in Table III. In the as-processed condition, analyses were made on coating/plasma-sprayed

barrier combinations on TDNi only, since the substrate itself would exert little or no influence on the composition of the NC11-A overcoat. In all cases, only NiAl and α Al_2O_3 were detected for the Hastelloy C barriers, and CoAl and α Al_2O_3 for the X40 (the α Al_2O_3 phase representing the embedded Al_2O_3 particles from the NC11-A coating process). The as-processed chromized/carburized barrier TDNiCr also showed only NiAl and α Al_2O_3 in the overcoat.

After the 1533° K (2300° F)/100-hour exposure, analyses were made of the coatings on the TDNiCr panels. On the specimen with the X40 barrier, 17b, only a cubic cobalt phase was found to be present. Though there was no evidence of Al_2O_3, it will be shown in a subsequent section on microprobe analysis that a significant amount of aluminum was present. However, the ASTM Diffraction Card File contains no cards that identify cobalt phases containing aluminum other than CoAl.

The chromized/carburized barrier layer specimens, NiCr 20 and NiCr 5, revealed patterns of γ and Cr_2O_3. γ' was present in the specimen that had the 5-hour chromizing treatment, but its existence is questionable in the one with the 20-hour chromizing treatment. γ and γ' have virtually identical indexes except that the latter has several weak superlattice lines. If the γ' is low in concentration, these lines may be too weak to be detected.

The AVCO gun-sprayed Hastelloy C-2 barrier specimens (19b and 21b) both showed the same phases to be present, γ, γ', and Al_2O_3. On the other hand, the Metco gun-sprayed Hastelloy C-2 barrier specimens (23b and 25b) and the AVCO gun-sprayed Hastelloy C-1 barrier specimens (27b and 29b) revealed positive identification for γ and α Al_2O_3 and the questionable presence of γ'. Mixed results were obtained with the Metco gun-sprayed Hastelloy C-1 barrier; the one using the -325 mesh/+20 μM powder, 31b, showed the phases γ, γ', and α Al_2O_3, while the one using the 50/50 powder mixture of -325 mesh/+20 μM and -20 μM showed positive identification only of γ and α Al_2O_3.

From the above results one can postulate that a major loss of the aluminum in the covercoat was due to:

1) Conversion to α Al_2O_3 through reaction with the oxygen in the argon gas

2) Volatilization at the 1533° K (2300° F) temperature, due to the argon flow through the retort

3) Diffusion into the barrier layer and substrate

3.1.4.3 Electron Microprobe Analysis

Nineteen specimens representative of the various coating/barrier combinations were submitted for electron microprobe analysis by both scan and trace techniques, Table IV. EBS and elemental scans were made on all specimens while traces were made for those that showed potential as coating combinations. In

reporting these results, pictures of the scans are not shown because of the variation in intensity of the different elements and background noise, and because of the difficulty in reproducing slight variations in concentration which are evident on the original glass copy but do not show up in print. However, the significant traces are all reproduced.

3.1.4.3.1 X40 Barrier/TDNiCr (AVCO Gun)

Aluminum - In the as-processed condition, the scan showed a high level of aluminum at the surface to a depth of 25 μM and segregated areas of high aluminum concentration to a depth of 50-75 μM in the barrier layer. The corresponding trace (Figure 21, left) shows: an aluminum concentration of 30-40% for the first 25 μM, a drop to 20% aluminum at 40 μM, a further drop to 5% Al at 50 μM, but a peak of 8% at 55 μM. Below 60 μM, the level decreased sharply to about 2%.

After exposure, the scan showed a depletion of aluminum at the surface and the highest concentration near the barrier/substrate interface with isolated concentrations of aluminum in the substrate 49-50 μM below the interface. These results are confirmed by the microprobe trace (Figure 21, right), which shows an aluminum peak of about 18% at 40 μM below the surface, and several small peaks, 4-6% Al, in the substrate.

Cobalt - The scan of the as-processed condition revealed cobalt to a depth of 150-175 μM, indicating some diffusion of cobalt into the substrate during processing. After exposure, cobalt diffusion appeared to be evident at the limits of the scan or a depth of 325-350 μM. The trace, Figure 22, shows a gradient of 10% Co down to 8% for the first 100 μM and a total depth of diffusion of between 375 and 400 μM.

Chromium - The scans showed no discernible difference between the as-processed and exposed samples, as would be expected, since the chromium levels in the barrier layer and in the substrate were very close in concentration, 25% and 20%, respectively. The corresponding trace, Figure 22, indicates equivalent concentrations in the barrier layer and the substrate. The slight dip at the surface would be due to some chromium loss in oxidation.

Tungsten - The scan of the as-processed coating showed tungsten to be of uniform concentration to the limits of the scan, 325-350 μM. The tungsten trace, Figure 22, did not confirm such extensive diffusion. It shows a drop in tungsten concentration to about 1% and a depth of diffusion not exceeding 300 μM.

Thorium - In the as-processed condition the scan showed thorium to be at a uniform concentration below the barrier layer. After exposure there were definite segregated areas of thorium in a 100 μM zone below the barrier layer. These areas are evident in the EM trace, Figure 22, at concentration of 12-3% Th.

3.1.4.3.2 X40 Barrier/TDNi, As-Processed, (AVCO Gun)

Probe analyses were obtained for this system only in the as-processed condition. The 1533° K (2300° F) exposure produced massive void formation, so that traces of the elements would not be meaningful. The Al trace is not shown since it was essentially the same as that of the X40 barrier TDNiCr system above. Diffusion of barrier layer elements into the substrate would be due to the 2-hour heat treatment in hydrogen at 1422°-1477° K (2100°- 2200°F) and the coating process of 4 hours at 1366° K (2000° F). EM traces are shown in Figure 23.

Cobalt - In the coating process, the Co level in the aluminide layer dropped from the original 56% to 23%. Diffusion into the TDNi substrate also reduced the Co level in the barrier layer. However, the overall reduction in the amount of Co in the barrier layer appeared to be greater than can be accounted for in converting to aluminide and diffusion into the substrate. Cobalt diffusion into the substrate was limited to about 30 μM.

Chromium - The chromium trace showed a normal chromium gradient in the coating layer and chromium diffusion from the barrier layer into the substrate to a depth of about 30 μM.

Tungsten - The tungsten trace indicated considerably less W to be present than would be anticipated from an original 8% level. Preferential oxidation of the tungsten during a spraying may account for some of this loss. There was virtually no diffusion into the substrate.

Thorium (Thoria) - The thorium trace is somewhat surprising because it would appear that thoria has diffused into the barrier layer. It would be difficult to explain how discrete thoria particles would have such mobility at 1422°-1477° K (2100°-2200° F). Note that a thoria peak is formed midway in the barrier layer.

3.1.4.3.3 Hastelloy C-1 Barrier/TDNi

EM scans were made for both the AVCO and Metco gun-deposited barriers, as-processed and after exposure. An Al trace was run only on the as-processed AVCO gun-deposited barrier specimen. Complete elemental traces were run on both coating combinations after the 1533° K (2300° F) exposure.

Aluminum - The scans for both coatings showed relatively high aluminum concentration on the outer 25 μM of coating, followed by a sharp drop through the barrier layer and extending to a depth of 100-125 μM below the surface. The corresponding trace (Figure 24, left) indicates a 30-35% aluminum level in the outer coating layer, 20% in the inner diffusion zone, and 5-15% in the barrier layer. Below the barrier layer, the level drops from 5% to 0% over a distance of about 50 μM. After the 1533° K (2300° F) exposure, the scans showed very intense aluminum concentration at the surface and in local areas in a zone 100-125 μM below the surface. Below this region the aluminum was uniformly

diffused. These areas of aluminum segregation, as shown by trace (Figure 24, right), range from 40-70% aluminum indicating areas of Al_2O_3 to a depth of 40 μM. Intermittent aluminum peaks of 5-20% extend an additional 60-80 μM. In contrast, the Metco gun-coated specimen (Figure 25) showed a surface concentration of 30-35% Al with concentration spikes within the barrier layer and at the barrier layer/substrate interface.

Chromium - As-processed, there was little evidence of chromium diffusion into the substrate from the scans. However, after exposure the chromium concentration appeared uniform to the limits of the scans. The EM traces, Figures 26 and 27, showed chromium diffusion in excess of 600 μM. Chromium concentration was greater in the Metco gun-coated specimen.

Molybdenum - As with the chromium above, the scans showed the molybdenum to be confirmed to the barrier layer in the as-processed condition. Marked differences were observed after exposure. On the AVCO gun-coated specimen an intermittent band of segregated molybdenum was observed in a zone 50 μM below the surface and in the substrate 50-75 μM below the barrier/substrate interface. In contrast, the molybdenum showed a uniform gradient in the Metco gun-coated specimen. These differences were not evident in the EM traces, Figures 26 and 27, except that the molybdenum concentration showed a marked dip in the AVCO gun-coated specimen at about 200 μM below the surface.

Tungsten - As-processed, the tungsten scans showed some diffusion into the substrate to a depth of 25-50 μM. After exposure the condition was similar to that of chromium, a uniform distribution to the limits of the scan. However, the EM traces (Figures 26 and 27) showed tungsten diffusion not to exceed 300 to 325 μM.

Thorium - In the as-processed condition thorium was uniformly distributed in the substrate. After exposure, areas of thorium segregation and depletion were observed. Both EM traces showed thorium peaks with greater segregation indicated for the Metco gun-coated specimen, Figures 26 and 27. The latter also showed thorium extending into the coating which is difficult to explain.

3.1.4.3.4 Hastelloy C-1 Barrier/TDNiCr

As-processed and after-1533° K (2300° F)-exposure scans were made for both the AVCO and Metco gun-deposited barrier specimens. An Al trace was run on the Metco gun-deposited as-processed specimen, and complete elemental traces were run on both specimens after exposure.

Aluminum - The scans of both specimens showed a very high aluminum level in the outer coating layer, and aluminum evident to a depth of about 100 μM below the surface. This very high level was reflected in the EM traces of the Metco gun-coated specimen, Figure 28, left. Readings of 40-60% Al in the outer coating layer (25 μM) were indicative of the high level of entrapped Al_2O_3 particles from the NC11-A coating process. After the 1533° K (2300° F) exposure, there was a sharp drop in the aluminum level of the outer coating layer in both specimens (Figure 28, right, and Figure 29), the drop being more

pronounced for the AVCO gun-coated specimen than the Metco gun-coated specimen. However, higher aluminum concentrations were found in the barrier layer of the former than in the latter. More surprising were the high aluminum peaks at the barrier/substrate interface and within the substrate itself. A low aluminum concentration, about 2%, was found at a depth exceeding 175 μM in the Metco gun-coated specimen and over 250 μM in the AVCO gun-coated specimen.

Chromium - EM traces for chromium were run only on the 1533° K (2300° F) specimens. The results for the AVCO gun-sprayed barrier (Figure 30) and the Metco gun-sprayed barrier (Figure 31) were virtually identical, except for a dip in the chromium level at approximately 30 μM for the Metco gun-sprayed sample and a chromium spike at the corresponding point in the AVCO gun-sprayed sample. In both cases the surface chromium level was approximately 14%, which increased gradually to 20% at a depth of 400-425 μM.

Molybdenum - Markedly different behavior was noted with molybdenum on the two specimens. Whereas the AVCO gun-coated specimen (Figure 30) showed a low concentration of only 5% at the surface and a uniform gradient to 0% at 525-550 μM, the Metco gun-coated specimen (Figure 31) showed segregations of 20% and 25% Mo in the coating/barrier layer region and a much higher level of Mo in the substrate than was found in the AVCO gun-coated specimen. However, the depth of diffusion was about the same, 525-550 μM.

Tungsten - The same differences noted for molybdenum were observed with tungsten. Again, the tungsten level was down to about 2% in the surface layer and reached a 0% level at about 325 μM. On the Metco gun-sprayed specimen, tungsten segregation was found in the same areas as the molybdenum, reaching levels as high as 20%. Tungsten concentration was also slightly higher in the substrate, but the extent of diffusion was about the same.

Thorium - Thorium segregation was detected on both specimens, Figure 30 and 31, with significantly high concentrations being noted on the Metco gun-coated specimen. A low concentration of thorium was recorded in the coating/barrier layer region on the AVCO gun-coated specimen. Since the thoria level in the substrate is slightly higher in the Metco gun-coated specimen, it may be that the trace was slightly displaced from the zero reading. Such was not the case where this condition was noted previously, Figure 26 and 27.

3.1.4.3.5 Hastelloy C-2/TDNi

For the Hastelloy C-2 barrier, EM scans were run on both the as-processed and exposed specimens of both coating combinations. A complete elemental trace was made on the AVCO gun-coated specimen, as-processed, and for aluminum only after exposure. On the Metco gun-coated specimen, traces were made for Mo, W, Cr, and Th.

Aluminum - Scans of the as-processed specimens showed a significantly higher aluminum concentration in the AVCO gun-coated specimen than in the Metco gun-coated equivalent. However, the depth of aluminum penetration was about the same in both. After the 1533° K (2300° F) exposure both samples showed highly segregated aluminum areas to a depth of about 100 μM. The EM trace on the AVCO gun-coated specimen (Figure 32, left) shows a high aluminum concentration, indicating a high level of Al_2O_3 particle entrapment in the outer coating layer. The aluminum level drops to less than 10% in the barrier layer. After exposure (Figure 32, right) the aluminum shows a peak of 55%, indicating that some oxidation has occurred. Al peaks of 8-10% were found in the barrier layer, while the level in the substrate was very low.

Chromium - In the as-processed AVCO gun-coated specimen, Figure 33, chromium diffusion into the substrate exceeded 75 μM. The level in the coating varied from about 2% at the surface to 4% at the outer coating layer/barrier diffusion zone interface. The 1533° K (2300° F) exposure of the Metco gun-coated specimen, Figure 34, produced two areas of chromium segregation in the barrier layer and extensive diffusion in excess of 600 μM.

Molybdenum - The as-processed AVCO gun-coated specimen, Figure 33, showed molybdenum levels in the barrier layer to be in excess of its concentration in the original powder. Molybdenum diffused into the substrate apparently 60 μM. In the Metro gun-coated specimen exposed at 1533° K (2300° F), diffusion of molybdenum into the substrate lowered the concentration in the coating/barrier layer to 8%, Figure 34. Depth of diffusion was approximately 450 μM.

Tungsten - Tungsten in the as-processed AVCO gun coating was confined predominantly to the barrier layer with only slight diffusion into the coating and substrate, Figure 33. In the exposed Metco gun-coated specimen the W concentration dropped from 5% to 2% in the coating/barrier layer and diffused into the substrate to a depth of about 250 μM.

Thorium - The as-processed AVCO gun-coated specimen trace showed a low level concentration of thorium in the coating/barrier layer area, while the exposed Metco gun-coated specimen showed thorium segregation as noted previously.

3.1.4.3.6 Hastelloy C-2/TDNiCr

For this coating combination scans were run on both the AVCO and Metco gun coatings as-processed and exposed specimens. Al traces were made for the as-processed and exposed AVCO gun-coated specimens only; and Mo, W, Cr, and thorium traces were made for the exposed Metco gun-coated specimen.

Aluminum - The scans for both the as-processed AVCO and Metco gun-coated specimens indicated a very high aluminum level on the outer 12-15 μM, then a sharp drop to a lower level for the next 25 μM at which point the concentration dropped to a low value. Isolated high-aluminum areas were observed to a depth of 150 μM below the surface. The corresponding Al trace (Figure 35, left) showed 45-50% Al in the first 10 μM, 25-33% in the following 12-15 μM, and

intermittent aluminum peaks through the barrier layer. A low aluminum level was indicated in the substrate. After exposure the scans showed highly concentrated areas of aluminum in both the coating and barrier layer. In the corresponding trace (Figure 35, right) these high aluminum concentrations peaked at 56% and 68% Al in the coating (indications of Al_2O_3) and at lower levels in the barrier layer. The aluminum level in the substrate was of the order of 2% and extended well beyond 175 μM.

Chromium - Scans indicated the chromium level to be slightly lower in the substrate in the as-processed condition for both specimens. After exposure, areas devoid or low in chromium were evident. These areas appeared to coincide with those high in aluminum. These depressions in the chromium level were observed in the Cr trace of the Metco gun-coated specimen, Figure 36.

Molybdenum - The scans revealed a fairly uniform concentration of molybdenum extending about 100 μM below the coating in the barrier layer for both specimens in the as-processed condition, and a molybdenum gradient into the substrate to a depth of about 50 μM. After exposure, the molybdenum concentration in the barrier layer of the AVCO gun-coated specimen was greatly reduced, and molybdenum diffusion into the substrate was apparent to a depth of 200-250 μM. However, on the Metco gun-coated specimen, high molybdenum concentrations were noted in the coating/barrier interfacial region, and the Mo trace (Figure 36) showed peaks up to 30%. Mo diffusion extended to a depth of about 400 μM.

Tungsten - The behavior of tungsten was very similar to that of molybdenum in both the as-processed and exposed condition. Tungsten concentrations appeared to coincide with the molybdenum concentration, Figure 36.

Thorium - In the as-processed condition thorium distribution was uniform below the barrier/substrate interface. As in other coating systems, scans indicated a depletion of thorium in some areas and a slight concentration in others after the 1533° K (2300° F) exposure. However, thorium peaks were absent from the trace on the Metco gun-coated specimen.

3.1.5 Barrier Layer Expansion Compatibility

As pointed out in an earlier section, the panels with the plasma-deposited barriers were coated on one side only to determine the compatibility of the barrier layers with the substrates in thermal expansion. During the NC11-A coating application, various degrees of deflection were produced. These deflections became more pronounced after the 1533° K (2300° F)/100-hour exposure in argon. A comparison of these deflections is presented in Figure 37. The least amount of deflection was induced by the X40 barrier layer, followed by the Hastelloy C-1 and the Hastelloy C-2. In general, greater deflections were obtained on TDNiCr than on TDNi.

Since the expansion coefficients of Hastelloy C-1 and Hastelloy C-2 were not known, dilatometric measurements were made on bars prepared from vacuum-hot-pressed

compacts of the powder. Duplicate tests were run of each material up to 2000° F (1366° K). Reruns were made after the first runs indicated slight shrinkage due to sintering. The retest results are presented in Figure 38, along with data for TDNi, TDNiCr, and X40. For the retest values, the Hastellov C-1 ranged from $11.1X10^{-6}$ cm/cm/°K ($6.2X10^{-6}$ in./in./°F) at 366°K (200°F) to $15.3X10^{-6}$ cm/cm/°K ($8.5X10^{-6}$ in./in./° F) at 1366°K (2000°F). The Hastelloy C-2 values were slightly lower, $10.5X10^{-6}$ cm/cm/°K ($5.8X10^{-6}$ in./in./°F) at 366°K (200°F) to $14.7X10^{-6}$ cm/cm/°K ($8.2X10^{-6}$ in./in./°F) at 1366° K (2000°F).

These values are somewhat lower than the values for TDNi and TDNiCr. The lower coefficient of expansion of the Hastelloy C-2 would explain the greater deflections over the Hastelloy C-1. The higher coefficient of expansion of TDNiCr compared with TDNi would also be reflected in the greater deflections noted. The greater compatibility of X40 is based on its coefficient of expansion lying midway between that of TDNi and TDNiCr.

3.1.6 Hardness Survey

The hardness surveys were conducted to determine the effect of elemental diffusion. Initial results were erratic when a low indentor load was used. With a heavier indentor load, the effects of small preferred local grain orientations were reduced. This was based on a review of a study by Killpatrick and Young[9] in which it was demonstrated that hardness measurement on TDNiCr was sensitive to indentor orientation with respect to rolling direction. They showed Knoop hardness variations from a minimum of 275 (with a long axis of the indentor at 45° to the rolling direction) to 377 (with the long axis parallel). For this survey, the long axis was held parallel to the rolling direction in all cases. Measurements were made at 125 μM intervals beginning at 125 μM below the barrier/substrate interface, and extending to a depth of 750 μM. Readings were also taken on the as-received TDNi and TDNiCr stock. These results are compiled in Table V.

TD Nickel

Comparison of the hardness of the as-processed TDNi specimens with the as-received material indicated a slight reduction in hardness only in the first 120 μM of the substrate for the Hastelloy C-1 and C-2 barriers, the balance of the substrate being unaffected. The reason for this slight reduction in hardness cannot be explained by diffusion effects of barrier layer constituents. Probe traces showed diffusion of Mo and Cr to be limited to ~ 50 μM and virtually no diffusion of tungsten, Figure 33. One would anticipate an increase in hardness from the diffusion of the above elements.

Subsequent exposure at 1533° K (2300°F) for 100 hours resulted in significant hardness increases to a depth of about 400 μM for the AVCO gun-sprayed Hastelloy C-1 and C-2 barriers, while the Metco gun-sprayed Hastelloy C-1

barrier produced an increase to the very center of the substrate. In contrast, the specimen with the X40 barrier showed no significant change from the as-received condition. This may be due to the excessive void formation which inhibited diffusion. Examination of the probe traces after the 1533° K (2300° F) exposure for the AVCO gun-sprayed Hastelloy C-1 (Figure 26), Metco gun-sprayed Hastelloy C-1 (Figure 27), and Metco gun-sprayed Hastelloy C-2 (Figure 36) indicates approximately the same depth of diffusion for chromium, molybdenum, and tungsten (500 μM, 350 μM, and 200 μM, respectively). One can conclude that the hardness increase is, at least, partially due to the diffusion of chromium and molybdenum. Probe traces were not made of the X40 barrier specimen after exposure because metallographic examination had revealed massive void formation at the barrier/substrate interface and in the substrate just below the interface. This void formation would tend to significantly reduce the extent of diffusion of the barrier layer constituents into the substrate.

TD Nichrome

The as-received TDNiCr varied considerably in hardness ranging from a high of 329 at 125 μM to lows of 277 and 265 at 250 and 500 μM, respectively. A core value of 299 was appreciably higher than the two low values noted above. This same variation in hardness was observed in the as-coated condition. However, all three barrier layer specimens showed a reduction in hardness, the most pronounced being with the X40, where the average hardness dropped over 40 points.

After the 1533° K (2300° F) exposure, the X40 barrier specimen showed a further drop in hardness at the 125 μM level, but average hardness remained the same. This same drop in hardness at the 125 μM level was noted with the AVCO gun-sprayed Hastelloy C-1 specimen, though the average hardness actually increased about 15 points. Neither the Metco gun-sprayed Hastelloy C-1 nor the AVCO gun-sprayed Hastelloy C-2 barrier specimens showed this drop at the same level. Both showed overall hardness increases of ~ 18 points.

3.1.7 Summary of Task I Results

The primary objectives of Task I were (1) to identify barrier layer materials that were compatible with TDNi and TDNiCr in that void formation was minimized at elevated temperature and the diffusion of coating constituents into the substrate was reduced, and (2) to provide a new surface for the formation of a protective aluminide-type coating. Of the three materials evaluated on TDNi, the Hastelloy C-1 and C-2 compositions appeared to meet these criteria. Excessive void formation occurred with the third material, X40. These same three materials showed satisfactory performance on TDNiCr. A combined chromizing/carburizing approach for the latter alloy did not prevent void formation at elevated temperature.

The NC11-A covercoat applied to the Hastelloy C-type barrier layers degraded when exposed in argon at 1533° K (2300° F) for 100 hours. This degradation was due, in part, to the volatilization of aluminum at the elevated

temperature, which was aggravated by the argon gas flow through the retort at 0.42 M^3/hour (12.5 CFH). Residual oxygen in the argon gas resulted in some oxidation of the coating, whereas the volatilization of the aluminum contributed to void formation in the coating. Some void formation is inherent from the method of applying the barrier materials. Plasma deposits generally have a porosity of 5-10%. The reduction of oxides during the hydrogen diffusion heat treatment would result in the coalescence of the voids.

In the case of the X40 barrier, void formation at the coating/barrier interface could also be a Kirkendall effect. Void formation of this type has been observed on aluminide-coated X40 after extended exposure at 1477° K (2200° F) where the substrate was not solutioned and aged before coating or certain alloying elements were out of balance. Plasma deposition of the X40 material may have adversely affected the balance of these alloying constituents.

Diffusion of barrier layer constituents into the substrates was extensive, with a corresponding counter diffusion of substrate constituent(s) into the barrier layer. In the case of the X40/TDNi and the chromized/carburized/TDNiCr combinations, the outward constituent diffusion apparently exceeded the inward diffusion, thereby producing extensive void formation. With the other combinations the interdiffusion appeared to be in balance.

One significant aspect of the elevated temperature exposure was the formation of a band of recrystallized grains in the substrate, 75-125 μM wide below the barrier layer. These recrystallized columnar grains appeared to originate in grain boundaries at the depth of 75-125 μM and grow outward toward the substrate/barrier interface. In the recrystallization and growth process the thoria was swept into the grain boundaries, as evidenced by the thorium spikes obtained on the electron microprobe traces and the segregated and depleted areas noted in the EM scans.

Analysis of elemental diffusion from the barrier layer by microprobe analysis was conducted in an attempt to identify which if any one element(s) was initiating recrystallization. Probe traces of chromium and molybdenum revealed elemental diffusion into TDNi to depths of 350-500 μM (Figures 26, 27, and 34) and of molybdenum into TDNiCr to a depth of 400 μM (Figure 30, 31, and 36). The diffusion of tungsten was significantly less, approximately 250 μM, which would be due, in part, to its lower concentration level in the barrier layer. This appears to be a minor factor, since there was no appreciable difference between the specimens with the Hastelloy C-1 barrier containing 10% W and the Hastelloy C-2 barrier containing 5% W. Similarly, the higher concentration of molybdenum in the Hastelloy C-2 (27% versus 17% in the Hastelloy C-1) did not appear to influence the extent of diffusion. Also, the diffusion of these elements into TDNi and TDNiCr was equivalent. Since both molybdenum and tungsten diffusion were well beyond the recrystallization zone, it is not likely that they triggered the recrystallization.

A remaining possibility is aluminum, though there is little support for this approach. The level of aluminum diffusion through the barrier layer into the substrate was very low, of the order of 1-2%. This level of aluminum appeared to extend past the recrystallization zone, Figures 24 and 28.

Consequently, from the data accumulated to date, there is no definitive evidence that the recrystallization is due to diffusion of any specific constituents in the barrier layer or from the aluminide covercoat. Further study is needed to identify the cause of recrystallization.

Hardness surveys reflected the influence of barrier constituent diffusion into the substrate. The coating process had little effect on the hardness of TDNi, as did the 1533° K (2300° F) exposure with the X40 barrier. In the latter case, the gross void formation at the barrier/substrate interface would have influenced the extent of diffusion. In contrast, after the 1533° K (2300° F) exposure, both the AVCO-deposited Hastelloy C-1 and C-2 barriers increased the hardness to a depth of 400-500 μM, while the Metco-deposited Hastelloy C-1 raised the hardness to the very core of the specimen.

The results on TDNiCr were not as definitive because the as-received material varied considerably in hardness, 265-329 Vickers. In most cases the hardness dropped in the first 125 μM (except for the as-processed Metco gun-sprayed Hastelloy C-1, which had no effect, and the as-processed AVCO gun-sprayed Hastelloy C-2, which increased hardness approximately 50 points Vickers). The largest reductions in hardness were experienced by the as-processed and exposed panels with the X40 barrier layers, ranging from 83 points in the first 125 μM to 56 at the core. Correlation of hardness values with mechanical properties has not been determined for TDNi and TDNiCr. The influence of processing and exposure on mechanical properties is covered in Task II.

Expansion compatibility of the barrier materials with the substrates was demonstrated by deflection and expansion measurements. The coefficient of expansion of X40 is very close to that of both TDNi and TDNiCr, actually lying halfway between. The expansions of Hastelloy C-1 and C-2 are both lower than either substrate, with the C-1 barrier closer than the C-2. These differences were reflected in the degree of permanent deflection that occurred in processing the panels and after exposure. From an expansion viewpoint, the X40 barrier is most compatible with either TDNi or TDNiCr with Hastelloy C-1 second.

3.2 Task II - Preliminary Oxidation Testing

3.2.1 Materials

Aluminum-Rich Compounds - Three heats of aluminum-rich compounds based on the stoichiometric compositions for Cr_5Al_8, $MoAl_2$, and CoAl were melted in the laboratory facilities and attributed to powder in the 3-5 μM range. Chemical analyses of these heats were as follows:

		w/o
Cr_5Al_8 -	Cr	- 54.0
	Al	- 45.0
CoAl -	Co	- 70.4
	Al	- 30.8
$MoAl_2$ -	Mo	- 62.0
	Al	- 37.3

Tensile Specimens - Sixteen TDNi and twenty TDNiCr tensile specimens were machined in the transverse direction from the materials described in Section 3.1.1.1. The specimens were 2.54X15.2 cm (1 inch X 6 inches) with a 7.6-cm (3-inch) reduced section and a 5.08-cm (2-inch) gage length. Specimen edges were radiused a minimum of 0.08 cm (1/32 inch).

3.2.2 Test Facility

One of the M&PTL flame tunnels was modified for the 1422°K (2100° F) test to accommodate the sheet tensile specimens as shown in Figure 39. Fixturing was provided to hold six specimens. The specimens were heated by a ring of eight Selas burners using an air/natural gas mixture for combustion. Velocity of the effluent was of the order of 0.05 Mach. The heat zone of the tunnel was adjusted so that a temperature of 1422° ± 11° K (2100° ± 25° F) was maintained over the reduced sections of the specimens. Tunnel temperature was monitored by thermocouple downstream from the specimens. Specimen temperature was read with an Ircon infrared pyrometer. An Ircon reading of the thermocouple was also taken periodically as a check.

3.2.3 Aluminum-Rich Compound Studies

3.2.3.1 Chemical Analysis

The analyses of the three aluminum-rich compound heats are reported in Section 3.2.1. All three compounds were very close to the stoichiometric composition. A comparison with the stoichiometric composition for these compounds follows:

		Composition, %	
Compound	Element	Stoichiometric	Actual
Cr_5Al_8	Cr	54.7	54.0
	Al	45.3	45.0
CoAl	Co	68.7	70.4
	Al	31.4	30.8
$MoAl_2$	Mo	64.2	61.9
	Al	36.0	37.3

3.2.3.2 X-Ray Diffraction Analysis

Samples of the individual heats were submitted for x-ray diffraction to identify the crystallographic structure. For the CoAl material, a definitive identification of the CoAl phase was obtained. The material prepared to the $MoAl_2$ composition showed a $MoAl_3$ dominant phase and a number of unidentified diffraction lines. There is no index card of d-spacings available for $MoAl_2$, and there is some doubt as to its existence as a stable phase[10]. When first examined, the material prepared to the Cr_5Al_8 composition contained no conclusively identifiable phases. An additional analysis was made after an homogenization heat treatment of 16 hours at 1116° K (1550° F), but no change in results was obtained. A subsequent heat treatment at 1366° K (2000° F) for 10 hours was more successful. A comparison of these results with the standard index card is presented in Table VI. The ASTM index card is based on a chromium-aluminum alloy containing 54.65% Cr which is very close to the composition of the M&PTL alloy (54.0% Cr). The card identifies this compound tentatively as Cr_3Al_5 rather than Cr_5Al_8. There appears to be good agreement as to d-spacings and corresponding intensities for the major lines. However, several of the standard d-spacings are missing from the M&PTL-prepared compound (namely 1.77 and 1.53), though the 1.512 and 1.504 spacings which are missing from the index may correspond to the latter. On the other hand, the M&PTL compound shows several d-spacings (2.34, 2.156, and 2.141) which do not appear on the index card. It should be pointed out that the data on the ASTM index card are based on very limited results and that the M&PTL compound may actually be Cr_5Al_8. Also, the data on the index card are derived using molybdenum radiation, whereas the M&PTL results were obtained with chromium radiation which is more discriminating.

3.2.3.3 Oxidation Testing-Bulk Material

Samples of the compounds in bulk- or coarse-particle form were placed in crucibles and exposed at 1366° K (2000° F) for 113 hours for a quick determination of oxidation behavior. Both the Cr_5Al_8 and CoAl indicated excellent oxidation resistance with the formation of tightly adherent scales and no evidence of scale growth (see Figure 40, left and center). On the other hand, the molybdenum-aluminum alloy failed catastrophically (Figure 40, right), the total material converting to oxide.

This catastrophic behavior led to an immediate coating run in which molybdenum-aluminum alloy particles were embedded in an aluminide coating. After a brief exposure [23 hours at 1394° K (2050° F) in air], considerable loose scale had formed on the surface and gross attack had occurred in localized areas, see Figure 41.

These unsatisfactory results were discussed with the NASA Project Manager with a recommendation that further work with the molybdenum-aluminum alloy be dropped. Based on the evidence presented, the NASA Project Manager concurred with the recommendation. The program was modified accordingly by substituting additional barrier layer combinations described in a subsequent section.

3.2.3.4 Particle Embedment Studies

In the particle embedment study, the initial efforts involved all three aluminum-rich compounds. The same application technique was used for the embedment of Al_2O_3 particles as in the General Electric NC11-A process. This method involves the spray application of a slurry consisting of fine particles in a carrier of acetone and nicrobraze cement to a thickness of approximately 250 μM. During the subsequent aluminiding step, the particles become embedded.

Various modifications were tried to ensure embedment of the aluminum-rich particles. The most successful approach was the formulation of a slurry using 4-6 parts of the alloy powder to one part of CaO. By this method a particle volume fraction of about 10% was obtained in the outer coating layer. Embedment was confirmed by electron microprobe scans showing the presence of Mo, Co, and Cr respectively for the three compounds, Figure 42. Metallographic evidence of embedded CoAl and Cr_5Al_8 particles and for Al_2O_3 in the NC11-A coating is presented in Figure 43.

One problem arose with the Cr_5Al_8 powder. When oven dried after the attriting operation, it tended to ignite. Extreme care was needed to produce powder without burning.

3.2.4 Coating Combination Selection

In the barrier layer diffusion studies, Section 3.1, void formation was minimized with the Hastelloy C-1 and C-2 barriers on TDNi and with Hastelloy C-1, C-2, and X40 on TDNiCr. Both the X40 and Hastelloy C-1 barrier were more compatible in matching the expansion of the substrates than the C-2. A total of 36 tensile specimens was coated using the more promising combinations of barrier and substrate. Because the $MoAl_2$ proved unsatisfactory as a particle embedment material, its application to eight of the specimens was dropped with the approval of the NASA Project Manager, and other combinations were substituted in its place. As a result, the following combinations were prepared.

Substrate	Barrier	Covercoat	No. of Specimens
TDNi	Hastelloy C-1	NC11-A	4
TDNi	Hastelloy C-1	Cr_5Al_8	4
TDNi	Hastelloy C-1	CoAl	4
TDNiCr	Hastelloy C-1	NC11-A	4
TDNiCr	Hastelloy C-1	Cr_5Al_8	4
TDNiCr	Hastelloy C-1	CoAl	4
TDNi	Hastelloy C-2	NC11-A	2
TDNi	Hastelloy C-2	Cr_5Al_8	2
TDNiCr	X40	NC11-A	4
TDNiCr	X40	Cr_5Al_8	4

Half of these specimens were exposed to cyclic oxidation at 1422° K (2100° F) and then tensile tested at room temperatures and 1422° K (2100° F) along with the as-processed ones.

3.2.5 Tensile Specimen Preparation

The 36 tensile specimens were divided into three groups, (I) 12 of TDNiCr, (II) 12 of TDNi, and (III) 8 of TDNiCr and 4 of TDNi. For the application of the barrier layers, the Metco gun and spray parameters were used because of the cleaner and denser deposits obtained under Task I. To assure uniformity of deposits, the spraying operation was automated except for coating of the specimen edges which were sprayed first. After grit blasting the surfaces and edges, the specimens as a group were stacked together so that the edges were all sprayed at one time. This prevented overheating the edges during spraying. The specimens then were mounted horizontally on a fixture, and the best of the barrier layer was applied with the gun traversing the specimen horizontally. A coating thickness of 125-150 μM was built up by successive overlapping passes. Earlier attempts to rotate the specimens during spraying produced a spiralling effect because of the high traversing speed that was needed to prevent overheating of the specimens and resulted in uneven deposits.

Following the spraying operation, the specimens from each group were given a diffusion heat treatment in dry hydrogen. Group I, TDNiCr, was processed at 1477° K (2200° F) for two hours in a sand-sealed retort. However, the specimens were still partially discolored with an oxide film from the spraying operation. A subsequent treatment at 1422° K (2100° F) for six hours was needed to reduce the oxide film. Groups II and III were diffusion heated in a special hydrogen atmosphere furnace at 1477° K (2200° F) for six hours which effectively removed all the oxide film, leaving a bright clean surface. The specimen faces were then hand ground and the edges sanded preparatory to the application of the aluminide coatings. The results of the barrier layer application and subsequent grinding are presented in Table VII.

The aluminide coating application was by the duplex process to ensure a maximum of embedded particles. This consisted of two 4-hour coating runs at 1324° K (1925° F). For the duplex process, the pack consisted of 10% high-activity aluminum alloy powder and 90% Al_2O_3 filler with an activator level at 0.1%. As in Task I, the specimens were suspended above the pack so that the coating was effected by the gaseous vapors. The slurry application for Al_2O_3 particle embedment was the same as described in Task I, Section 3.1.2.3. The Cr_5Al_8 and CoAl slurries consisted of one part CaO to six parts of Cr_5Al_8 or CoAl powder with equal additions of Nicrobraze cement and acetone for proper spraying consistency. The results of the aluminiding operation are presented in Table VII.

3.2.6 1422° K (2100° F) Cyclic Oxidation Testing

The oxidation test cycles consisted of a 1-hour exposure at 1422° K (2100° F) followed by an air blast that cooled the specimens to approximately 533° K (500° F) in 80 seconds and a reheat to 1422° K (2100° F) in 120 seconds. Three 300-hour tests were scheduled to be run on the following specimens.

Group	Substrate	Coating Combination	No. of Specimens
I	TDNiCr	NC11-A/Hastelloy C-1	2
		Cr_5Al_8/Hastelloy C-1	2
		CoAl/Hastelloy C-1	2
II	TDNi	NC11-A/Hastelloy C-1	2
		Cr_5Al_8/Hastelloy C-1	2
		CoAl/Hastelloy C-1	2
III	TDNiCr	NC11-A/X40	2
	TDNiCr	Cr_5Al_8/X40	2
	TDNi	NC11-A/Hastelloy C-2	1
	TDNi	Cr_5Al_8/Hastelloy C-2	1

The six specimens from each group were mounted in the rotating fixture as shown in Figure 39. During the initial stages of the testing the specimens were weighed at approximately 25-hour intervals and at longer intervals as the test proceeded. The specimens were photographed each time they were weighed. The tunnel temperature was monitored by a control thermocouple positioned 2.54 cm (1 inch) downstream from the rotating fixture at an elevation approximately at the center of the specimens. Specimen temperature was read several times daily with an Ircon pyrometer. Periodically, an Ircon reading of the thermocouple was also taken as a check. Several complete temperature surveys of specimens were made to determine specimen temperature variation. Typical surveys from the third test are presented in Figure 44.

Testing of Groups I and II was terminated after 200 hours and 145 hours, respectively, due to coating failure. Only the TDNiCr specimens from Group III with the NC11-A/X40 and Cr_5Al_8/X40 coating combinations completed the 300-hour test.

Cumulative weight change data are compiled in Tables VIII, IX, and X with a commentary on coating behavior. Coating failure generally initiated at the specimen edges which tended to overtemperature during the heat-up portion of the cycle. These areas were particularly vulnerable because of the difficulty in applying a dense uniform barrier layer to such a thin section by plasma deposition (in particular, the radiused area of the edge).

In the first test of the coated TDNiCr specimens, Table VIII, both specimens with the CoAl particles in the coating failed before 200 hours (one after 50 hours and the other after 158 hours). One specimen of each of the other two systems (NCl1-A and Cr_5Al_8) failed after 200 hours, at which point the test was terminated. The other two specimens had weight changes of -0.7 and +2.4 mg/cm^2, respectively. Figure 45 shows the failure of the CoAl specimen after 50 hours and the edge spalling of the Cr_5Al_8 and NCl1-A specimens. The condition of the specimens after 158 hours (when the second CoAl specimen was removed) and after 200 hours (when the test was terminated) is shown in Figure 46. Note the severe edge spalling of one of the NCl1-A specimens and the initiation of edge spalling on one of the Cr_5Al_8 specimens. However, the flat surface areas appeared to be intact and still providing protection to the substrates.

In the second test of the coated TDNi specimens, Table IX, a premature failure of one of the CoAl specimens resulted in its corrosion products contaminating the NCl1-A coatings after 100 hours of testing, Figure 47. The corresponding positions of the specimens are shown in Figure 48. The other CoAl specimen and both Cr_5Al_8 specimens were unaffected except for a small local attack at the edge of one Cr_5Al_8 specimen in the center of the reduced section. It was necessary to withdraw the CoAl and both NCl1-A specimens before proceeding with the test. These were replaced with spare Cr_5Al_8 and NCl1-A specimens plus a bare TDNi specimen. Because of rapid weight loss on one of the two original Cr_5Al_8 specimens and the remaining CoAl specimens, the test was discontinued at 145 hours, Figure 49.

The third test, which included both coated TDNi and TDNiCr specimens, Table X, was the only one that completed the full 300 hours. However, only the NCl1-A/X40 and the Cr_5Al_8/X40 combinations on TDNiCr completed the test with weight changes under the 3 mg/cm^2 weight loss criterion. Both of the TDNi specimens with the Hastelloy C-2 barrier failed earlier, the NCl1-A failed after 175 hours, and the Cr_5Al_8 failed after 150 hours (Figure 50). After 300 hours there was no visual evidence of coating failure on one of the Cr_5Al_8/X40 coated TDNiCr specimens (Figure 51, top) and only slight spalling on one edge of the other. However, weight losses of 1.05 and 0.67 mg/cm^2 were sustained. On the other hand, the two NCl1-A/X40 specimens (Figure 51, bottom) showed attack of about 60% of one edge on one and only slight attack on the other. The edge conditions are shown more clearly in Figure 52. Note that one of the NCl1-A/X40 specimens is bent. This resulted from a failure of the test fixture between 96 and 124 hours of testing. The deformation of the specimen did not cause damage to the coating and did not appear to affect the coating performance in subsequent testing. The latter specimens showed little weight change in testing; weight change was still positive at the conclusion of the test 1.0 and 1.06 mg/cm^2.

3.2.7 Evaluation

3.2.7.1 Metallographic Examination

Group I Specimens - TDNiCr

As-processed specimens are shown metallographically in Figure 53 and the exposed specimens in Figures 54 and 55. In the as-processed condition a line

of voids is evident at the barrier/substrate interface on all specimens. These voids originated from the coalescence of voids present at the interface from the spraying operation and voids within the as-sprayed deposit. However, this void level is excessive in comparison with that obtained in prior studies and may be due to the high traversing rates needed for the automated spraying setup. In subsequent oxidation testing these voids had a detrimental effect by promoting spalling of the coatings. Particle embedment in the outer coating layer was particularly heavy in the NC11-A specimen, Figure 53, top. Sections at higher magnifications, showing the level of embedded particles for these three systems, are presented in Figure 43. The quality of the other two coatings, Cr_5Al_8 and CoAl, is definitely poorer than that of the NC11-A, Figure 53, center and bottom. It appears that in many areas the aluminum-rich particles conglomerated during the slurry application and became entrapped as clusters rather than as discrete particles during the coating process. These loosely formed clusters apparently were removed in polishing, leaving numerous voids.

After 200 hours of exposure at 1422° K (2100° F) considerable attack was evident in the Al_2O_3 particle-free areas of the outer coating layer of the NC11-A coating, Figure 54, top. Scattered small voids were present throughout the barrier layer and for a short distance (25-50 μM) into the substrate. The line of intermittent voids observed at the barrier/substrate interface in the as-processed condition (Figure 53, top) was not noted.

The Cr_5Al_8 specimen (Figure 54, bottom) after the same exposure showed gross attack of the outer coating layer with fingers of oxide penetrating into the apparent void areas noted in Figure 53, center. Still, the attack appears to be restricted to the outer coating layer. The line of intermittent voids observed in Figure 53, center, is also evident in this specimen. Scattered small voids are present in the substrate to a depth of ~ 50 μM.

The very poor performance of the CoAl specimen after 50 hours at 1422° K (2100° F) is reflected in the microstructure, Figure 55. Virtually all of the outer coating layer was converted to oxide, and there was minor attack of the inner diffusion zone. This specimen also showed the intermittent line of voids at the barrier/substrate interface.

Group II Specimens - TDNi

The oxidation-tested specimens are shown in Figures 56 and 57. Figure 56, top, presents the NC11-A coating after 100 hours at 1422° K (2100° F) from the side of the specimen that was not contaminated by the corrosion products from the premature failure of the CoAl specimen. Again, there was considerable attack of the Al_2O_3 particle-free areas of the outer coating layer. Pronounced void formation occurred in the substrate to a depth of 50-75 μM below the barrier/substrate interface. Gross attack was evident in the outer coating layer of the CoAl specimen after the same exposure period, Figure 56, bottom. Extensive void formation was also apparent in the same area of the substrate noted above with the NC11-A coating. Both of these areas show evidence of the same grain recrystallization and growth and thoria segregation observed under Section 3.1.3.1, Task I.

The Cr_5Al_8 specimen after 145 hours of 1422° K (2100° F) oxidation showed nearly complete degradation of the outer coating layer, Figure 57. The same void formation in the substrate was observed as with the other two coatings.

Group III Specimens

The Group III specimens in the as-processed condition are shown in Figure 58. All coating combinations showed evidence of grain recrystallization and growth in the substrate just below the interface and a minor pullout of these grains. Some voids were still present from the spraying operation. The grain recrystallization is shown more clearly at higher magnification in Figure 59 for the X40 barriers on TDNiCr.

The 1422° K (2100° F)/300-hour exposures resulted in various degrees of attack and structural changes on the TDNiCr specimens, Figure 60. Several sections of the Cr_5Al_8 specimen are shown in Figure 60, top; a typical NC11-A specimen is shown in Figure 60, bottom. Figure 60, top left, shows only minor coating attack and scattered voids whereas very extensive void formation (possible grain pullout) is indicated in Figure 60, top right. On the NC11-A specimen, Figure 60, bottom, coating attack is intermittent and void formation (grain pullout) fairly extensive.

On the other hand, the Cr_5Al_8 coating over the Hastelloy C-2 barrier on TDNi was nearly totally degraded in 150 hours (Figure 61, top left); and, there was more extensive attack of the NC11-A coating in 175 hours than was observed after 300 hours on the NC11-A/X40/TDNiCr specimen (Figure 61, top right). Grain growth and pullout are very evident in these photographs. A failed area of the NC11-A coating on TDNi is shown in Figure 61, bottom.

3.2.7.2 Electron Microprobe Analysis

Electron microprobe scans and traces were run on all the coating combinations, both as-processed and after the 1422° K (2100° F) exposure. As mentioned under Section 3.1.3.2 Task I, the scans are not shown in this report because of reproduction difficulties. Of the traces only those have been reproduced for the specimens which completed the 1422° K (2100° F) 300-hour test (Figures 62 through 69) are discussed in detail.

NC11-A/X40/TDNiCr

Aluminum: As-processed, the aluminum content varied from 15-35% in the outer coating layer, Figure 62, left. A sharp drop in the aluminum level occurred in the inner diffusion zone where segregated areas of Co, Cr, and W are found. Aluminum diffusion at a 2% level extended into the substrate a minimum distance of 150 μM. After the 1422° K (2100° F) exposure, Figure 62, right, the surface aluminum dropped to about 2% with 25% and 35% peaks within the coating. (The low aluminum may actually represent a void area at the surface, and the first aluminum peak may represent the actual surface.) Aluminum concentration of 2-2.5% extended a minimum of 200 μM into the substrate.

Nickel: Figure 63, left, shows that nickel diffusion from the substrate raised the nickel concentration in the barrier layer from about 10% as deposited to a high of 34% for an average of 25%. After the 1422° K (2100° F)/300-hour exposure (Figure 63, right), the nickel level increased above 50% except for the first 25 M of coating.

Cobalt: In the as-processed condition (Figure 64) the cobalt level dropped from 56% to about 35%, the difference being accounted for by diffusion into the substrate to a depth exceeding 100 M. 1422° K (2100° F) exposure further lowered the Co level in the coating to 25% and extended the diffusion into the substrate over 150 M, Figure 65.

Chromium: As-processed, the chromium concentration in the outer coating layer dropped from about 10% at the interface to 1% at the surface, Figure 64. Fluctuations in the chromium concentration in the barrier layer indicate chromium segregation. After exposure, Figure 65, the chromium in the coating leveled off at 15%. The Cr peak near the surface is probably Cr_2O_3 particles in the scale.

Tungsten: In the as-processed condition, the tungsten concentration (Figure 64) appears low in comparison with the 8% level in the as-deposited material. During processing, tungsten diffused into the substrate 50 M. The 1422° K (2100° F) exposure specimen, Figure 65, showed a tungsten content more comparable with that deposited. The level in the barrier layer dropped to 5%, and tungsten diffused to a depth of 225 M.

Cr_5Al_8/X40/TDNiCr

Aluminum: Appreciably higher aluminum levels were found in the as-processed condition (Figure 66, left) in comparison with the NC11-A coating (Figure 62). After the 1422° K (2100° F) exposure (Figure 66, right), the still higher aluminum concentration reflected the conversion of the first 25 M to oxide Figure 60, top Diffusion into the substrate, in either case, was limited to 150-200 M.

Nickel: Nickel behavior in the as-processed condition (Figure 67, left) was also appreciably different than on the NC11-A specimen. Much less nickel diffused into the X40 barrier. After exposure, the behavior was more comparable, (Figure 67, right). The two sharp dips in the nickel level coincided with voids i the barrier layer.

Cobalt: Cobalt behavior was essentially the same for the as-processed specimen (Figure 68) as it was for the NC11-A/X40 specimen. However, the exposed specimen, Figure 69, was radically different. A major loss of cobalt occurred; the maximum Co concentration dropped to 15%.

Chromium: The same behavior was noted with chromium, in that the as-processe specimen (Figure 68) showed the same pattern as the NC11-A coating, but the exposed specimen (Figure 69) showed grossly segregated areas in the coating and barrier layer.

Tungsten: The tungsten level in the as-processed condition was more comparable with that of the as-deposit barrier layer, Figure 68. After the 1422° K (2100° F) exposure (Figure 69), the level of residual tungsten indicated that a major portion of the tungsten had been lost.

3.2.7.3 X-Ray Diffraction Analysis

X-ray diffraction analysis was conducted on the coating combinations that completed the 1422° K (2100° F)/300-hour oxidation test. The results are compiled in Table XI.

NC11-A/X40/TDNiCr

In the as-processed condition the predominant phases present were α Al_2O_3 and CoAl. The CoAl phase could also be partially NiAl, since the microprobe traces indicated appreciable nickel diffusion into the X40 barrier layer. The ASTM indexes for CoAl and NiAl are nearly identical. Several additional lines of low intensity were recorded that could not be identified. After the 1422° K (2100° F)/300-hour exposure, only α Al_2O_3 and a γ face-centered cubic phase were identified. The latter is the γ phase detected in nickel-base superalloys. Again, several low intensity lines were recorded that could not be identified.

Cr_5Al_8/X40/TDNiCr

The only phases positively identified in the as-processed condition were α Al_2O_3, CoAl, and Cr. Al_2O_3 would be present due to some oxidation of the Cr_5Al_8 powder when attrited to 3-5 μM size and subsequently dried. (See Section 3.2.3.4.) The predominant phase was CoAl. The chromium indication is probably the chromium-aluminum solid solution which can contain up to 25% Al. The d-spacing for the strongest line, 110, was 2.042 Å compared with the standard line of 2.039 Å. Other weak lines corresponded to some of the lines found in the pattern for Cr_5Al_8, but other stronger lines for that compound were not present. (See Section 3.2.3.2). One can conclude that the entrapped Cr_5Al_8 particles observed metallographically were altered in composition during the coating process and no longer were Cr_5Al_8.

Subsequent exposure at 1422° K (2100° F) for 300 hours resulted in the same phases detected for the exposed NC11-A/X40 specimen, α Al_2O_3 and γ. Again, there were several weak lines that defied identification.

3.2.7.4 Mechanical Property Testing

Tensile testing at room temperature and at 1422° K (2100° F) were conducted on specimens from each group (Tables XII, XIII, and XIV). Specimens were tested in the as-processed condition and after exposure. Uncoated specimens were also tested to provide baseline data. Strength values for the coated specimens are based on the original cross section.

Group I - TDNiCr (Table XII)

In the as-coated condition at room temperature, all three coatings exhibited a slight drop in ultimate strength and a loss in ductility compared with that of the as-received material. Yield strength was unaffected. At 1422° K (2100° F), the coatings had no significant effect on any of the properties. After 1422° K (2100° F) oxidation testing, the room temperature ultimate strengths were very close to that of the as-received material, and the yield strengths were slightly higher. The 1422° K (2100° F) exposure did not change the ductility from that of the as-coated condition. Testing at 1422° K (2100° F) resulted in a slight increase in ultimate strength, but no effect on yield or ductility.

Group II - TDNi (Table XIII)

For this group of specimens the coating process had no effect on ultimate strength, but increased the yield strength by 15-20% in testing at room temperature. However, ductility was lowered by 50%. Testing at 1422° K (2100° F) showed no significant difference in properties between the coated and uncoated specimens. The 1422° K (2100° F) exposure had little effect on the room temperature properties except for some loss in yield strength. The exposure also did not degrade the 1422° K (2100° F) properties.

Group III - TDNi and TDNiCr (Table XIV)

The Group III TDNiCr specimens with the X40 barrier showed the least effect of coating on the room temperature tensile properties, both as-processed and after the 1422° K (2100° F)/300-hour exposure. Only the elongation was reduced from 17% to between 9-10%. None of the tensile properties were degraded at 1422° K (2100° F) for the specimens, either as-coated or after the extended 1422° K (2100° F) exposure.

The data on TDNi were very limited since only one specimen of each coating was available for the two test temperatures in the as-processed and exposed conditions. However, these limited results indicated no appreciable effect on the properties.

3.2.8 Discussion and Coating Selection

The influence of the Hastelloy C-1 and C-2 barrier layers on void formation was significantly different in the 1422° K (2100° F) oxidation test compared with the 1533° K (2300° F) exposure in argon. Whereas in the latter test neither barrier showed a tendency for void formation with either the TDNi or TDNiCr substrates, both produced voids in the cyclic oxidation test. This is difficult to understand since the extent of diffusion of barrier layer constituents in the substrates was greater in the 1533° K (2300° F) exposure.

Three factors may be responsible. Part of the problem may be in the sensitivity of these materials to metallographic preparation. In the as-processed condition there was evidence of grain recrystallization and growth in the substrate in a band 75 - 100 μM wide below the barrier layers. These recrystallized grains appeared to be devoid of thoria particles which were found to be concentrated at the grain boundaries. Probably as a result of this condition, grains were sometimes pulled out during normal polishing operations. In this regard the TDNi material appears to be more sensitive than the TDNiCr. Secondly, it should be pointed out that the bonding achieved in the fully automated spraying setup was not as good as that produced by the semiautomatic setup used in the preparation of panels for the 1533° K (2300° F) test. As a result, more residual voids from the spraying operation were present in the former case. A third factor may be the difference in expansion coefficients of the barriers compared with the substrates. Both of the barriers have lower expansions, which would induce stresses during the cycling of the specimens in the oxidation test, whereas there was no cycling in the 1533° K (2300° F) test.

With the X40 barrier on TDNiCr, the void formation was not as pronounced as with the Hastelloy barriers. Again, the voids in this case may be a polishing artifact (compare Figure 60, top left, with Figure 60, top right - two sections from the same Cr_5Al_8/X40 specimen). Similar evidence can be seen in the as-processed condition in Figures 58 and 59.

A major consideration is whether or not this recrystallized structure with grain boundary thoria is detrimental to the mechanical properties. Since this total affected area (200 μM for both sides) represents approximately 12% of the cross section, one would anticipate a lowering of the strength properties. This was not the case as shown in Section 3.2.7.4. In some combinations the strength has actually increased. Another consideration would be separation of the coating in the recrystallized area due to cycling. Again, there was no evidence of this occurring with either of the X40 combinations.

Though aluminide covercoats over the X40 barrier sustained considerable attack, the oxide scale that was formed did adhere very tenaciously to the surface, and there was no evidence of coating loss except along the edge of one of the NC11-A specimens. The NC11-A covercoat was more resistant to oxidation than the aluminide coating with the Cr_5Al_8 dispersoids, although the latter held its oxide very tenaciously. Actually, there was no evidence that

the Cr_5Al_8 particles existed as such after the duplex processing cycle. In essenc the aluminum-reservoir concept did not materialize in practice as expected. With the NC11-A covercoat, the attack was predominantly in those areas that were devoid of Al_2O_3 particles. A more uniform distribution of these particles apparently would lead to better oxidation resistance. It is significant that during the 300-hour test this coating combination had a maximum weight gain under 2 mg/cm^2; and, at the completion, the gain was still of the order of 1 mg/cm^2.

Though the coatings (as processed or after exposure) did not significantly affect the strength properties, they did (in some cases) affect ductility. Processing lowered the room temperature ductility of both TDNi and TDNiCr by approximately 50%. Subsequent exposure at 1422° K (2100° F) did not have any further effect. On the other hand, at 1422° K (2100° F) as-coated TDNi had greater ductility than the uncoated material, while TDNiCr showed no significant effect. Extended exposure at 1422° K (2100° F) produced no change from the as-received materials.

From the above evidence, it is apparent that two coating/barrier combinations (NC11-A/X40 and Cr_5Al_8/X40) on TDNiCr warrant further testing. Of the two, the NC11-A/X40 coating appeared to be the better.

However, for better coating performance improved techniques for applying the barrier layer are needed so that a denser deposit of more-uniform quality is achieved. Composite coatings have been successfully deposited by physical vapor deposition (PVD). Particularly the FeCrAlY, CoCrAlY and NiCrAlY type materials. The latter materials have demonstrated exceptional high temperature properties. Successful application of the X40 barrier layer by this technique would also warrant a reevaluation of one of the Hastelloy C modifications (preferably C-1) on either TDNi or TDNiCr in combination with the NC11-A covercoat. On this basis the following coating combinations were selected for evaluation in Task III:

Coating	Substrate
PVD X40 Barrier + NC11-A Aluminide	TDNiCr
PVD Hastelloy C-1 Barrier + NC11-A Aluminide	TDNiCr
PVD Hastelloy C-1 Barrier + NC11-A Aluminide	TDNi

At this point recent advances had been made on a in-house developed PVD NiCrAlY type coating that had demonstrated exceptional performance on TDNiCr. Thus an excellent opportunity was provided to compare the performance of aluminide vs PVD type coatings. It was recommended to the project manager that the fourth coating be the in-house NiCrAlY coating. The selection of this coating received NASA approval.

3.3 TASK III - ADVANCED TESTING

As discussed in section 3.2.8, a change in the method of applying the barrier layer coatings was proposed to produce a denser and more uniform barrier layer than was produced by plasma spraying. This was to be achieved by physical vapor deposition. Feed bars of X40 and the Hastelloy C-1 and C-2 compositions were prepared and the barrier coatings were applied in the laboratory vapor coater. However, the composition of the deposited layer deviated markedly from that of the feed bars as described in Section 3.3.2.3. Consequently, it was necessary to drop this approach and revert to the thermal spray technique, but to use better application methods. One of these methods was with the Union Carbide detonation-gun that can produce deposits with a density of 95 - 98 percent of theoretical compared with ~ 90 percent for the plasma deposited layers produced in Task I and Task II. The X40 material was selected to be deposited by this method. For the application of the Hastelloy C-1 material an improved plasma spray technique was utilized. This involved a new design of nozzle which produced a higher velocity plasma and a correspondingly higher density of the spray deposit. Accordingly, the modified program included the following coating combinations:

Coating	Substrate
Detonation-gun Deposited X40 Barrier + NC11-A Aluminide	TDNiCr
High Velocity Plasma Deposited Hastelloy C-1 Barrier + NC11-A Aluminide	TDNiCr
High Velocity Plasma Deposited Hastelloy C-1 Barrier + NC11-A Aluminide	TDNi
Physical Vapor Deposition NiCrAlY	TDNiCr

These coatings were applied to both tensile specimens and erosion bars. The tensile specimens were to be oxidation tested at 1533° K (2300° F) for 100 hours, cycling to room temperature once per hour; and, the erosion bars were to be oxidation tested on a Mach 1 burner rig at 1422° K (2100° F) for 500 hours and at 1477° K (2200° F) for 100 hours, also cycling once per hour. After exposure, the tensile specimens were to be rupture tested at room temperature, 1422° K (2100° F), and 1533° K (2300° F).

3.3.1 MATERIALS

3.3.1.1 Test Specimens

The test specimens for this phase of the investigation were of two types: (1) tensile, and (2) oxidation/erosion wedges. The tensile specimens were fabricated from sheet material of the same heats of TDNi and TDNiCr used in Tasks I and II. Specimen length was transverse to the rolling direction. Modification was made to the standard specification configuration to facilitate application of the vapor-deposited coating (as shown in Figure 70a) and the sprayed barrier layer coatings (as shown in Figure 70b). The tag end extension in Figure 70a served to mount the specimen in the holding fixture during the vapor-coating operation. The tag was removed after subsequent heat treatment and prior to exposure testing. For the barrier layer coating specimens, Figure 70b, the grip holes were not drilled prior to coating application and subsequent exposure testing; these were drilled prior to tensile testing.

Material for the oxidation/erosion bars was procured from Fansteel, Inc. in the form of 0.71 cm (0.280 inch) plate. Compositions were as follows:

Material	Heat Number	Composition, Weight Percent				
		C	S	Cr	ThO2	Ni
TDNiCr	3699	0.02	0.0035	19.87	2.12	Balance
TDNi	3746	0.01	0.0023	---	2.25	Balance

It should be pointed out that material of this section size does not have the same structure and mechanical properties as the 0.0152 cm (0.060 inch) sheet material used for the tensile specimens. Test pieces were machined in accordance with NASA drawing CB301680, Figure 71, except that surface finish was 10 to 15 RMS.

3.3.1.2 Barrier Layer Powders

X40 powder (Stellite 31) from the same lot used in Tasks I and II (No. 2546) was applied as the barrier layer in Task III. Particle size was 20 to 45 microns. New Hastelloy C-1 powder of the following composition was obtained from Alloy Metals, Inc., Troy, Michigan:

Element	Weight Percent
Chromium	15.87
Tungsten	11.51
Molybdenum	11.29
Silicon	0.35
Nickel	Balance

The powder was screened and only the 20 to 45 micron range material was used.

3.3.2 COATING APPLICATION

3.3.2.1 Barrier Layer Systems

3.3.2.1.1 Cobalt-Base Alloy X40, Detonation-Gun Process

The X40 barrier layer on both the TD Nichrome oxidation/erosion bars and the tensile specimens was applied by the detonation-gun process at the Union Carbide plant in Indianapolis, Indiana. Spraying parameters were proprietary with Union Carbide. Coating thickness varied from 0.0075 to 0.0127 cm (0.003 to 0.005 inch). The as-sprayed finish ranged between 150 and 200 RMS. The as-sprayed coating structure is shown at the bottom of Figure 72.

3.3.2.1.2 Hastelloy C-1, Thermal-Spray Process

The Hastelloy C-1 barrier layer was applied to TD Nickel and TD Nichrome oxidation/erosion bars and tensile specimens by the plasma-spray process at General Electric's Material & Process Technology Laboratories. Powder size was in the 20 to 45-micron range. The plasma unit was a Metco 3M with a special high velocity nozzle. Spray parameters were as follows:

Nozzle	-	GP
Powder Port	-	No. 2
Argon	-	0.69 MPa/4670 liters H (0.1 ksi/165 CFH)
Helium	-	0.69 MPa/141 liters H (0.1 ksi/5 CFH)
Amps	-	500
Volts	-	50
Powder Feed Rate	-	3.18 K/hr (7 lbs/hr)
Spray Distance	-	7.5 cm (3.0 inches)
Deposition	-	0.005 cm/pass (0.002 inch)
Coating Thickness	-	0.0075 to 0.0127 cm (0.003 to 0.005 inch)

The as-sprayed finish was 125 to 150 RMS. The as-sprayed coating structure is shown at the top of Figure 72.

3.3.2.2 NC11A Aluminide Covercoat

Prior to the application of the NC11A aluminide coating, the barrier layer deposits were heat treated in dry hydrogen [at a dew point of 211° K (-80° F) or lower] at 1366° K (2000° F) for a period of four hours. The purpose of this heat treatment was to diffusion bond the barrier layer to the substrate and to effect some reduction of the oxides produced during spraying. The latter objective applied more to the Hastelloy C-1 coating than to the X40 coating. Coatings deposited by the detonation-gun process are inherently cleaner than those by the plasma process when sprayed in air. Following heat treatment, the coatings were hand polished to provide a smoother surface.

Application of the NC11A coating was the same as described in Tasks I and II. Briefly, the process consisted of the following:

Pack composition	-	10% CODEP B, balance Al_2O_3
Slurry coating	-	2-micron Al_2O_3
Pack atmosphere	-	Hydrogen, 211° K (-80° F) or better, entering
Specimen position	-	Above pack
Cycle	-	1353° K (1975° F)/4 hours
Number of cycles	-	Two

Weight gains were measured on selected specimens. Results were as follows:

Specimen	Barrier/Coating	Weight Gain, mg/cm^2
TDNiCr	X40/NC11A	4.15/3.88
TDNiCr	Hastelloy C-1/NC11A	8.61/8.77
TDNi	Hastelloy C-1/NC11A	9.09/8.18

Typical as-processed coatings are shown in Figure 73.

3.3.2.3 Physical Vapor Deposition

3.3.2.3.1 Barrier Layer Coating

The original intent under Task III was to vapor deposit the barrier layers so that (in comparison with thermal spraying) cleaner, denser, and more homogeneous deposits would be obtained. For this purpose, feedbars of the following compositions were processed:

Element	Ingot Weight Percent	
	X40	Hastelloy C-1
Nickel	15.8	54.60
Chromium	20.6	16.13
Tungsten	8.2	11.1
Molybdenum	---	17.8
Cobalt	54.3	---
Iron	1.1	---
Carbon	0.38	---

The PVD coatings were applied to test specimens using processing parameters developed for nickel- and cobalt-based alloys. The PVD process was conducted in the GE-M&PTL apparatus which utilizes electron beam melting of the feedbar. A vacuum of 10^{-4} torr was maintained in the vapor coater.

Analyses of the PVD coatings revealed compositions that were widely divergent from the feedbar compositions. As shown in Table XV, very little or none of the tungsten was transported during the physical vapor deposition of the X40 material; the same condition existed with tungsten and molybdenum for the Hastelloy C-1. Also, there was considerable variation from run to run. The use of the PVD technique had been based on consultations with personnel at Battelle Memorial Institute (BMI) regarding the feasibility of vapor depositing coatings with high refractory metal contents. Work with pure and alloyed refractory metals had been performed at BMI using electron beam melting equipment with a 17 KW power rating. Little difficulty was anticipated with the higher powered GE-M&PTL facility. In this technique nonequilibrium evaporation is employed to limit fractionation.

The inability to transfer tungsten or molybdenum under nonequilibrium conditions led to a critical review of the process. Analysis of refractory metal vapor pressures showed that, with the vacuum level maintained in the system, a pool temperature in excess of 4033° K (5000° F) would be needed to volatilize tungsten and a somewhat lower temperature for molybdenum. Under such conditions, both the nickel and chromium (in the case of Hastelloy C-1) and the cobalt and chromium (in the case of X40) would volatilize at prodigious rates so that the desired steady-state evaporation was extremely difficult (if not impossible) to maintain. On that basis, it was recommended that this approach be abandoned, and that the thermal spray technique be used for application of the barrier layers. The NASA Project Manager concurred with this recommendation. It was agreed that the X40 powder would be deposited by the detonation-gun process at Union Carbide, and that the Hastelloy C-1 powder would be deposited by an improved (high velocity) plasma spray process.

3.3.2.3.2 NiCrAlY Coating

The NiCrAlY coating was deposited using a vacuum of 10^{-4} torr. Coating thickness varied from 0.0076 to 0.0125 cm (0.003 to 0.005 inch). Processed coatings were then heat treated in vacuum at 1366° K (2000° F) for four hours. The coating structure is shown in Figure 74. Coating composition is proprietary to General Electric.

3.3.3 TEST FACILITIES

3.3.3.1 High Velocity Burner Rig

Two overall views and one closeup of the high velocity burner rig (modeled after the NASA facility) are presented in Figure 75. The rig is located in a soundproofed test cell. Specimens are heated by the combustion of pressurized JP-4 fuel and air through a converging-diverging nozzle designed to produce Mach 1 gas velocity. This hot-gas stream impinges upon rotating specimens, which approach within 2.54 cm (1.0 inch) of a 5.7 cm (2.25 inch) long nozzle duct. For this test, the specimens were rotated at 350 rpm, a typical value for most testing. Eight specimens at a time are held in the test fixture, which has a diametral distance from specimen center to specimen center of about 7.6 cm (3 inches). Figure 76 shows the test fixture with one oxidation/erosion specimen in position.

The rig can be placed on automatic control and cycled at programmed intervals. Cycling is achieved by the test fixture dropping from the "up" position in the hot-gas stream to the "down" position in a blast of ambient air. The specimen fixture drops in a fraction of a second into the air blast where it is held for about 1½ minutes and where the specimens are cooled to below 370° K (200° F). It is then returned to the "up" position where approximately 30-45 seconds are required to bring the specimens up to test temperature. Fixture rotation is always maintained during cycling. The cycling time is not counted as part of the total test time at test temperature.

The specimen metal temperature is obtained by three independent sources. These are thermocouple, Ircon (automatic pyrometer), and optical pyrometer. A chromel/Alumel thermocouple inserted into a specimen is used to indicate the "real" temperature and as a standard for obtaining the proper fuel and air flows. The thermocouple is inserted into the specimen through a 0.20 cm (0.080 inch) hole drilled to a depth corresponding to the test area hot zone as shown in Figure 77. At least one specimen is thermocoupled.

The design of the test fixture's thermocouple slip ring necessitated the use of a chromel/Alumel thermocouple rather than Pt-Pt/Rh, since the lower EMF of the Pt-Pt/Rh at test temperatures around 1422° K (2100° F) is not within the sensitivity of the slip ring. At the temperatures used in these tests [1422° K (2100° F) and 1477° K (2200° F)], it was necessary to make frequent thermocouple changes to maintain accurate readings. Once temperature was established, the Ircon was "locked in" to monitor operation. Any change in combustion causing a temperature change was compensated for by the Ircon control. The Ircon temperature usually read some constant value lower than the internal thermocouple. A tripod-mounted, precision micro-optical pyrometer (sighted through a window in the test cell upon a mirror reflection of the specimens) was used to obtain periodic temperature checks. For test temperatures of 1422° K (2100° F) to 1477° K (2200° F), a 55° K (100° F) temperature correction factor must be added to the optical reading to compensate for transmission losses.

The temperature of the individual specimens is assumed to be the same regardless of variation in specimen emissivities and conductivities. Heat transfer for the specimens is by convection, and specimen rotation is rapid enough to minimize heat loss when the specimens are at the maximum distance from the nozzle. Heat loss by conduction through the test fixture is assumed to be the same for all specimens. Simultaneous thermocouple checks of several different specimens have indicated no significant differences in temperature.

An "annunciator" control panel is located outside the test cell. Any significant change in a control setting will cause the rig to shut down and to light up the annunciator panel. Combustion air pressure, atomizing air pressure, main air line pressure, rear and front combustion liner temperatures, flame signal, downstream temperature, test cell toxicity levels, and other functions are monitored.

3.3.3.2 1533° K (2300° F)/100-Hour Cyclic Oxidation Test

Originally, the facility for conducting the 1533° K (2300° F)/100-hour cyclic oxidation test was to have been a radiant heater capable of producing a net heat flux at rated voltage of 40 watts/cm^2 and a total power of 12 KW. However, difficulties were experienced in achieving the rated power. Instead, a Hevi-Duty Lindberg Furnace with a 1644° K (2500° F) temperature capability was used. A high temperature ceramic heater element support plate, designed for 1644° K (2500° F) operation, was used to support the coated tensile specimens in a vertical position. Because of the close spacing of the heater element slots, all 16 specimens could be tested at one time. The furnace was calibrated by potentiometer for 1533° K (2300° F) operation. Repeat checks during the test indicated a temperature variation of 1533° K ± 14° K (2300° F ± 25° F). Specimens were held at temperature for one hour and then removed from the furnace. They were allowed to cool to room temperature before replacing them in the furnace. Heat-up time was approximately 20 minutes. The specimens were weighed after 5, 10, 20, 25, 35, 40, 50, 60, 70, 80, and 100 hours of exposure. Photographs were taken of all specimens that failed in less than five hours and of all specimens that survived after 5, 10, 20, 40, 60, 80, and 100 hours.

3.3.4 TEST RESULTS

3.3.4.1 1422° K (2100° F) Mach 1 Burner Rig Test

3.3.4.1.1 Visual Examination and Weight Change

In the 1422° K (2100° F) Mach 1 burner rig test, there were four TD Nichrome specimens, one TD Nickel specimen, and three X40 dummy specimens to fill the remaining three stations in the test fixture. The TD Nichrome specimen coatings consisted of: 1) NiCrAlY, 2) X40/NC11A, 3) Hastelloy C-1/NC11A, and 4) uncoated. The latter specimen was drilled and contained the thermocouple for calibrating temperature. The TD Nickel specimen had the Hastelloy C-1/NC11A coating. The specimens prior to test are shown at the top of Figure 78. Specimens were weighed and photographed after 46, 118, 284, and 350 hours of testing.

The test was terminated after 350 hours of the scheduled 500 hours due to the failure of one of the specimens in fatigue and localized failure of all the other coatings. Cumulative weight change data are presented in Table XVI and shown graphically in Figure 79. At 46 hours, the X40-barrier/NC11A-coated specimen fractured in the slotted area where it was clamped in the fixture and was replaced with a new specimen. The condition of the specimens after 46 hours is shown at the bottom of Figure 78. Modifications were made in the holding fixture to improve the clamping arrangement before testing resumed. After 118 hours, examination revealed that the NiCrAlY-coated specimen and several dummy specimens had worked their way partially out of the holding fixture slots and had rubbed against an end cap which enclosed the tip sections of the specimens. As a result, the NiCrAlY-coated specimen lost by abrasion a portion of its leading edge in an area extending approximately 2.5 cm (1.0 inch) down from the tip. Weight of

material removed was projected to be 0.873 gram, based on the weight loss of 0.026 gram which the specimen had experienced after 46 hours.

After 118 hours, the Hastelloy C-1-barrier/NC11A-coated TDNi specimen showed coating distress on the trailing edge portion and some minor damage on the leading edge, Figure 80. A weight loss of 1.768 grams indicated coating failure.

After 196 hours, a major portion of the coating was lost from the Hastelloy C-1-barrier/NC11A-coated TDNi specimen. Consequently, the specimen was removed from test. On the Hastelloy C-1-barrier/NC11A-coated TDNiCr specimen, spalling was evident on the leading edge with penetration to the substrate on the very edge. Both the X40 barrier/NC11A (second specimen) and NiCrAlY coatings were still intact, Figure 81.

After 284 hours, the Hastelloy C-1 barrier/NC11A coating on TDNiCr spalled further, exposing the substrate at the leading and trailing edges. Spalling of the coating on the X40 barrier/NC11A TDNiCr specimen* also had occurred, penetrating to the substrate in local areas of the leading and trailing edges. On the NiCrAlY-coated specimen, coating degradation had initiated; but, penetration to the substrate was not apparent, Figure 82.

At 326 hours the NiCrAlY-coated TDNiCr specimen failed in fatigue, but the test did not terminate until 350 hours of operation (the test was run over the weekend between 284 and 350 hours). At this point all the specimens showed significant loss of coating at the leading and trailing edges. The uncoated TDNiCr specimen, which was instrumented to monitor test temperature, sustained a 4.651-gram or 3.91% weight loss. This compares with a weight loss of 1.150 grams or 0.90% for the NiCrAlY-coated TDNiCr. The X40-barrier/NC11A-coated TDNiCr was next best with a loss of 1.709 grams or 1.38%. However, the latter specimen was exposed for 46 fewer hours than the bare TDNiCr. The condition of these specimens at the conclusion of the test is shown in Figure 83.

3.3.4.1.2 Metallographic Examination

X40/NC11A/TDNiCr

The X40/NC11A-coated TDNiCr specimen which failed in fatigue after 46 hours is shown in Figure 84. The coating is still intact, though oxidation is evident in all sections. The greatest degree at attack is at the corners of the trailing edge section (Figure 84, bottom), where there has been a considerable reduction in coating thickness. It would appear that temperature at the trailing edge was higher than at the leading edge. All sections show intermittent scale or voids at the coating substrate interface. The as-coated specimens also showed a similar condition indicating that application of the barrier layer needs to be improved.

* Actual test time was 238 hours, replacement specimen.

The coating on the X40/NC11A specimen which was a replacement at 46 hours, and was exposed for the remaining 304 hours of testing, degraded completely at the leading and trailing edge sections, Figure 85. No coating remained on the leading edge from the tip back 0.30 cm (0.120 inch). There were intermittent patches of residual coating along the side faces of the specimen (Figure 85, center) from the balance of the leading edge to approximately the center of the specimen. The rear half of the hot zone area showed severe attack of the substrate. It should be noted that the only area where the coating was still present corresponded to the location of the internal thermocouple on the instrumented specimen used for direct temperature readout.

The mechanism of coating failure essentially was the same as that observed in the low velocity 1422° K (2100° F) flame tunnel testing of the X40/NC11A coating under Task II, Section 3.2.7. Oxidation of the outer coating layer is accelerated as the aluminum level is depleted. Concurrently, grain recrystallization and void formation progress in the substrate just below the barrier layer/substrate interface, leading (eventually) to spallation of the coating. However, both grain recrystallization and void formation apparently progressed at a slower rate in these erosion specimens machined from plate material than in the tensile specimens in Task II which were machined from sheet. This would be expected due to the increased amount of working of the latter material.

NiCrAlY/TDNiCr

Some coating degradation had been observed after 284 hours of testing. After 326 hours, coating failure was complete at the leading and trailing edges (Figure 86) but was still intact along the side faces. Coating loss on the leading edge extended 0.20 cm (0.080 inch) back from the tip of the leading edge. On the trailing edge, the entire back face coating was lost, and coating loss continued along the side faces for approximately 0.25 cm (0.10 inch). On the balance of the wedge section of the leading edge and along the side faces, the coating was still intact (Figure 86, center), though oxidation spikes generally penetrated to two-thirds of the coating thickness. Coating loss at the tip of the leading edge and at the trailing edge appears to be associated more with complete oxidation attack rather than erosion or spalling due to higher temperatures in these areas. In the section corresponding to the internal thermocouple readout, there was still residual intact coating.

Hastelloy C-1/NC11A/TDNiCr and Hastelloy C-1/NC11A/TDNi

No coating remained in the hot zone section of either the Hastelloy C-1/NC11A/TDNiCr specimen which was on test for the entire 350 hours (but had shown visual coating failure at 196 hours) or the Hastelloy C-1/NC11A/TDNi specimen which failed after 118 hours (but was not removed until 196 hours). However, examination of sections below the hot zone section [where temperatures were approximately 100° K (180° F) lower] offered clues to the failure mechanism. At the leading and trailing edges, oxidation attack and void formation were similar to that observed in the 1422° K (2100° F) low

velocity flame tunnel test in Task II [See Figure 54, top and Figure 56, top]. Coating loss would have been the result of a combination of outer coating layer oxidation and coating spallation due to the extensive void formation at the barrier-layer/substrate interface.

Uncoated TDNiCr

For comparative purposes, the extent of material loss to the uncoated TDNiCr specimen after 350 hours at exposure is shown in Figure 87 for the leading and trailing edge sections. Note the significant increase in radius of curvature of the leading edge and the corner of the trailing edge in comparison with similar sections in Figure 84.

3.3.4.2 1477° K (2200° F) Mach 1 Burner Rig Test

3.3.4.2.1 Visual Examination and Weight Change

The 1477° K (2200° F) burner rig test consisted of four coated TDNiCr specimens and four X40 dummy specimens. The coated TDNi specimen which had been prepared for this test was not included in the initial setup because of the poor performance of the Hastelloy C-1/NC11A-coated TDNi specimen in the 1422° K (2100° F) test. Of the four TDNiCr specimens, two were X40/NC11A-coated, one was Hastelloy C-1/NC11A, and one was NiCrAlY coated. The latter specimen was drilled and instrumented to calibrate the test temperature.

After 20 hours of testing, the Hastelloy C-1/NC11A-coated TDNiCr specimen was removed because of a small localized area of attack in the hot zone section. Weight loss was less than 0.3 mg/cm^2. Testing continued with the remaining specimens until 36 hours, when one of the X40/NC11A-coated specimens failed due to fatigue in the dovetail slot section. Visually, the coating was still intact.

The failed specimen was replaced with an X40 dummy, and the test continued for another two hours at which time the rotating fixture jammed due to overheating. The rotating fixture stopped with one of the X40 dummy specimens positioned directly in front of the burner. This stoppage triggered the interlock mechanism that immediately cut off the fuel supply. However, there was sufficient fuel remaining in the lines to continue burning just long enough to melt the X40 dummy specimen, thereby causing molten droplets to splatter on some of the other specimens; the NiCrAlY-coated specimen received the most splatter. When the specimens were removed at this point for weighing, the second X40/NC11A specimen broke in the slotted section on removal. Figure 88 shows the condition of the Hastelloy C-1/NC11A-coated specimen which was removed after 20 hours, the fatigue-failed X40/NC11A specimen, and the two remaining specimens after 38 hours. The darkened area on the lower view of the NiCrAlY-coated specimen is splatter from the melted X40 dummy specimen.

Though only the NiCrAlY-coated specimen remained intact, the decision was made to continue with the test and to fill one of the positions with the Hastelloy C-1/NC11A-coated TDNiCr specimen which had been removed after

20 hours. Weight loss on this specimen had been less than 0.3 mg/cm^2. In addition, the unused Hastelloy C-1/NC11A-coated TDNi specimen replaced one of the failed X40/NC11A specimens. After an additional 32 hours of test time, the TDNi specimen also failed in fatigue. Testing continued until 100 hours had been accumulated on the NiCrAlY-coated specimen and 82 hours had been accumulated on the Hastelloy C-1/NC11A-coated specimen. The condition of the specimens after the conclusion of the test are shown in Figure 89. Cumulative weight changes are compiled in Table XVII. From Figure 89, it is evident that the trailing edge experienced higher temperatures than the leading edge based on the extent of coating attack.

3.3.4.2.2 Metallographic Examination

Metallographic sections were prepared from the hot-zone area of each coating/substrate combination and are shown in Figures 90 through 93.

Hastelloy C-1/NC11A/TDNi

After 32 hours of exposure at 1477° K (2200° F), the leading edge sections showed some coating degradation and void formation in the substrate in the region adjacent to the barrier-layer/substrate interface, Figure 90, top. In local areas some oxide penetration to the interface had occurred. Lesser attack is evident on the side faces (Figure 90, center), and there is no void formation in the substrate. However, at the trailing edge (Figure 90, bottom) there was coating failure and attack into the substrate at both corners, indicating higher trailing-edge than leading-edge temperatures.

Hastelloy C-1/NC11A/TDNiCr

After 82 hours of exposure at 1477° K (2200° F), the coating spalled at the very tip of the leading edge, extending back approximately 0.10 cm (0.040 inch) (Figure 91, top). The residual coating in this area shows extensive oxidation of the barrier layer material and clearly indicates the mechanism of coating failure. Along the side faces (Figure 91, center) the coating is still protective, though coating degradation has progressed to a considerable extent. The most severe attack was at the trailing edge (Figure 91, bottom) where the coating spalled on the back face, and coating loss extended approximately 0.25 cm (0.100 inch) along the side faces. The extensive coating loss at the trailing edge further confirms higher trailing-edge than leading-edge temperatures.

X40/NC11A/TDNiCr

Due to mechanical fatigue failure, this coating combination experienced only 36 hours of 1477° K (2200° F) exposure. Though the coating experienced varying degrees of oxidation attack, Figure 92, it essentially was still intact and providing protection to the substrate. Again, the most severe attack was at the trailing edge where oxidation extended into the X40 barrier layer. There are numerous areas below the barrier-layer/substrate interface where grain recrystallization is evident. Some limited void formation also is present.

NiCrAlY/TDNiCr

The only specimen to complete 100 hours at 1477° K (2200° F) showed localized attack of the coating at the leading edge (Figure 93, top) with several points of penetration into the substrate. Most of the coating showed little attack. Along the side faces the attack was limited to intermittent oxide spikes along grain boundaries that penetrated into the substrate. Attack was most severe at the trailing edge (Figure 93, bottom) where the deepest penetration into the substrate occurred. The least attack took place in the section where the internal thermocouple was located. This section most closely represented the 1477° K (2200° F) test temperature.

3.3.4.3 1533° K (2300° F) Static Oxidation Test

3.3.4.3.1 Visual Examination and Weight Change

The four sets of coated tensile specimens exposed in the 1533° K (2300° F) static oxidation test are shown in Figures 94 and 95. Cumulative weight changes during the 100-hour test are compiled in Table XVIII and shown graphically for the two best coatings in Figure 96. The Hastelloy C-1/NC11A coating failed in five hours or less on both the TDNi and TDNiCr, and the X40/NC11A coating on TDNiCr failed in four hours on two specimens, Figures 97 and 98. Most of these failures were due to sections of coating spalling from the grip ends of the specimens. In most cases the reduced section remained intact. All four of the NiCrAlY-coated TDNiCr specimens and two of the X40/NC11A-coated TDNiCr specimens continued past the 5-hour period. After 40 hours, one of the NiCrAlY-coated specimens and one of the X40/NC11A-coated specimens failed, Figure 99. A second NiCrAlY-coated specimen failed after 80 hours, and the two remaining NiCrAlY-coated specimens and one of the X40/NC11A-coated specimens completed the 100-hour test, Figure 100.

3.3.4.3.2 Metallographic Examination

Metallographic sections were prepared for each coating system from the reduced section of the tensile specimens. Where applicable, photomicrographs were taken of both intact and failed coating areas.

Hastelloy C-1/NC11A/TDNi 1533° K (2300° F)/5 Hours

Metallographic examination was made of the Hastelloy C-1/NC11A specimen with the longest exposure time, 5 hours. This specimen had failed in the grip areas, but the coating was intact in the reduced section from which the metallographic specimen was prepared. Isolated attack of the outer coating layer has occurred (Figure 101, top), and there is no evidence of void formation at the coating/substrate interface. The barrier layer coating is well bonded to the substrate.

Hastelloy C-1/NC11A/TDNiCr, 1533° K (2300° F)/4 Hours

The coating in the reduced section showed both intact and failed areas. Figure 101,center, shows a heavily attacked outer coating layer, but the coating is still protective to the substrate. Figure 101,bottom, represents a failed area where the coating has spalled and the substrate has been attacked.

X40/NC11A/TDNiCr, 1533° K (2300° F)/4 Hours

Metallographic examination was made from one of the blistered specimens shown in Figure 98. Figure 102,top, presents an area where considerable degradation of the coating has occurred and oxide penetration to the substrate is imminent. A section through a blister is shown in Figure 102, bottom. Oxidation attack into the substrate has taken place.

X40/NC11A/TDNiCr, 1533° K (2300° F)/100 Hours

Two metallographic sections are shown, Figure 103, top and bottom. The former represents an area where the coating has been severely attached but is still protective to the substrate. In the latter, the coating attack is more severe with local areas of oxide penetration into the substrate. Recrystallization is present in the region below the coating, and void formation is evident in many areas.

NiCrAlY/TDNiCr, 1533° K (2300° F)/80 Hours and 1533° K (2300° F)/100 Hours

Metallographic sections after 80 and 100 hours of exposure both show grain boundary attack of the NiCrAlY coating and intermittent void formation at the coating/substrate interface. Two views of the 80-hour specimen are shown in Figure 104,left. The top photomicrograph represents the grain boundary type of attack and several local areas where the attack has accelerated. The bottom photomicrograph demonstrates the void formation at the interface. Failure mechanism is predominately grain boundary attack followed by a lateral attack into the grain.

After 100 hours of exposure, attack of the coating is somewhat more severe (Figure 104,right). Also, both views show intermittent void formation at the interface. Oxide penetration into the substrate had initiated at several points.

3.3.4.4 Tensile Test Results

Tensile testing was conducted to determine the effect of 1533° K (2300° F) exposure on the mechanical properties of TDNi and TDNiCr. Specimens were tested in the as-coated condition and after exposure at 1533° K (2300° F) for various times depending on coating life. Testing was at room temperature, 1422° K (2100° F), and 1533° K (2300° F). Results are compiled in Table XIX.

Testing at room temperature after exposure at 1533° K (2300° F) showed that the NiCrAlY on TDNiCr lowered both the ultimate and 0.2% yield strengths about 10% and reduced the elongation about 20%. The X40/NC11A coating apparently did not affect the strength properties but reduced the elongation about 25%. On the other hand, the Hastelloy C-1/NC11A coating lowered tensile strength between 15 and 25% and the 0.2% yield strength approximately 10%. The most severe effect was on the elongation which was reduced about 80%.

1422° K (2100° F) testing of the as-coated specimens yielded ultimate and 0.2% yield strength results that were slightly higher than the as-received material. Elongation also was greater for the coated TDNi specimens (4.1% vs. 2.8%) and for two of the three coated TDNiCr specimens (1.6 and 2.3% vs. 0.9%).

Testing at 1422° K (2100° F) after prior exposure at 1533° K (2300° F) produced higher tensile values for both TDNi and TDNiCr, compared with unexposed TDNi and TDNiCr, except for the Hastelloy C-1/NC11A-coated TDNiCr which had a lower tensile but higher yield strength. Moreover, this is only a single datum point and may be due to an error in testing. Elongation for both coated materials was higher. In this test only the NiCrAlY-coated specimen had appreciable exposure at 1533° K (2300° F), 80 hours versus 4 to 5 hours for the other specimens. Still, the results show little significant differences.

1533° K (2300° F) testing after 1533° K (2300° F) exposure showed little difference in the strength properties of Hastelloy C-1/NC11A-coated TDNi, Hastelloy C-1/NC11A-coated TDNiCr, and X40/NC11A-coated TDNiCr, though the latter specimen was exposed for 100 hours; whereas, the former specimens experienced only 4 and 2 hours, respectively. The NiCrAlY-coated TDNiCr specimens (both of which had 100-hour exposures) had slightly higher tensile values, but significantly lower elongation.

4.0 DISCUSSION

The barrier layer/aluminide coating concept which was the basis for this investigation to provide an improved coating for TDNi and TDNiCr was not successfully demonstrated. The in-house-developed NiCrAlY vapor-deposited coating, introduced in Task III of the program which was for comparative purposes, also fell short of the desired goals for life at 1422°K (2100°F) and 1477°K (2200°F). The least successful coating combinations were those with the plasma-sprayed Hastelloy C-1 barrier layers. Many specimens failed prematurely because of local coating separation due to poor bonding of the barrier layer to the substrate. With TDNi, void formation on exposure also played a role in coating loss. This condition was most evident in the 1477°K (2200°F) burner rig test, where the specimen failed in fatigue after 32 hours (Figure 21). The coating was intact at the leading edge and along the flats, but failed locally at the trailing edge. Void formation is particularly evident at the leading edge and, in all probability, contributed to the spalling of the coating at the trailing edge. Consequently, it can be concluded that the Hastelloy C-1 barrier approach holds little promise in a combination coating over either TDNi or TDNiCr.

The X40 barrier which was applied by the detonation-gun process was more successful than the Hastelloy C-1. This may have been due to several factors: (1) the coating as deposited is less porous; (2) it is more compatible with the substrate; and, (3) the aluminide coating produced is more oxidation resistant than the one formed over Hastelloy C-1. The erratic behavior of the coating in the 1533°K (2300°F) static oxidation test, where two specimens failed in less than four hours due to blistering and two specimens survived 40 and 100 hours of testing, is not understood. The former were the only specimens that exhibited this failure pattern, indicating the presence of some contaminant. The coating did demonstrate approximately 150 hours of life on the 1422°K (2100°F) burner rig test, but received only limited testing at 1477°K (2200°F) due to mechanical failure. In the latter test, it was still intact after 36 hours though some areas had experienced some degradation. Still the X40 barrier has some limited potential for 1422° to 1477°K (2100° to 2200°F) Mach 1 application. Diffusion of X40 constituents into the substrate apparently promote grain recrystallization and void formation which ultimately are detrimental to coating adherence.

The NiCrAlY coating proved to be the best of the systems tested, but its performance also failed to meet the program goal. In the 1422°K (2100°F) burner rig test it began to fail after 284 hours and in the 1477°K (2200°F) testing it began to fail after 100 hours. Coating behavior was different in the two tests. At 1422°K (2100° F) the degradation of the coating was primarily frontal (Figure 86); at 1477° K (2200°F) the attack was preferentially along the grain boundaries which were oriented perpendicular to the substrate (Figure 93). Also, single boundaries extended from the surface to the substrate. This appears to be a limiting feature with the NiCrAlY coating. Its potential would be greatly enhanced if a fine-grained rather

than coarse-grained coating could be produced and retained at high temperatures. This is an area that warrants further investigation.

Several aspects of the burner rig test warrant further investigation. Based on the severity of attack, it was apparent that the trailing edge temperature was higher than the leading edge temperature. Also, attack was more severe at the tip of the leading edge than at the area where temperature readout was recorded with an internal thermocouple. Thus, there is a strong possibility that local temperatures on the test specimen were higher than the control temperature. A modification in specimen configuration may be necessary to more closely control specimen temperature.

Another feature of the test specimen that presented problems was the slot design for supporting the specimen in the rotating fixture. The testing of some of the coatings had to be terminated due to mechanical fatigue failure. Two specimens failed in the 1422° K (2100° F) test and two in the 1477° K (2200° F) test. Modifications were made to improve the design after the failures at 1422° K (2100° F). Still the problem persisted in the 1477° K (2200° F) test. These modifications included: (1) redesigning the clamping arrangement, (2) polishing the clamping area to a high finish to reduce notch sensitivity, and (3) improving the heat shielding to lower the temperature in the clamped section. A further modification in specimen design that is recommended is the reduction in overall specimen length.

With regard to the effect of coatings on tensile properties, only the room temperature properties were adversely affected. At 1422° K (2100° F), after exposure at 1533° K (2300° F), the properties were equivalent or better than as-received TDNi or TDNiCr tested at the same temperature. Tensile properties for uncoated TDNi and TDNiCr exposed and tested at 1533° K (2300° F) were not available. However, the results obtained for the coated specimens fall within the range projected from 1422° K (2100° F) and 1477° K (2200° F) data.

5.0 CONCLUSIONS

1. The cobalt-base alloy, X40, and both Hastelloy C modifications, C-1 and C-2, proved to be somewhat effective barriers to the diffusion of aluminum into the TDNi and TDNiCr substrates.

2. Extensive diffusion of barrier layer constituents into the TDNi and TDNiCr substrates occurred in the 1533° K (2300° F) and 1422° K (2100° F) exposures. Diffusion was more pronounced at the higher temperature.

3. Grain recrystallization and growth occurred in a 75 - 100 μM wide band in the TDNi and TDNiCr substrates adjacent to the barrier layer. The recrystallized grains were thoria-depleted with thoria concentrated in the grain boundaries.

4. Application of the X40 barrier layer by the detonation-gun process resulted in denser coating of more uniform quality than the coating applied by plasma deposition.

5. Application of the barrier layer materials by physical vapor deposition was unsuccessful due to the inability to effect transfer of Mo and W from the feed bar to the coating.

6. The NiCrAlY coating on TDNiCr was far superior to X40/NC11A on TDNiCr or Hastelloy C-1/NC11A on either TDNi or TDNiCr.

7. At 1422° K (2100° F) under a Mach 1 gas stream, coating life for NiCrAlY was approximately 275 hours;at 1477°K (2200°F) coating life was approximately 100 hours. In the latter case, occasional oxide spikes had just penetrated into the substrate.

8. The Hastelloy C-1/NC11A coating on both TDNi and TDNiCr performed poorly, with Hastelloy C-1/NC11A/TDNi combination having the shorter life.

9. The X40/NC11A coating performance on TDNiCr was intermediate between the NiCrAlY and Hastelloy C-1/NC11A. Its behavior in static oxidation testing at 1533° K (2300° F) was erratic, with two specimens failing in less than five hours and two specimens completing 40 and 100 hours.

10. The best coating, NiCrAlY, falls short of the program goal of 500 hours at 1477°K (2200°F) and 1000 hours at 1422° K (2100°F), both at Mach 1.

11. All coatings reduced room temperature tensile properties after exposure at 1533° K (2300° F), but to varying degrees. The X40/NC11A coating lowered ductility only;the NiCrAlY reduced strengths about 10% and ductility 20%;and, the Hastelloy C-1/NC11A lowered strengths between 15 and 25% and ductility 80%.

12. 1422° K (2100° F) properties were slightly higher for the as-coated specimens than for the TDNi and TDNiCr specimens as received.

13. After 1533° K (2300° F) static exposure, 1422° K (2100° F) properties were also higher than the as-received material except for Hastelloy C-1/NC11A-coated TDNiCr, which showed a lower ultimate strength but a higher yield strength.

6.0 REFERENCES

1. Baker, I.R., Lambert, J.B., Monson, L.A., and Alexander, G.B., "Further Development of Coatings for Protection of Dispersion Strengthened Nickel from Oxidation." E.I. DuPont de Nemours & Co., AFML-TR-67-230, August 1967, Part I.

2. Neijedlik, J.F. and Gadd, J., "Further Development of Coatings for Protection of Dispersion Strengthened Nickel from Oxidation." TRW, Inc., AFML-TR-67-230, August 1967, Part II.

3. Sama, L., Lawthers, D.D., and Pepino, G.T., "Development of Ductile Cladding for TD Nickel Turbine Vane Application." Sylvania Electric Products, Inc., NASA Contract NAS3-10489, NASA Cr-72521, Dec. 1968.

4. Hill, V.L., Misra, S.K., and Wheaton, H.L., "Development of Ductile Claddings for Dispersion-Strengthened Nickel-base Alloys." IIT Research Institute, NASA Contract NAS3-10494, NASA Cr-72522.

5. Grisaffe, S.J., "Review of Some Current NASA-Lewis Sponsored Coating Research," NASA-Lewis Research Center. 17th Refractory Composites Working Group Meeting, June 1970.

6. Levinstein, M.A. and Stanley, J.R., "Improved Aluminide Coatings for Nickel-Base Alloys." General Electric Co. NASA Contract NAS3-11160, NASA Cr-72863, March 1971.

7. Yount, R.E., Kutchera, R.E., and Keller, D.L., "Development of Joining Techniques for TD Nickel." General Electric Co. Tech Report AFML-TR-66-137, May 1966.

8. "Joining Techniques for TD Nickel-Chromium." General Electric Co. AFML-TR-67-224, October 1967.

9. Killpatrick, D.H. and Young, J.D. - "Texture and Room Temperature Mechanical Properties of Dispersion Strengthened NiCr Alloys," Metallurgical Trans., Vol. I, April 1970, p.959-960.

10. Shunk, F.A., "Constitution of Binary Alloys," Second Supplement, McGraw-Hill Book Co., 1969, p.30.

11. L.A. Monson and W.I. Pollock, "Development of Coatings for Protection of Dispersion-Strengthened Nickel From Oxidation". AFML-TR-66-47, Part 1, March 1966, Air Force Materials Laboratory, Wright-Patterson Air Force Base.

12. J.V. Peck, "Development of Production Manufacturing Techniques for Application of Protective Coatings to Their Dispersion-Strengthened Alloys." IR-483-9(IV), Fourth Interim Technical Report, 1 Sept. 1970 - 30 Nov. 1970, TRW, Inc.

Table I. Barrier Layer Combinations.

Substrate	Barrier Layer
TDNi	Hastelloy C-1
TDNi	Hastelloy C-2
TDNi	X40 (Stellite No. 31)
TDNiCr	Hastelloy C-1
TDNiCr	Hastelloy C-2
TDNiCr	X40 (Stellite No. 31)
TDNiCr	Chromizing/Carburizing

Table II. Barrier Layer/NC11-A Coating Combinations.

Barrier Material	Powder Mesh Size	Plasma Gun	Substrate	Specimen Number
X40	-325, +20 μ	AVCO	TDNi	16a, 16b
X40	-325, +20 μ	AVCO	TDNiCr	17a, 17b
Hastelloy C-1a[1]	-325, +20 μ	AVCO	TDNi	26a, 26b
Hastelloy C-1a	-325, +20 μ	AVCO	TDNiCr	27a, 27b
Hastelloy C-1b	50% -325, +20 μ 50% -20 μ	AVCO	TDNi	28a, 28b
Hastelloy C-1b	50% -325, +20 μ 50% -20 μ	AVCO	TDNiCr	29a, 29b
Hastelloy C-1a	-325, +20 μ	Metco	TDNi	30a, 30b
Hastelloy C-1a	-325, +20 μ	Metco	TDNiCr	31a, 31b
Hastelloy C-1b	50% -325, +20 μ 50% -20 μ	Metco	TDNi	32a, 32b
Hastelloy C-1b	50% -325, +20 μ 50% -20 μ	Metco	TDNiCr	33a, 33b
Hastelloy C-2a[2]	-325, +20 μ	AVCO	TDNi	18a, 18b
Hastelloy C-2a	-325, +20 μ	AVCO	TDNiCr	19a, 19b
Hastelloy C-2b	50% -325, +20 μ 50% -20 μ	AVCO	TDNi	20a, 20b
Hastelloy C-2b	50% -325, +20 μ 50% - 20 μ	AVCO	TDNiCr	21a, 21b
Hastelloy C-2a	-325, +20 μ	Metco	TDNi	22a, 22b
Hastelloy C-2a	-325, +20 μ	Metco	TDNiCr	23a, 23b
Hastelloy C-2b	50% -325, +20 μ 50% -20 μ	Metco	TDNi	24a, 24b
Hastelloy C-2b	50% -325, +20 μ 50% - 20 μ	Metco	TDNiCr	25a, 25b
Chromize - 5 hrs Carburize - 1 hr	---	---	TDNiCr	NiCr5
Chromize - 20 hrs Carburize - 1 hr	---	---	TDNiCr	NiCr20

[1] Ni-55.4, Cr-16.0, Mo-17.0, W-10.6, Si-0.43 w/o

[2] Ni-50.4, Cr-17.0, Mo-27.5, W-4.8, Si-0.36 w/o

Table III. X-Ray Diffraction Analyses of Barrier Layer/NC11-A Coating Combinations.

Specimen	Substrate	Barrier	Plasma Gun	Condition	Indexed Phases
16a	TDNi	X40	AVCO	As-Processed	βCoAl, α Al_2O_3
18a	TDNi	Hast C-2a	AVCO	As-Processed	NiAl, α Al_2O_3
20a	TDNi	Hast C-2b	AVCO	As-Processed	NiAl, α Al_2O_3
22a	TDNi	Hast C-2a	Metco	As-Processed	NiAl, α Al_2O_3
24a	TDNi	Hast C-2b	Metco	As-Processed	NiAl, α Al_2O_3
26a	TDNi	Hast C-1a	AVCO	As-Processed	NiAl, α Al_2O_3
28a	TDNi	Hast C-1b	AVCO	As-Processed	NiAl, α Al_2O_3
30a	TDNi	Hast C-1a	Metco	As-Processed	NiAl, α Al_2O_3
32a	TDNi	Hast C-1b	Metco	As-Processed	NiAl, α Al_2O_3
NiCr20	TDNiCr	Cr(20)C	---	As-Processed	NiAl, α Al_2O_3
NiCr5	TDNiCr	Cr(5)C	---	As-Processed	NiAl, α Al_2O_3
17b	TDNiCr	X40	AVCO	Exposed	Co (Cubic)
NiCr20	TDNiCr	Cr(20)C	---	Exposed	γ, γ'(?),Cr_2O_3
NiCr5	TDNiCr	Cr(5)C	---	Exposed	γ, γ', Cr_2O_3
19b	TDNiCr	Hast C-2a	AVCO	Exposed	γ, γ', α Al_2O_3
21b	TDNiCr	Hast C-2b	AVCO	Exposed	γ, γ', α Al_2O_3
23b	TDNiCr	Hast C-2a	Metco	Exposed	γ, γ'(?), α Al_2O_3
25b	TDNiCr	Hast C-2b	Metco	Exposed	γ, γ'(?), α Al_2O_3
27b	TDNiCr	Hast C-1a	AVCO	Exposed	γ, γ'(?), α Al_2O_3
29b	TDNiCr	Hast C-1b	AVCO	Exposed	γ, γ'(?), α Al_2O_3
31b	TDNiCr	Hast C-1a	Metco	Exposed	γ, γ', α Al_2O_3
31b	TDNiCr	Hast C-1b	Metco	Exposed	γ, γ'(?), α Al_2O_3

Notes: (1) Hast C-2a -325/+20 μ powder
Hast C-2b 50% (-325/+20 μ) -50% (-20 μ) powder
Hast C-1a -325/+20 μ powder
Hast C-1b 50% (-325/+20 μ) -50% (-20 μ) powder
Cr(20)C Chromized 20 hours
Cr(5)C Chromized 5 hours

Table IV. Electron Microprobe Analyses of Barrier Layer/NC11-A Coating Combinations.

Substrate	Barrier/Gun	Condition	Elemental Traces	Figures
TDNiCr	X40/AVCO	As-Processed	Al	21
TDNiCr	X40/AVCO	Exposed	Al, Co, Cr, W, Th	21,22
TDNi	X40/AVCO	As-Processed	Co, W, Cr, Th	23
TDNi	Hastelloy C-1/AVCO	As-Processed	Al	24
TDNi	Hastelloy C-1/AVCO	Exposed	Al, Mo, W, Cr, Th	24,26
TDNi	Hastelloy C-1/Metco	Exposed	Al, Mo, W, Cr, Th	25,27
TDNiCr	Hastelloy C-1/Metco	As-Processed	Al	28
TDNiCr	Hastelloy C-1/Metco	Exposed	Al, Mo, W, Cr, Th	28,31
TDNiCr	Hastelloy C-1/AVCO	Exposed	Al, Mo, W, Cr, Th	30,29
TDNi	Hastelloy C-2/AVCO	As-Processed	Al, Mo, W, Cr, Th	32,33
TDNi	Hastelloy C-2/AVCO	Exposed	Al	32
TDNi	Hastelloy C-2/Metco	Exposed	Mo, W, Cr, Th	34
TDNiCr	Hastelloy C-2/AVCO	As-Processed	Al	35
TDNiCr	Hastelloy C-2/Metco	Exposed	Mo, W, Cr, Th	36

Table V. Hardness Surveys of Coated and Uncoated TDNi and TDNiCr.

(Square Diamond Indicator, Leitz, 50-gm Load)

Vickers Hardness (Converted)

Barrier/Substrate	Gun	Condition	Distance From Barrier Layer, mm					
			125	250	375	500	625	750
TDNi	---	As-Received	197	183	175	178	182	175
Hast C-1/TDNi	AVCO	As-Coated	169	168	188	175	172	171
Hast C-2/TDNi	AVCO	As-Coated	168	185	168	185	172	166
X40/TDNi	AVCO	Exposed	178	185	177	178	186	168
Hast C-1/TDNi	AVCO	Exposed	227	208	204	172	183	186
Hast C-1/TDNi	Metco	Exposed	277	251	218	227	199	204
Hast C-2/TDNi	AVCO	Exposed	218	249	221	190	186	188
TDNiCr	---	As-Received	329	277	319	265	310	299
X40/TDNiCr	AVCO	As-Coated	280	254	251	236	257	277
Hast C-1/TDNiCr	AVCO	As-Coated	293	260	274	280	299	268
Hast C-1/TDNiCr	Metco	As-Coated	321	293	299	277	262	262
Hast C-2/TDNiCr	AVCO	As-Coated	381	303	283	274	286	283
X40/TDNiCr	AVCO	Exposed	244	251	296	265	257	221
Hast C-1/TDNiCr	AVCO	Exposed	244	286	313	296	303	310
Hast C-1/TDNiCr	Metco	Exposed	306	325	299	306	289	296
Hast C-2/TDNiCr	AVCO	Exposed	303	293	325	299	303	306

Table VI. X-Ray Diffraction Pattern for Cr_5Al_8 Compound, Chromium Target Radiation.

Index d - Spacings	Observed d - Spacings	Index I/I_1	Observed I/I_1
3.67 A.V.	3.712 A.V.	20	30
2.60	2.613	10	11
---	2.34	---	10
---	2.156	---	100
---	2.141	---	85
2.132	2.132	100	94
---	1.958	---	6
1.91	1.928	40	15
---	1.873	---	8
1.84	1.849	40	12
1.77	---	10	---
1.53	---	40	---
---	1.512	---	14
---	1.504	---	13
1.46	1.471	10	10
1.33	1.33	40	11
1.30	1.30	60	28
1.27	1.274	20	13
1.24	1.247	20	29

Table VII. Thickness and Weight Gain Measurements of Coated TDNi and TDNiCr Tensile Specimens.

Specimen No.	Barrier Substrate	Coating Thickness, mm (Inch) As Sprayed	Coating Thickness, mm (Inch) After Grinding	Coating Thickness, mm (Inch) After Coating	Aluminiding Weight Gain mg/cm^2
C	TDNiCr/C-1/Cr_5Al_8	0.11 (.0045)	0.062 (.0025)	0.100 (.004)	9.1
D	TDNiCr/C-1/NC11-A	0.11 (.0045)	0.038 (.002)	0.085 (.0035)	8.5
E	TDNiCr/C-1/Cr_5Al_8	0.11 (.0045)	0.050 (.002)	0.085 (.0035)	8.8
F	TDNiCr/C-1/CoAl	0.125 (.005)	0.062 (.0025)	0.100 (.004)	10.2
G	TDNiCr/C-1/CoAl	0.100 (.004)	0.050 (.002)	0.085 (.0035)	10.5
I	TDNiCr/C-1/Cr_5Al_8	0.125 (.005)	0.062 (.0025)	0.100 (.004)	8.8
N	TDNiCr/X-40/Cr_5Al_8	0.075 (.003)	0.038 (.0015)	0.062 (.0025)	7.9
R	TDNiCr/X-40/Cr_5Al_8	0.125 (.005)	0.075 (.003)	0.100 (.004)	7.4
S	TDNiCr/X-40/NC11-A	0.125 (.005)	0.075 (.003)	0.100 (.004)	6.5
T	TDNiCr/X-40/NC11-A	0.137 (.0055)	0.085 (.0035)	0.11 (.0045)	6.4
2	TDNi/C-1/Cr_5Al_8	0.137 (.0055)	0.085 (.0035)	0.125 (.005)	10.5
4	TDNi/C-1/Cr_5Al_8	0.137 (.0055)	0.085 (.0035)	0.125 (.005)	10.1
5	TDNi/C-1/Cr_5Al_8	0.125 (.005)	0.075 (.003)	0.11 (.0045)	12.4
8	TDNi/C-1/CoAl	0.125 (.005)	0.075 (.003)	0.11 (.0045)	12.4
11	TDNi/C-1/CoAl	0.137 (.0055)	0.075 (.003)	0.11 (.0045)	10.9
12	TDNi/C-1/NC11-A	0.125 (.005)	0.075 (.003)	0.11 (.0045)	10.2
15	TDNi/C-1/NC11-A	0.150 (.006)	0.085 (.0035)	0.125 (.005)	10.2
16	TDNi/C-1/NC11-A	0.125 (.005)	0.075 (.003)	0.11 (.0045)	9.9
19	TDNi/C-2/Cr_5Al_8	0.150 (.006)	0.100 (.004)	0.137 (.0055)	14.0
20	TDNi/C-2/NC11-A	0.125 (.005)	0.075 (.003)	0.11 (.0045)	11.8

Table VIII. Cumulative Weight Changes of Coated TDNiCr Specimens at 1422° K (2100° F) in Test No. 1, Hastelloy C-1 Barrier[1].

Specimen	Weight Changes in Grams During Flame Tunnel Tests						Appearance of Specimens at End of Test
	Coating	25 Hr	50 Hr	100 Hr	158 Hr	200 Hr	
C	Cr_5Al_8	+0.1746	+0.2311	+0.1444	-0.0910	-0.1963	Spalled on edges over entire gage length. Flat surface of gage length retained most of the coating.
E	Cr_5Al_8	+0.1541	+0.2423	+0.2449	+0.1732	+0.1444	Spalled on edges over ~ 50 percent of gage length. Flat surface of gage length retained all of the coating.
F	CoAl	+0.1357	-0.1714	---	---	---	After 50 hr the specimen lost ~ 50 percent of the edge coating and spalled badly on the flat surface of gage length.
G	CoAl	+0.1630	+0.2859	-0.0560	-0.2950	---	After 158 hr the specimen lost ~ 25 percent of the edge coating and retained most of the flat surface coating over gage length. Large weight loss attributed to spalling on areas outside gage length.
I	NC11-A	+0.1473	+0.2004	+0.1084	-0.1153	-0.2292	Spalled edges over entire gage length. Flat surface of gage length retained most of the coating.
D	NC11-A	+0.1377	+0.1664	+0.1590	+0.0193	-0.0400	Spalled edges over ~ 25 percent of gage length. Flat area of gage length is blistered and ~ 25 percent spalled off.

NOTE: (1) Surface Area - 66.7 cm^2

Table IX. Cumulative Weight Changes of Coated TDNi Specimens at 1422° K (2100° F) in Test No. 2, Hastelloy C-1 Barrier.

Specimen	Barrier	Coat[1]	Cumulative Weight Change,[1] Grams					Comments
			24 Hr	45 Hr	49 Hr	100 Hr	145 Hr	
2	C-1	Cr_5Al_8	---	+0.2591[2]	---	---	---	No evidence of failure.
4	C-1	Cr_5Al_8	+0.1323	---	+0.2257	+0.3289	+0.1751	Spalled over 80 percent of gage length edges. Faces of gage length good.
5	C-1	Cr_5Al_8	+0.1622	---	+0.2878	+0.3281	-0.1467	Spalled over 90 percent of gage length edges. Faces of gage length blistered over ~ 10 percent of area.
8	C-1	CoAl	+0.1625	---	+0.2094	+0.1738	-0.0190	Very bad erosion with melted appearance at one place on face of gage length. Remainder blistered.
11	C-1	CoAl	+0.1572	---	+0.2056	-0.1337[3]	---	Entire gage length either blistered badly or spalled.
12	C-1	NC11-A	---	+0.1262[4]	---	---	---	~ 10 percent of surface area beginning to spall or blister.
15	C-1	NC11-A	+0.1150	---	+0.1665	-0.1728	---	Coating blistered over 70-80 percent of edges and faces of gage length.
16	C-1	NC11-A	+0.1091	---	+0.1565	+0.0313	---	~ 50 percent of edge and face surface area either blistered or spalled.

NOTES:
(1) Surface area - 66.7 cm^2
(2) Replaced specimen No. 11 after 100 hours
(3) Replaced with uncoated specimen after 100 hours
(4) Replaced specimen No. 15 after 100 hours

Table X. Cumulative Weight Changes of Coated TDNi and TDNiCr Specimens at 1422° K (2100° F) in Test No. 3.

Panels	Barrier	Coat	Cumulate Weight Change, Grams Surface Area 66.7 cm^2							Comments
			25 Hr	48 Hr	94 Hr	124 Hr	150 Hr	200 Hr	300 Hr	
N TDNiCr	X-40	Cr_5Al_8	+.0990	+.0897	+.0800	+.0142	-.0137	-.0335	-.0701	No evidence of failure on any surface
R TDNiCr	X-40	Cr_5Al_8	+.1249	+.0974	+.0923	+.0394	.0229	-.0051	-.0445	Very slight spalling occurred on one edge. The other edge and both faces showed no evidence of failure.
S TDNiCr	X-40	NC11-A	+.0519	+.0746	+.0973	+.1105	+.1089	+.1029	+.0708	One edge showed ~ 60% spalled. The other edge and both faces showed no evidence of failure.
T TDNiCr	X-40	NC11-A	+.0451	+.0645	+.0856	+.0966	+.1006	+.0946	+.0673	Slight amount of spalling on one edge. The other edge and both faces showed no evidence of failure.
19 TDNi	C-2	Cr_5Al_8	+.1557	+.1731	+.1784	+.1252	-.0851(1)	---	---	Edges spalled over ~ 50% of area. No evidence of face failure.
20 TDNi	C-2	NC11-A	+.0354	+.0656	+.0986	+.1292	+.1365	+.0573(2)		Edges spalled over ~ 40% and one face blistered ~ 50% of area. The other face showed no evidence of failure.

NOTES: (1) Replaced with bare TDNi specimen at 150 hours.
(2) Replaced at 175 hours with X40/NC11-A specimen V. Cumulative weight at end of test was +.1007 gms. No evidence of failure on any surface.

Table XI. X-Ray Diffraction Analysis of NC11-A/X40 and Cr_5Al_8/X40 Coatings on TDNiCr.

Specimen	Coating	Condition	Phase Observed
W	NC11-A/X40	As-coated	Al_2O_3, CoAl (NiAl)
S	NC11-A/X40	1422° K (2100° F)/300 Hours	Al_2O_3, γ (FCC)
T	NC11-A/X40	1422° K (2100° F)/300 Hours	Al_2O_3, γ (FCC)
Q	Cr_5Al_8/X40	As-coated	Al_2O_3, CoAl (NiAl) Cr (solid solution), Many unidentified lines.
N	Cr_5Al_8/X40	1422° K (2100° F)/300 Hours	Al_2O_3, γ (FCC)
R	Cr_5Al_8/X40	1422° K (2100° F)/300 Hours	Al_2O_3, γ (FCC)

Table XII. Group I Tensile Test Results on TDNiCr with Hastelloy C-1 Barrier Layer at Room Temperature and 1422° K (2100° F).

Specimen	Condition	Coat	Type Tensile	Corrected to Substrate Cross-Section				
				UTS (Ksi)	(MPA)	0.2% YS (Ksi)	(MPA)	% Elongation (2 inches) (5.08 cm)
A A	As-received	---	RT	127.6	880	83.0	572	17.0
A	As-coated	Cr_5Al_8	RT	116.8	802	82.9	570	12.1
H	As-coated	CoAl	RT	116.8	806	83.5	576	9.2
K	As-coated	NC11-A	RT	111.1	766	82.9	570	8.6
B B	As-received	---	1422° K	12.7	88	10.5	72	0.9
B	As-coated	Cr_5Al_8	1422° K	13.1	90	11.0	76	0.3
J	As-coated	CoAl	1422° K	11.7	81	9.4	65	1.3
L	As-coated	NC11-A	1422° K	13.5	93	10.6	73	2.0
E	1422° K/200 Hour	Cr_5Al_8	RT	120.8	830	87.3	601	6.0
F	1422° K/50 Hour	CoAl	RT	127.1	878	87.3	601	12.8
D	1422° K/200 Hour	NC11-A	RT	122.7	845	86.7	598	8.1
C	1422° K/200 Hour	Cr_5Al_8	1422° K	13.9	96	11.0	76	1.3
G	1422° K/158 Hour	CoAl	1422° K	15.4	106	12.4	86	1.2
I	1422° K/200 Hour	NC11-A	1422° K	15.0	103	10.8	75	1.7

Table XIII. Group II Tensile Test Results on TDNi with Hastelloy C-1 Barrier Layer at Room Temperature and 1422° K (2100° F).

Specimen	Condition	Coat	Type Tensile	Corrected to Substrate Cross-Section				
				UTS (Ksi)	(MPA)	0.2% YS (Ksi)	(MPA)	% Elongation (2 inches)
21	As-received	---	RT	64.1	442	46.1	316	15.8
1	As-coated	Cr_5Al_8	RT	66.1	455	52.1	360	7.1
7	As-coated	CoAl	RT	70.5	486	52.7	362	6.7
13	As-coated	NC11-A	RT	67.7	471	55.5	382	6.8
22	As-received	---	1422° K	12.8	89	10.4	72	2.8
3	As-coated	Cr_5Al_8	1422° K	13.4	92	9.7	67	4.5
9	As-coated	CoAl	1422° K	13.5	93	10.4	71	4.9
14	As-coated	NC11-A	1422° K	13.9	96	10.3	71	4.6
4	1422° K/145 Hour	Cr_5Al_8	RT	63.6	438	37.6	255	5.4
11	1422° K/100 Hour	CoAl	RT	60.6	417	40.6	280	5.9
16	1422° K/100 Hour	NC11-A	RT	64.1	442	45.8	316	6.4
5	1422° K/145 Hour	Cr_5Al_8	1422° K	13.5	93	11.2	71	2.6
8	1422° K/145 Hour	CoAl	1422° K	12.8	89	10.0	69	2.6
15	1422° K/100 Hour	NC11-A	1422° K	13.4	92	11.2	71	4.7

Table XIV. Group III Tensile Test Results on TDNi and TDNiCr.

Specimen	Coating/Substrate	Condition	Test Temperature	Corrected to Substrate Cross Section				
				UTS		0.2% YS		Elongation 5.08 cm (2 Inches)
				Ksi	MPA	Ksi	MPA	
U	Cr_5Al_8/X40/TDNiCr	As-Coated	RT	125.5	864	90.3	620	8.8
N	Cr_5Al_8/X40/TDNiCr	1422° K/300 Hours	RT	121.5	837	81.2	559	9.4
T	NC11-A/X40/TDNiCr	1422° K/300 Hours	RT	123.0	849	84.4	580	10.0
W	NC11-A/X40/TDNiCr	As-Coated	1422° K	14.8	102	11.1	76	1.8
V	NC11-A/X40/TDNiCr	1422° K/125 Hours	1422° K	12.5	86	11.2	77	1.1
R	Cr_5Al_8/X40/TDNiCr	1422° K/300 Hours	1422° K	13.5	93	12.4	85	1.1
18	NC11-A/C-2/TDNi	As-Coated	RT	65.8	450	56.8	392	6.5
19	Cr_5Al_8/C-2/TDNi	1422° K/150 Hours	RT	66.8	460	41.2	285	7.8
17	Cr_5Al_8/C-2/TDNi	As-Coated	1422° K	12.2	84	10.1	70	4.8
20	NC11-A/C-2/TDNi	1422° K/175 Hours	1422° K	12.6	87	10.2	70	4.8

Table XV. Chemical, SEM, and Microprobe Analyses of PVD Feedbars and Coatings.

	Wet Chemistry Feedbar, Weight %	PVD Coatings, Weight %			
		Run No. 1		Run No. 2	
		SEM	Microprobe	SEM	Microprobe
X40					
Carbon	0.38	---	---	---	---
Nickel	15.76	77.3	32-35	27.2	27
Chromium	20.65	8.5	22	35.4	27
Iron	1.14	3.7	---	---	---
Tungsten	8.23	---	< 1	---	< 1
Cobalt	54.30	10.6	43	37.3	47
Hastelloy C-1					
Nickel	54.60	65	75	79	60-75
Chromium	16.13	35	20	21	25-35
Tungsten	11.10	---	< 1	---	< 1
Molybdenum	17.80	---	< 1	---	< 1

Table XVI. 1422° K (2100° F) Mach 1 Burner Rig Testing of Coated and Uncoated TDNi and TDNiCr.

Specimen	Cumulative Weight Change, grams					Percent Total Loss	Remarks
	46 Hr	118 Hr	196 Hr	284 Hr	350 Hr		
Uncoated TDNiCr	-0.352	-1.279	- 2.200	-3.746	-4.651	3.91	Attack severe at leading edge and corners of trailing edge
NiCrAlY/TDNiCr	-0.026	-0.065*	- 0.158	-0.660	-1.150	0.90	Coating failure at leading and trailing edges at 284 hours
Hast C-1/NC11A-TDNiCr	+0.069	+0.034	- 0.504	-1.786	-3.809	3.28	Coating failure at 196 hours
X40/NC11A-TDNiCr	-0.074	---	---	---	---	---	Failed in fatigue in base slot
X40/NC11A-TDNiCr	---	-0.069	- 0.356	-0.934	-1.709	1.38	Replacement at 46 hours Coating failure at 284 hours (238 actual)
Hast C-1/NC11A-TDNi	-0.096	-1.768	-14.175	---	---	---	Coating failure at 118 hours; removed at 196 hours

*Estimated. Specimen rubbed at tip, removing material. Value projected from weight loss at 46 and 196 hours.

Table XVII. 1477° K (2200° F)/100-Hour Mach 1 Burner Rig Test.

Specimen/Coating	Cumulative Weight Changes, grams Exposure Time, Hours 7	20	27	32	36	38	45	82	100	Remarks
No. 1 NiCrAlY/TDNiCr	---	---	---	---	---	+0.045	-0.127	---	-0.222	Specimen Splattered with Molten X40 at 38 hours
No. 3 Hast C-1/NC11A/TDNiCr	---	-0.010	---	---	---	---	---	-0.395	---	Removed at 20 hours Returned at 38 hours
No. 5 X40/NC11A/TDNiCr	---	---	---	---	-0.235	---	---	---	---	Fatigue Failure at 36 hours
No. 7 X40/NC11A/TDNiCr	---	---	---	---	---	-0.814	---	---	---	Specimen Broke when Removed from Fixture
No. 5A Hast C-1/NC11A/TDNi	+0.045	---	---	---	---	---	---	---	---	Failed in Fatigue after 32 hours Local Coating Failure

Table XVIII. 1533° K (2300° F) Static Oxidation Testing of Coated TDNi and TDNiCr Tensile Specimens, One Hour Cycles.

Specimen	Cumulative Weight Change, grams							Remarks
	5	10	20	40	60	80	100	
No. 8 Hast C-1/NC11A/TDNi	+0.029	---	---	---	---	---	---	Local Coating Failure Removed after 5 Hours
No. 10 Hast C-1/NC11A/TDNi	---	---	---	---	---	---	---	Local Coating Failure Removed after 4 Hours
No. 11 Hast C-1/NC11A/TDNi	---	---	---	---	---	---	---	Local Coating Failure Removed after 4 Hours
No. 12 Hast C-1/NC11A/TDNi	---	---	---	---	---	---	---	Local Coating Failure Removed after 1 Hour
No. 19 Hast C-1/NC11A/TDNiCr	---	---	---	---	---	---	---	Local Coating Failure Removed after 1 Hour
No. 20 Hast C-1/NC11A/TDNiCr	---	---	---	---	---	---	---	Local Coating Failure Removed after 4 Hours
No. 21 Hast C-1/NC11A/TDNiCr	---	---	---	---	---	---	---	Local Coating Failure Removed after 2 Hours
No. 22 Hast C-1/NC11A/TDNiCr	---	---	---	---	---	---	---	Local Coating Failure Removed after 2 Hours
No. 3 X40/NC11A/TDNiCr	+0.090	+0.085	+0.096	+0.053	---	---	---	Local Coating Failure Removed after 40 Hours
No. 4 X40/NC11A/TDNiCr	---	---	---	---	---	---	---	Coating Blistered Removed after 4 Hours
No. 5 X40/NC11A/TDNiCr	---	---	---	---	---	---	---	Coating Blistered Removed after 4 Hours
No. 6 X40/NC11A/TDNiCr	+0.068	+0.114	+0.165	+0.213	+0.237	+0.246	+0.234	Coating Intact
No. 1 NiCrAlY/TDNiCr	+0.020	+0.026	+0.040	+0.047	+0.042	+0.027	-0.003	Coating Intact
No. 2 NiCrAlY/TDNiCr	+0.045	+0.038	+0.063	+0.033	-0.034	-0.136	---	Coating Failure Removed after 80 Hours
No. 3 NiCrAlY/TDNiCr	+0.052	+0.048	+0.059	+0.060	+0.049	+0.021	-0.028	Coating Intact
No. 4 NiCrAlY/TDNiCr	+0.026	+0.032	+0.051	+0.060	---	---	---	Coating Failure Removed after 40 Hours

Table XIX. Tensile Test Results of Uncoated and Coated TDNi and TDNiCr.

Material	Coating	Condition	Test Temperature	Corrected to Substrate Cross Section				
				UTS		0.2% Y.S.		
				MPa	Ksi	MPa	Ksi	% Elongation
TDNiCr	Uncoated	As-Received	RT	880	127.6	572	83.0	17.0
TDNiCr	Hast C-1/NC11A	4 Hrs/1533° K (2300° F)	RT	745	108.3	518	75.3	4.9
TDNiCr*	Hast C-1/NC11A	4 Hrs/1533° K (2300° F)	RT	656	95.3	509	74.0	2.4
TDNiCr	NiCrAlY	40 Hrs/1533° K (2300° F)	RT	808	117.5	490	71.2	13.8
TDNiCr	X40/NCiiA	4 Hrs/1533° K (2300° F)	RT	860	125.0	550	80.0	12.0
TDNi	Uncoated	As-Received	1422° K (2100° F)	89	12.8	72	10.4	2.8
TDNiCr	Uncoated	As-Received	1422° K (2100° F)	88	12.7	72	10.5	0.9
TDNi	Hast C-1/NC11A	As-Coated	1422° K (2100° F)	90	13.1	75	10.9	4.1
TDNiCr	Hast C-1/NC11A	As-Coated	1422° K (2100° F)	93	13.5	78	11.3	1.6
TDNICr	X40/NC11A	As-Coated	1422° K (2100° F)	90	13.1	78	11.3	2.3
TDNiCr	NiCrAlY	As-Coated	1422° K (2100° F)	94	13.7	89	12.9	0.9
TDNi	Hast C-1/NC11A	5 Hrs/1533° K (2300° F)	1422° K (2100° F)	93	13.3	75	10.9	4.3
TDNiCr	Hast C-1/NC11A	4 Hrs/1533° K (2300° F)	1422° K (2100° F)	81	11.7	78	11.3	1.4
TDNiCr	X40/NC11A	4 Hrs/1533° K (2300° F)	1422° K (2100° F)	99	14.4	91	13.2	1.8
TDNiCr	NiCrAlY	80 Hrs/1533° K (2300° F)	1422° K (2100° F)	98	14.2	85	12.4	1.6
TDNi	Hast C-1/NC11A	4 Hrs/1533° K (2300° F)	1533° K (2300° F)	62	9.0	52	7.6	2.6
TDNiCr	Hast C-1/NC11A	2 Hrs/1533° K (2300° F)	1533° K (2300° F)	63	9.1	59	8.5	2.3
TDNiCr	X40/NC11A	100 Hrs/1533° K (2300° F)	1533° K (2300° F)	65	9.4	60	8.7	1.8
TDNiCr	NiCrAlY	100 Hrs/1533° K (2300° F)	1533° K (2300° F)	74	10.8	65	9.4	0.9
TDNiCr	NiCrAlY	100 Hrs/1533° K (2300° F)	1533° K (2300° F)	72	10.3	62	9.0	0.9

*Specimen Mislabelled TDNi.

TASK I

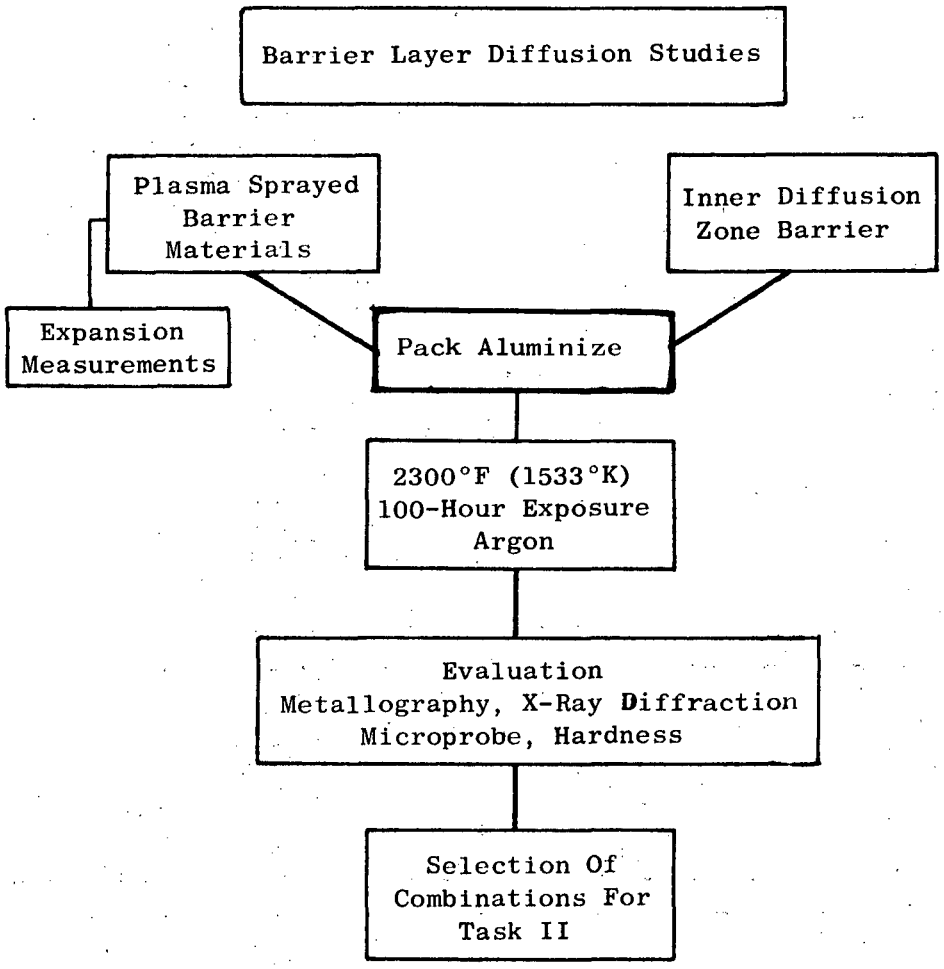

Figure 1. Flow Sheet for Task I

TASK II

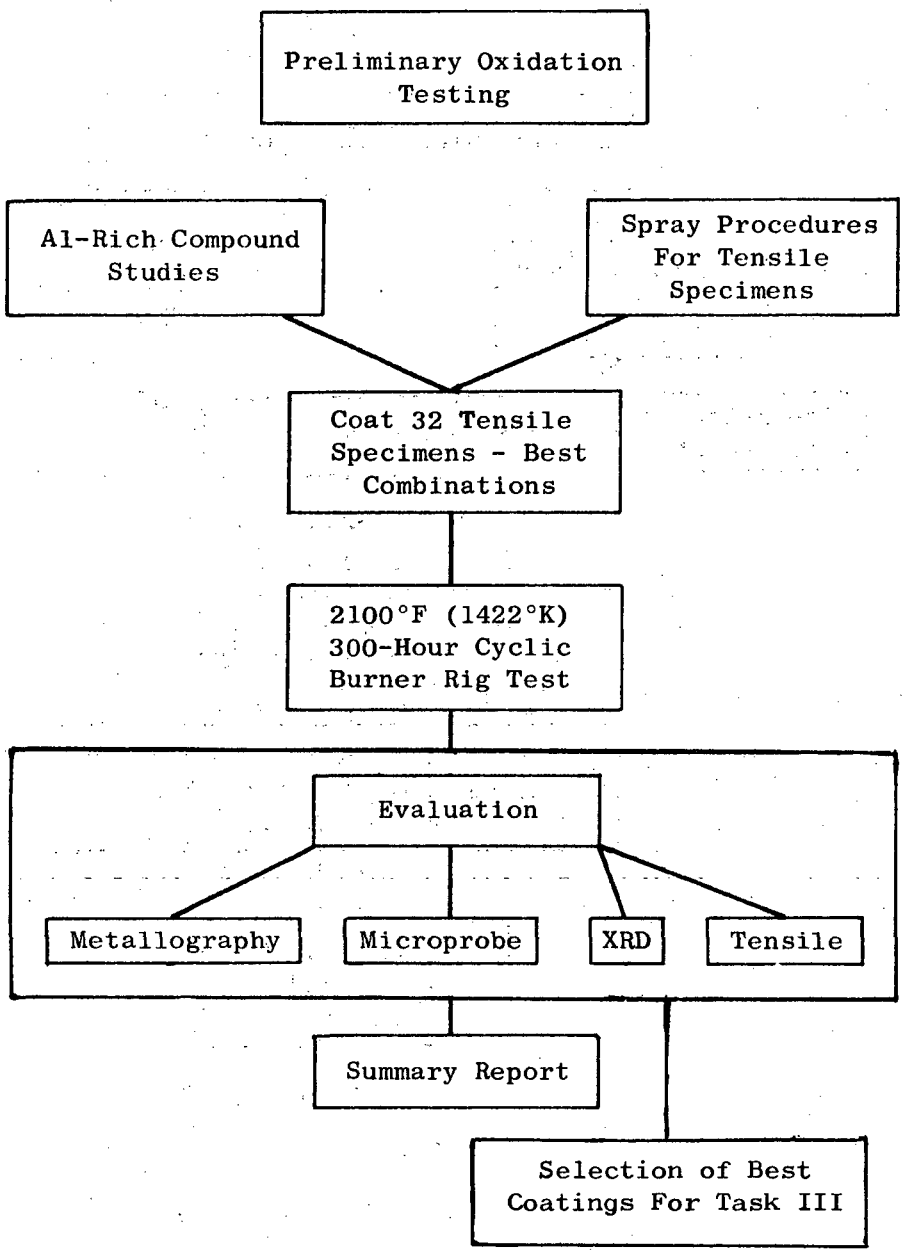

Figure 2. Flow Sheet for Task II

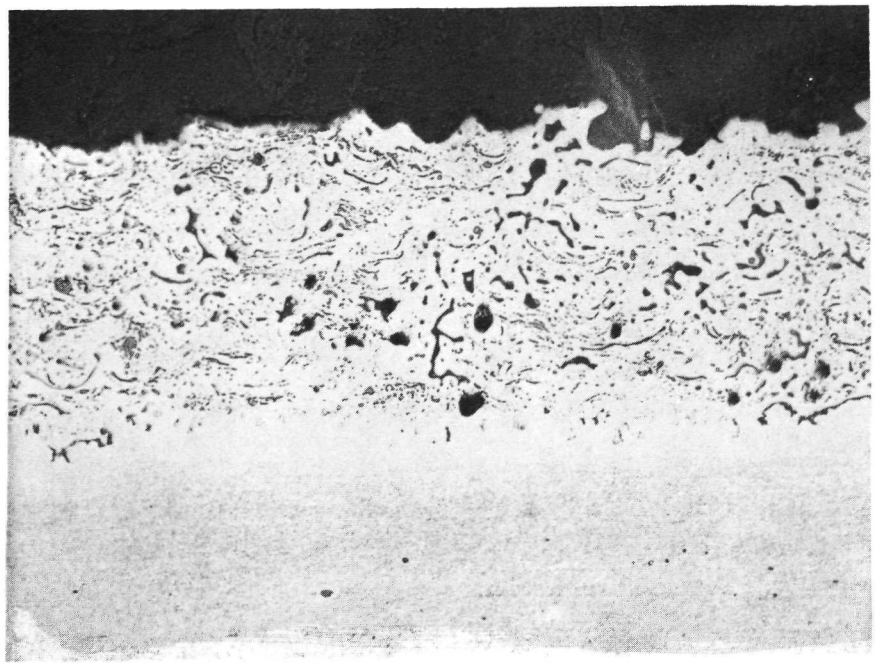

TDNi

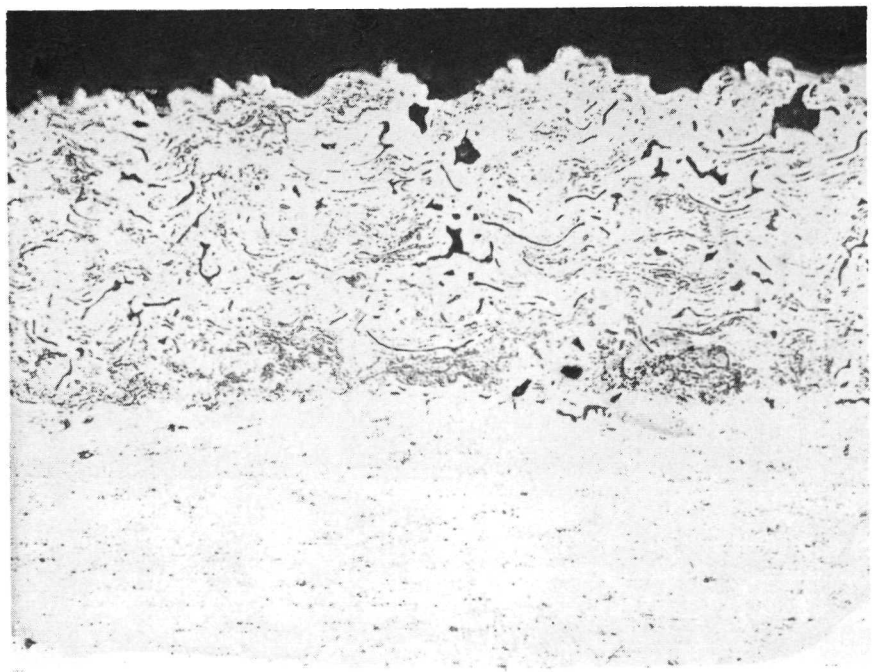

TDNiCr

Figure 3. AVCO Plasma-Gun Sprayed X40 Coating, #1 Spray Parameters. 1477°K (2200°F)/2 Hr/H_2 Diffusion Heat Treatment. Etched - 250X

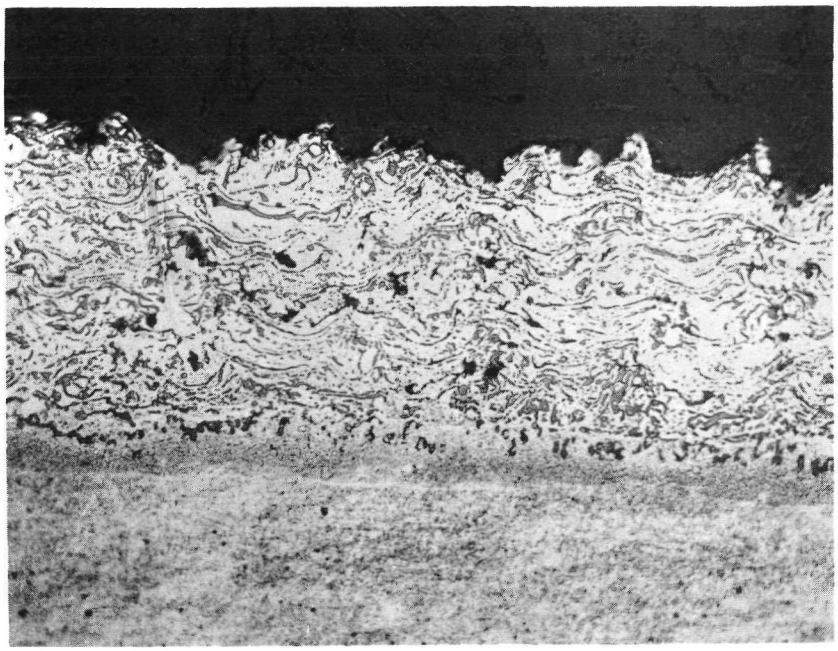

TDNi

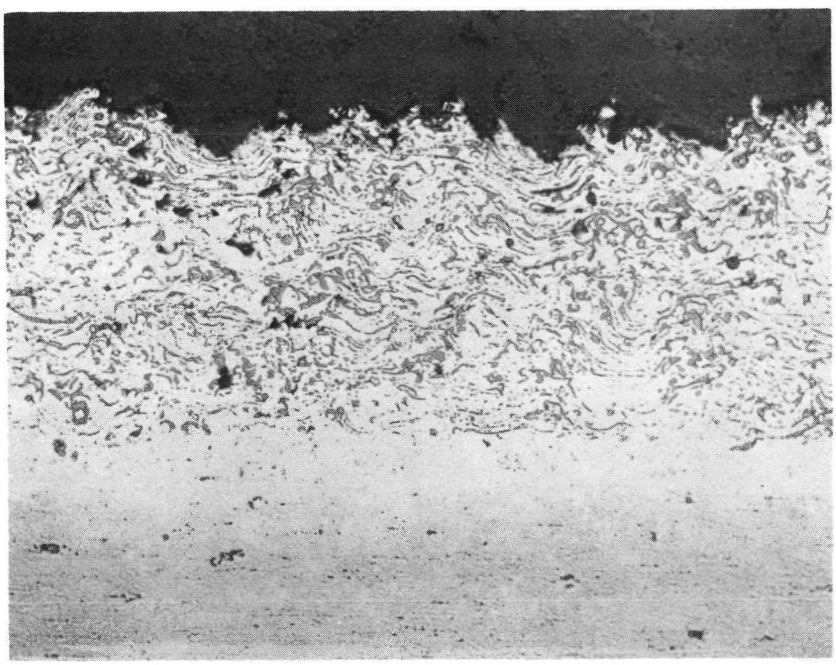

TDNiCr

Figure 4. AVCO Plasma-Gun Sprayed X40 Coating, #1 Spray Parameters. 1477°K (2200°F)/2 Hr/Vac. Diffusion Heat Treatment. Etched - 250X

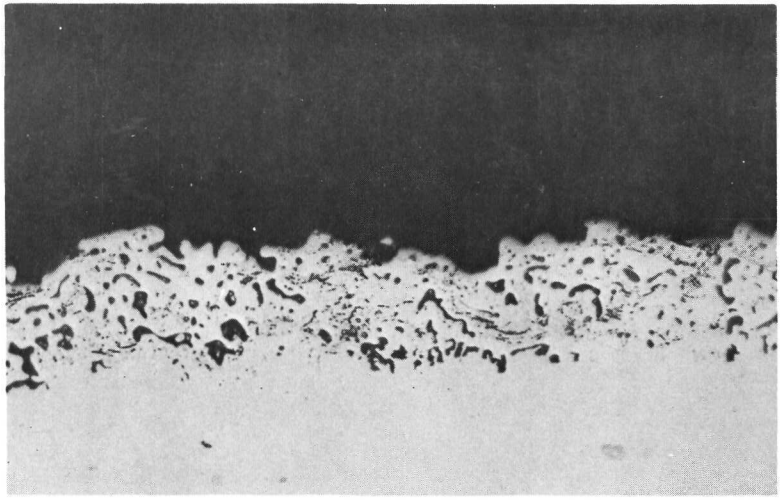

X40 - TDNi

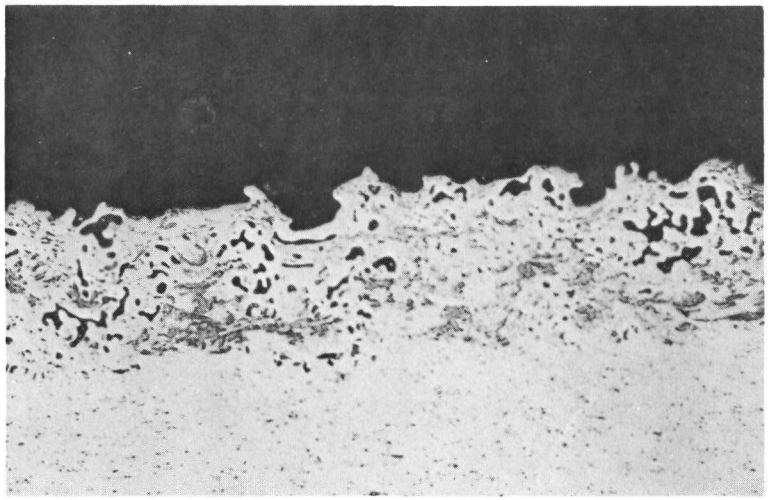

X40 - TDNiCr

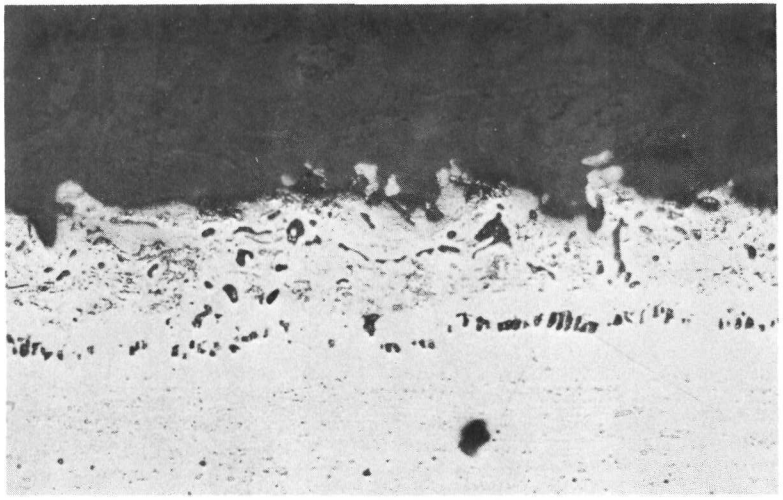

Hastelloy C-la - TDNi

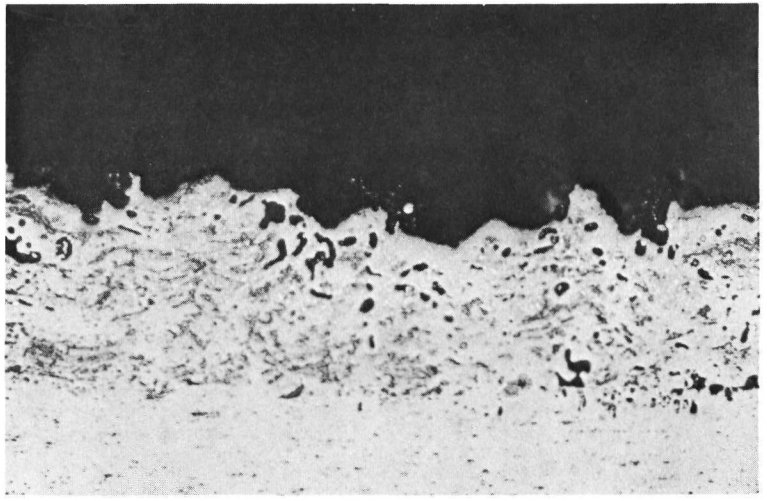

Hastelloy C-la - TDNiCr

Figure 5. AVCO Plasma-Gun Sprayed Coatings After Hydrogen Diffusion Heat Treatment. Unetched 250X

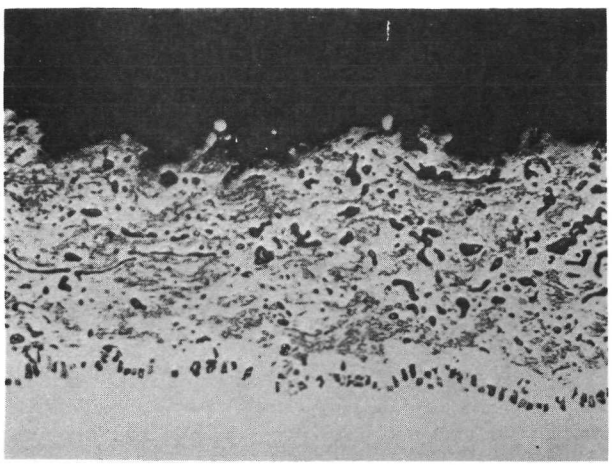

Hastelloy C-1b - TDNi

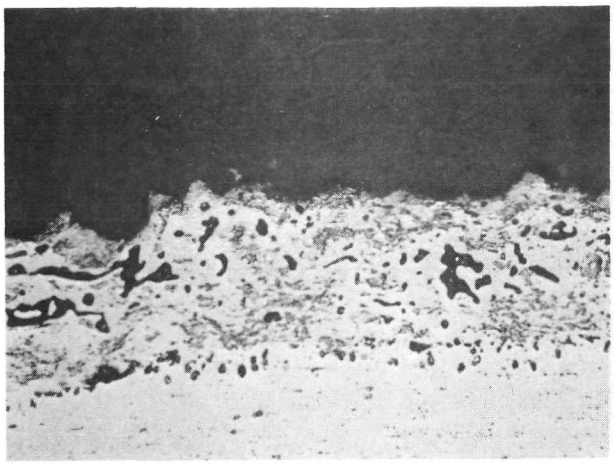

Hastelloy C-1b - TDNiCr

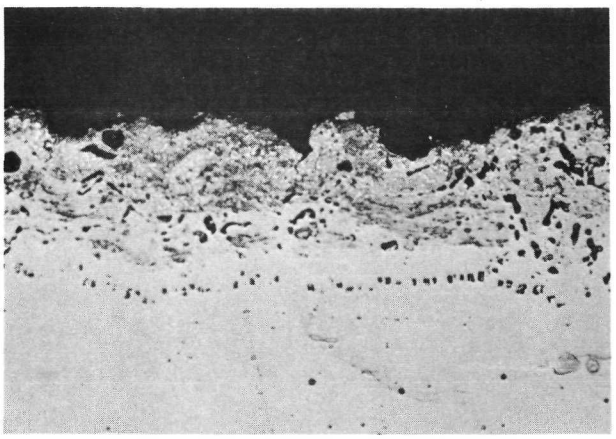

Hastelloy C-2a - TDNi

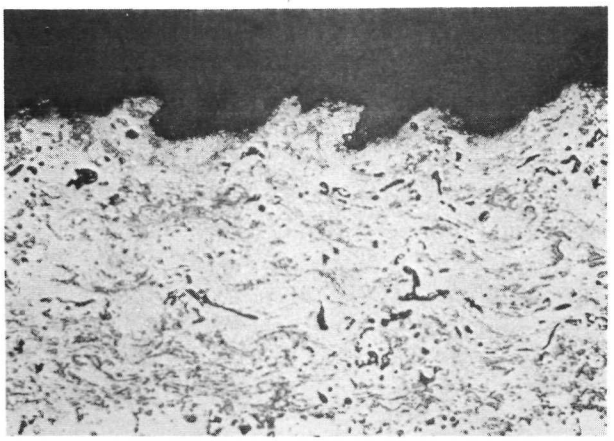

Hastelloy C-2a - TDNiCr

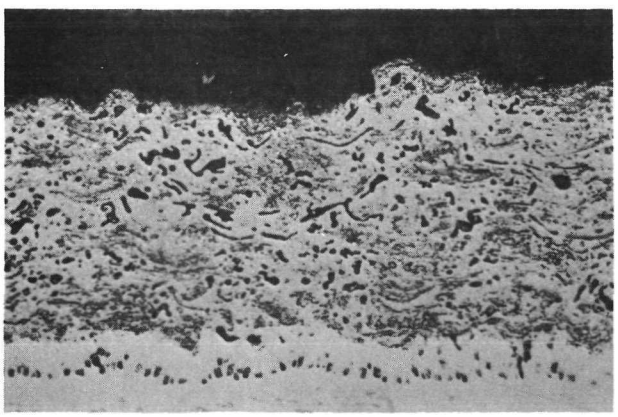

Hastelloy C-2b - TDNi

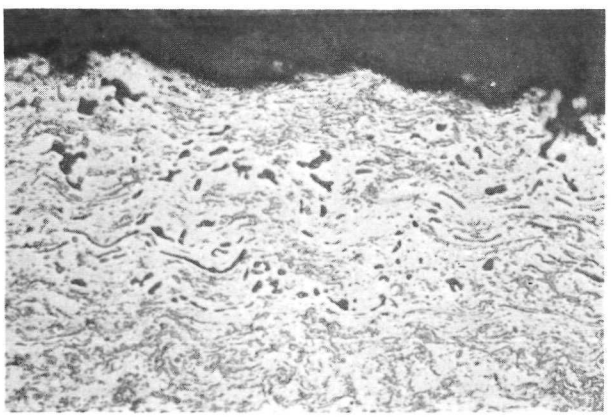

Hastelloy C-2b - TDNiCr

Figure 6. AVCO Plasma-Gun Sprayed Hastelloy C-1b, C-2a, and C-2b Coatings After Hydrogen Diffusion Heat Treatment. Unetched 250X

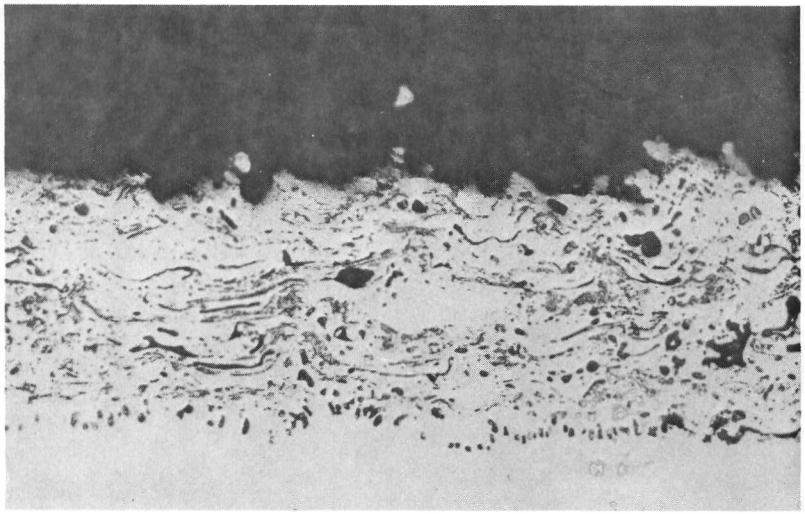

Hastelloy C-1a - TDNi

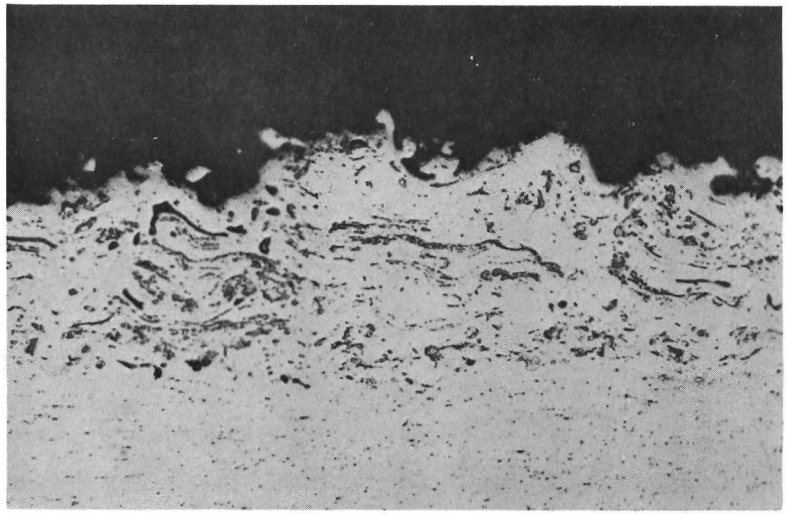

Hastelloy C-1a - TDNiCr

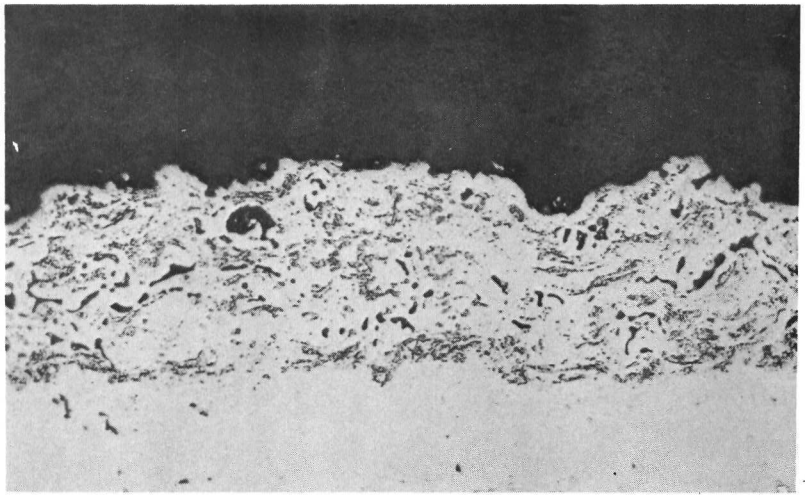

Hastelloy C-1b - TDNi

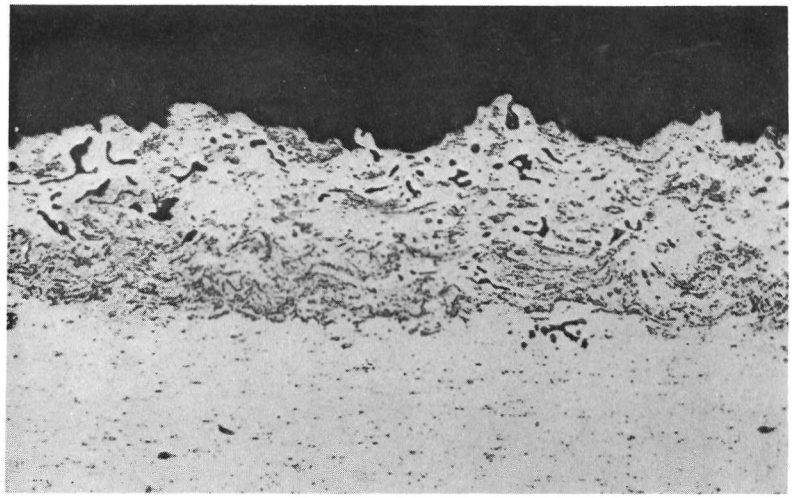

Hastelloy C-1b - TDNiCr

Figure 7. Metco Plasma-Gun Sprayed Hastelloy C-1a and C-1b Coatings After Hydrogen Diffusion Heat Treatment. Unetched 250X

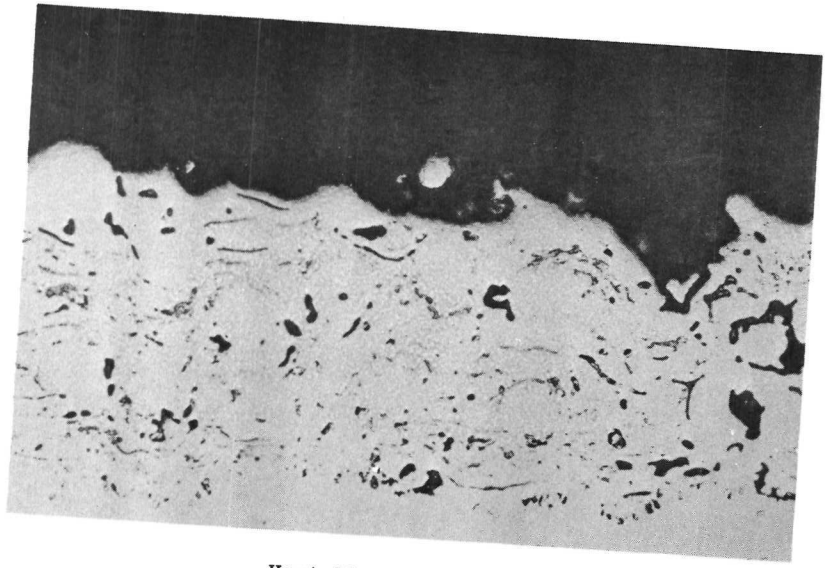

Hastelloy C-2a - TDNi

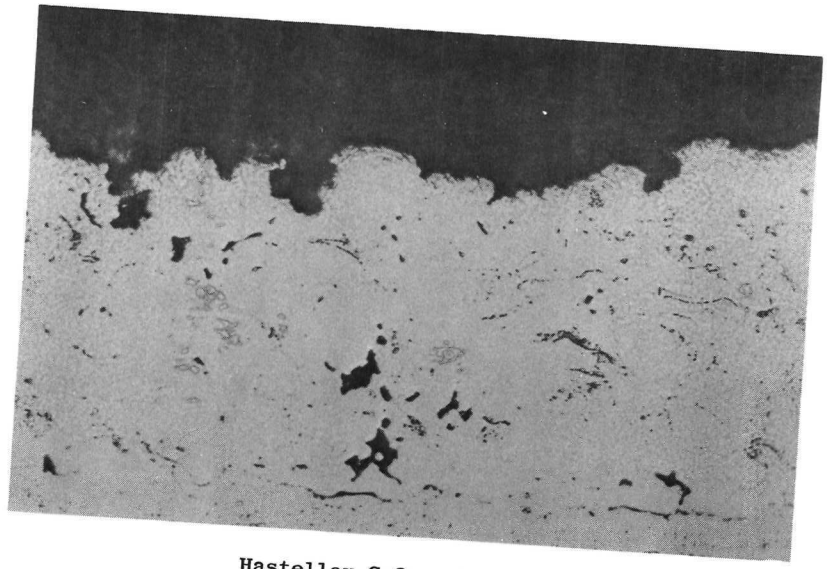

Hastelloy C-2a - TDNiCr

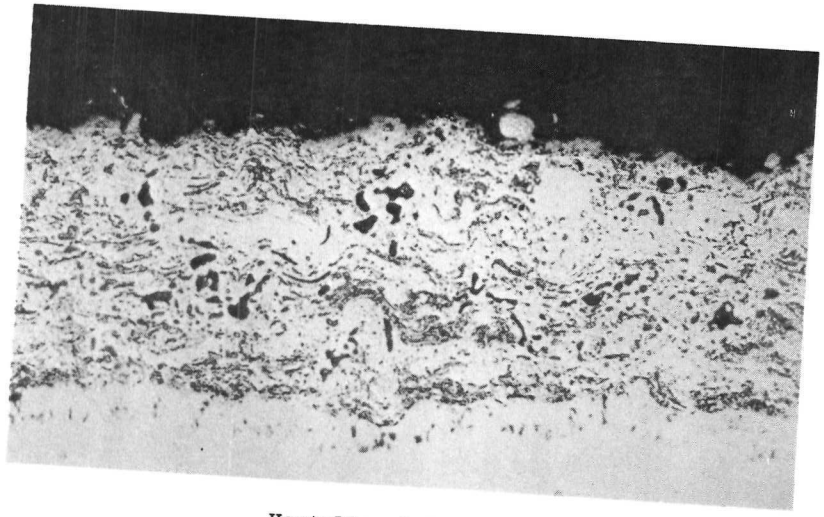

Hastelloy C-2b - TDNi

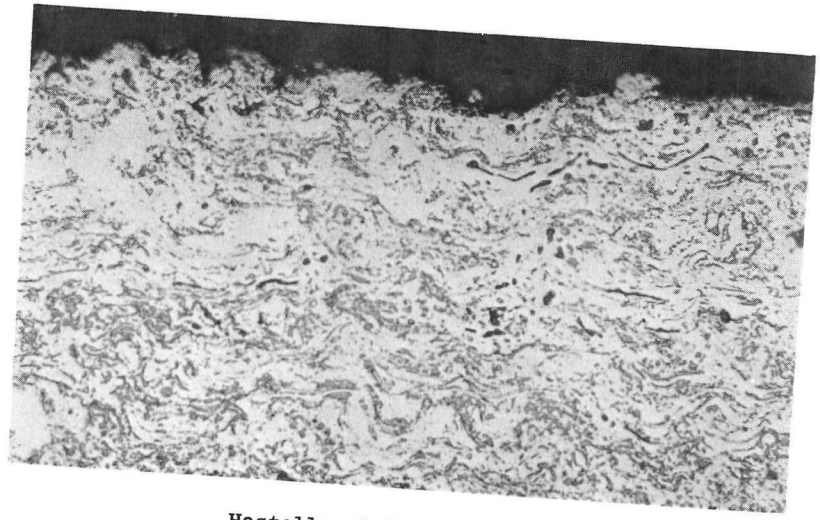

Hastelloy C-2b - TDNiCr

Figure 8. Metco Plasma-Gun Sprayed Hastelloy C-2a and C-2b Coatings After Hydrogen Diffusion Heat Treatment. Unetched 250X

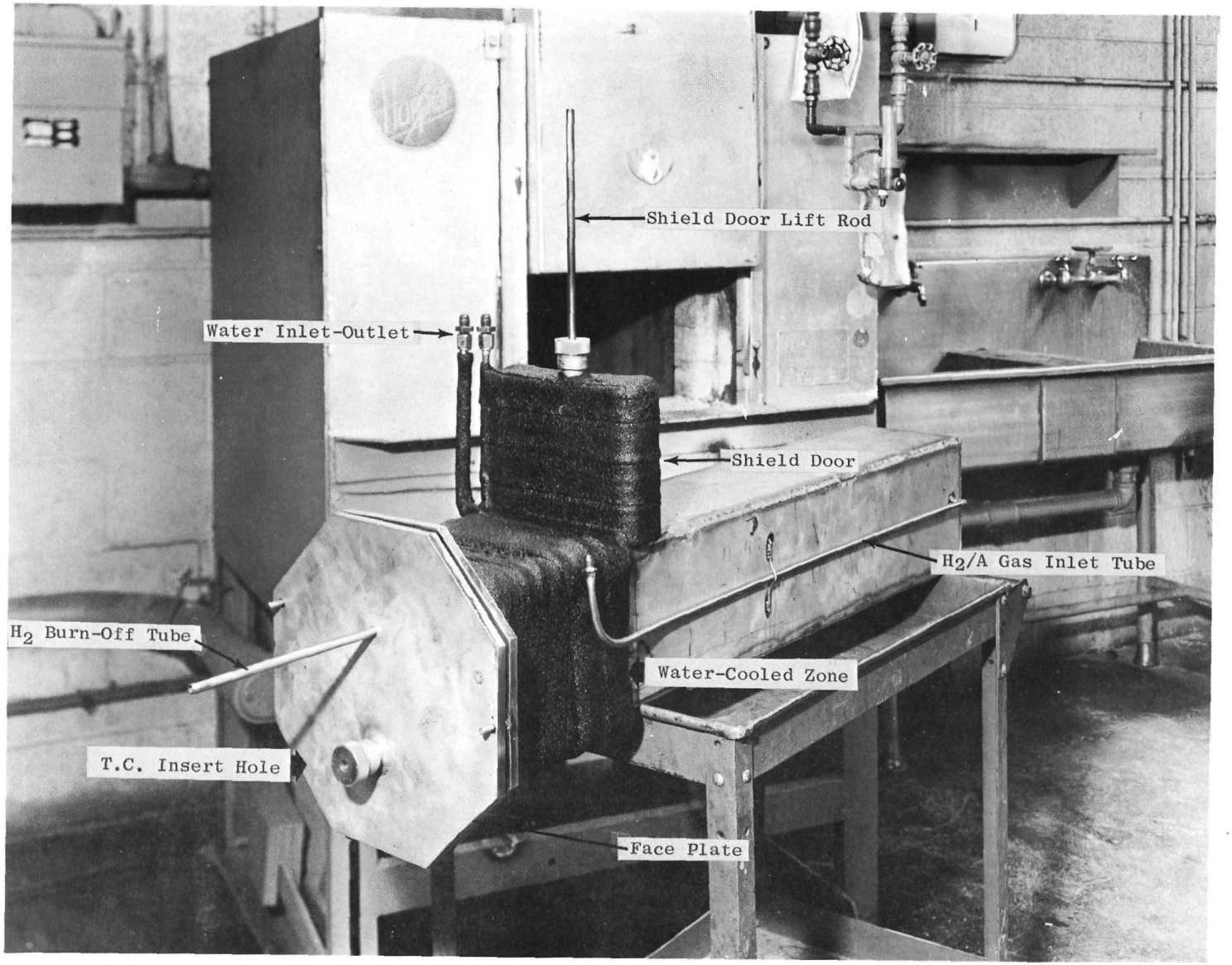

Figure 9. Controlled Atmosphere Coating Retort.

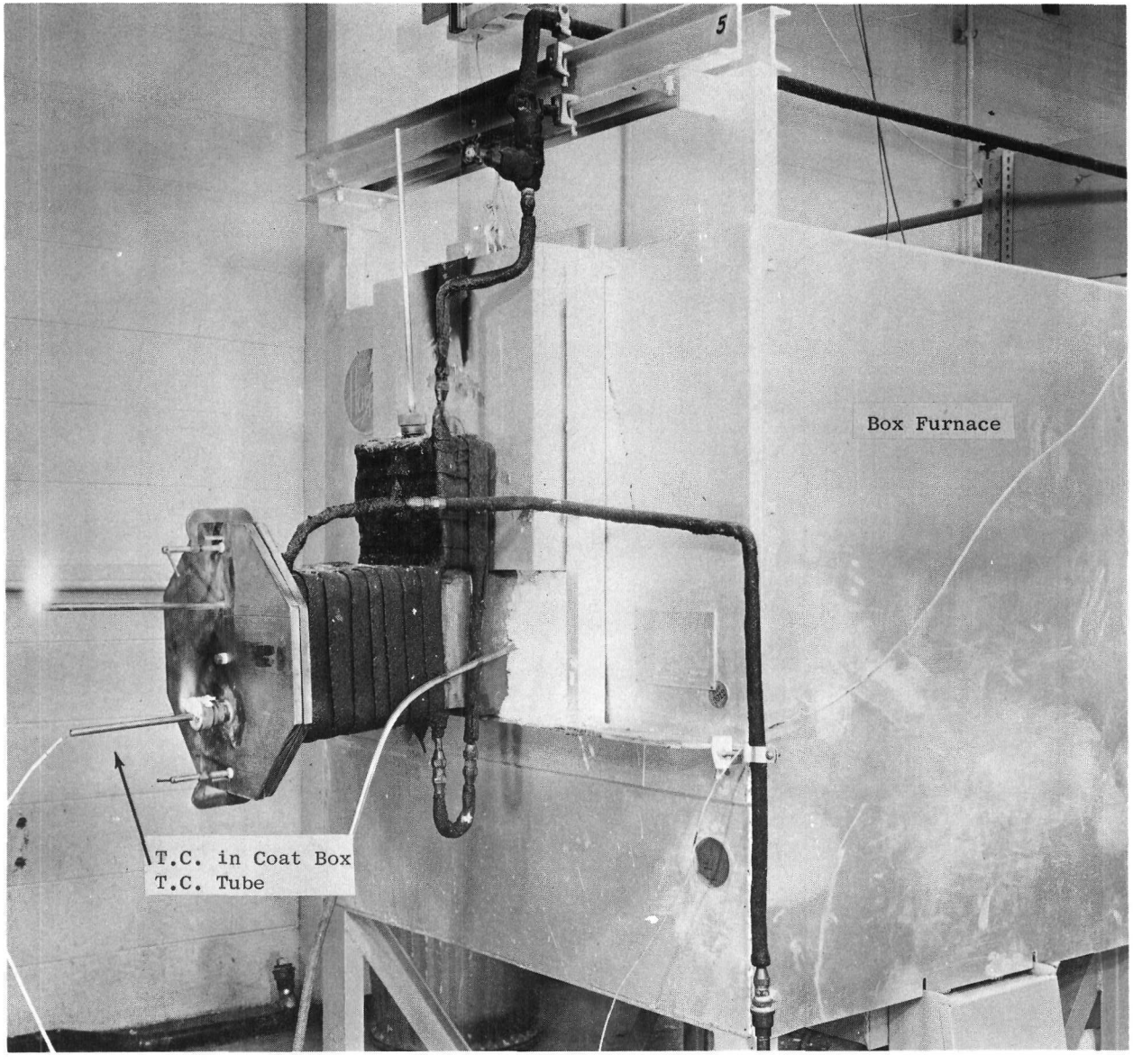

Figure 10. Coating Process Setup with Coating Box in Place.

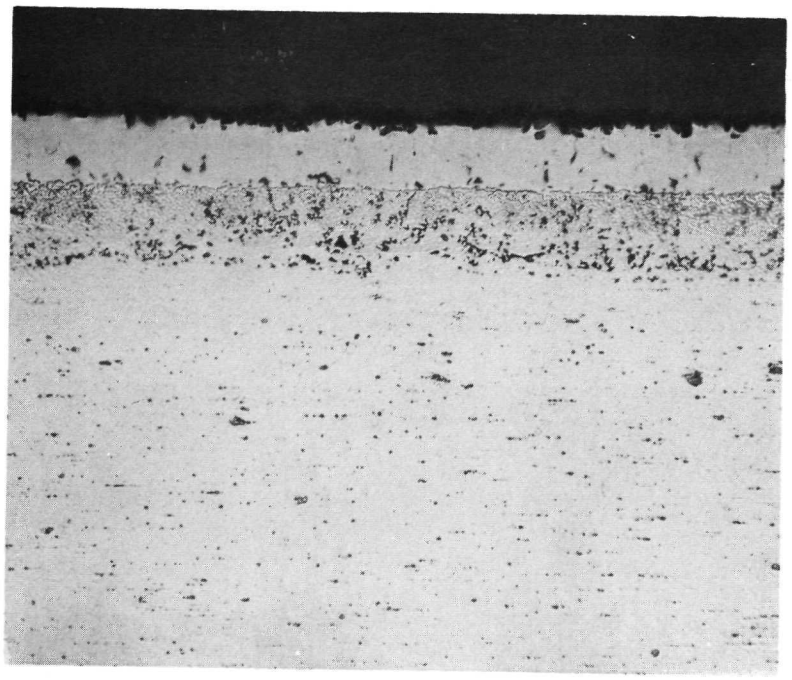

Carburized - 1 Hr @ 1366°K (2000°F)

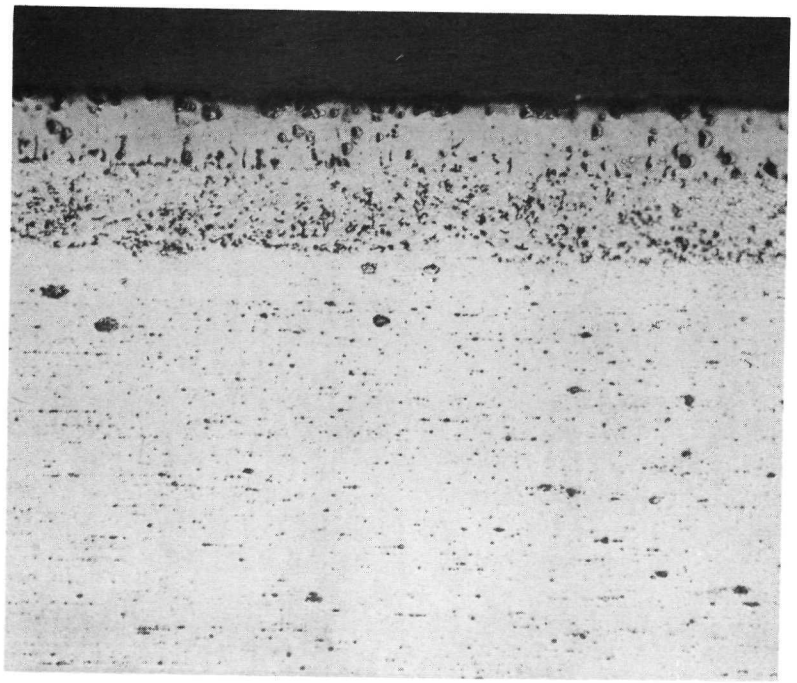

Carburized - 4 hr @ 1366°K (2000°F)

Figure 11. Codep B Coating on Chromized Plus Carburized Barrier Layer on TDNiCr. Etched 500X

As-Processed

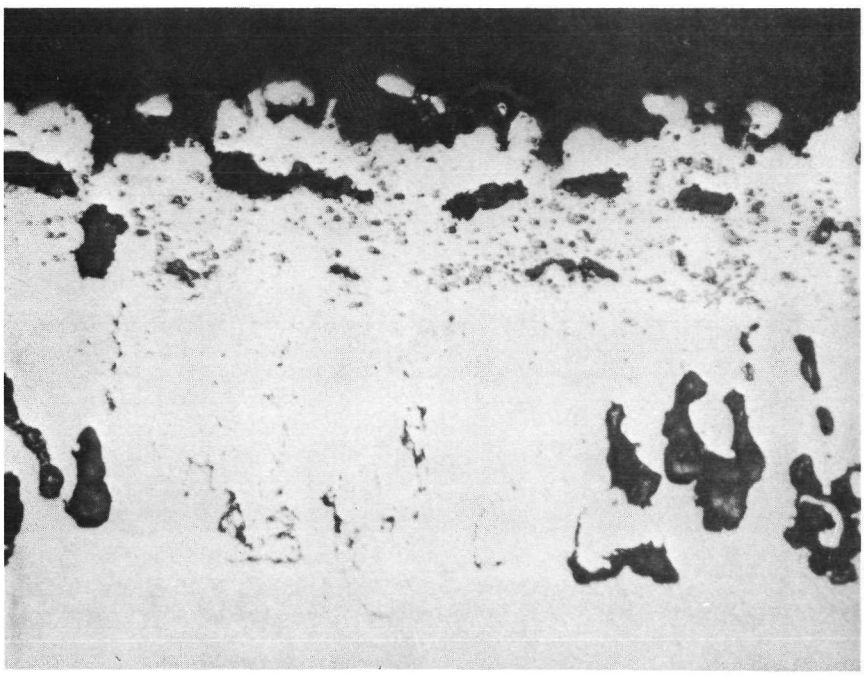

1533°K (2300°F)/100 Hrs/Argon

Figure 12. AVCO Plasma-Gun Sprayed X40 Barrier Layer with NC11-A Covercoat on TDNi. Unetched 500X.

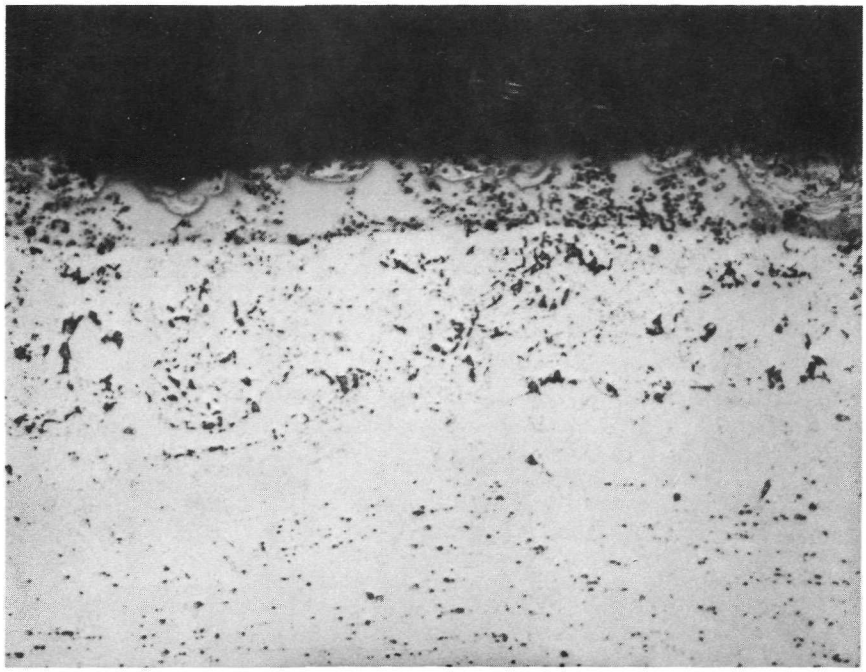

As-Processed

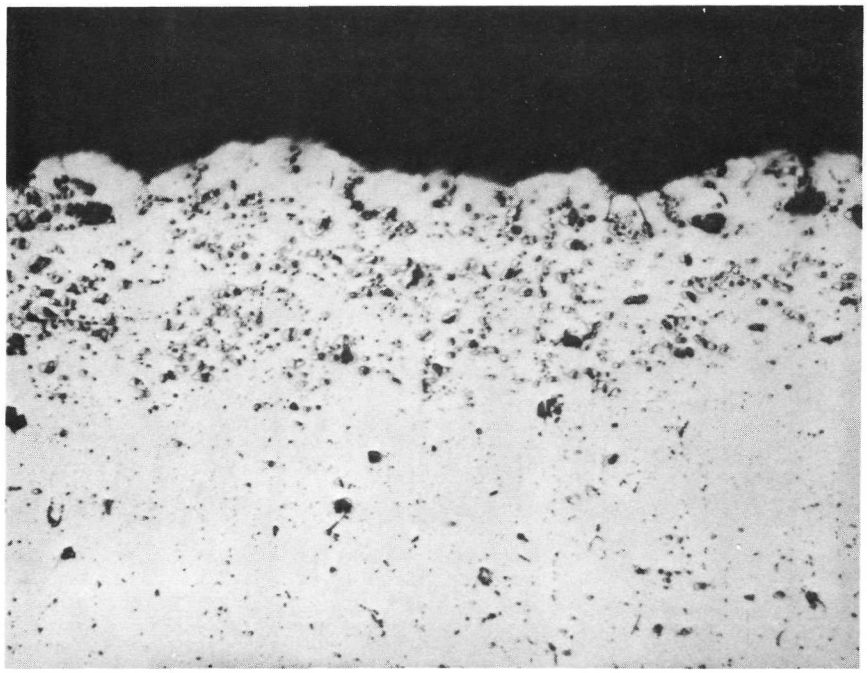

1533°K (2300°F)/100 Hrs/Argon

Figure 13. AVCO Plasma-Gun Sprayed X40 Barrier Layer with NC11-A Covercoat on TDNiCr. Unetched 500X.

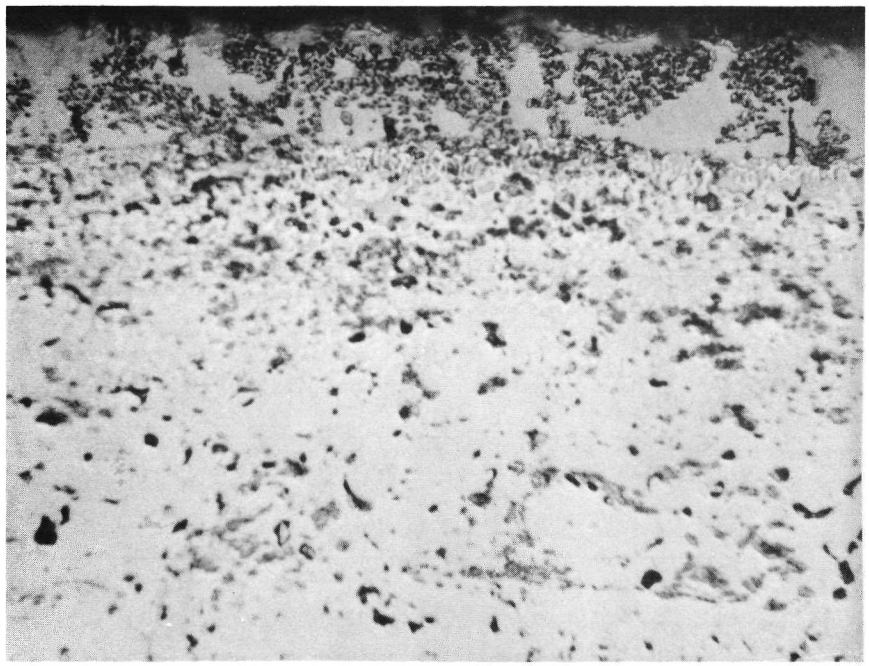

As-Processed

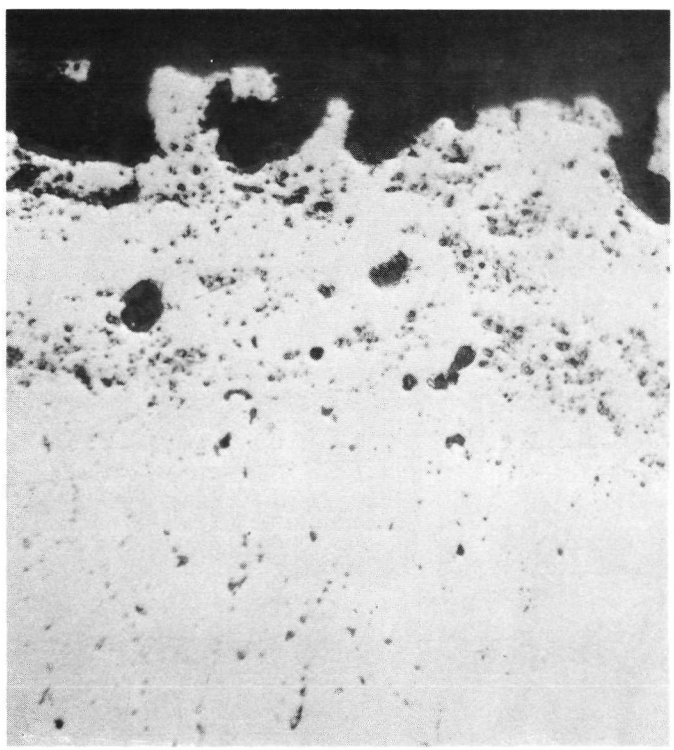

1533°K (2300°F)/100 Hrs/Argon

Figure 14. Metco Plasma-Gun Sprayed Hastelloy C-1a Barrier Layer with NC11-A Covercoat on TDNi. Unetched 500X

As-Processed

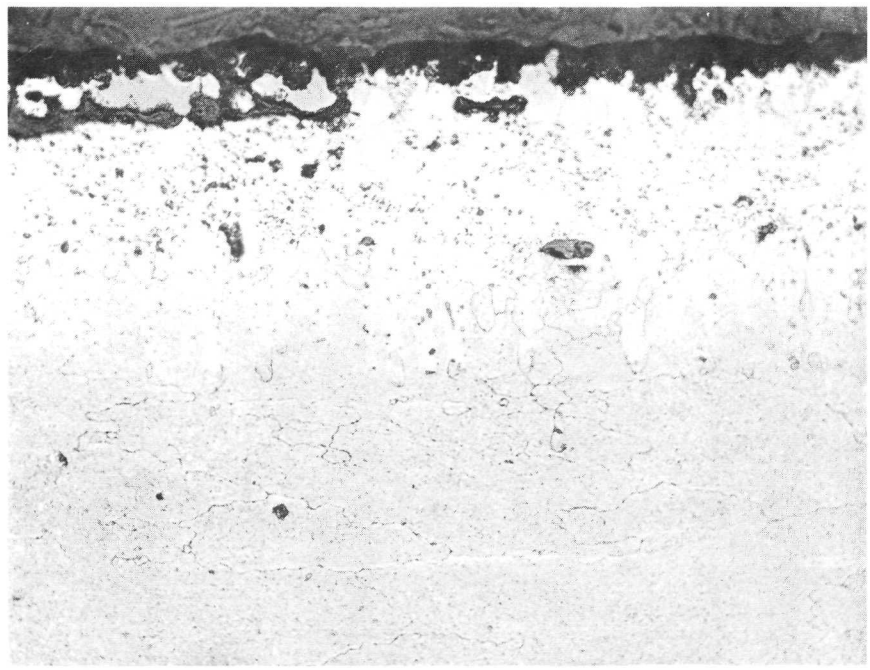

1533°K (2300°F)/100 Hrs/Argon

'igure 15. AVCO Plasma-Gun Sprayed Hastelloy C-1a Barrier Layer with NC11-A Covercoat on TDNiCr. Etched 250X, 2% Chromic

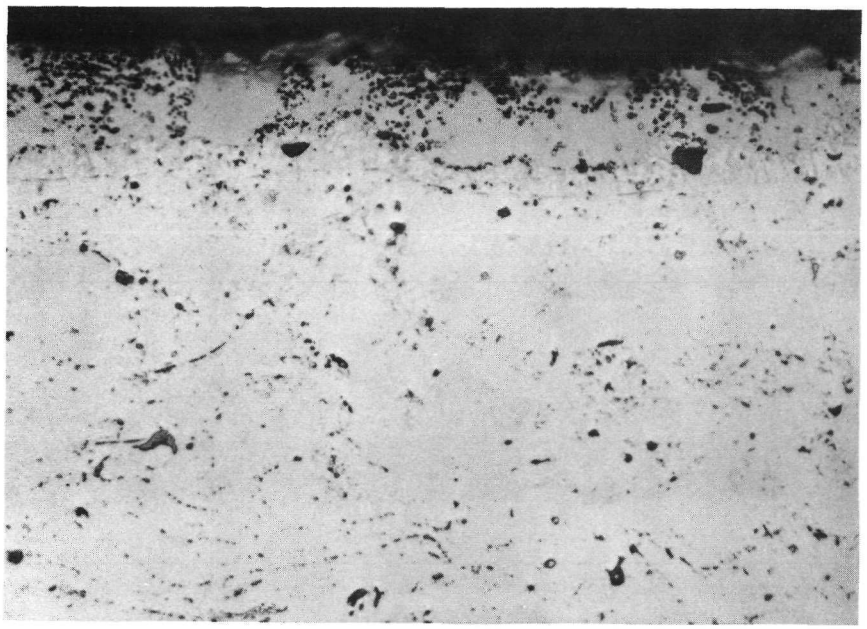

As-Processed

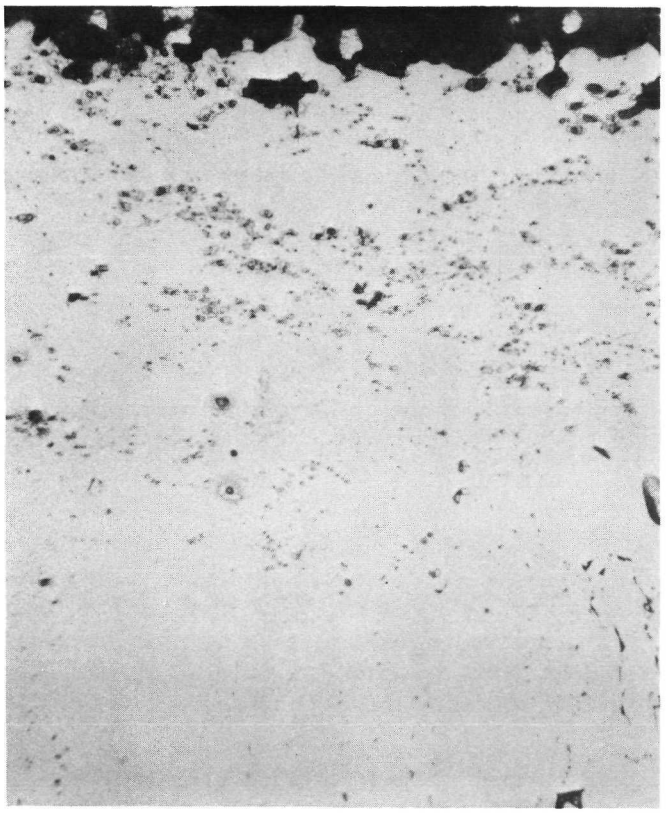

1533°K (2300°F)/100 Hrs/Argon

Figure 16. Metco Plasma-Gun Sprayed Hastelloy C-2a Barrier Layer with NC11-A Covercoat on TDNi. Unetched 500X

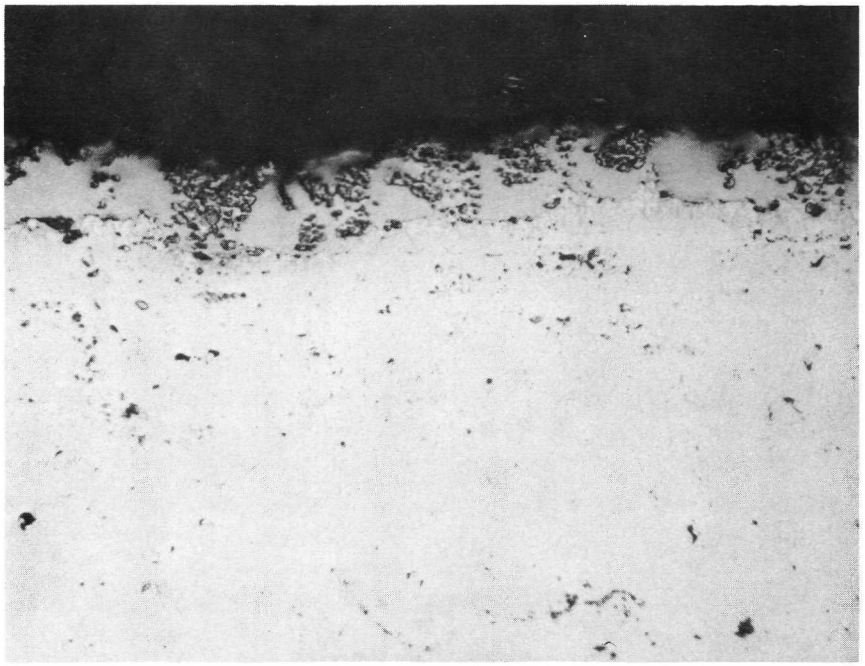

As-Processed

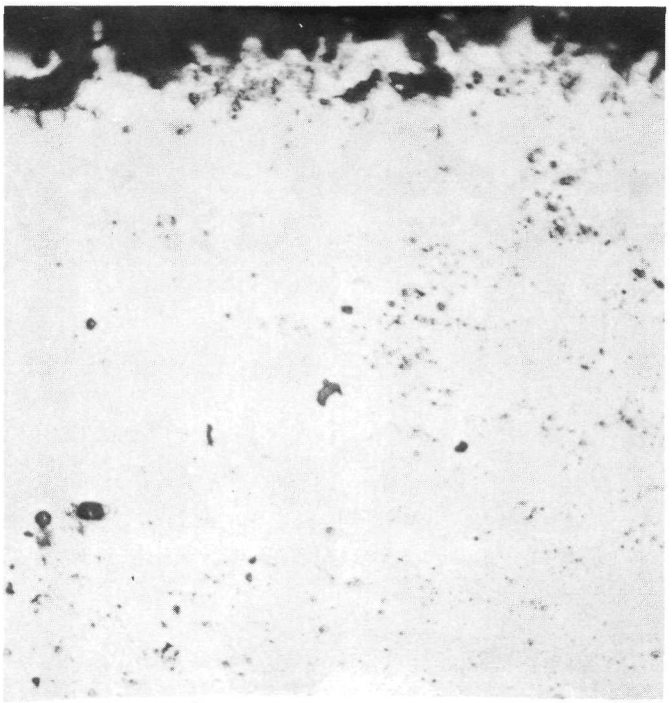

1533°K (2300°F)/100 Hrs/Argon

Figure 17. Metco Plasma-Gun Sprayed Hastelloy C-2a Barrier Layer with NC11-A Covercoat on TDNiCr. Unetched - 500X

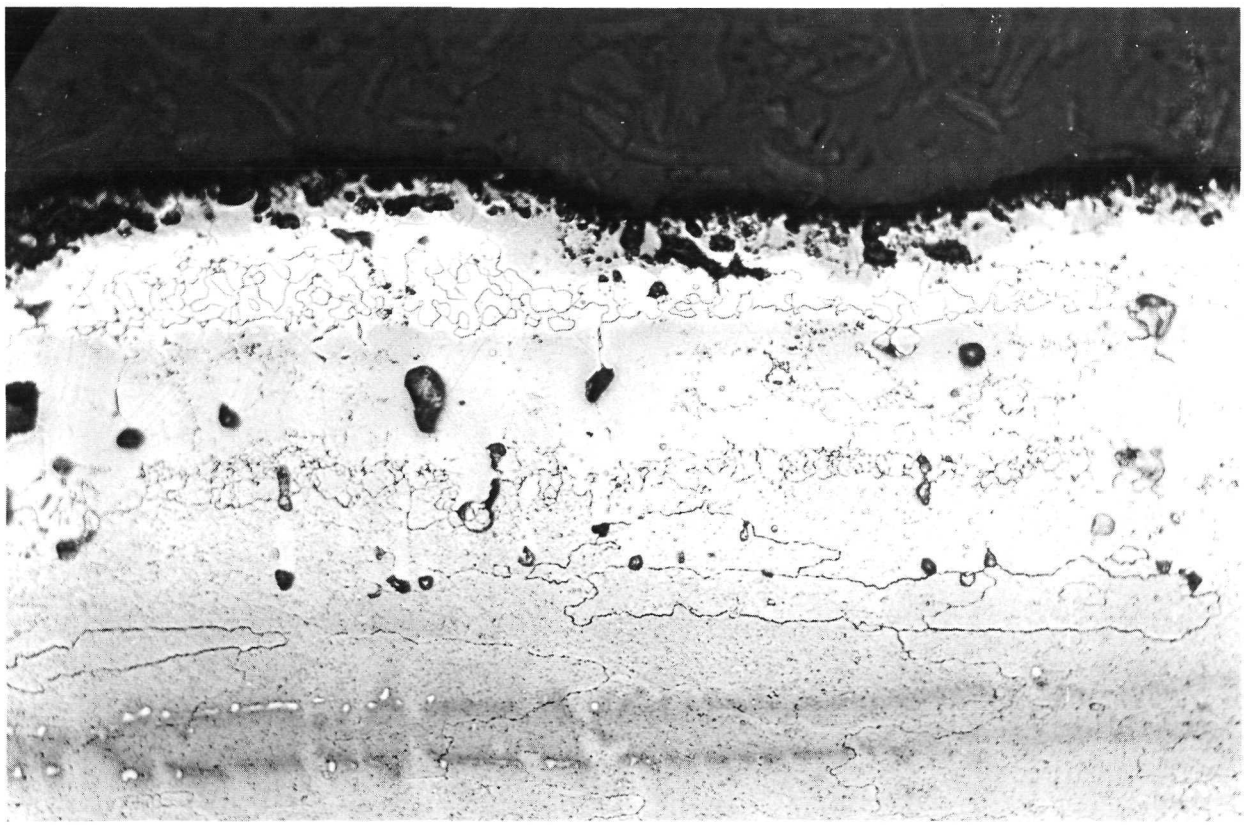

Figure 18. Metco Plasma-Gun Sprayed Hastelloy C-2a Barrier Layer with NC11-A Covercoat on TDNiCr. 1533°K (2300°F) Exposure. Etched - 250X, Chromic

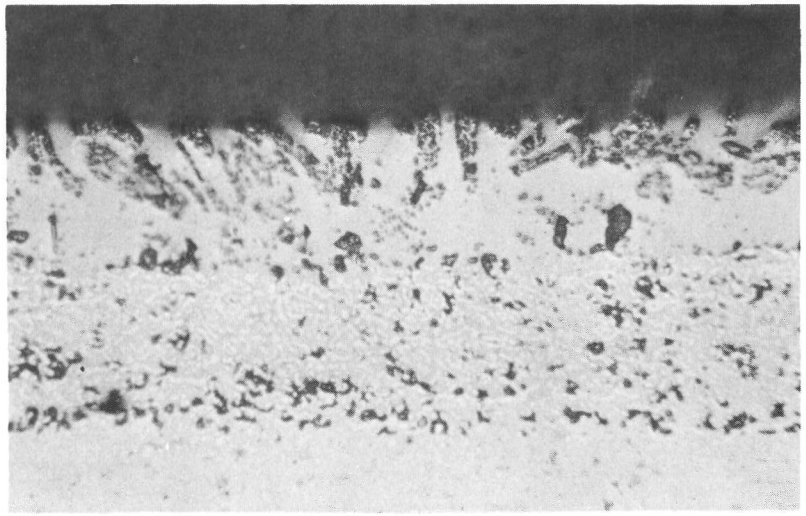

Chromized 1477°K (2200°F)/5 Hr
(As-Processed)

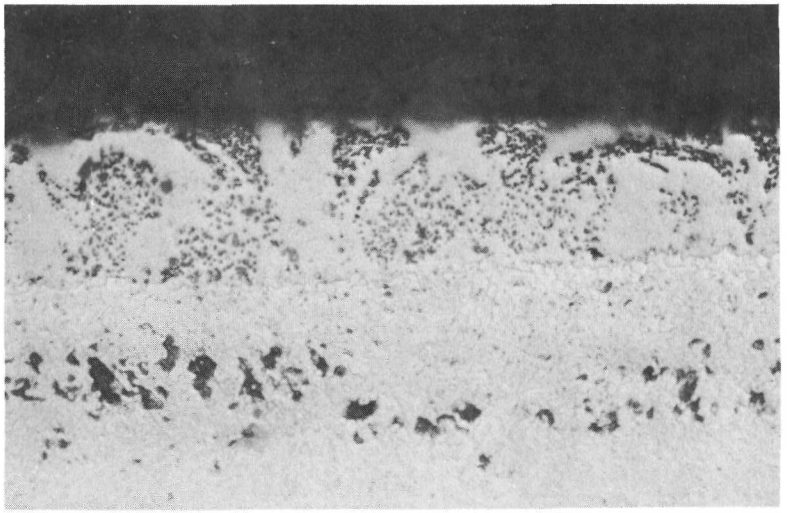

Chromized 1477°K (2200°F)/20 Hr
(As-Processed)

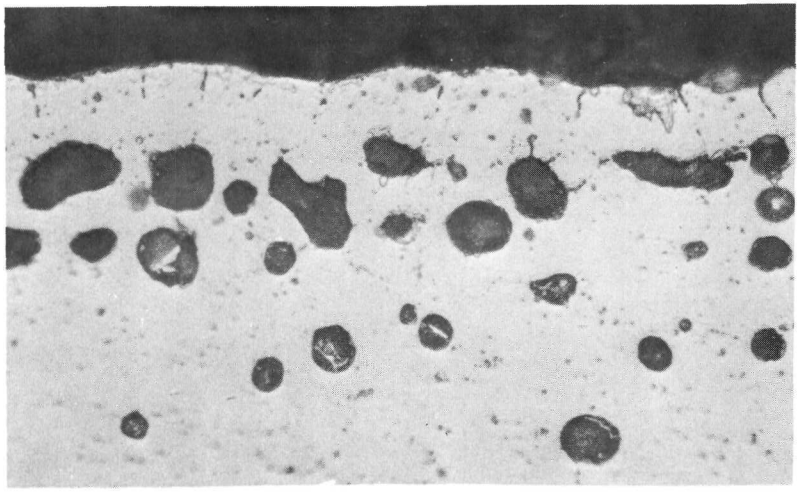

Chromized 1477°K (2200°F)/5 Hr
1533°K (2300°F)/100 Hr/A

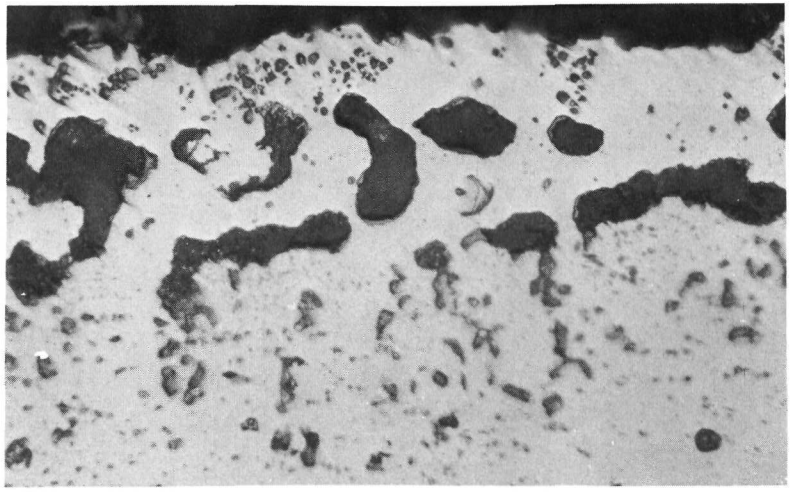

Chromized 1477°K (2200°F)/20 Hr
1533°K (2300°F)/100 Hr/A

Figure 19. Chromized/Carburized Barrier Layer and NC11-A Covercoat on TDNiCr As-Processed and After 1533°K (2300°F)/100 Hr Exposure. Unetched 500X

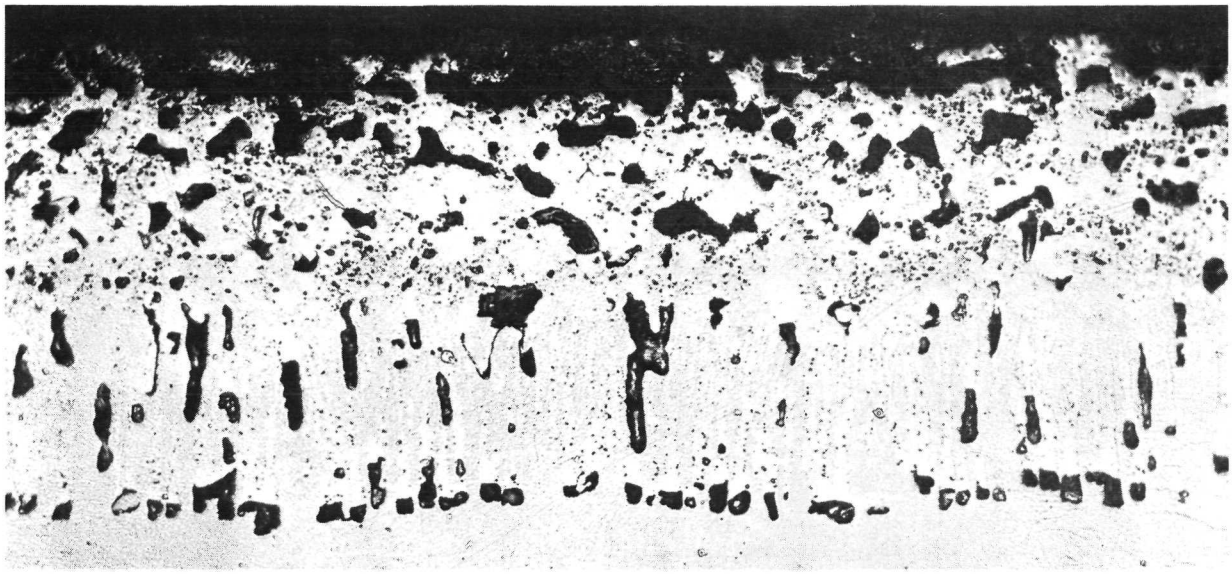

"Pullout" of Recrystallized TDNi Grains Due to Improper Polishing Technique

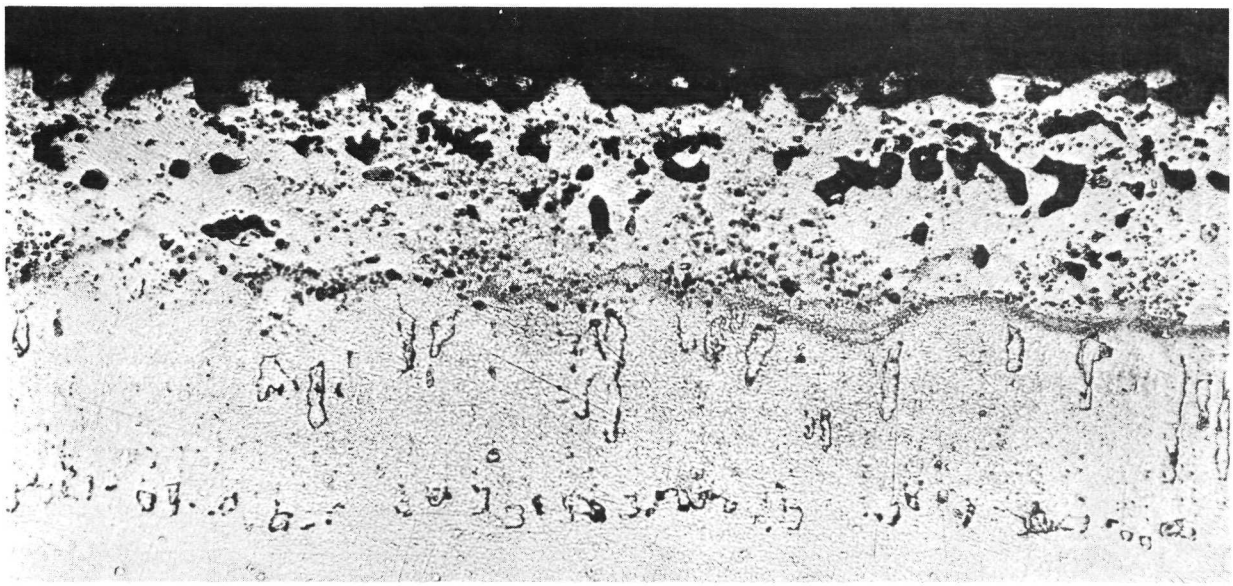

Retention of Recrystallized TDNi Grains with Proper Polishing Technique

Figure 20. Effect of Polishing Techniques on Appearance of Metallographic Structure of TDNi with NC11-A/Hastelloy C-2a Barrier After 1533°K (2300°F)/100 Hrs/Argon. Etched 250X

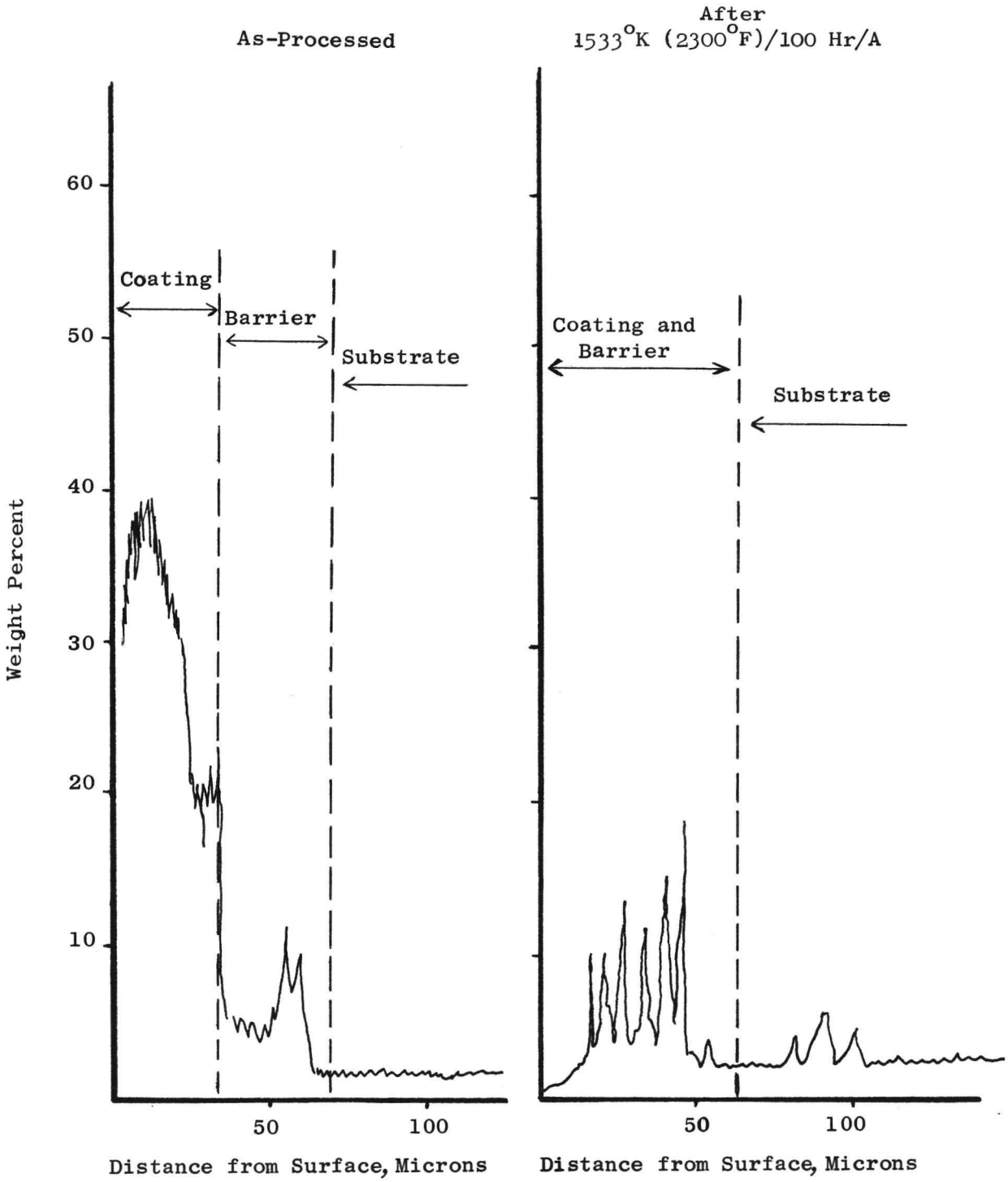

Figure 21 Electron Microprobe Traces for Al. X40 Barrier Layer on TDNiCr (AVCO Gun).

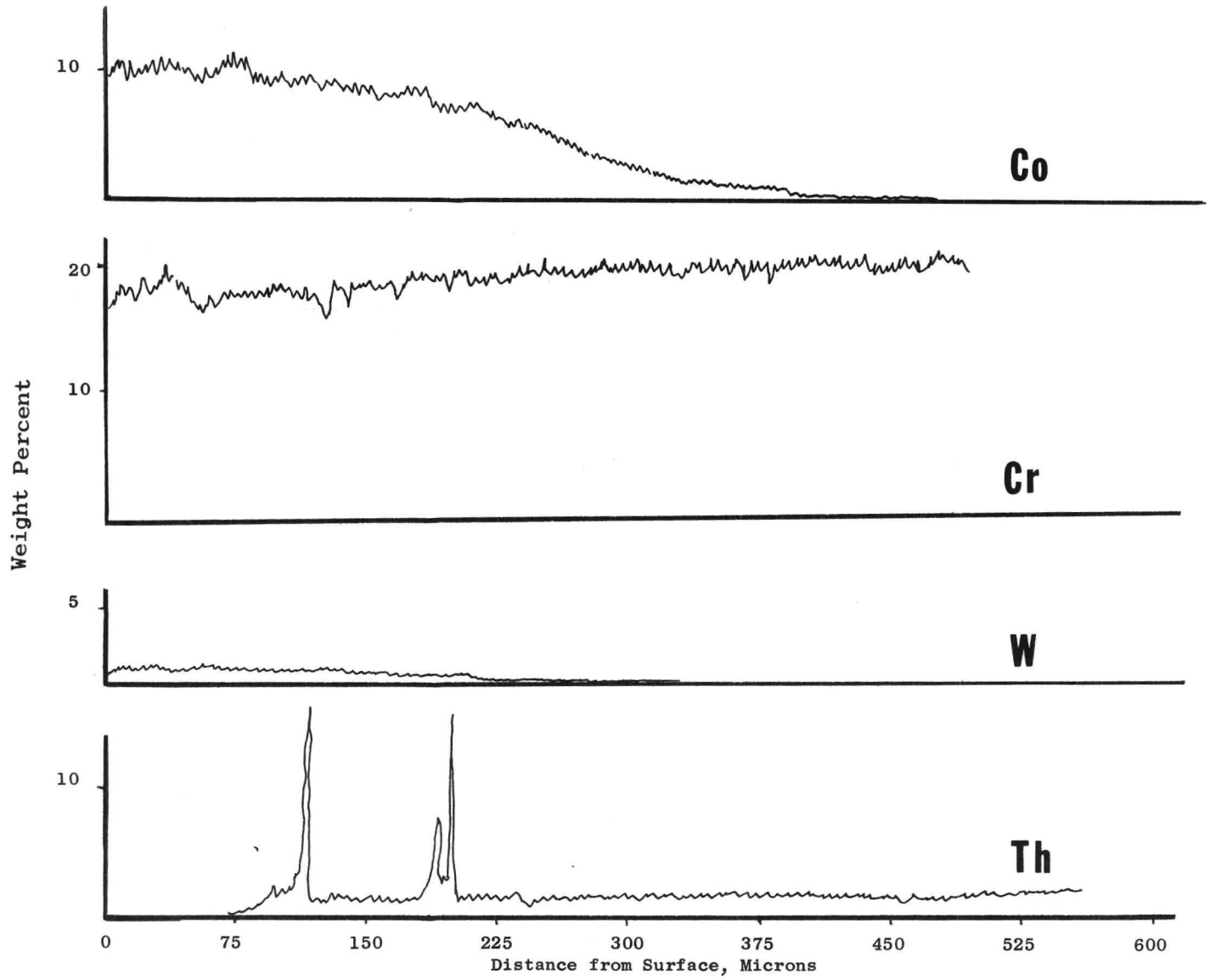

Figure 22. Electron Microprobe Elemental Traces for X40 Barrier Layer on TDNiCr After 1533°K (2300°F)/100 Hr/A Exposure (AVCO Gun).

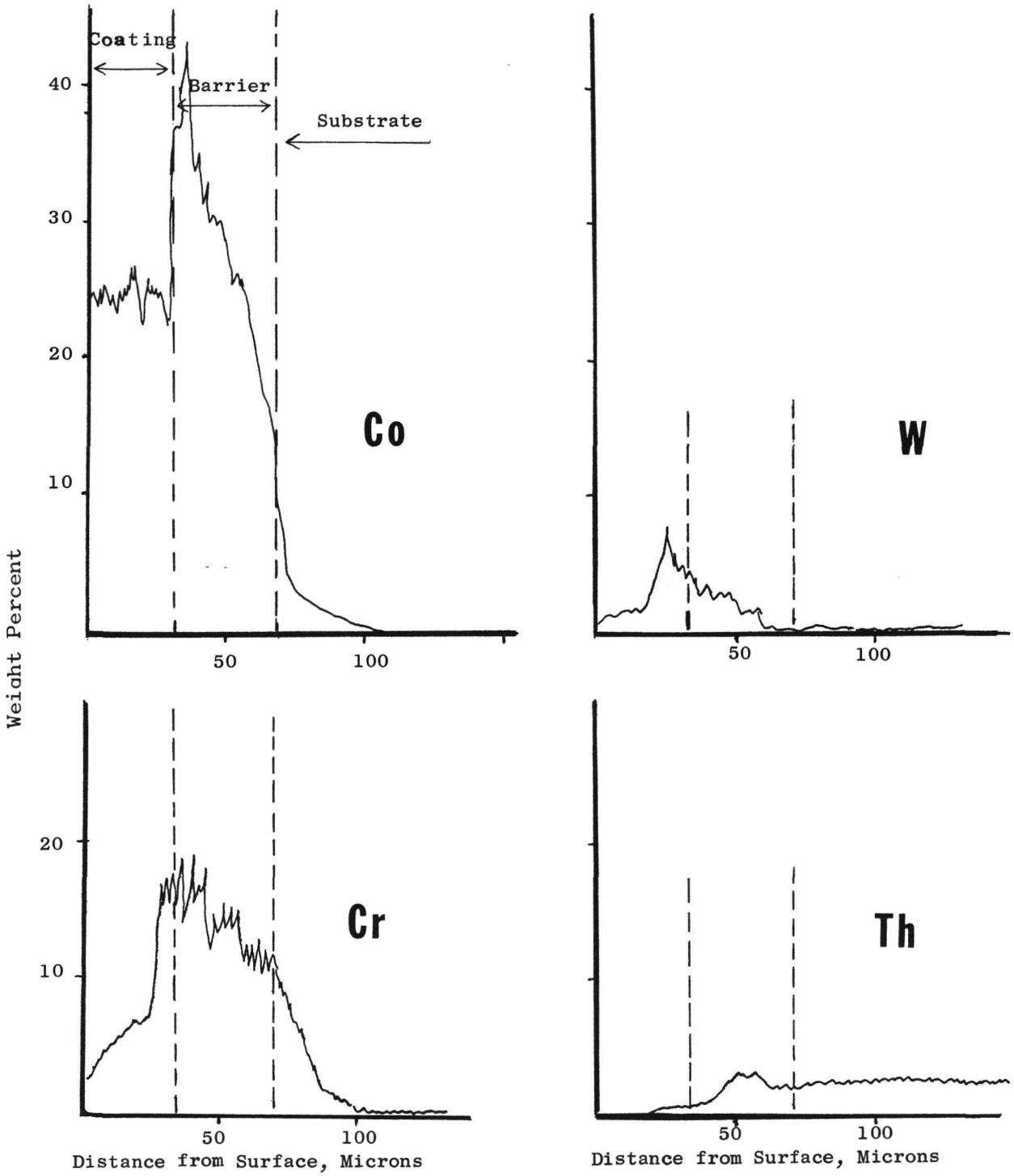

Figure 23. Electron Microprobe Elemental Traces for X40 Barrier Layer on TDNi, As-Processed (AVCO Gun).

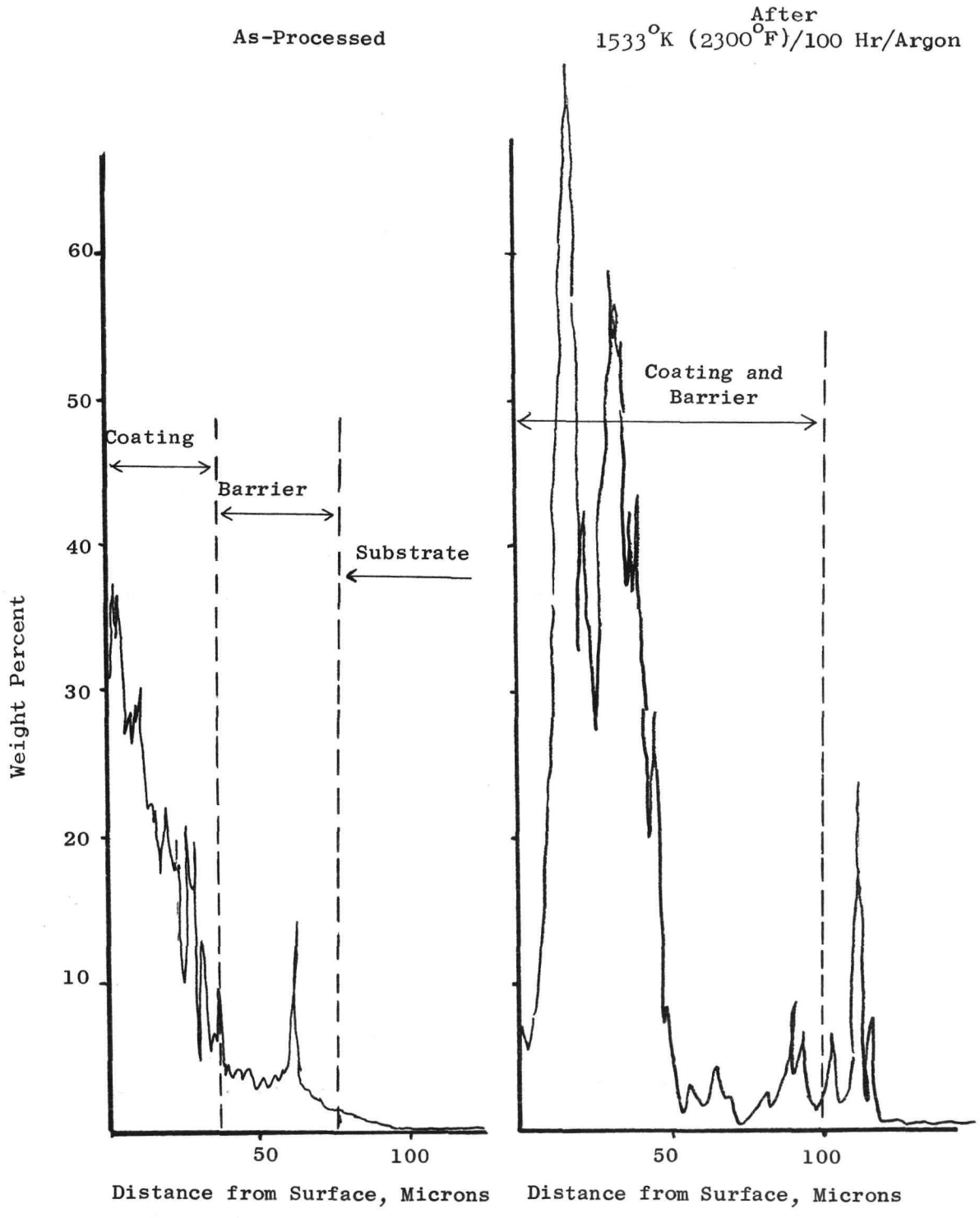

Figure 24 Electron Microprobe Traces for Al. Hastelloy C-1 Barrier Layer on TDNi (AVCO Gun).

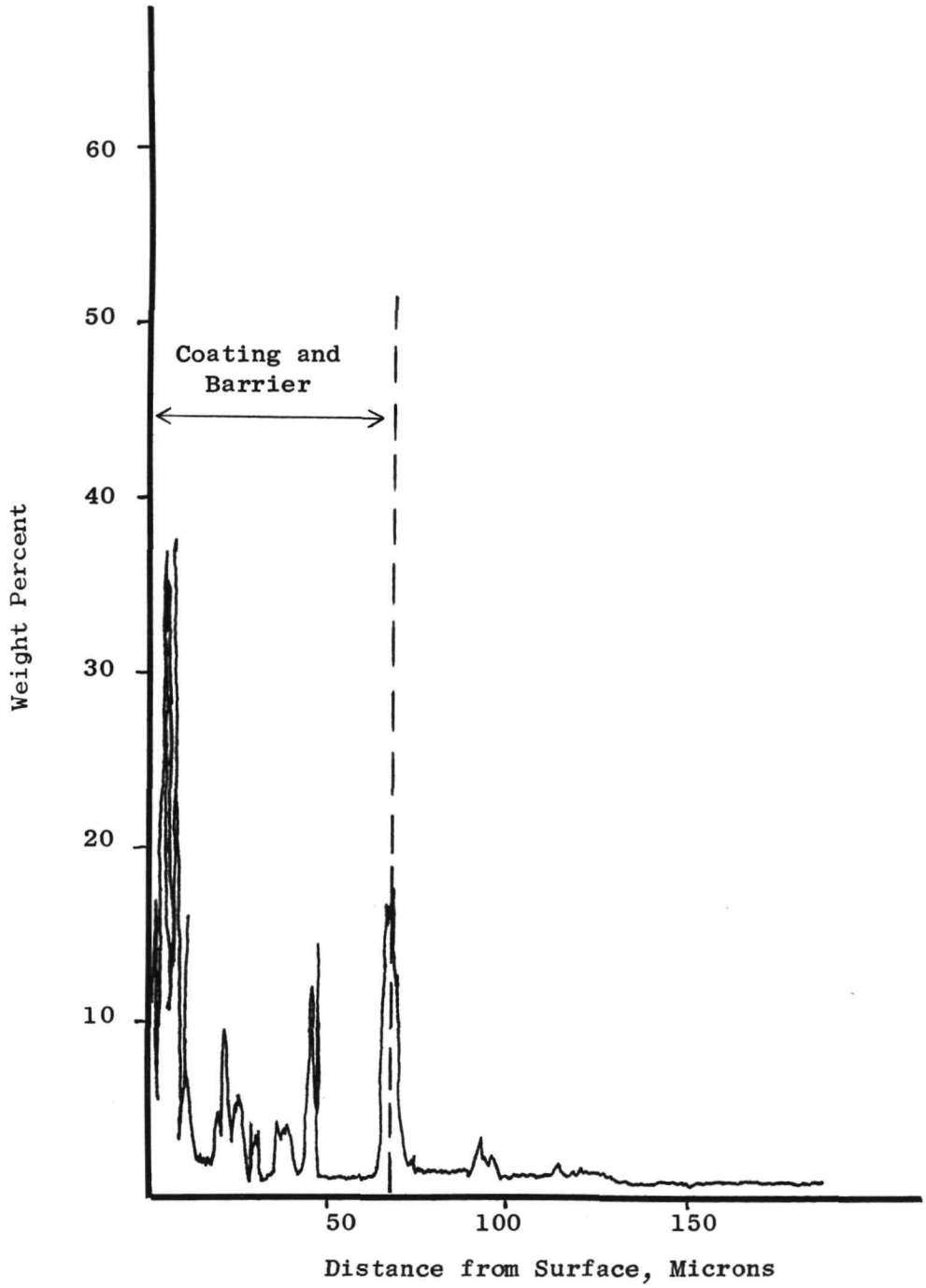

Figure 25 Electron Microprobe Traces for Al. Hastelloy C-1 Barrier Layer on TDNi After 1533°K (2300°F)/100 Hr/A Exposure (Metco Gun).

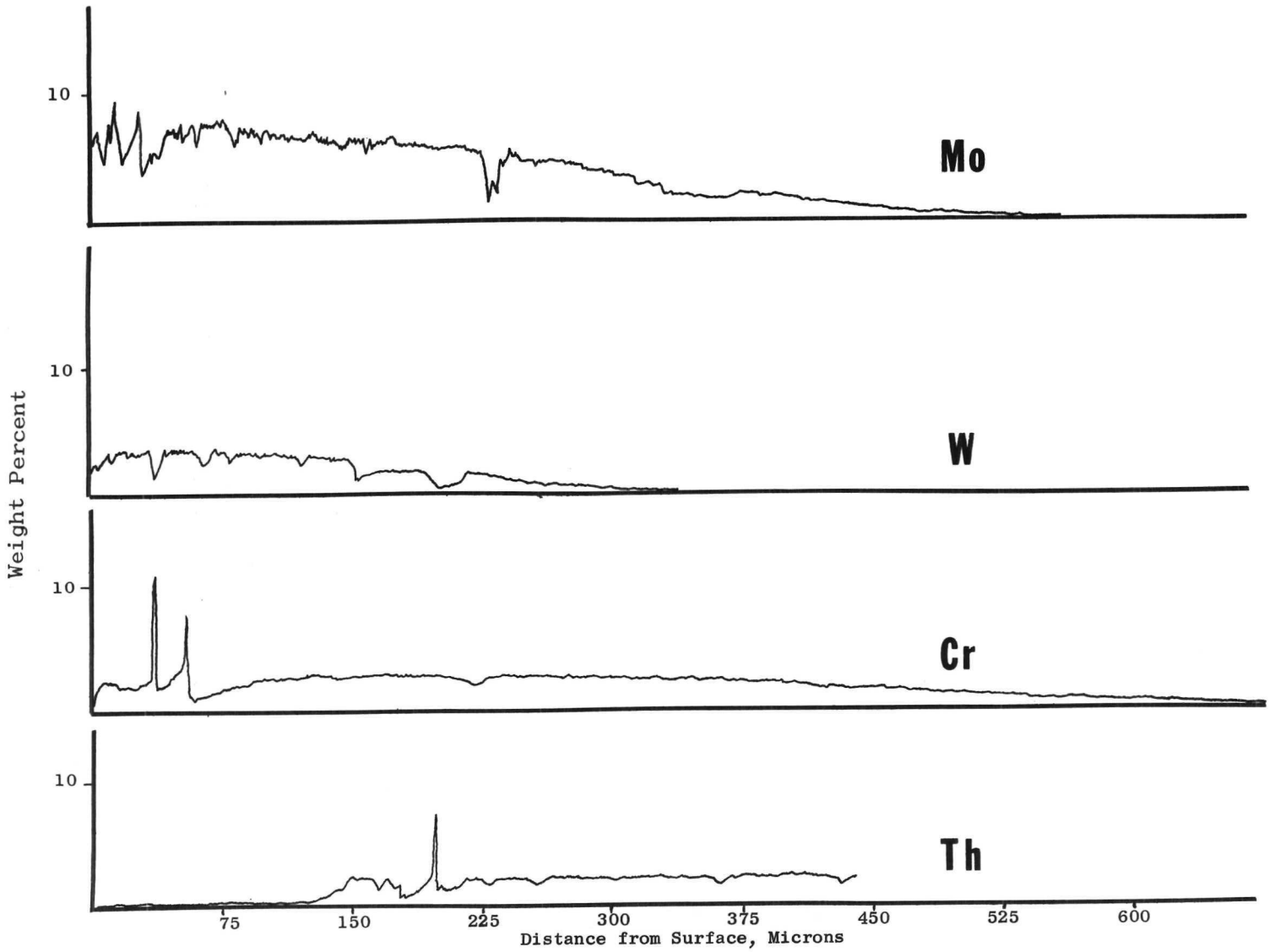

Figure 26. Electron Microprobe Traces for Hastelloy C-1 Barrier Layer on TDNi After 1533°K (2300°F)/100 Hr/A Exposure (AVCO Gun).

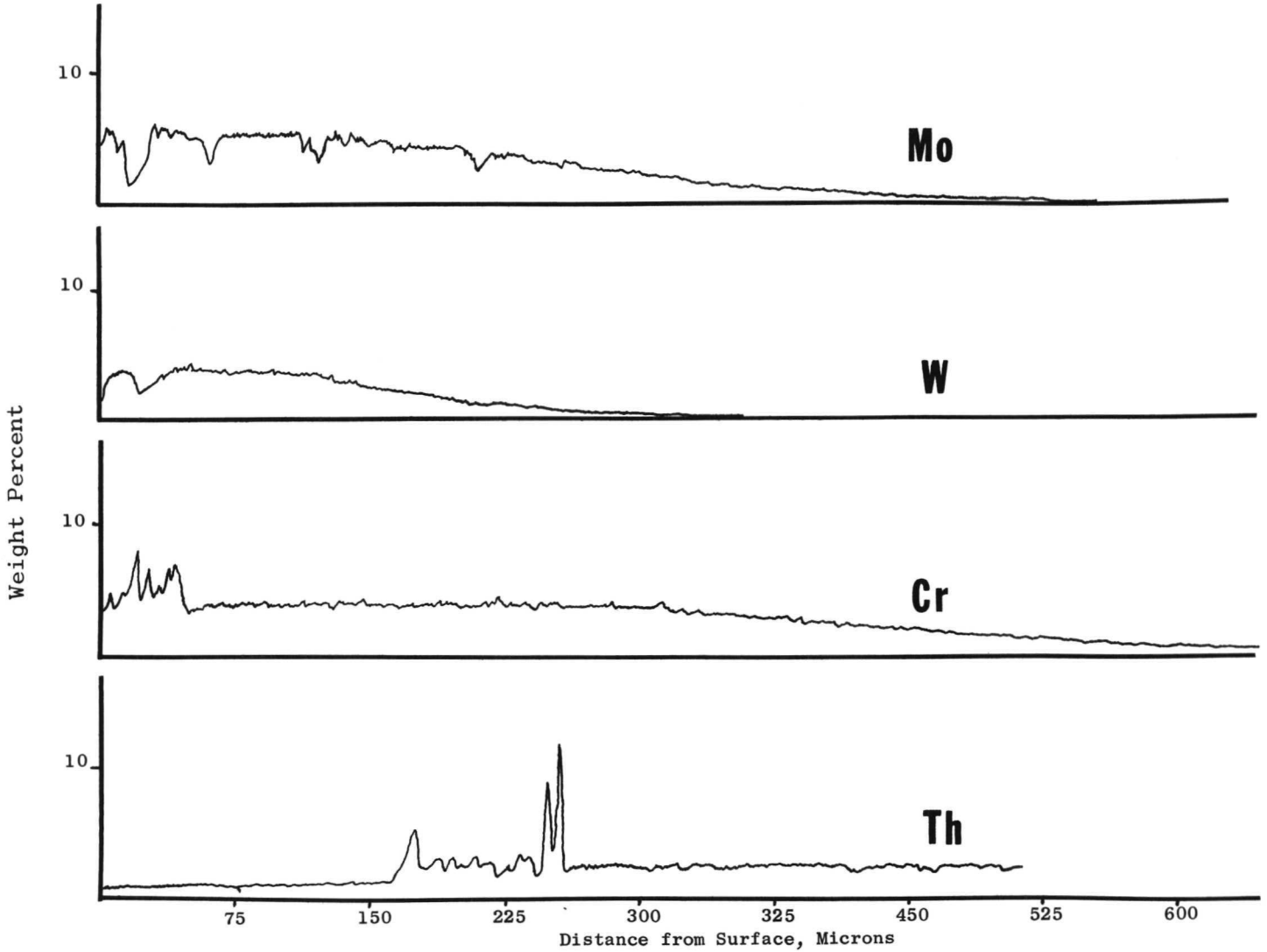

Figure 27. Electron Microprobe Traces for Hastelloy C-1 Barrier Layer on TDNi After 1533°K (2300°F)/100 Hr/A Exposure (Metco Gun).

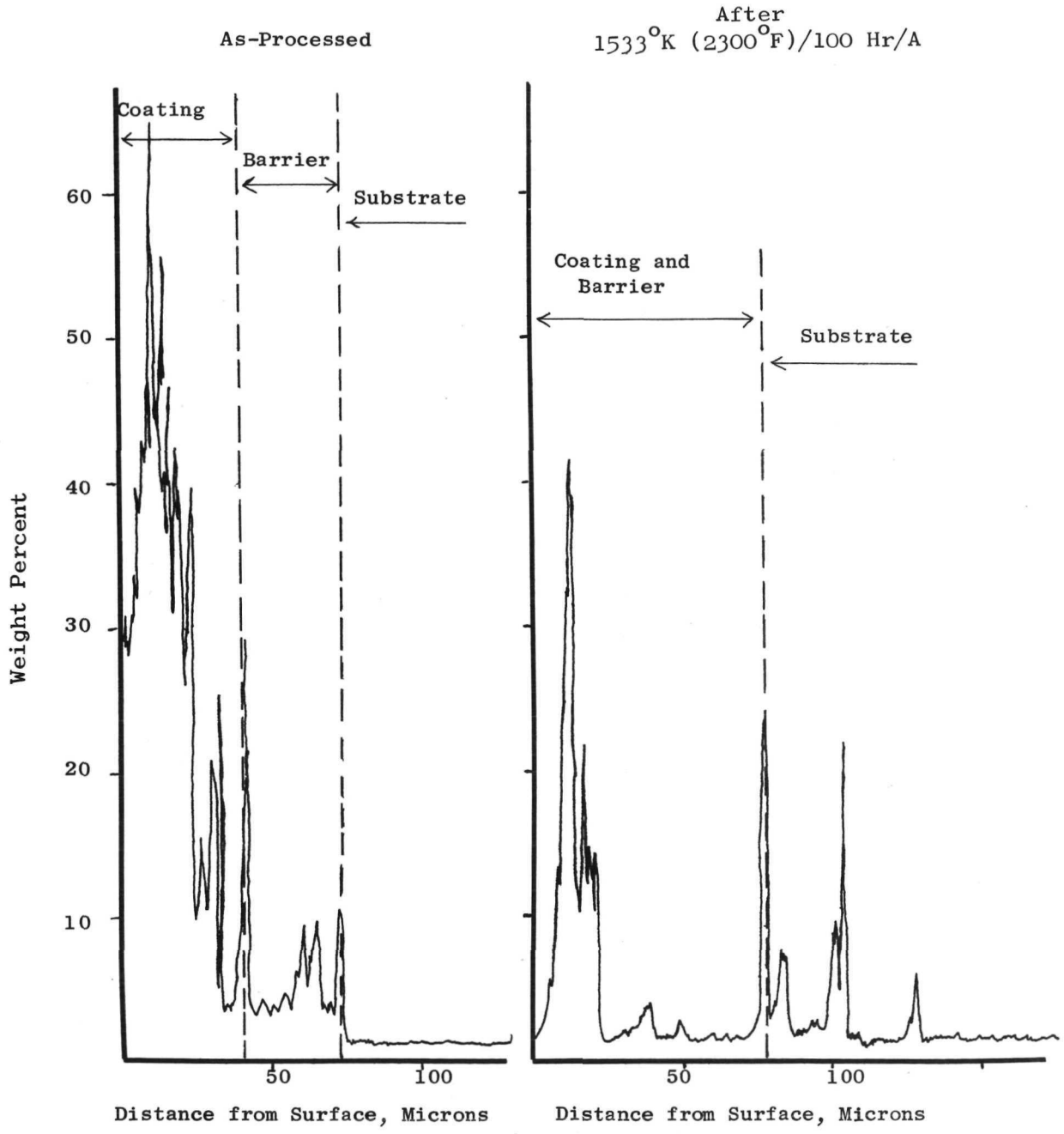

Figure 28 Electron Microprobe Traces for Al. Hastelloy C-1 Barrier Layer on TDNiCr (Metco Gun).

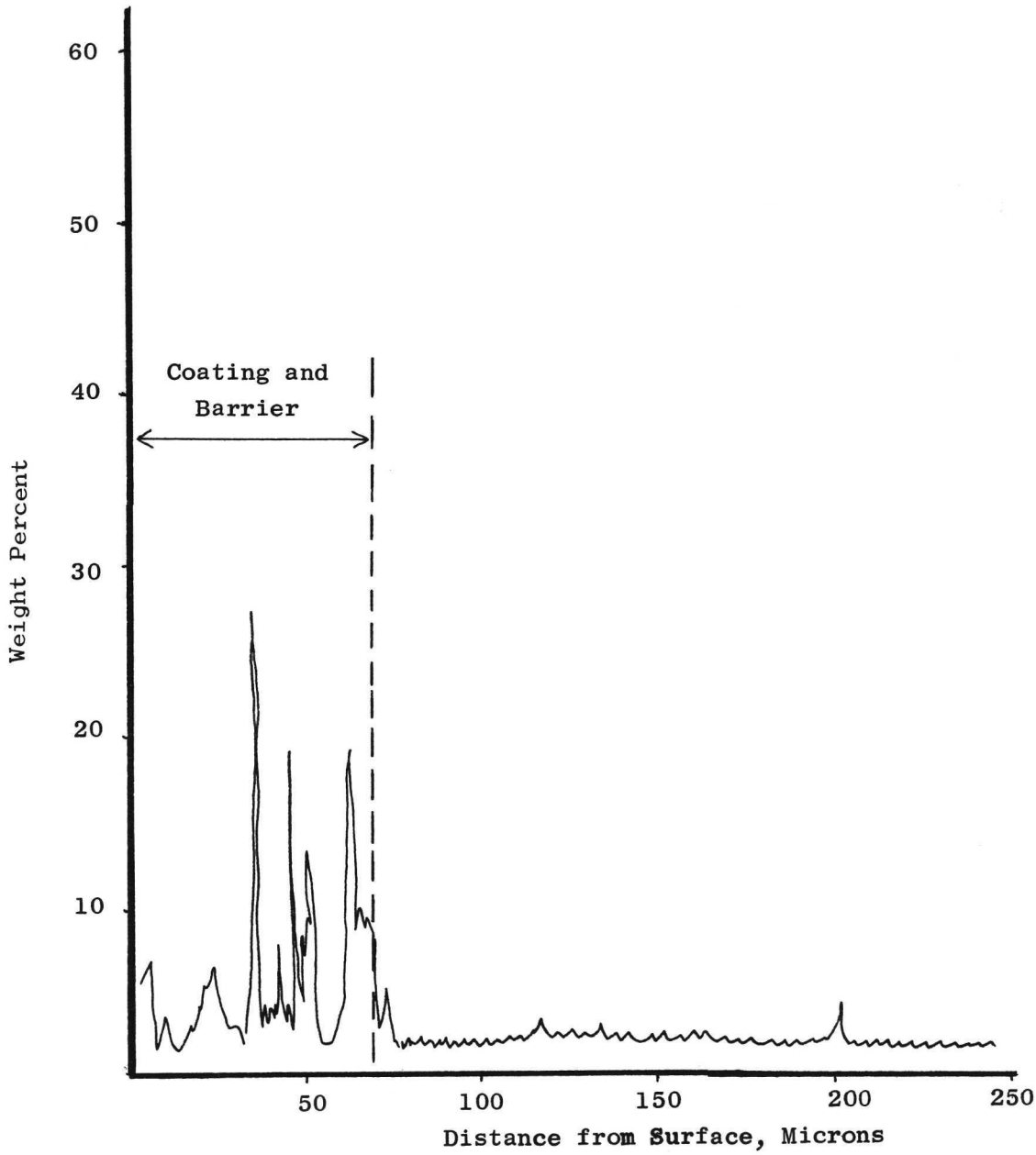

Figure 29 Electron Microprobe Traces for Al. Hastelloy C-1 Barrier Layer on TDNiCr After 1533°K (2300°F)/100 Hr/A Exposure (AVCO Gun).

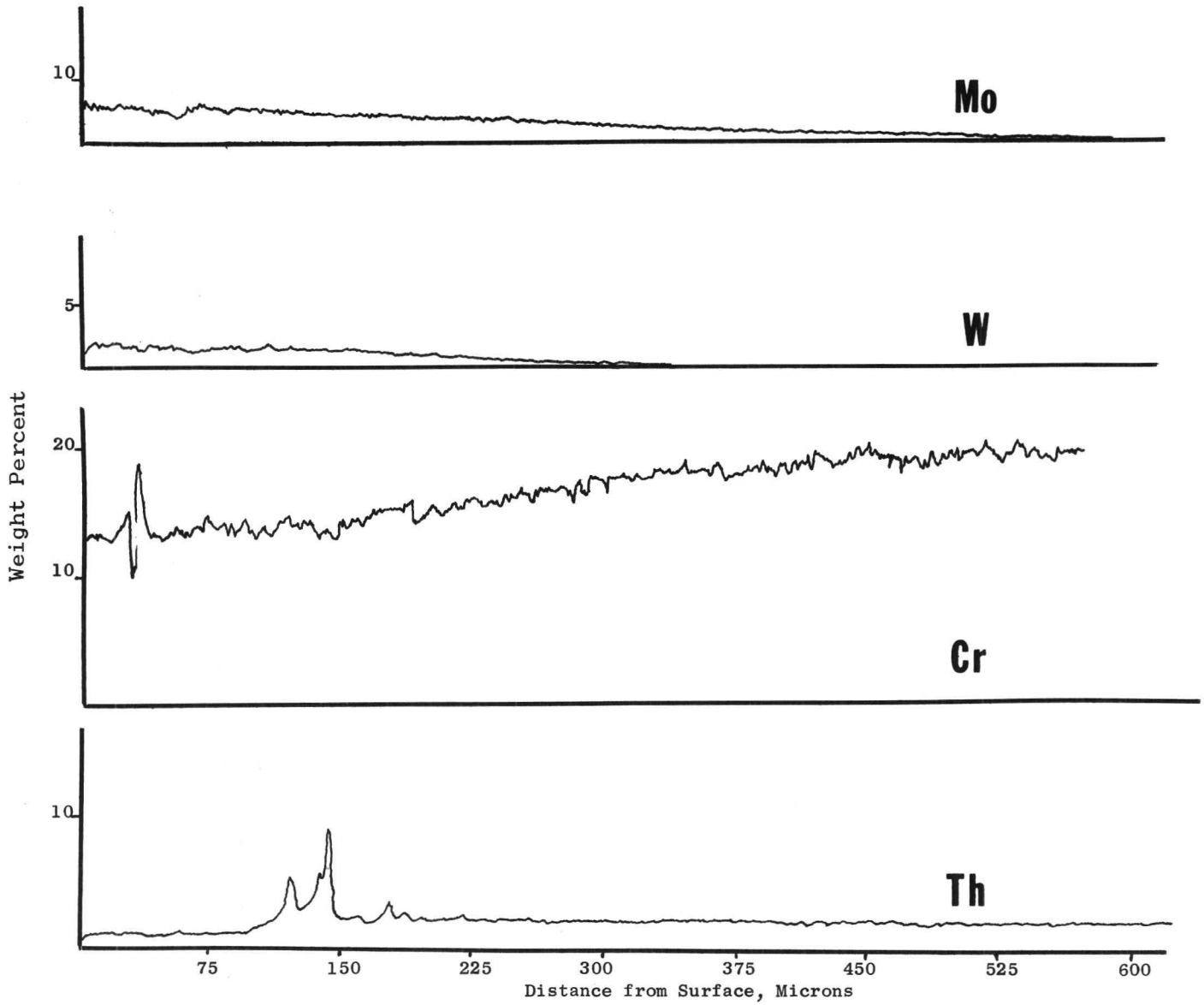

Figure 30. Electron Microprobe Traces for Hastelloy C-1 Barrier Layer on TDNiCr After 1533°K (2300°F)/100 Hr/A Exposure (AVCO Gun).

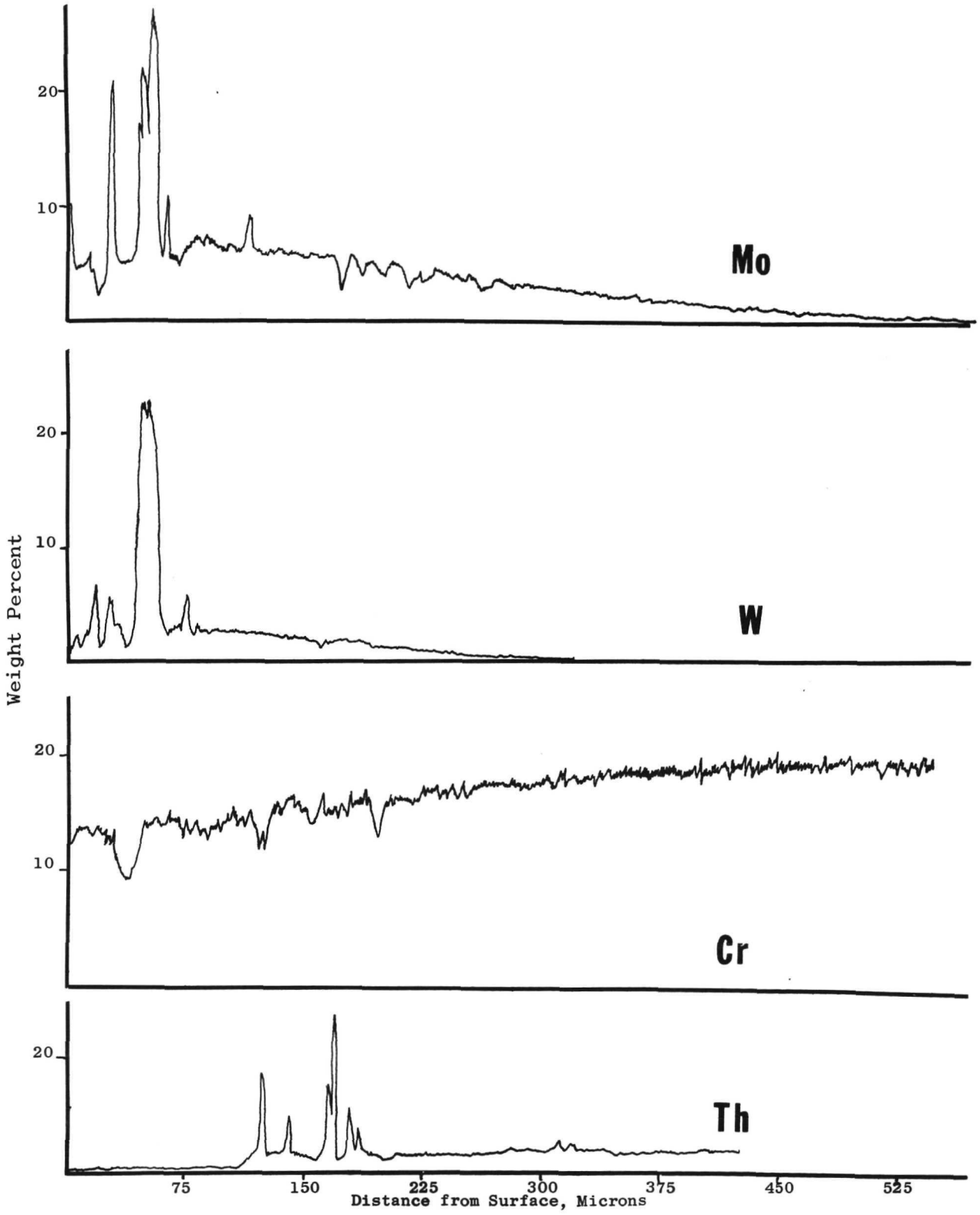

Figure 31. Electron Microprobe Elemental Traces for Hastelloy C-1 Barrier Layer on TDNiCr After 1533°K (2300°F)/100 Hr/A Exposure (Metco Gun).

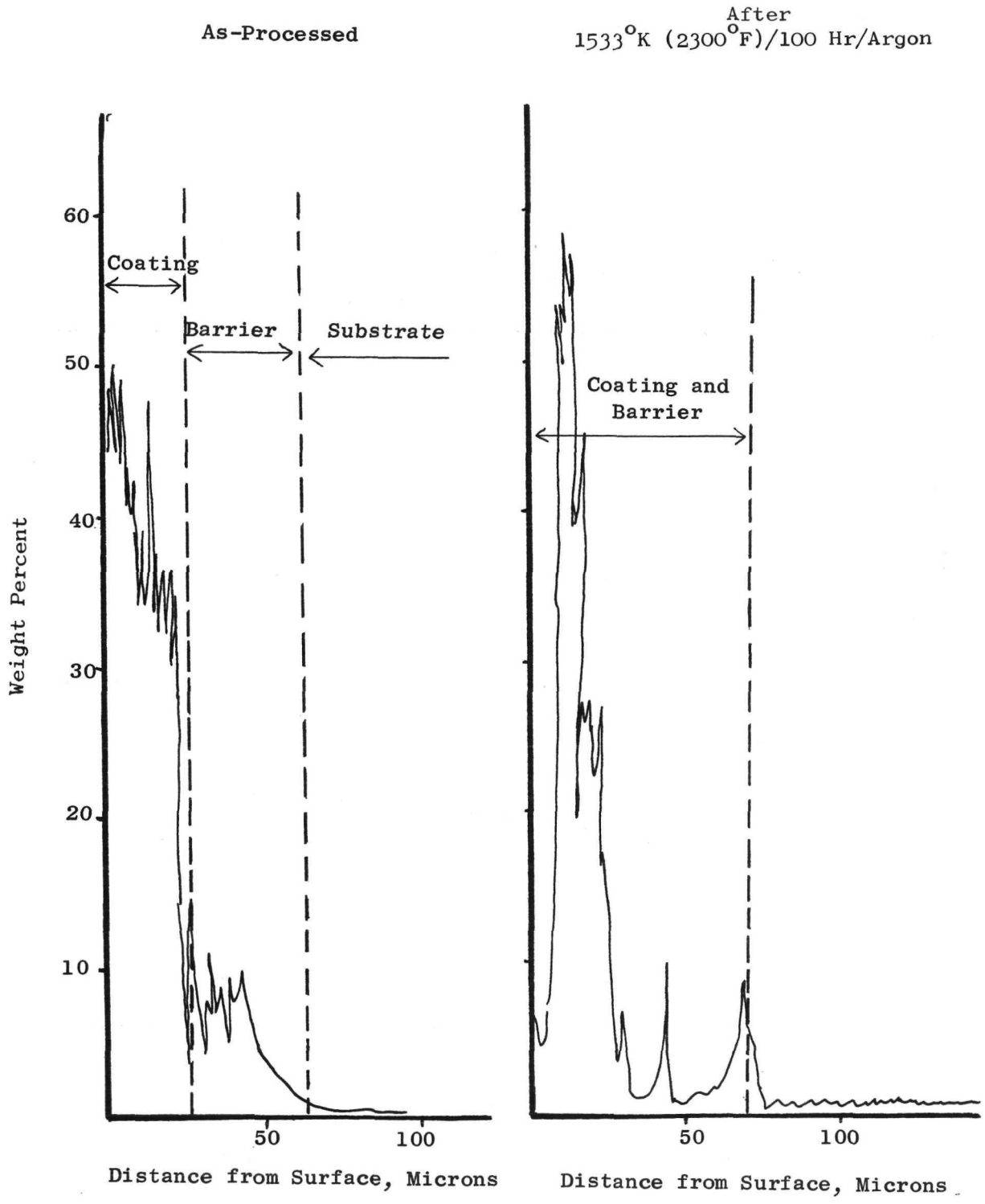

Figure 32 Electron Microprobe Traces for Al. Hastelloy C-2 Barrier Layer on TDNi (AVCO Gun).

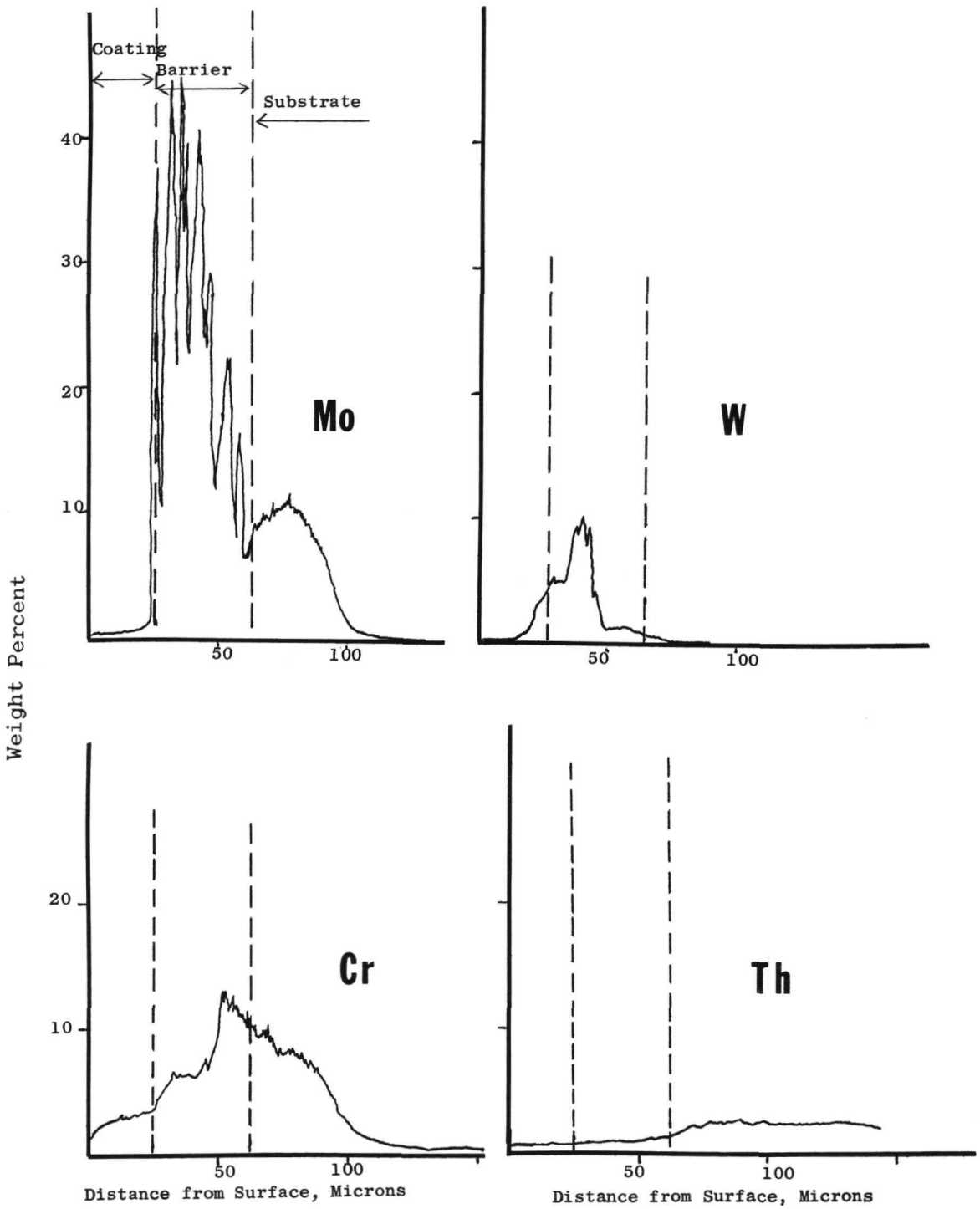

Figure 33. Electron Microprobe Traces for Hastelloy C-2 Barrier Layer on TDNi, As-Processed (AVCO Gun).

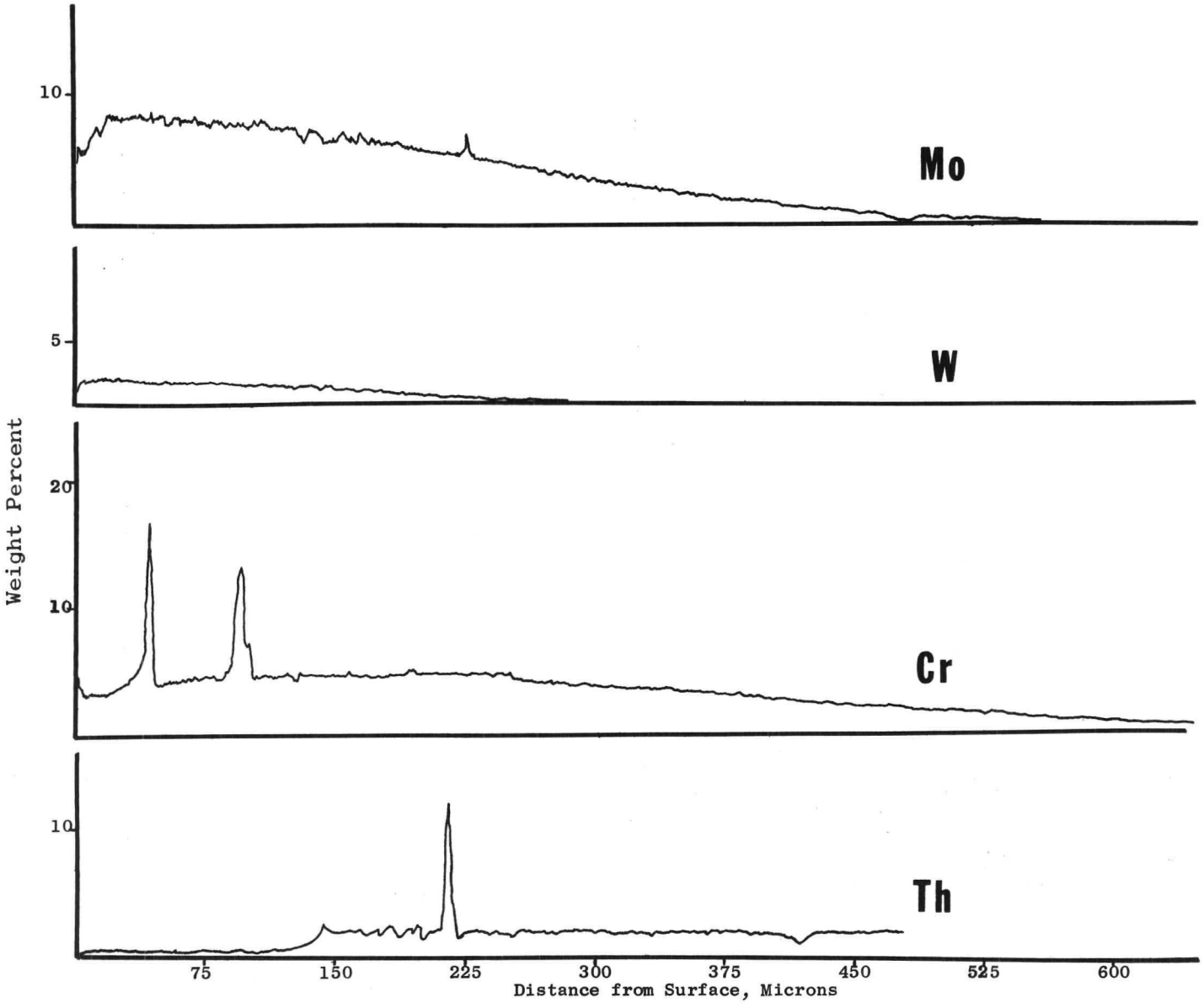

Figure 34. Electron Microprobe Elemental Traces for Hastelloy C-2 Barrier Layer on TDNi After 1533°K (2300°F)/100 Hr/A Exposure (Metco Gun).

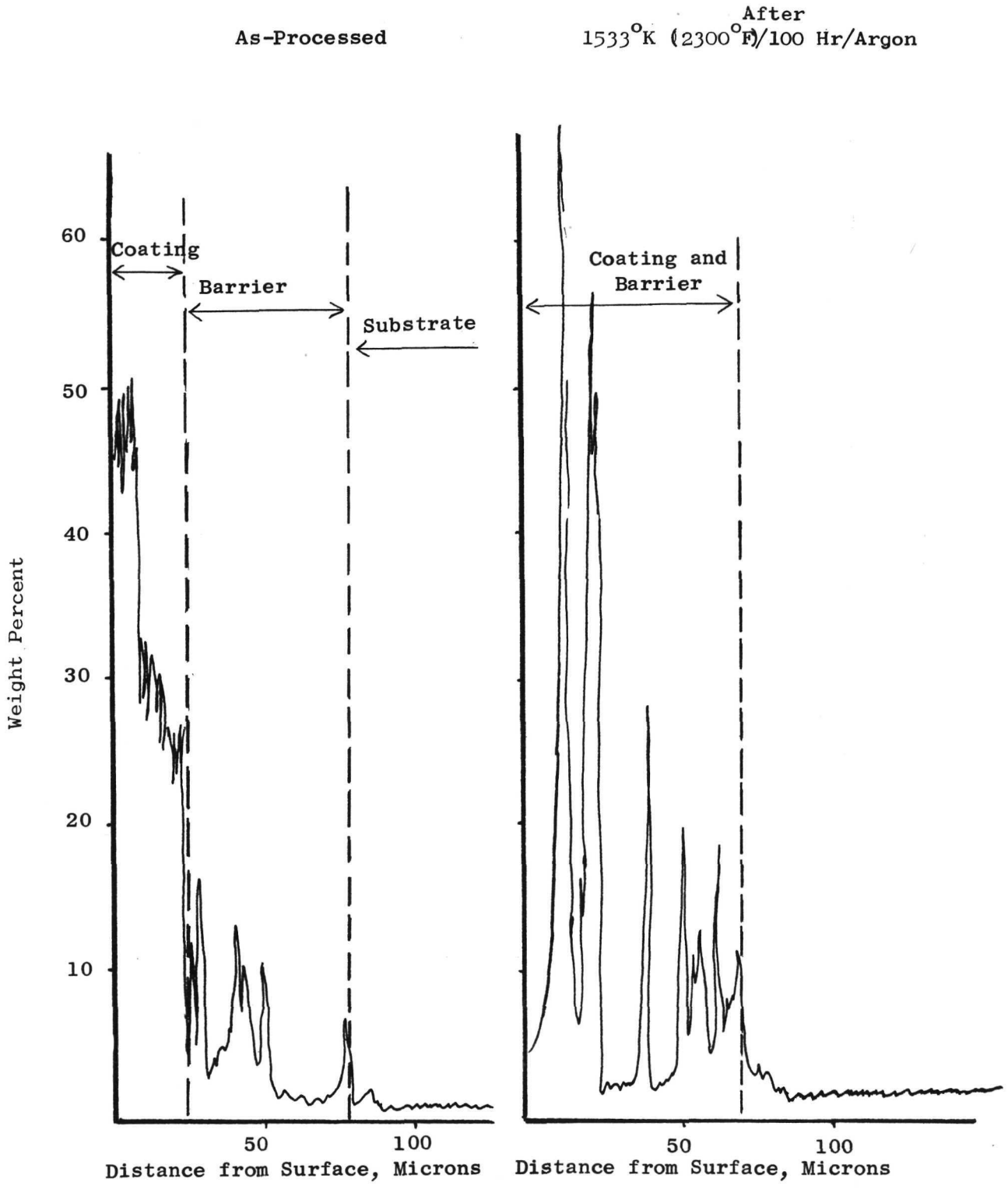

Figure 35 Electron Microprobe Traces for Al. Hastelloy C-2 Barrier Layer on TDNiCr (AVCO Gun).

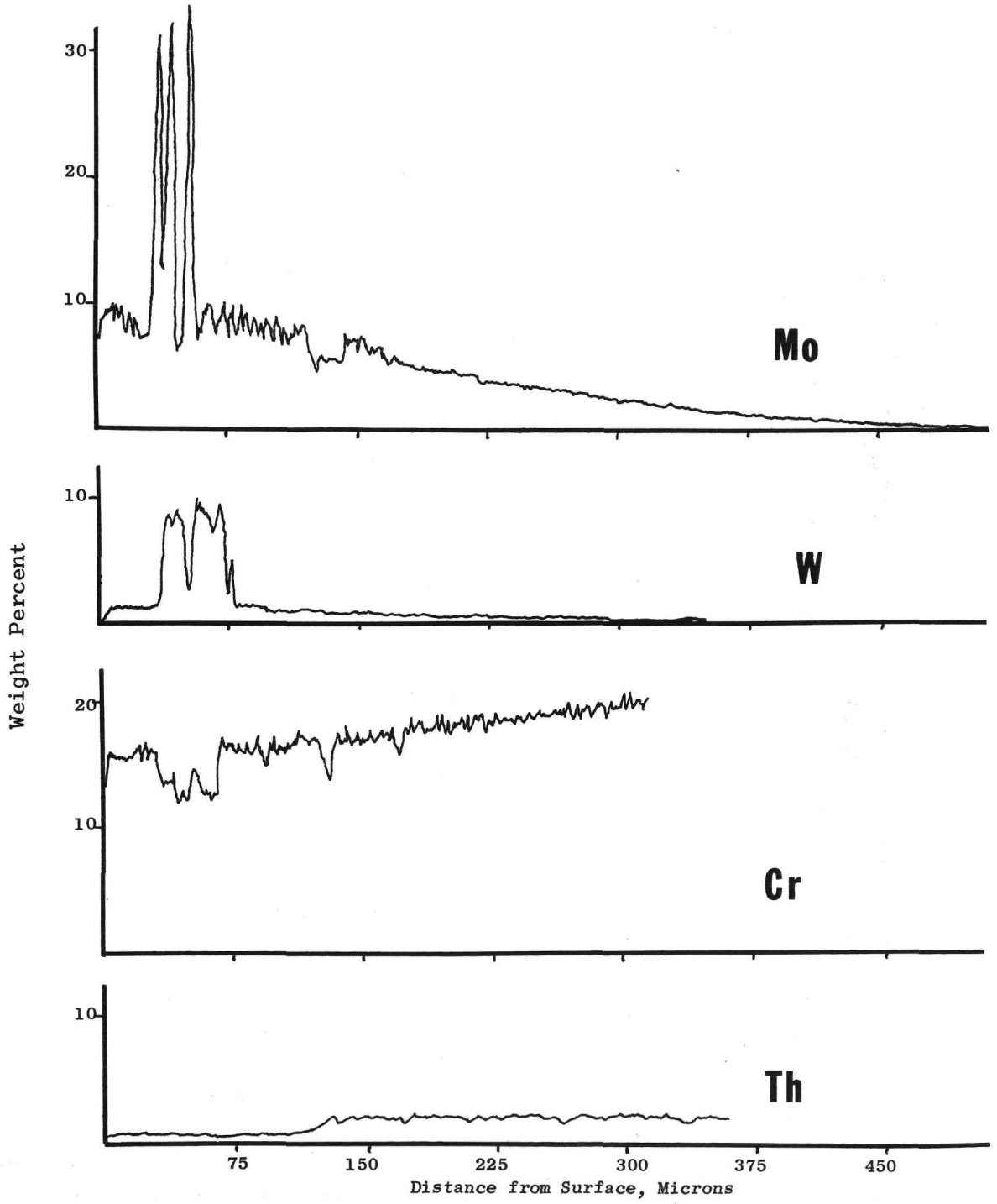

Figure 36. Electron Microprobe Traces for Hastelloy C-2 Barrier Layer on TDNiCr After 1533°K (2300°F)/100 Hr/A Exposure (Metco Gun).

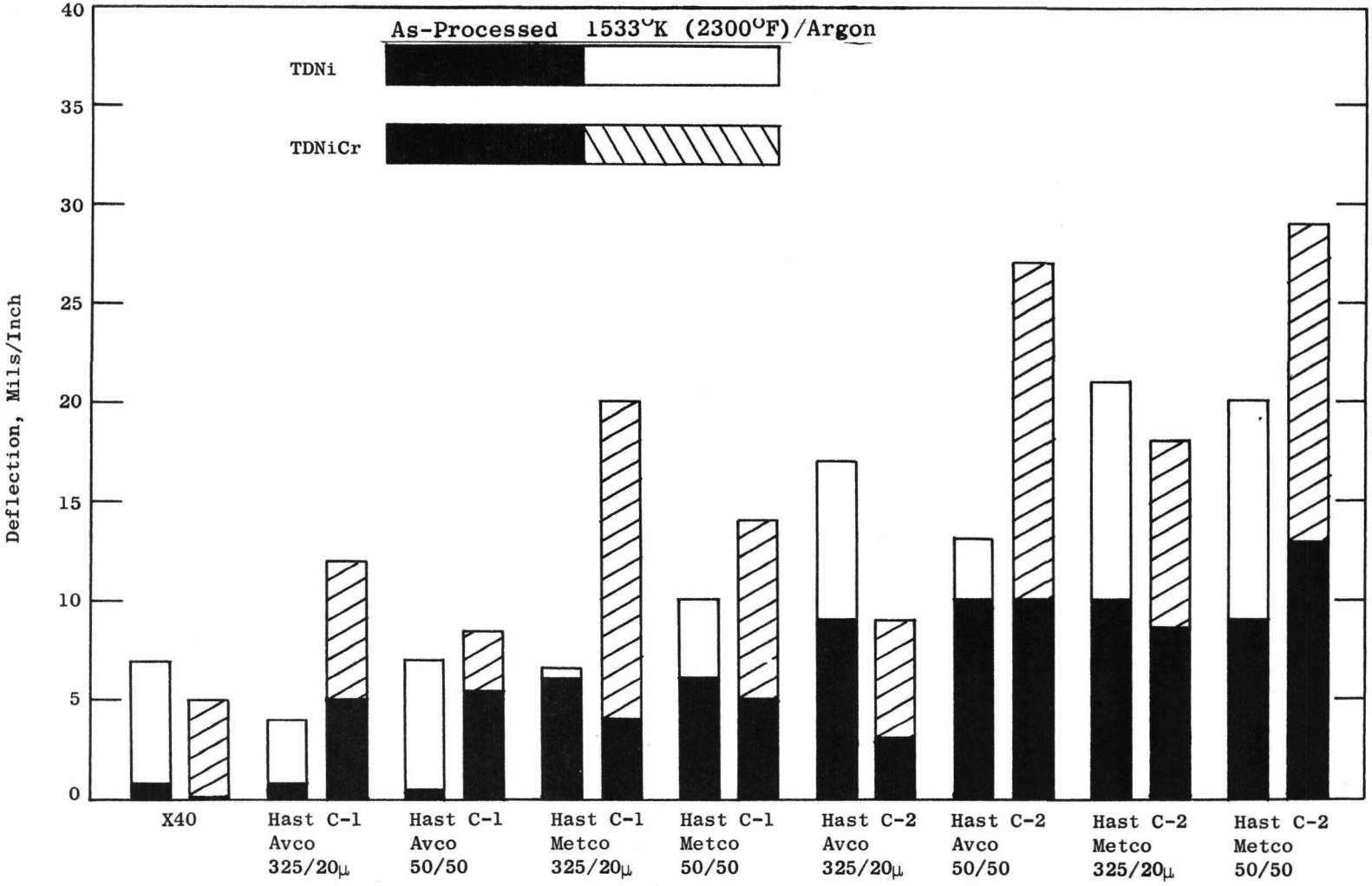

Figure 37. Deflection of TDNi and TDNiCr Panels Due to Barrier Layer, As-Processed and After 1533°K (2300°F)/100 Hr/Argon

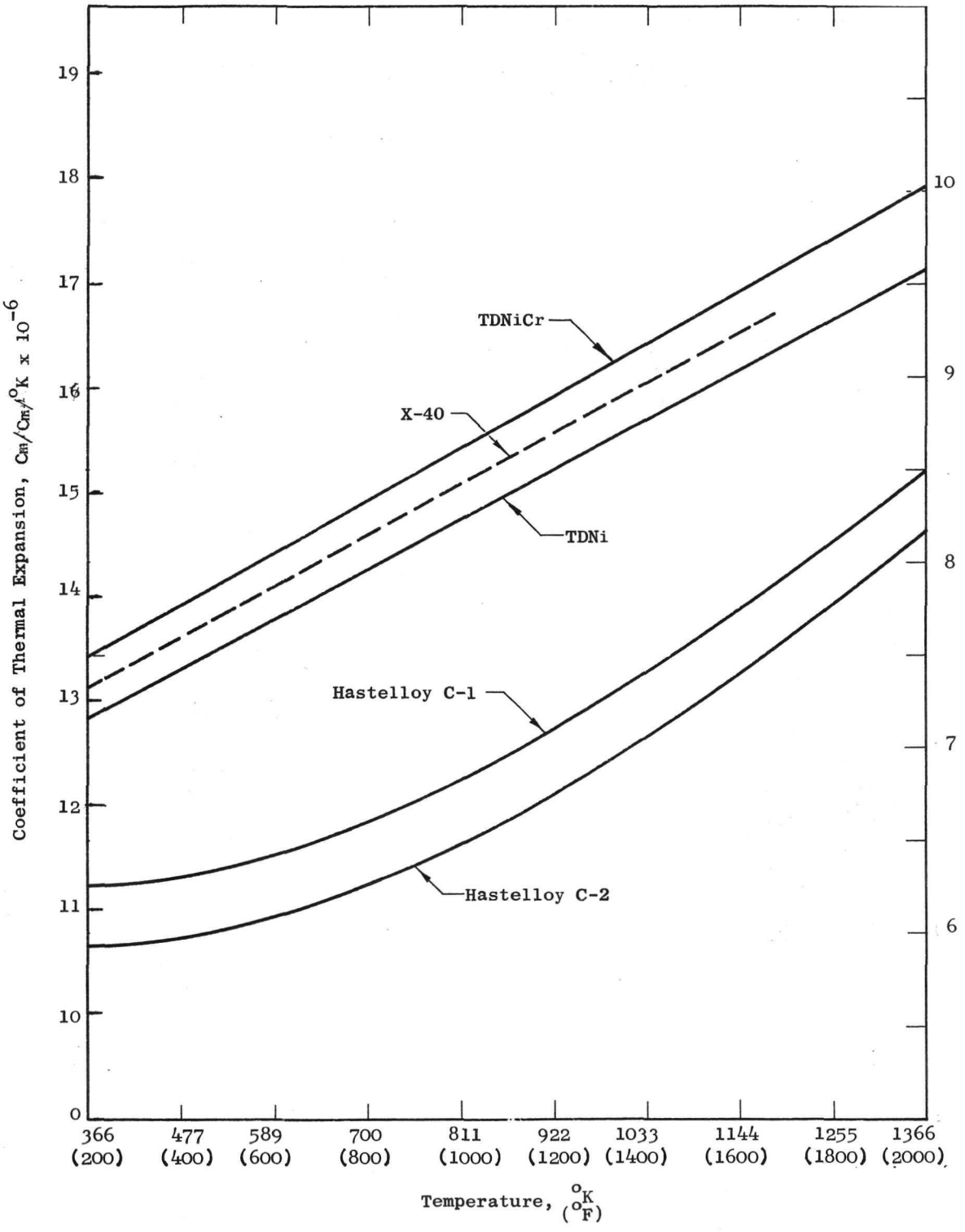

Figure 38. Coefficient of Expansion of TDNi, TDNiCr, and Barrier Layer Materials.

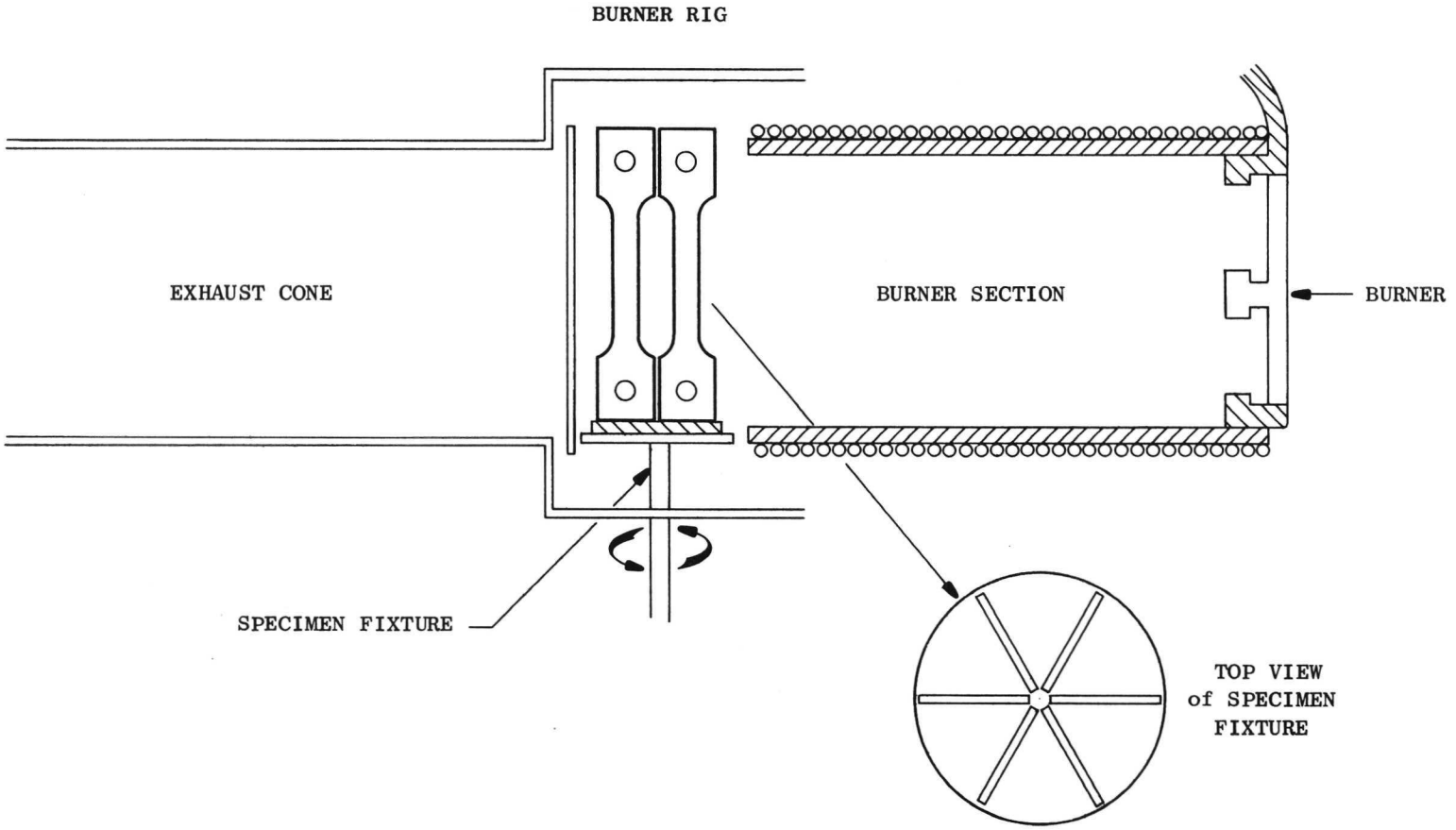

Figure 39. Modified M&PTL Burner Rig for Cycle Testing of Coated TDNi and TDNiCr Tensile Specimens.

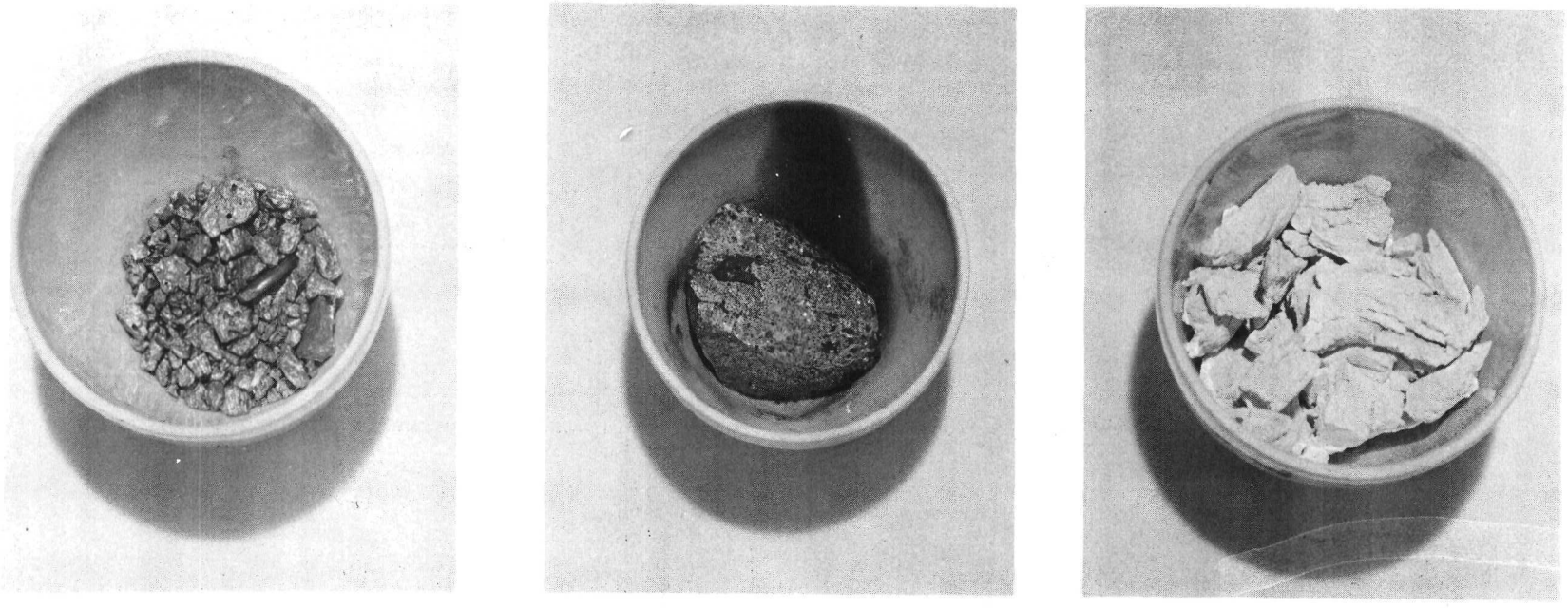

Cr_5Al_8 CoAl $MoAl_2$

Figure 40. Aluminum-Rich Compounds After 113 Hours at 1366°K (2000°F). Note Catastrophic Oxidation of $MoAl_2$.

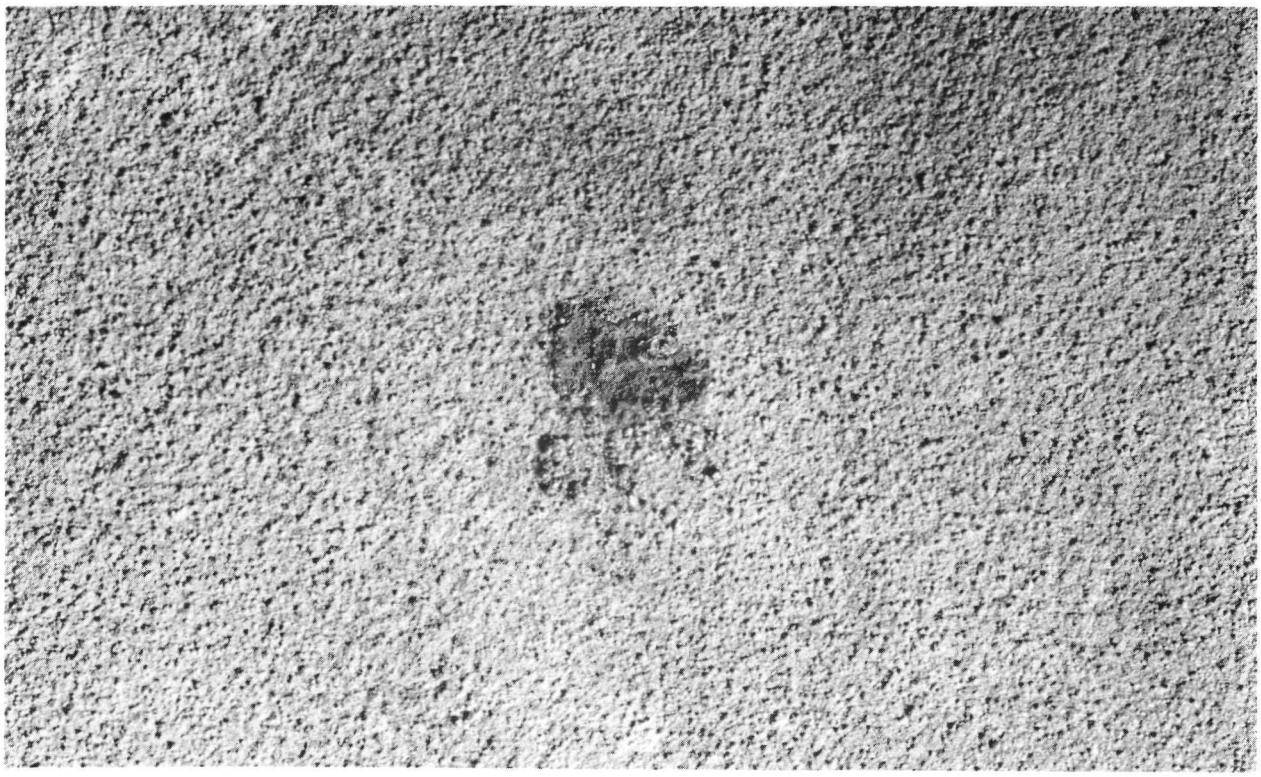

Figure 41. Localized Attack of Coating with Embedded $MoAl_2$ Particles After 23 Hours at 1422°K (2100°F). 5X

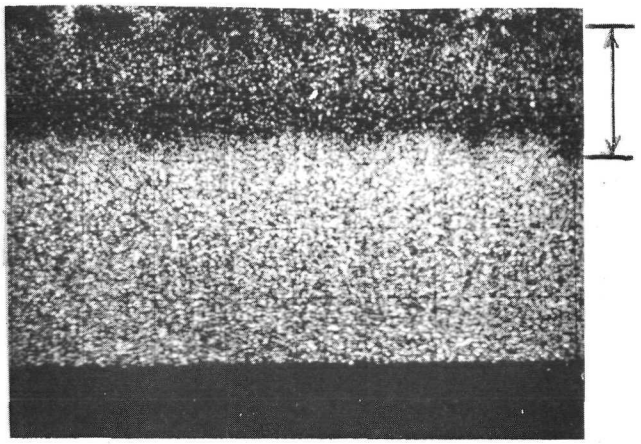

Coating
Additive
Layer

Cr Scan
Cr_5Al_8 Embedment

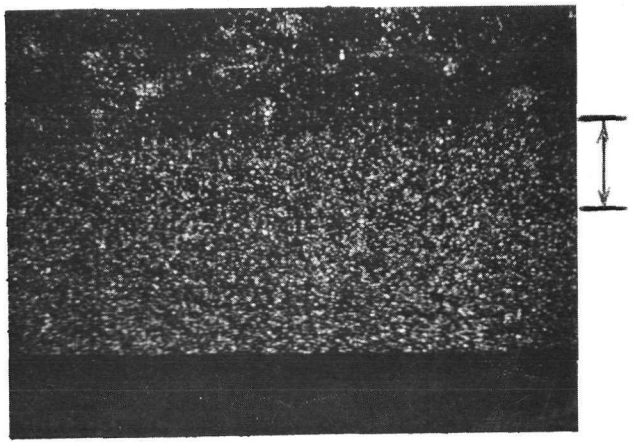

Coating
Additive

Co Scan
CoAl Embedment

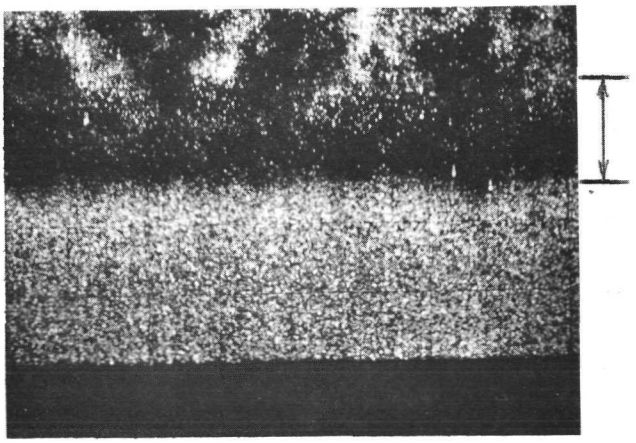

Coating
Additive
Layer

Mo Scan
$MoAl_2$ Embedment

Figure 42. Microprobe Scans of Aluminum-Rich Particles Embedded in Additive Coating Layer. Note: Indications Above Coatings are Due to Residual Slurry. 360X

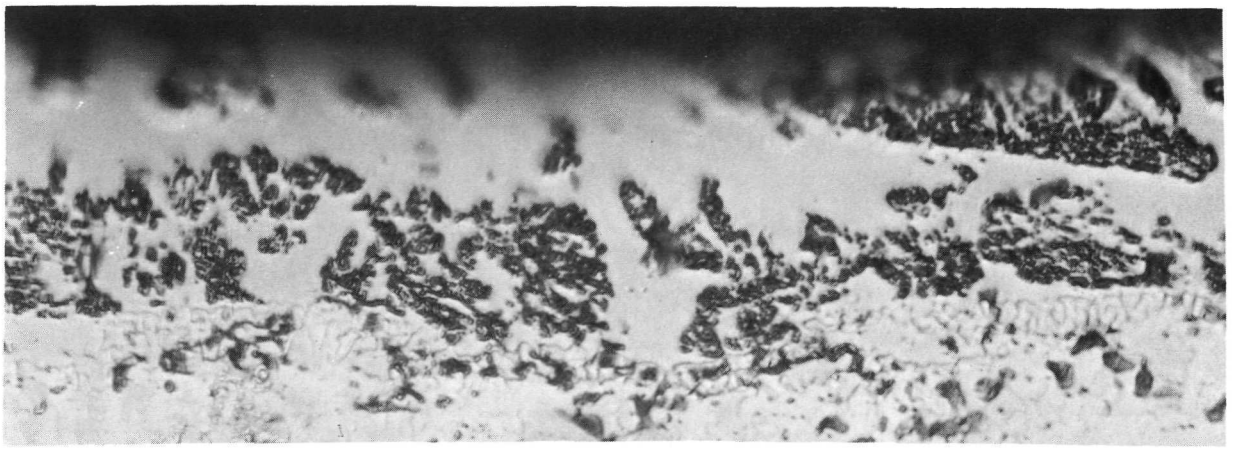

NC11-A (Al_2O_3)

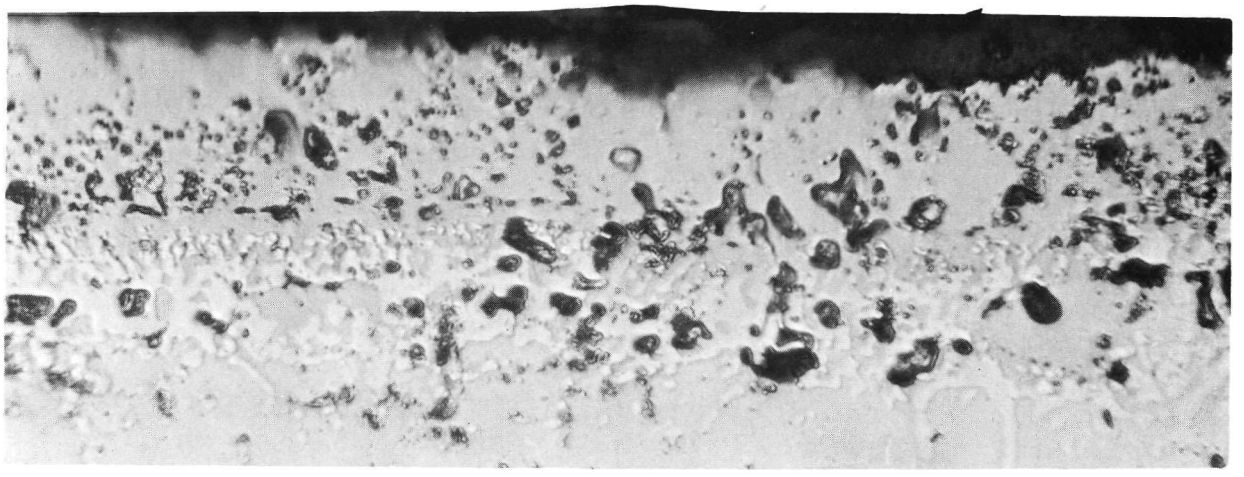

Cr_5Al_8

CoAl

Figure 43. Particle Embedment of Aluminum-Rich Compounds in Outer Coating Layer. Unetched - 750X

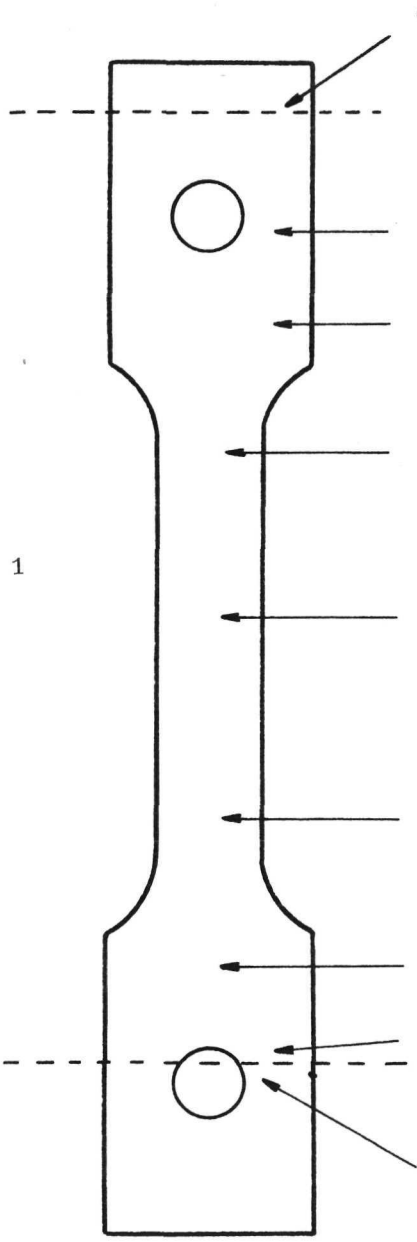

75 Hour	125 Hour	175 Hour	263 Hour
1280°K (1850°F)	1300°K (1880°F	1311°K (1900°F)	1280°K (1850°F)
1377°K (2020°F)	1383°K (2030°F)	1383°K (2030°F)	1372°K (2010°F)
1422°K (2100°F)	1411°K (2080°F)	1411°K (2080°F)	1411°K (2080°F)
1422°K (2100°F)	1422°K (2100°F)	1422°K (2100°F)	1422°K (2100°F)
1411°K (2080°F)	1411°K (2080°F)	1416°K (2090°F)	1394°K (2050°F)
1388°K (2040°F)	1366°K (2000°F)	1405°K (2070°F)	1394°K (2050°F)
1339°K (1950°F)	1328°K (1930°F)	1388°K (2040°F)	---

Figure 44. Specimen Temperature Surveys at Various Stages of Test No. 3.

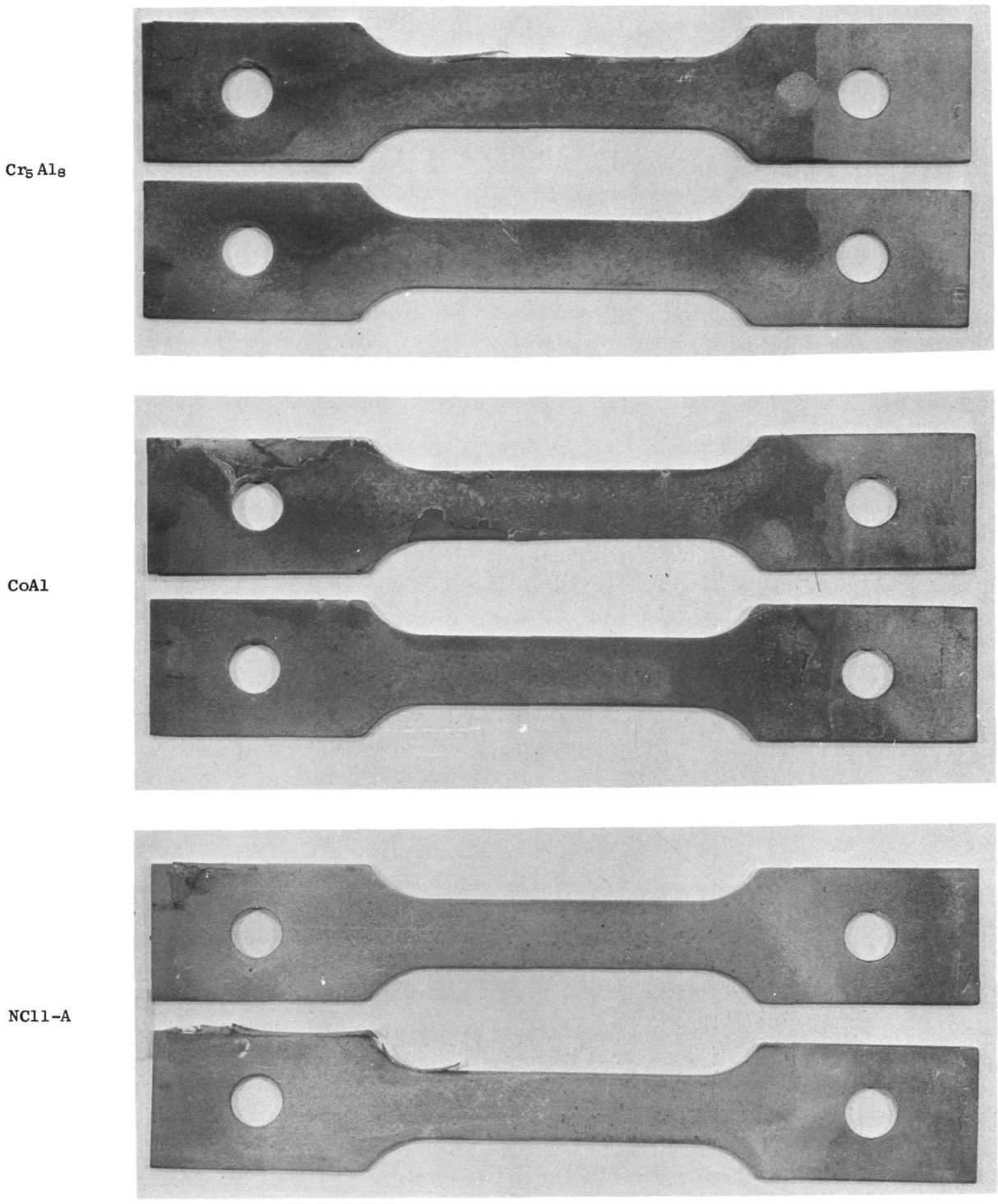

Figure 45. Group I Specimens After 50 Hours of Oxidation Testing at 1422°K (2100°F). Note Failed CoAl Specimen.

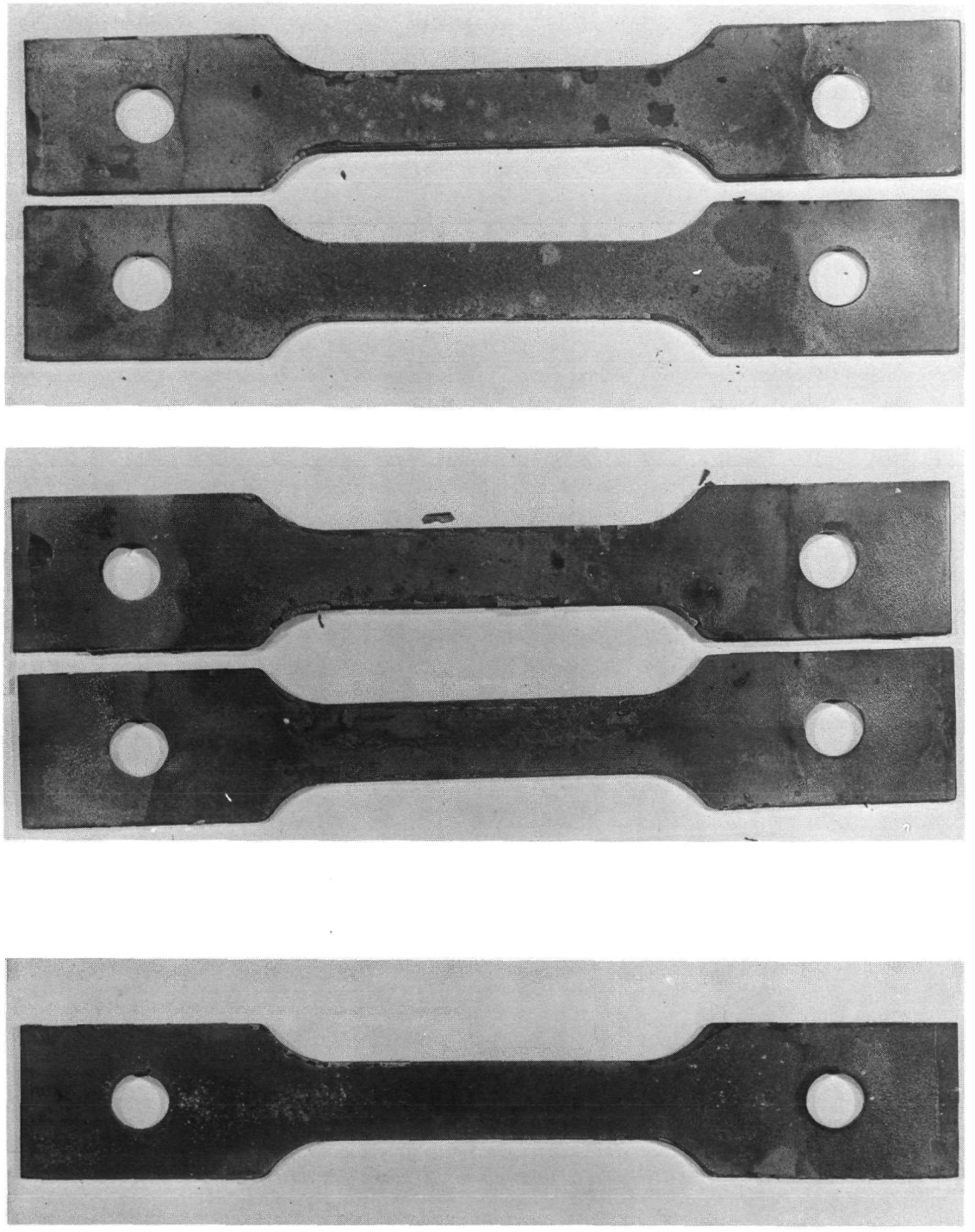

Figure 46. Group I Specimens After Oxidation Testing At 1422°K (2100°F).

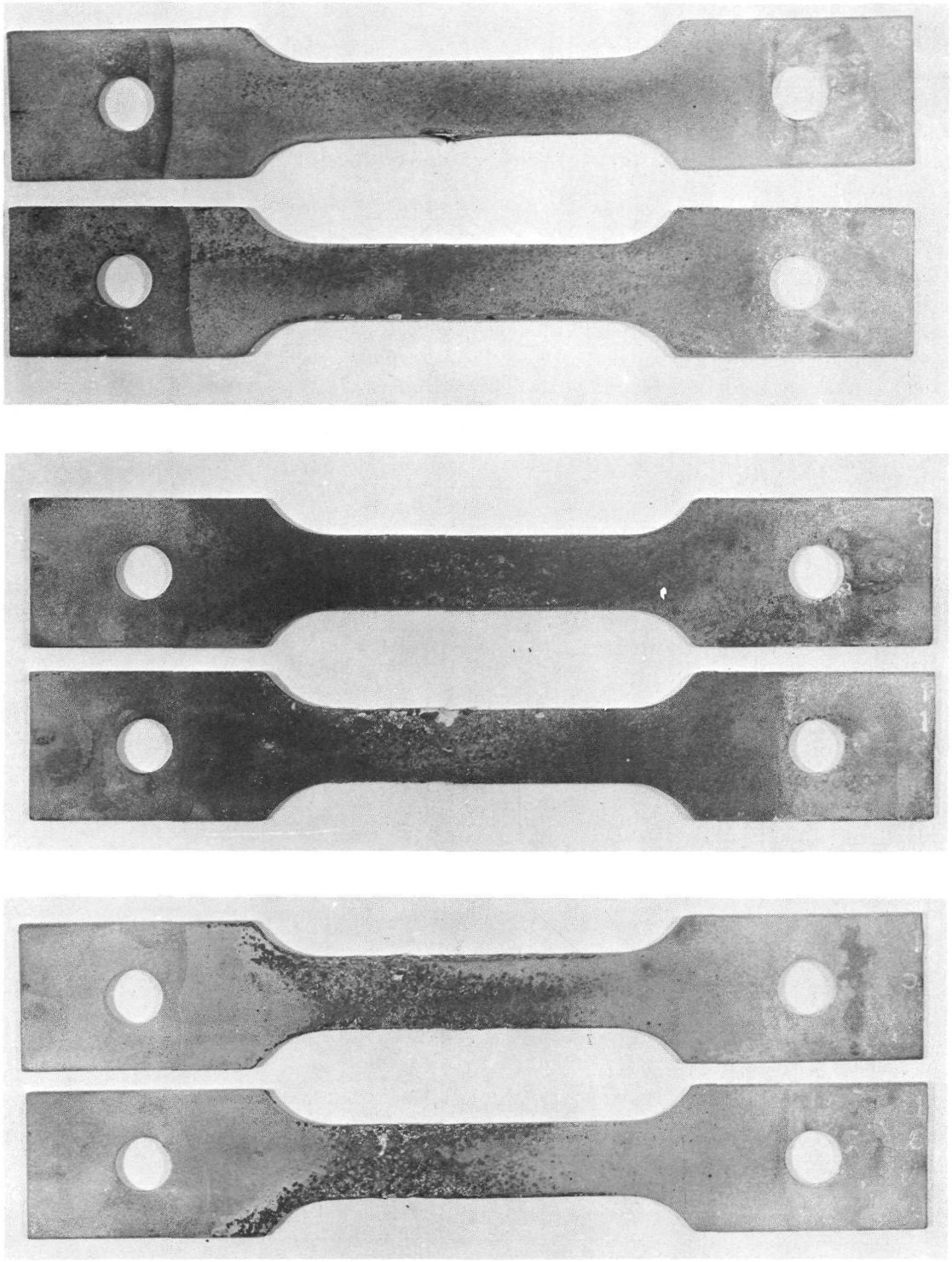

Figure 47. Group II Specimens After 100 Hours of Oxidation Testing at 1422°K (2100°F). Note NC11-A Specimen Contamination From Corrosion Products of Failed CoAl Specimen.

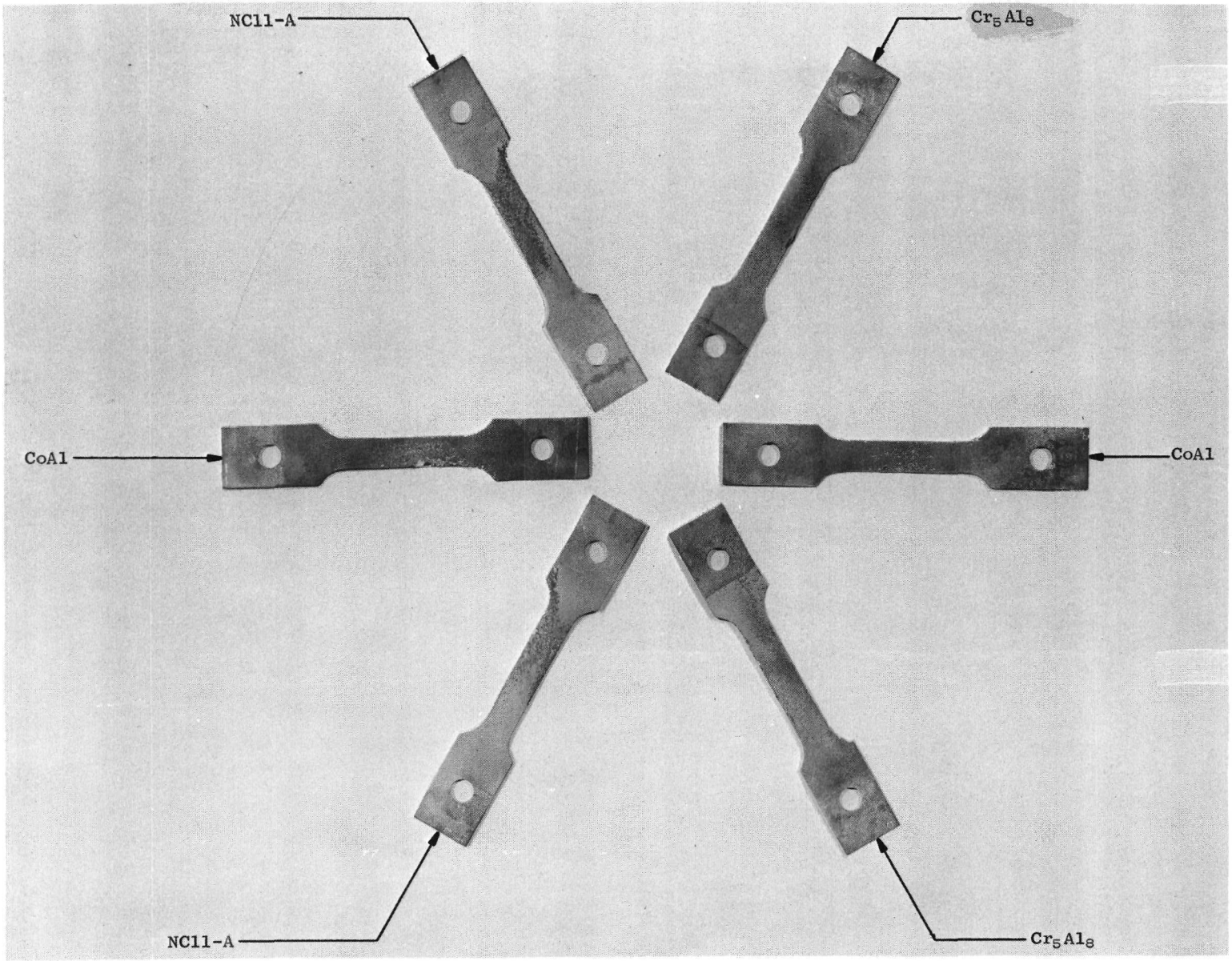

Figure 48. Position of Group II Specimens in Fixture in Test No. 2.

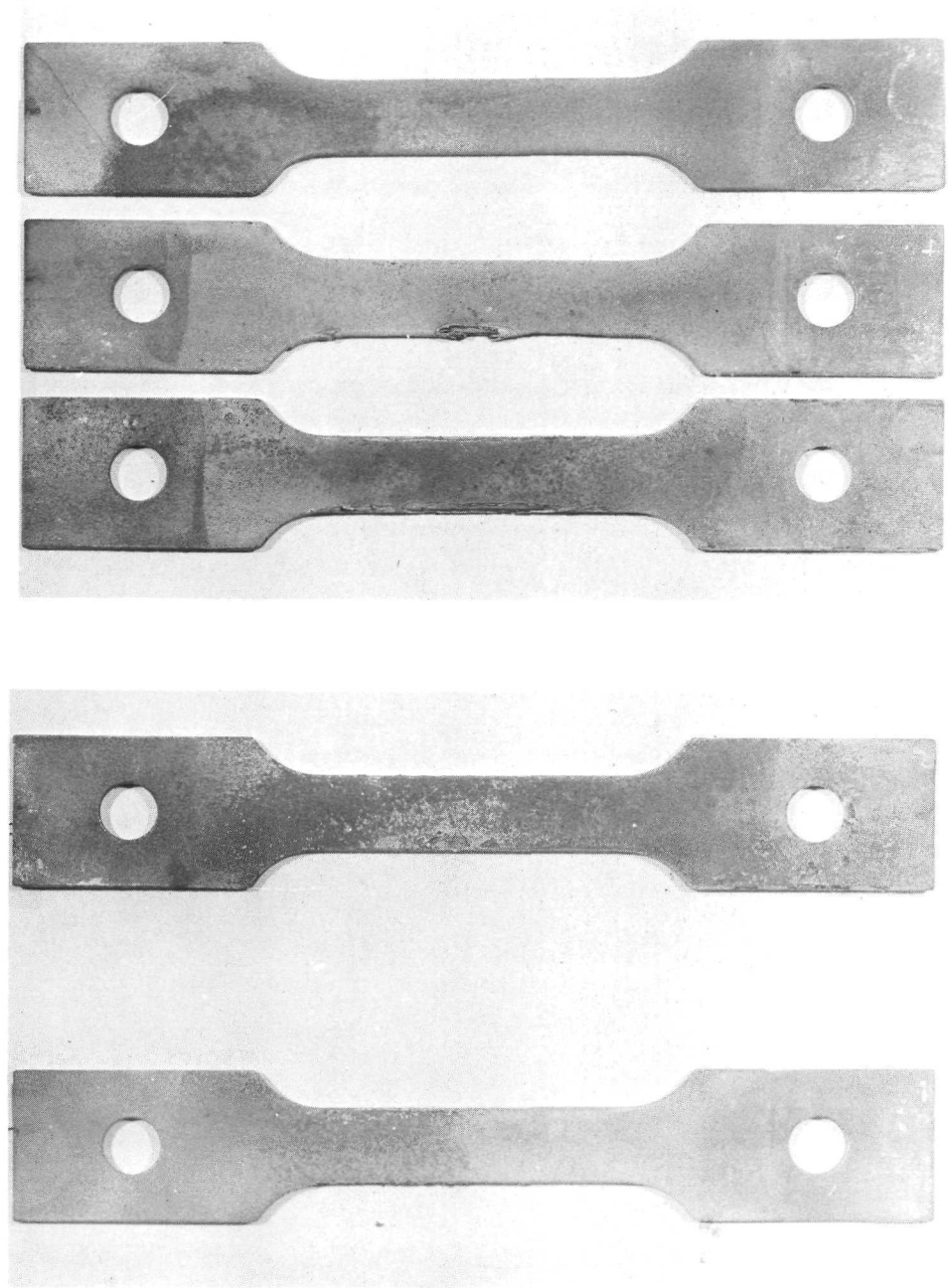

Figure 49. Group II Specimens After 145 Hours of Oxidation Testing at 1422°K (2100°F) at Which Point Test was Terminated.

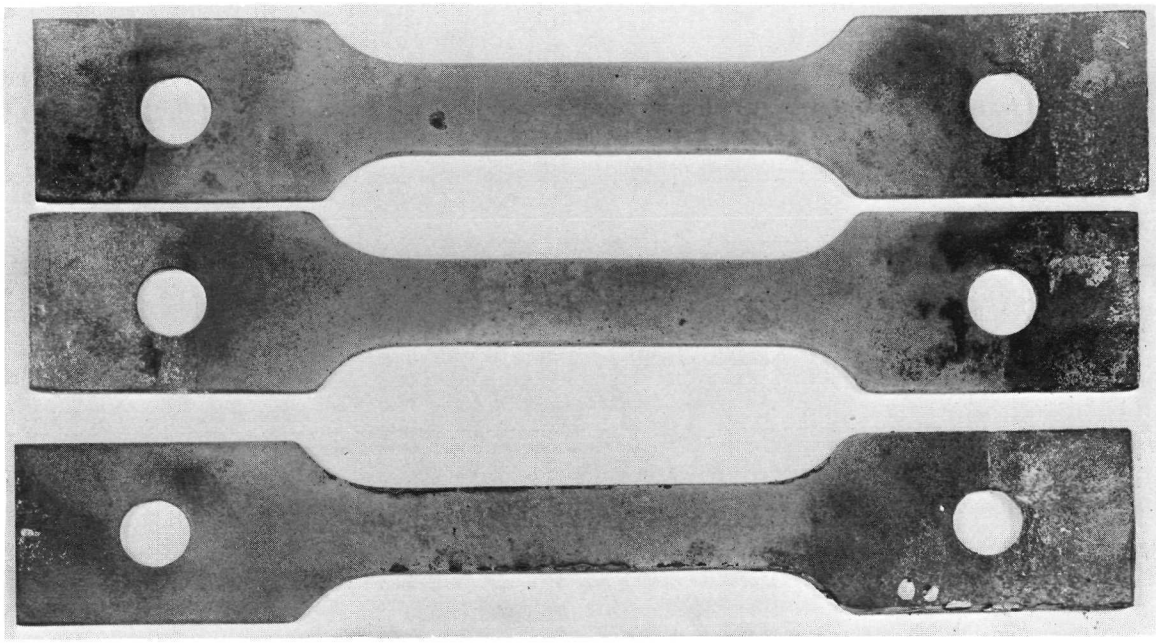

Cr_5Al_8 Coated Specimens
150 Hrs

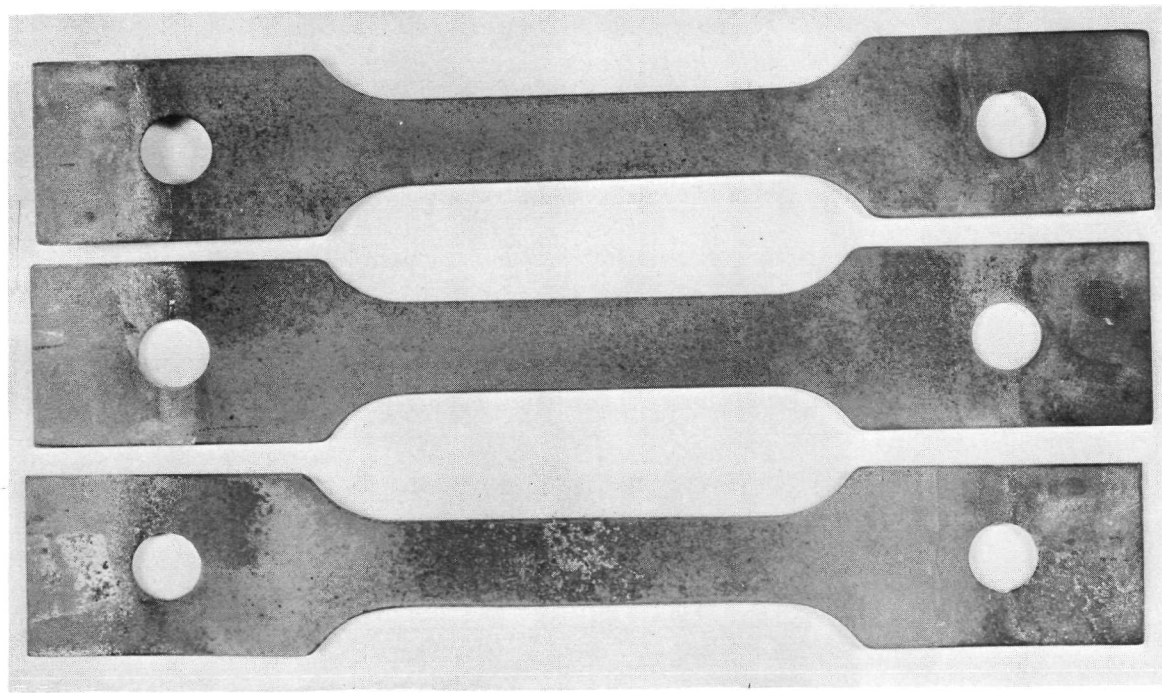

NC11-A Coated Specimen
175 Hrs

Figure 50. Group III Specimens. The Cr_5Al_8/C-2-Coated TDNi Specimen was Removed After 150 Hours of Oxidation Testing at 1422°K (2100°F); the NC11-A-Coated TDNi Specimen was Removed 25 Hours Later due to Spalled Edges and Coating Attack in Gage Section.

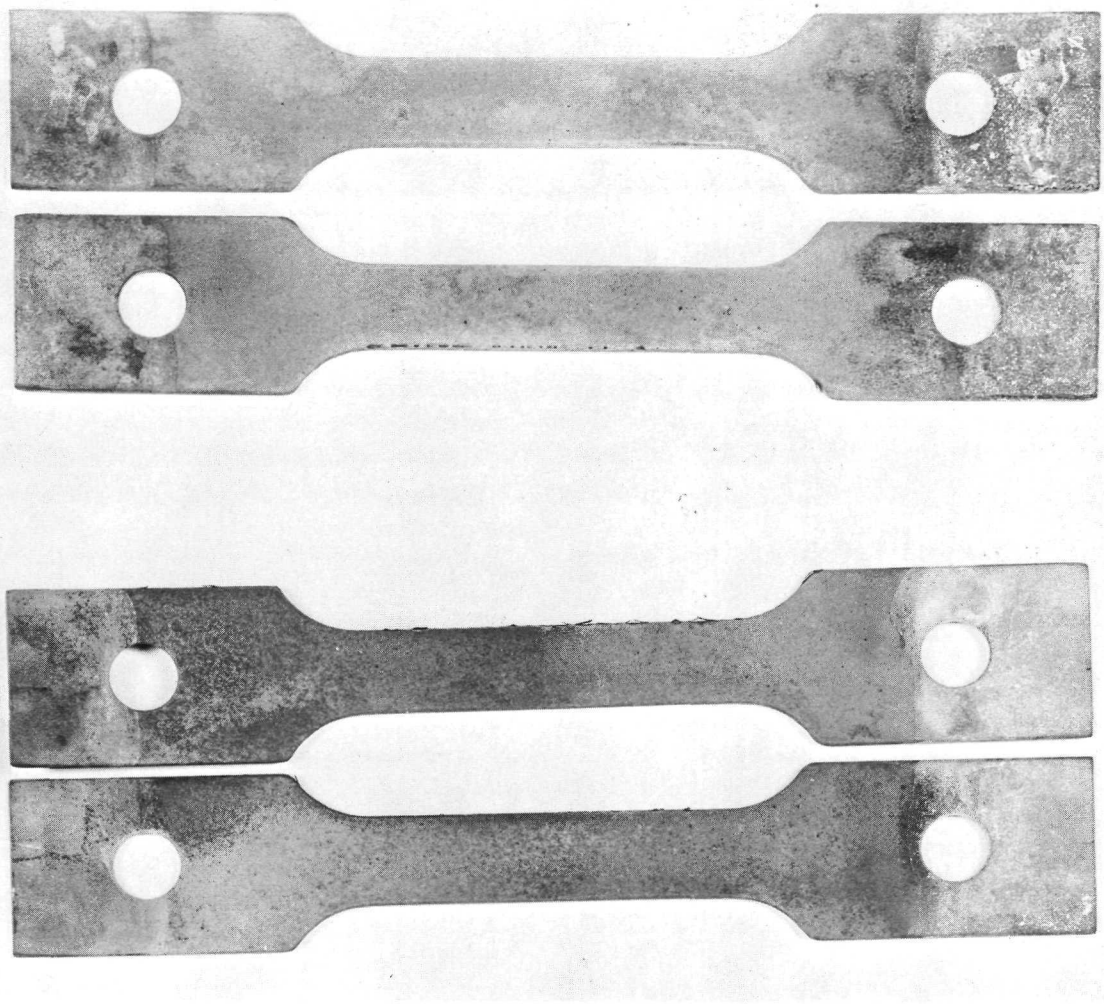

Figure 51. Group III TDNiCr Specimens, X40 Barrier, After 300 Hours of Oxidation Testing at 1422°K (2100°F)

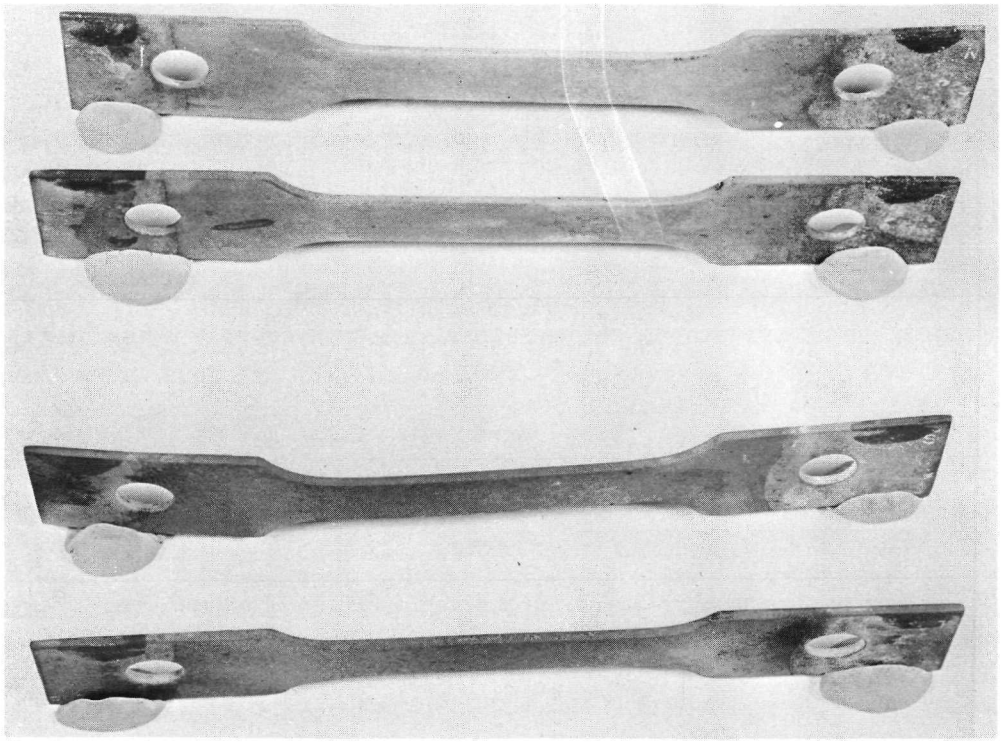

Left Edge View

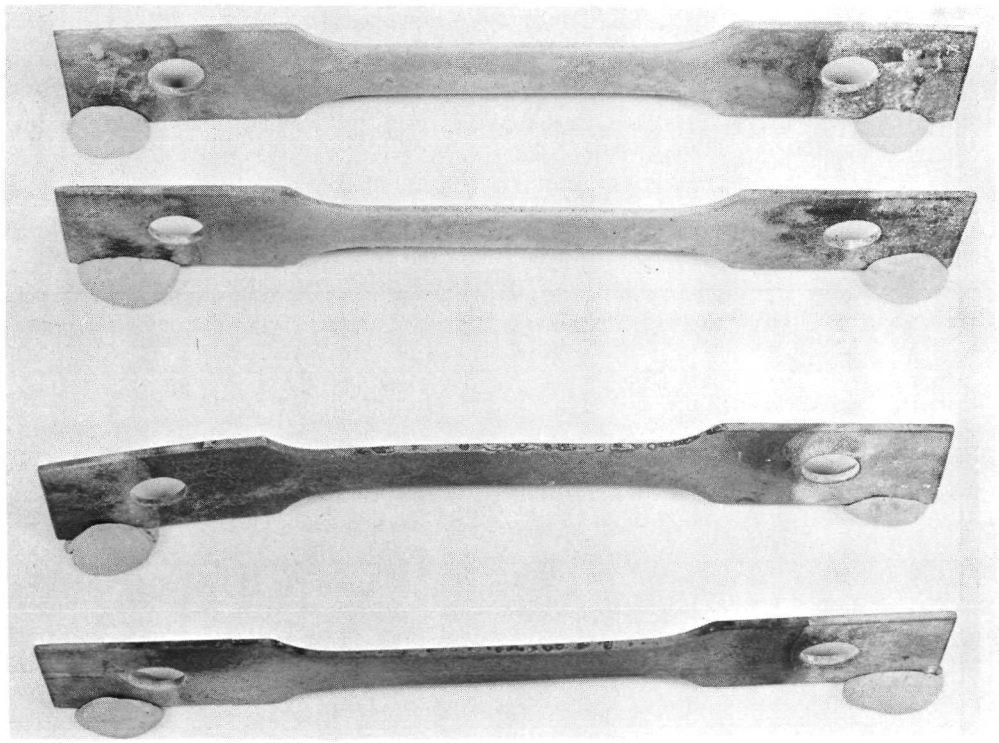

Right Edge View

Figure 52. Edge Condition of Group III TDNiCr Specimens, X40 Barrier, After 1422°K (2100°F)/300 Hours. Note: One Specimen was Bent due to Fixture Failure Between 96 and 124 Hours.

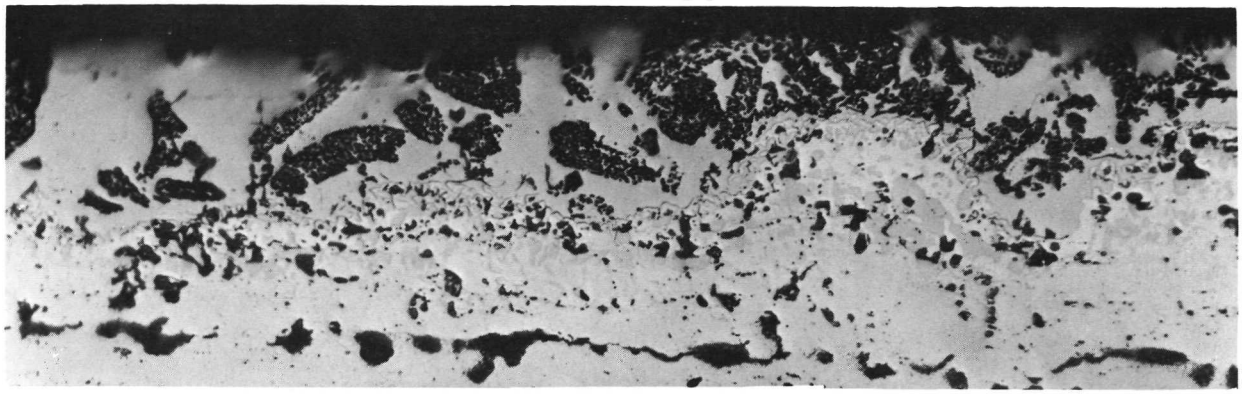

NCl1-A/Hastelloy C-1 Barrier

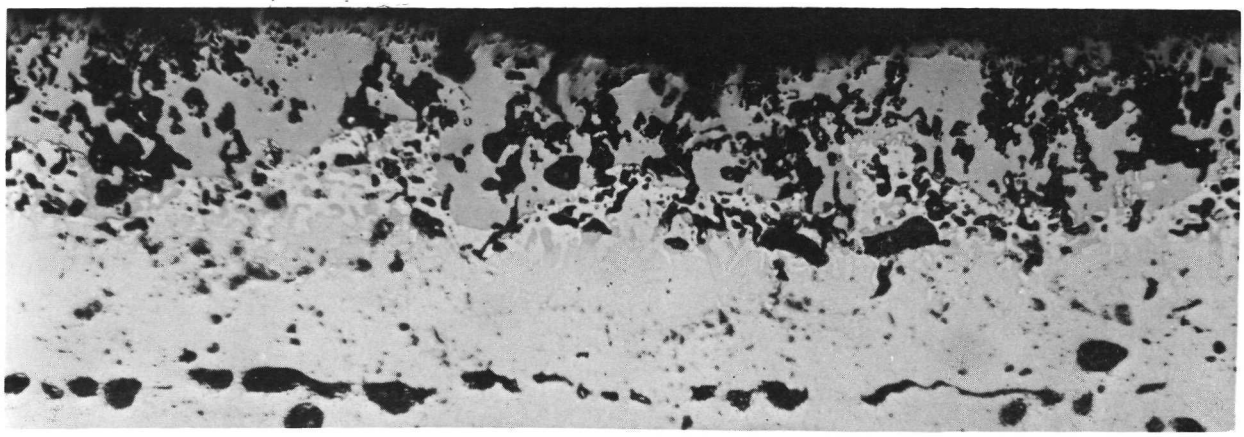

Cr_5Al_8/Hastelloy C-1 Barrier

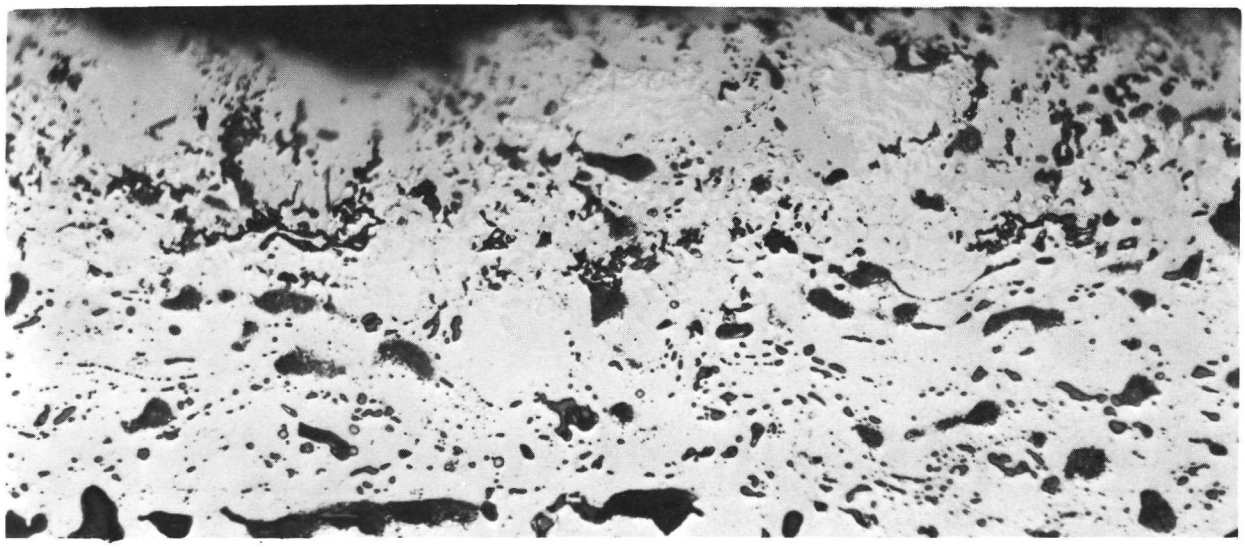

CoAl/Hastelloy C-1 Barrier

Figure 53. As-Processed Group I Coated TDNiCr Specimens. Unetched - 500X

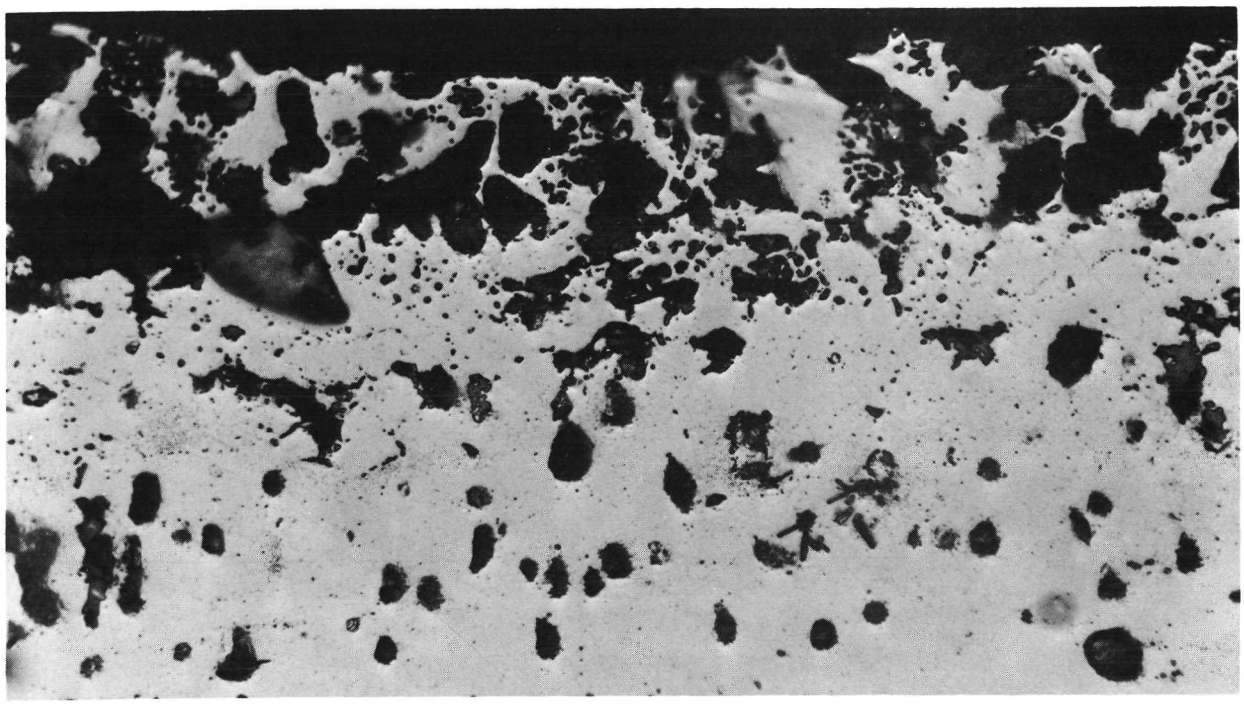

NC11-A/Hastelloy C-1

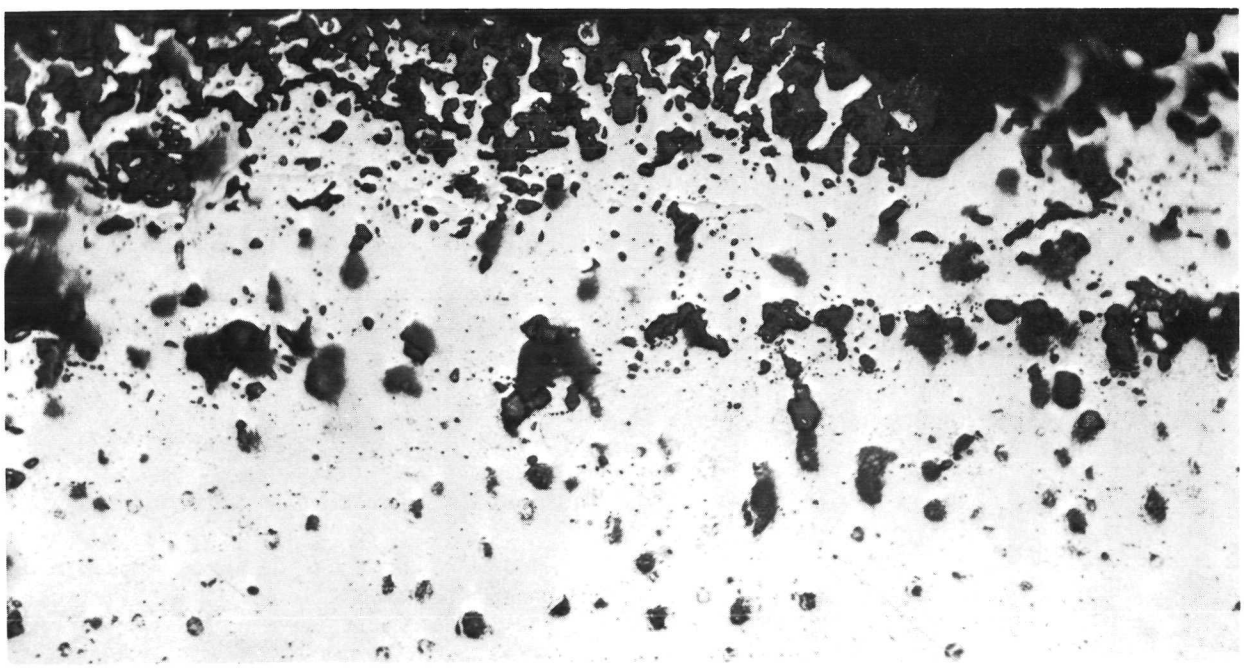

Cr_5Al_8/Hastelloy C-1

Figure 54. Group I Coated TDNiCr Specimens After 1422°K (2100°F)/200 Hour Oxidation Test. Unetched - 500X

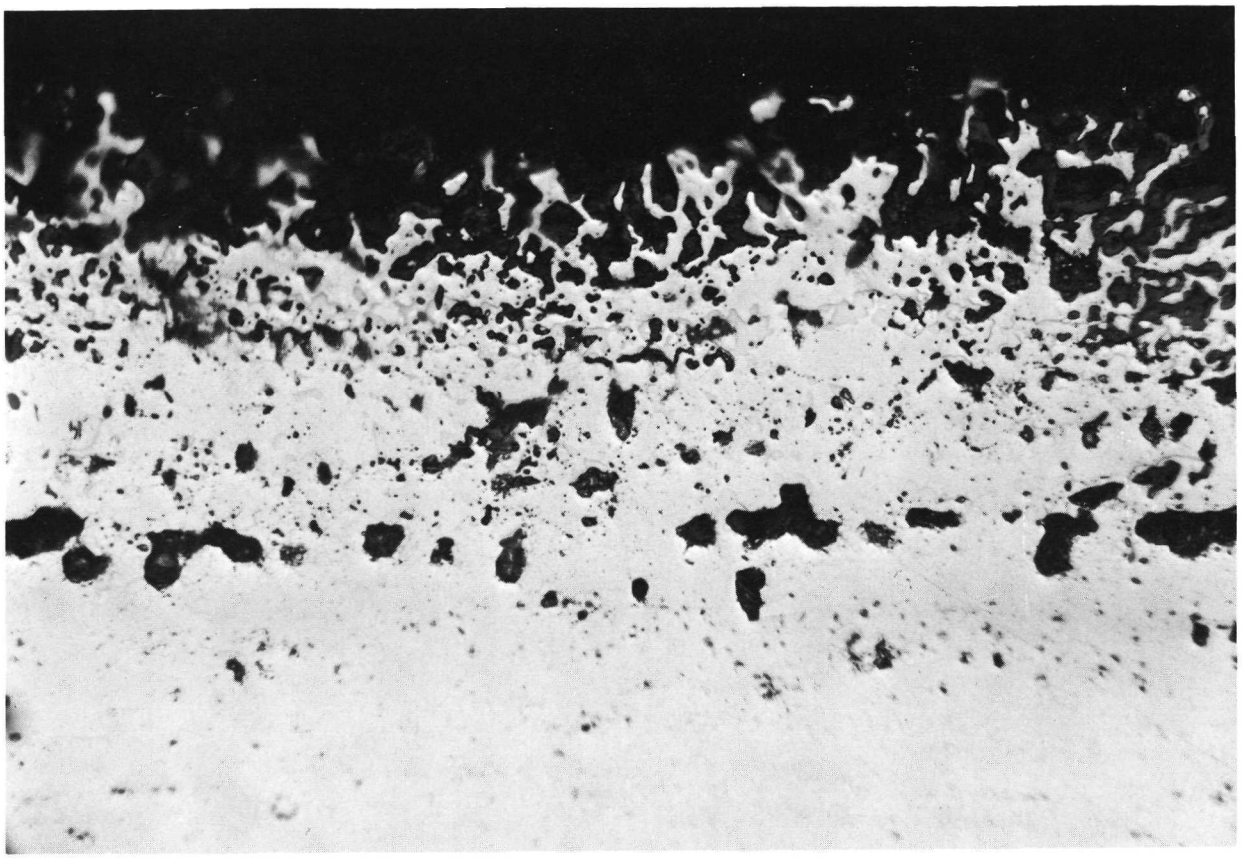

Figure 55. CoAl/Hastelloy C-1 TDNiCr Specimens After 1422°K (2100°F)/ 50-Hour Oxidation Test. Unetched - 500X

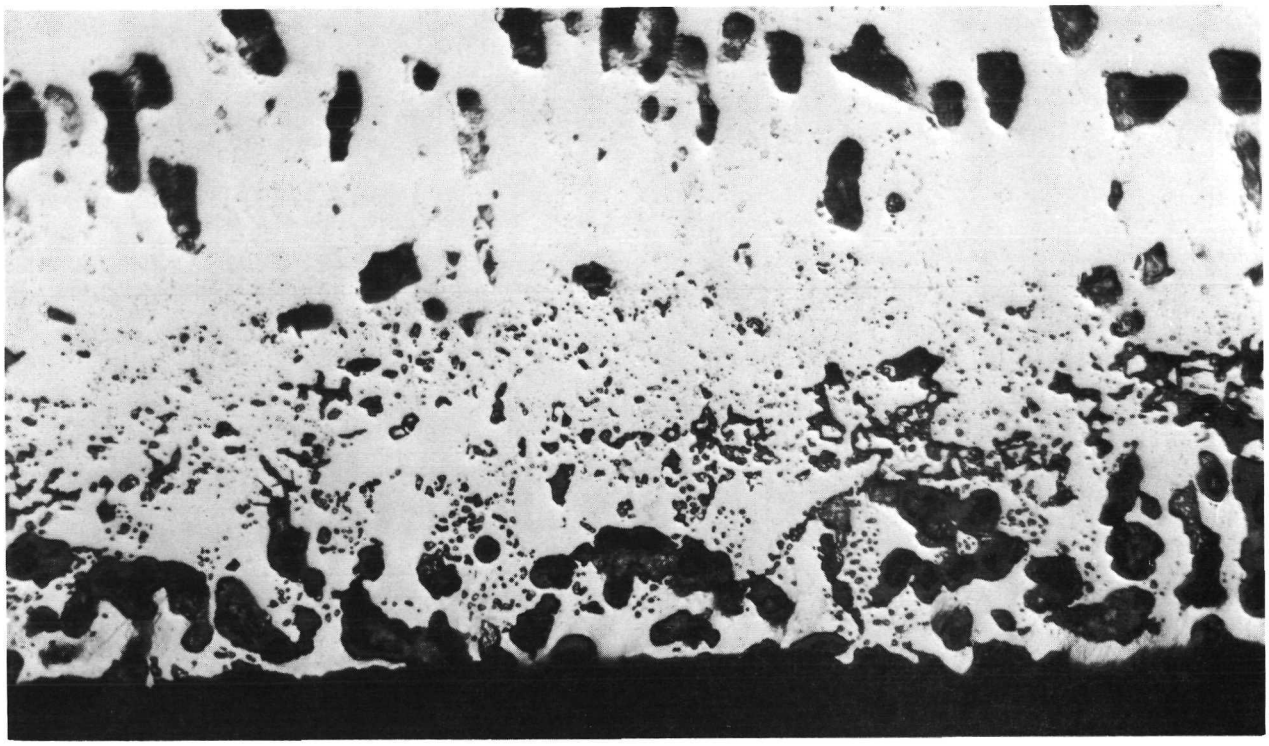

NC11-A

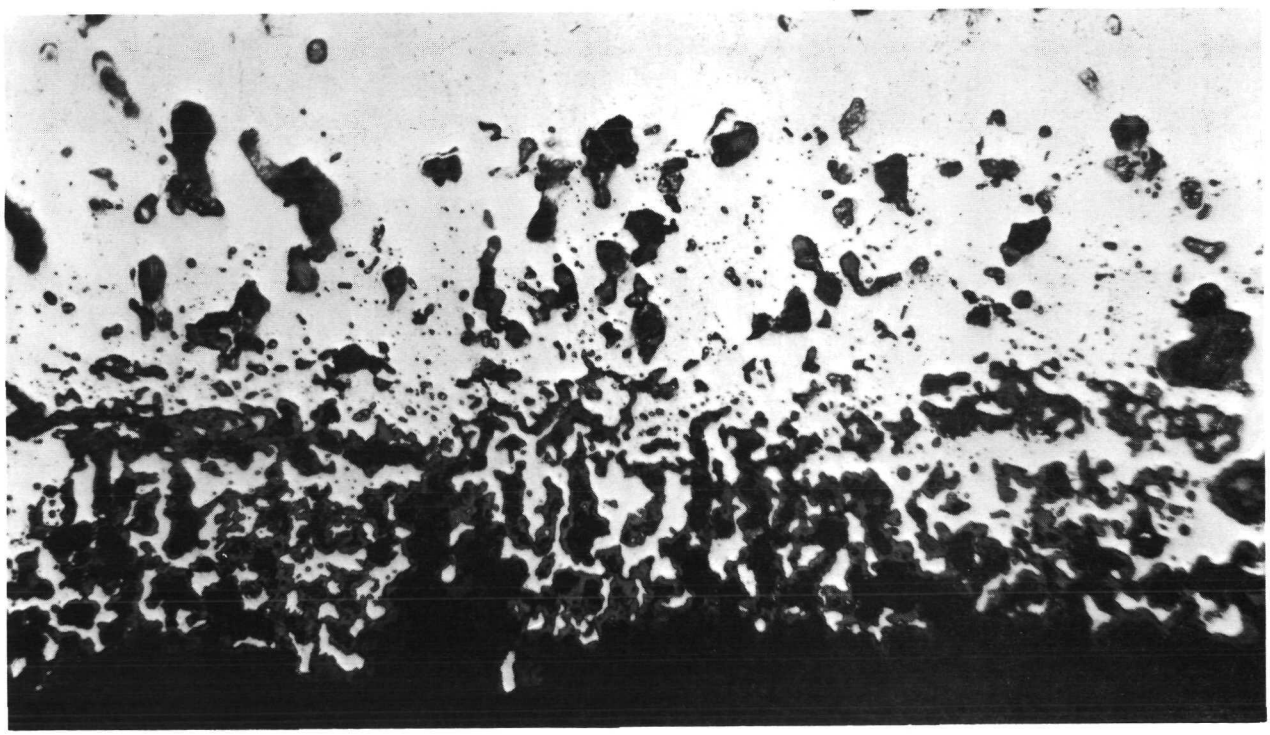

CoAl

Figure 56. NC11-A/Hastelloy C-1 and CoAl/Hastelloy C-1-Coated TDNi After 1422°K (2100°F)/100-Hour Oxidation Test. Unetched 500X.

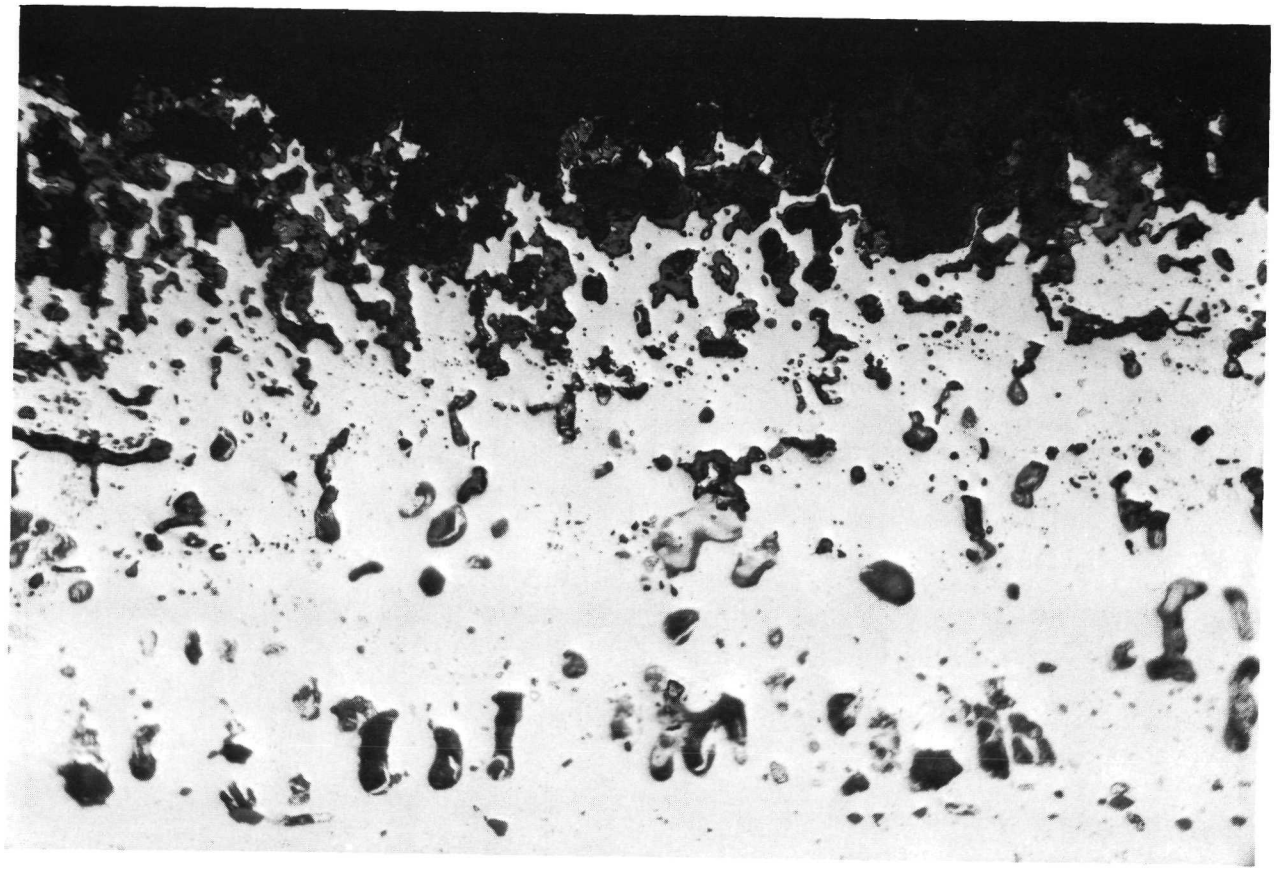

Figure 57. Cr_5Al_8/Hastelloy C-1 Coated TDNi After 1422°K (2100°F)/ 145-Hour Oxidation Test. Unetched - 500X.

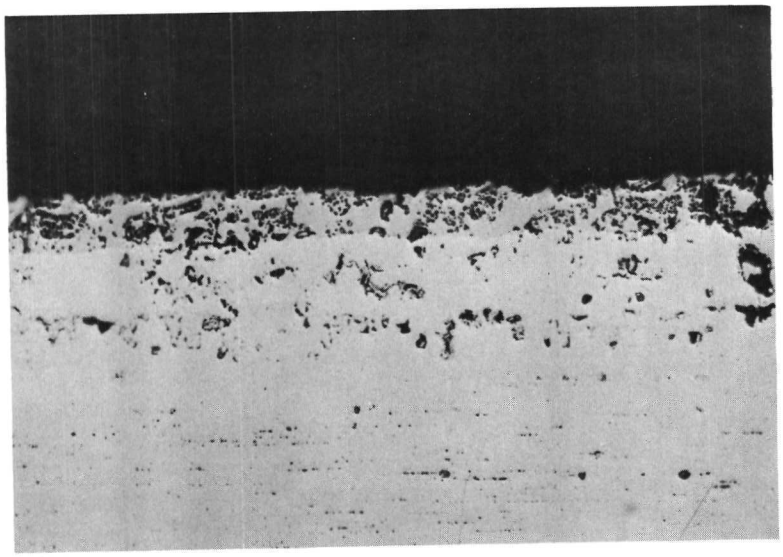

NC11-A/X40/TDNiCr

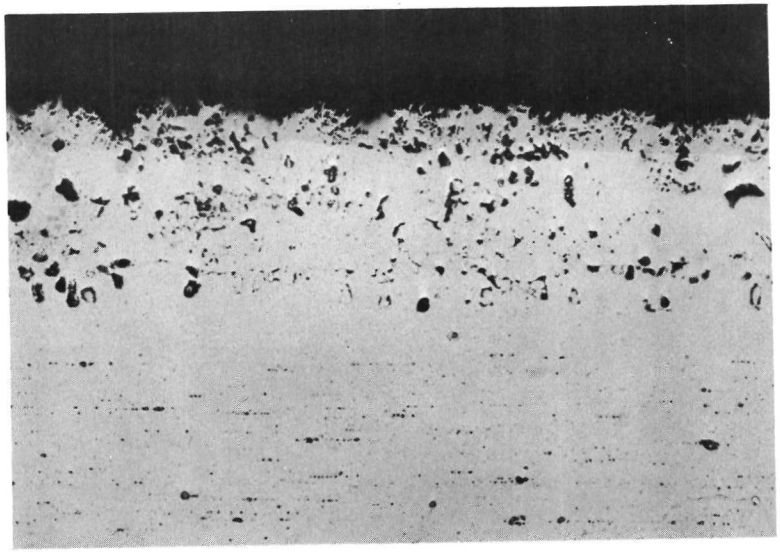

Cr_5Al_8/X40/TDNiCr

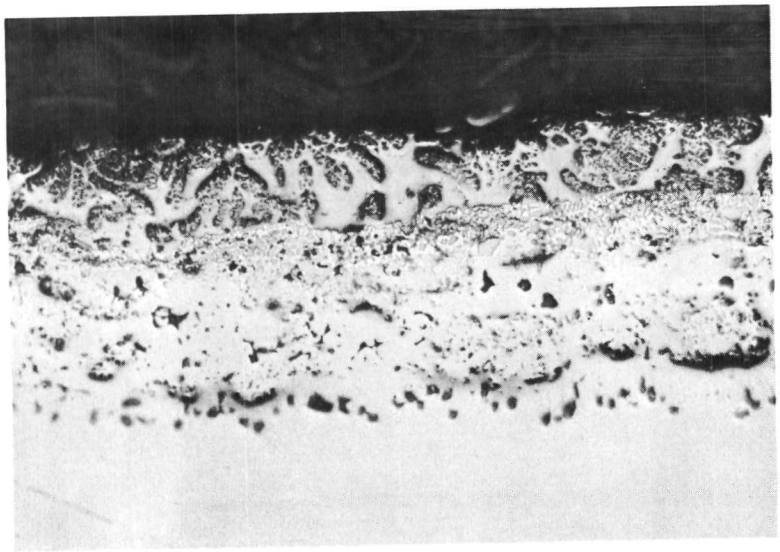

NC11-A/C-2/TDNi

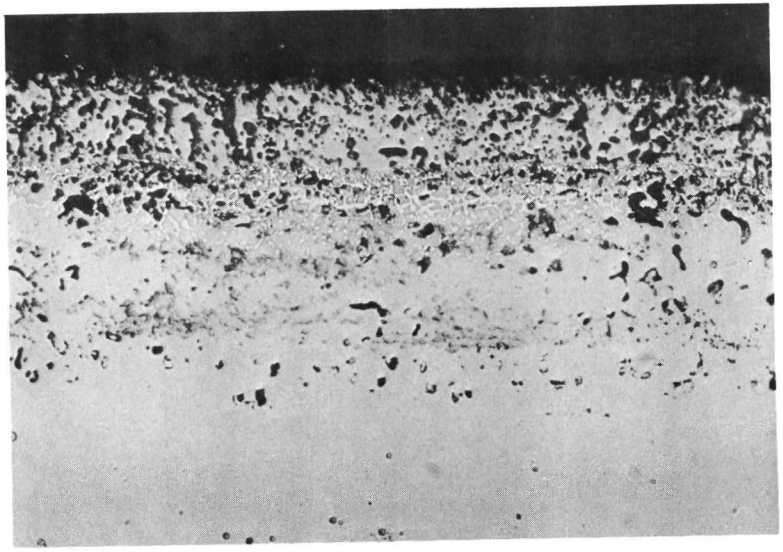

Cr_5Al_8/C-2/TDNi

Figure 58. As-Processed Group III Specimens. Unetched - 250X

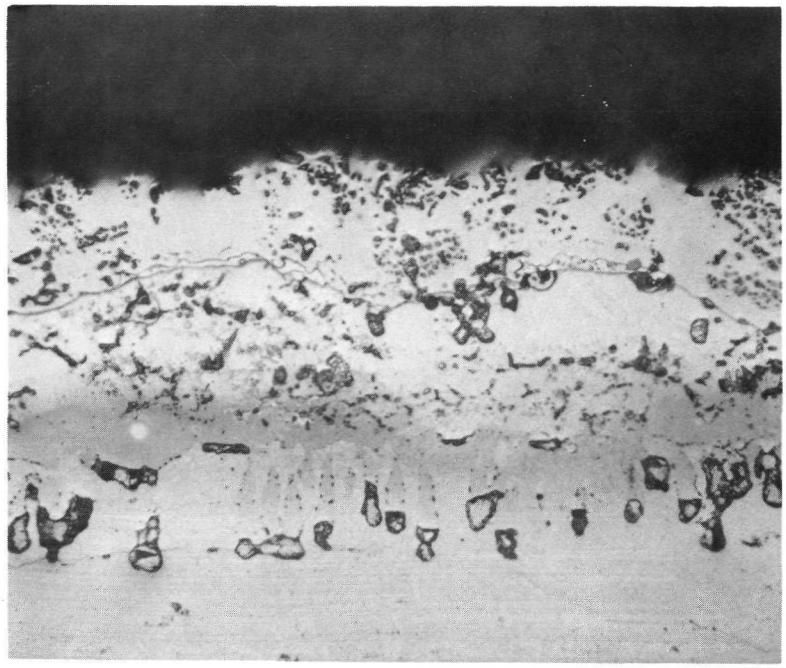

NC11-A

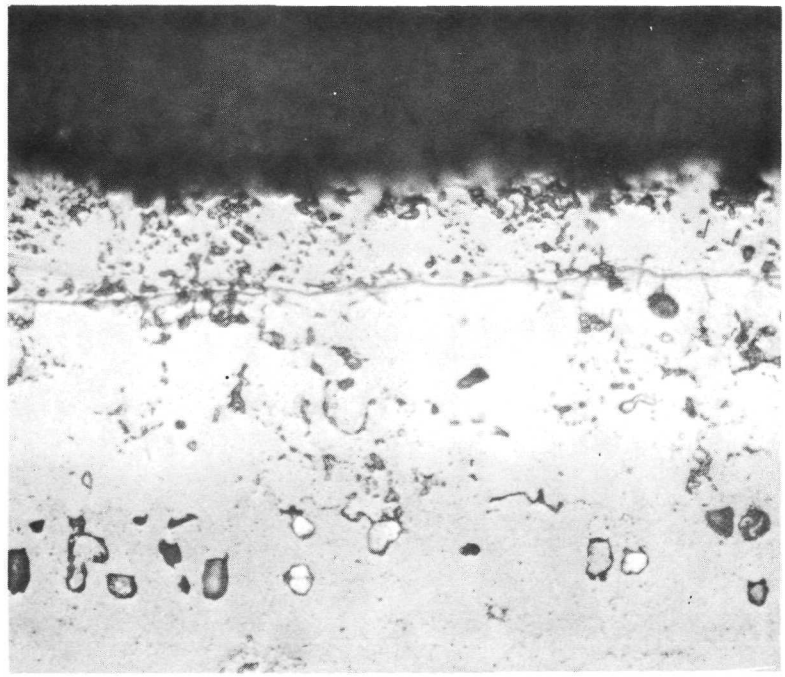

Cr_5Al_8

Figure 59. Grain Recrystallization and Growth of X40 Barrier on TDNiCr. Etched, 2% Chromic - 500X

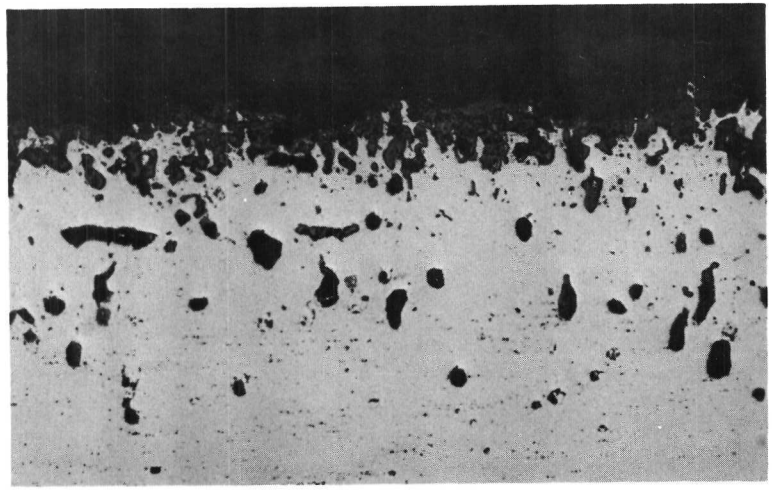

Cr_5Al_8/X40

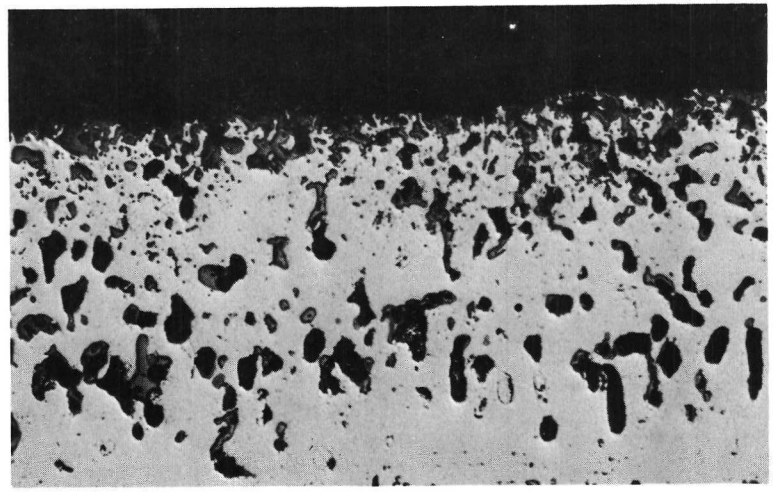

Cr_5Al_8/X40

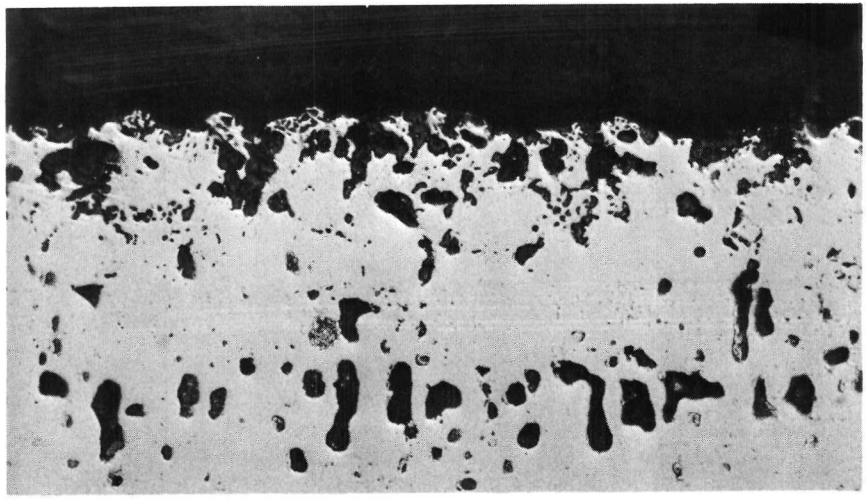

NC11-A/X40

Figure 60. Group III Coated TDNiCr Specimens After 1422°K (2100°F) 300-Hour Oxidation Test. Unetched - 250X.

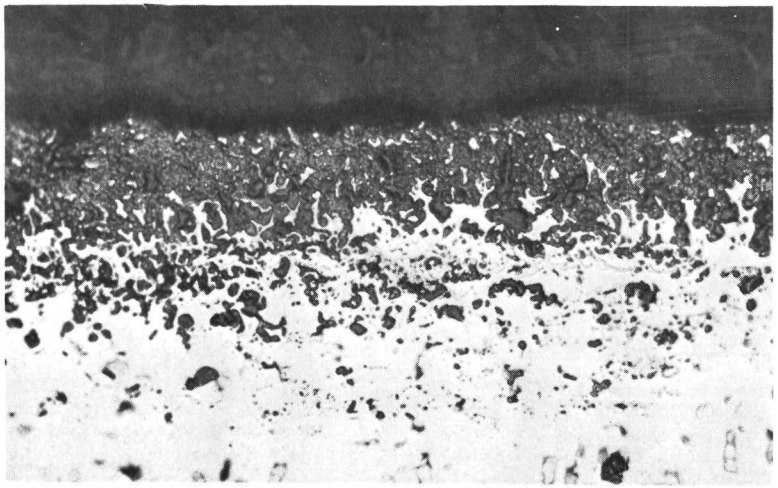

Cr_5Al_8/Hastelloy C-2

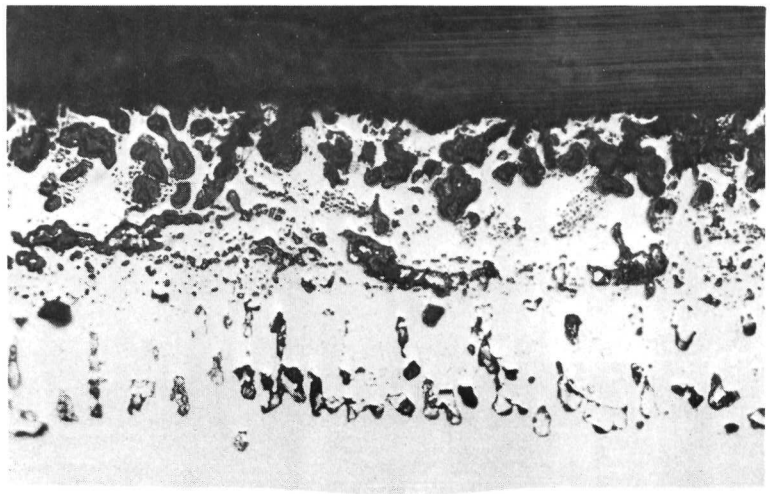

NC11-A/Hastelloy C-2

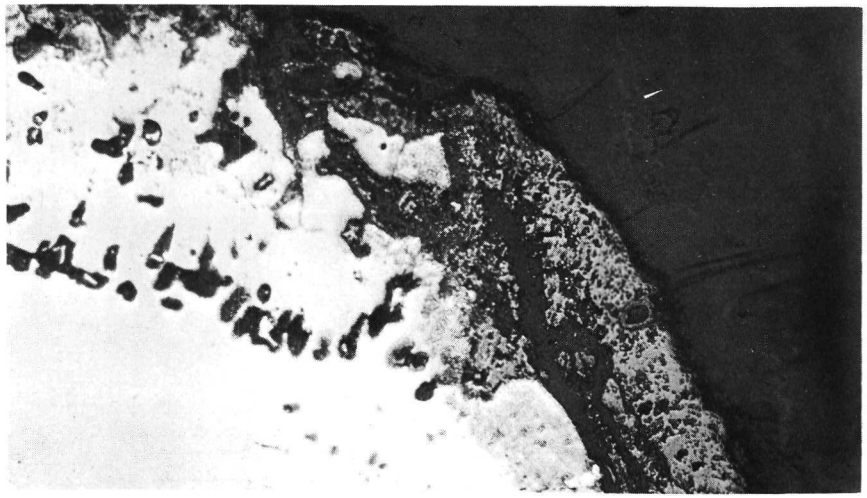

NC11-A/Hastelloy C-2

Figure 61. Cr_5Al_8 - and NC11-A-Coated TDNi Specimens After 150 and 175 Hours, Respectively, of Oxidation Testing at 1422°K (2100°F). 250X

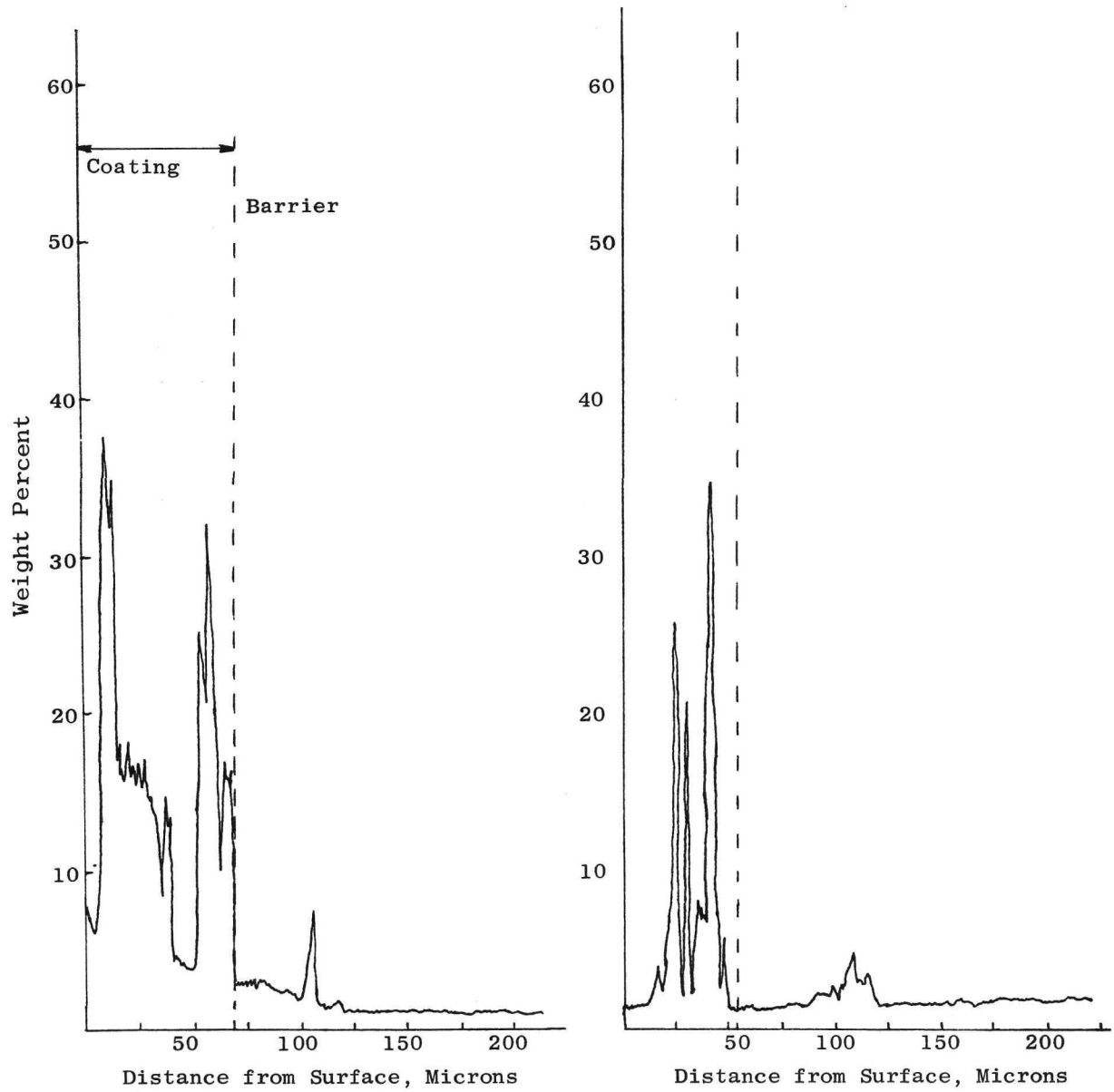

Figure 62. EM Aluminum Traces of NC11-A/X40 Coating on TDNiCr, As-Processed and After 1422°K (2100°F)/300-Hour Oxidation Exposure.

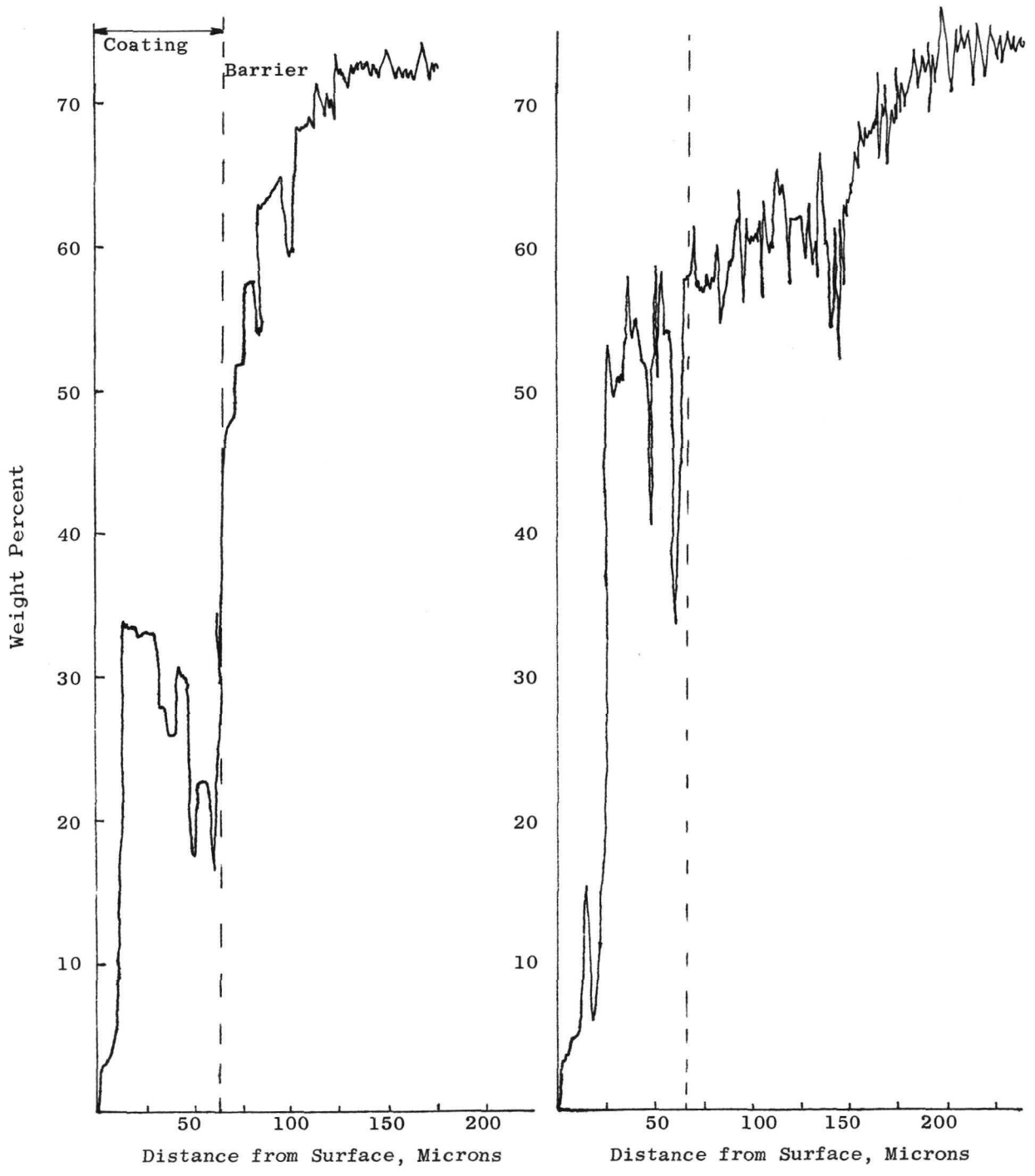

Figure 63. EM Nickel Traces of NC11-A/X40 Coating on TDNiCr, As-Processed and After 1422°K (2100°F)/300-Hour Oxidation Exposure.

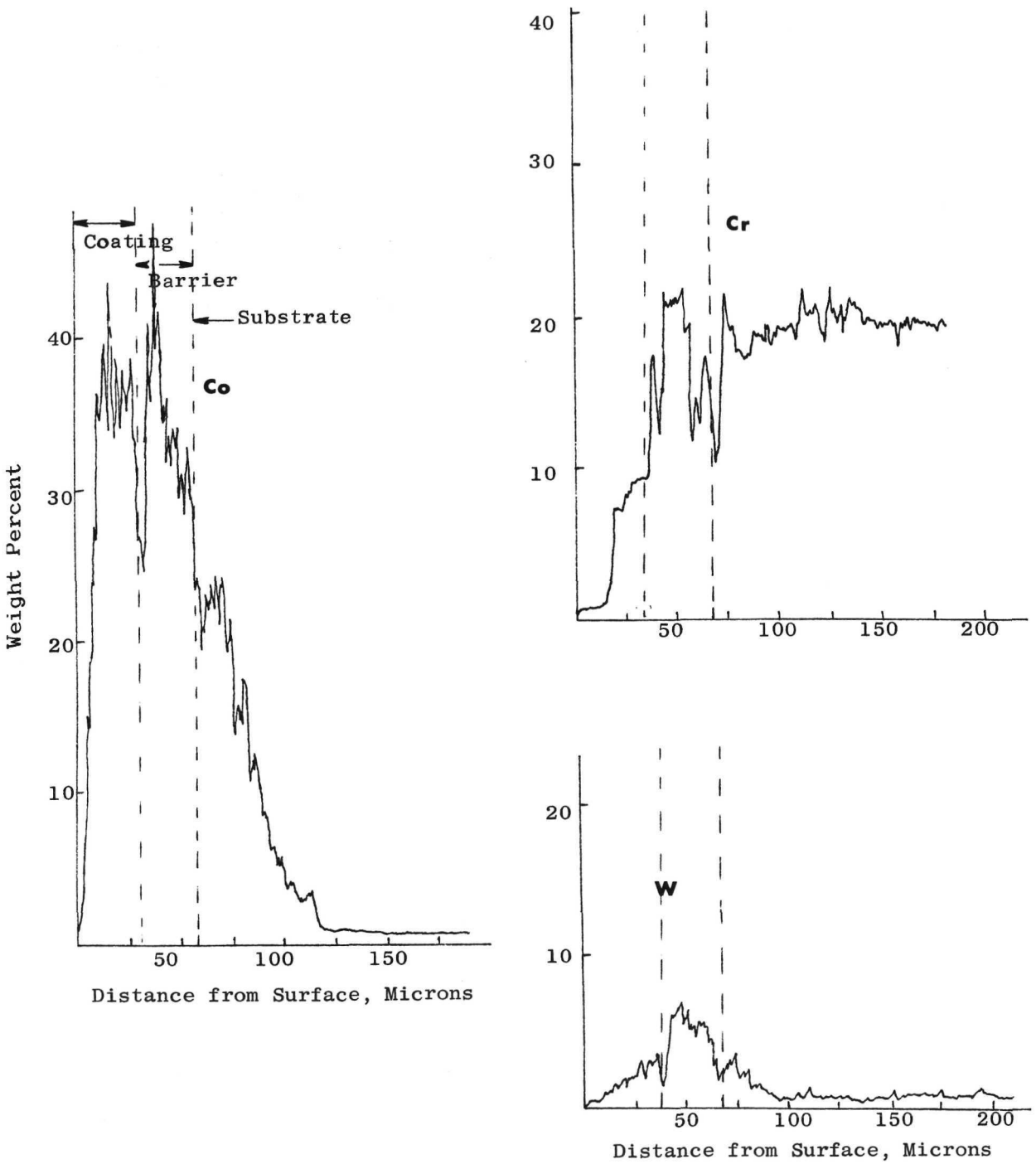

Figure 64. EM Co, W and Cr Traces of NC11-A/X40 Coating on TDNiCr, As-Processed.

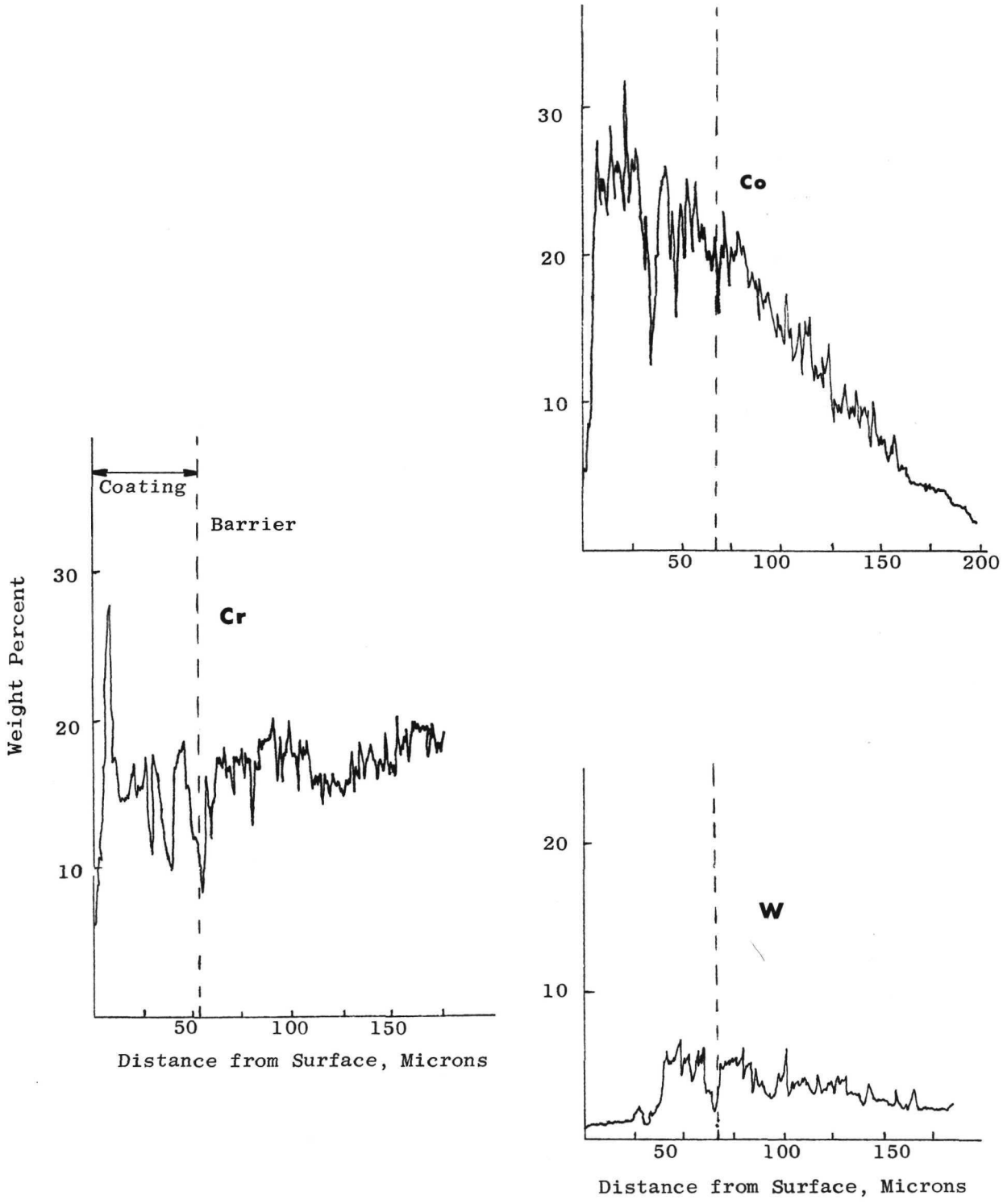

Figure 65. EM Co, W and Cr Traces of NC11-A/X40 Coating on TDNiCr After 1422°K (2100°F)/300-Hour Oxidation Exposure.

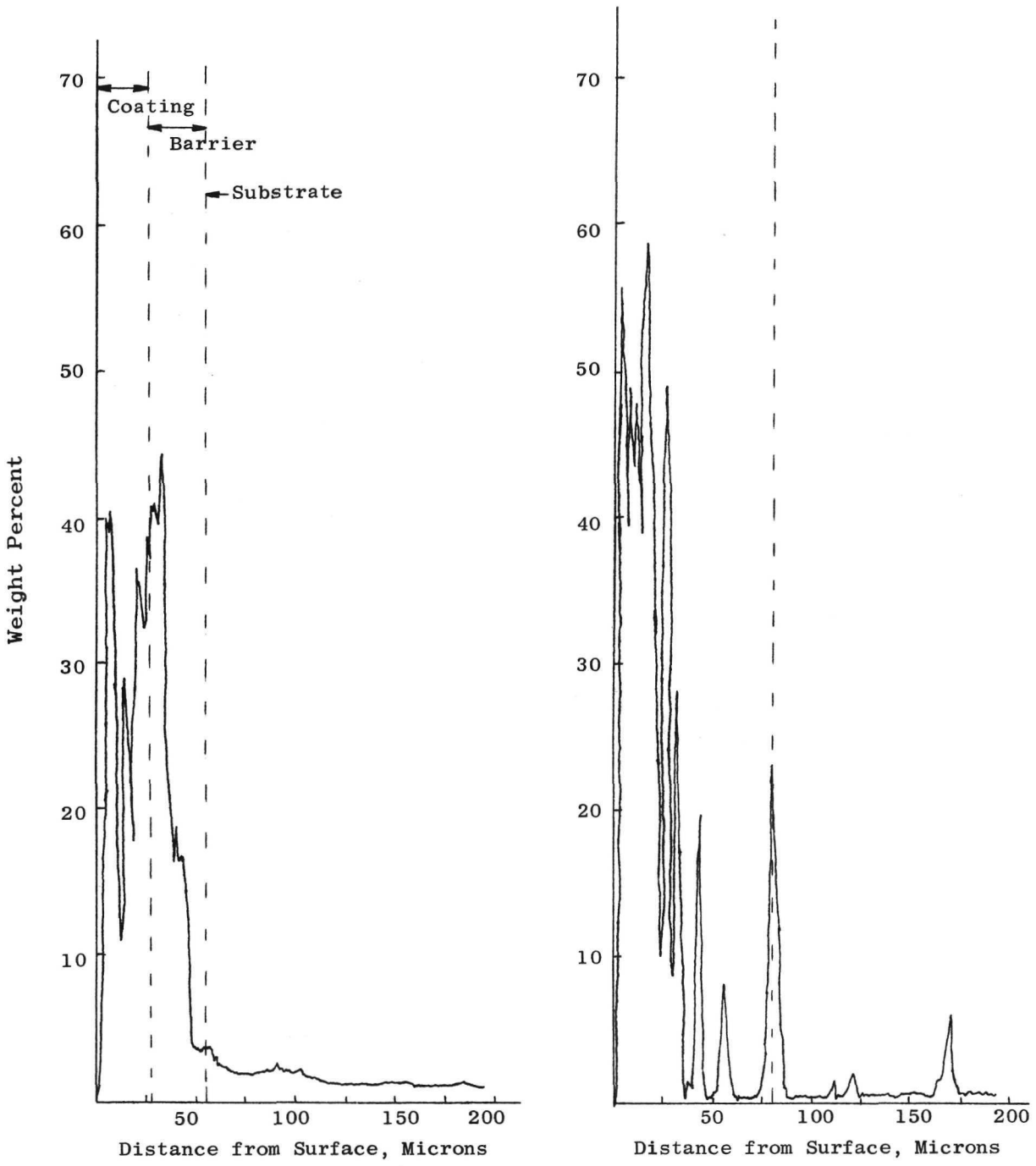

Figure 66. EM Aluminum Traces of $Cr_5Al_8/X40$ Coating on TDNiCr, As-Processed and After 1422°K(2100°F)/300-Hour Oxidation Exposure.

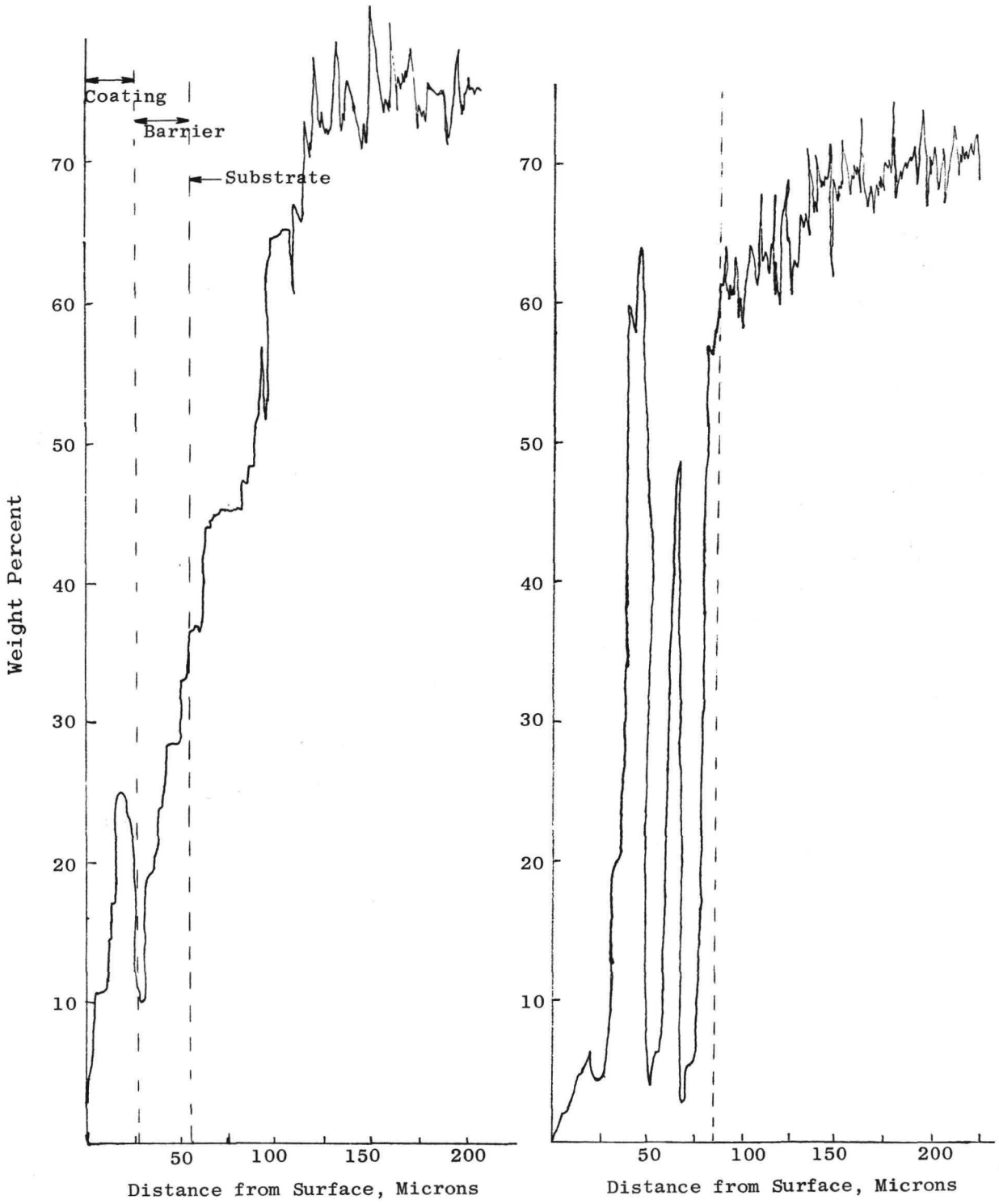

Figure 67. EM Nickel Traces of Cr_5Al_8/X40 Coating on TDNiCr, As-Processed and After 1422°K (2100°F)/300-Hour Oxidation Exposure.

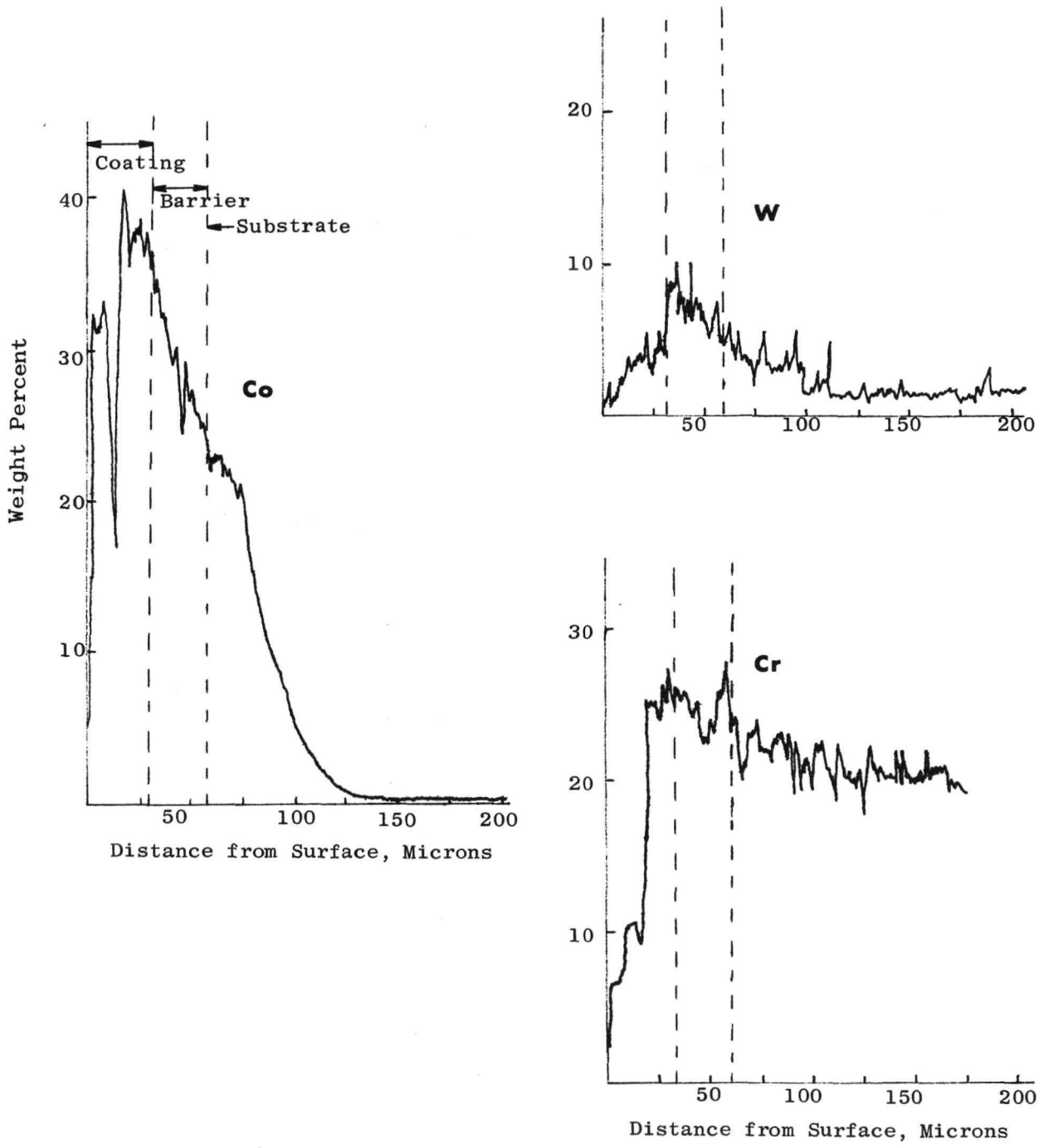

Figure 68. EM Co, Cr, and W Traces of Cr_5Al_8 Coating on TDNiCr, As-Processed.

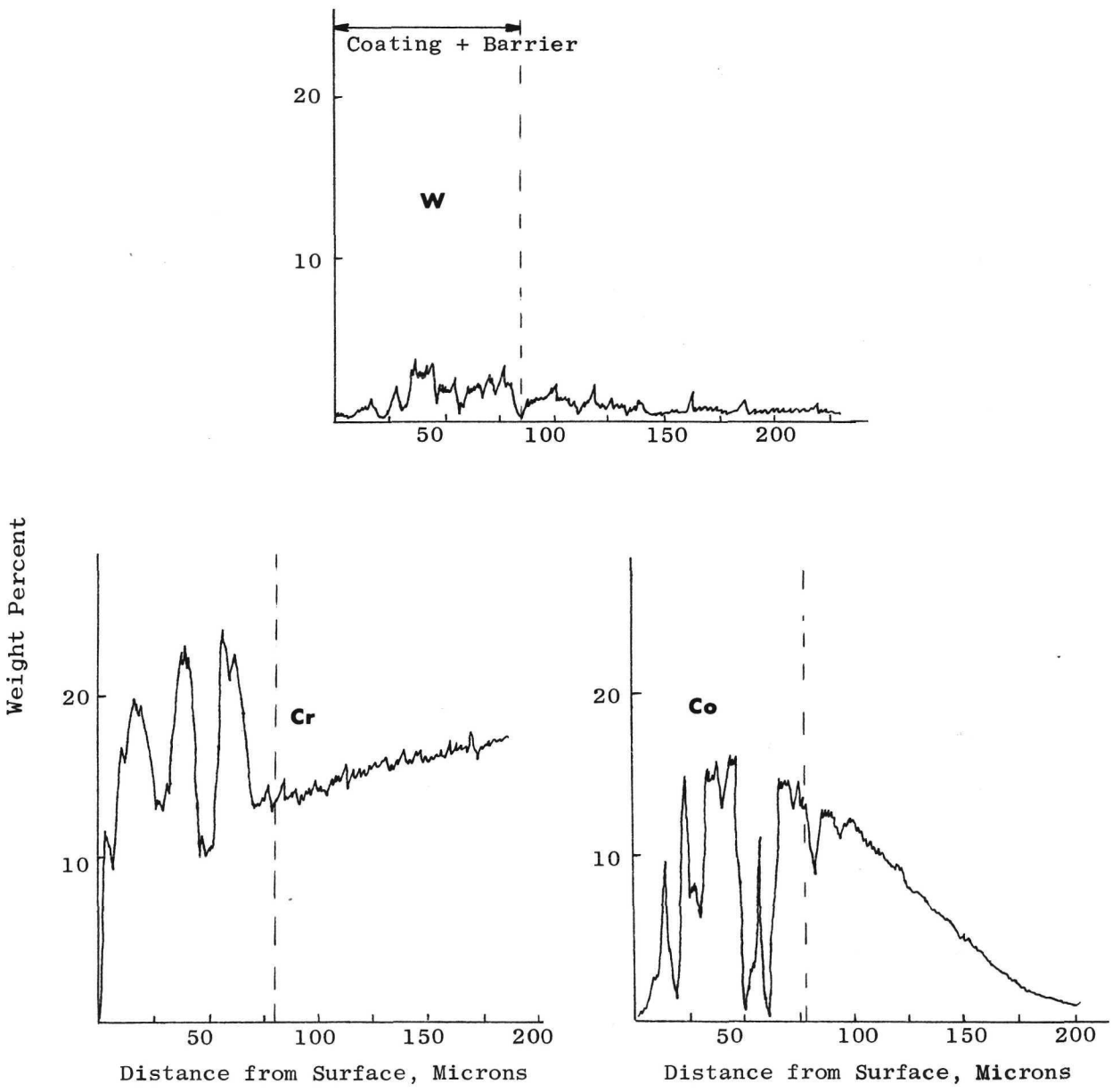

Figure 69. EM Co, Cr and W Traces of Cr_5Al_8 Coating on TDNiCr After 1422°K (2100°F)/300-Hour Oxidation Exposure

(a) Vapor Coated Specimen

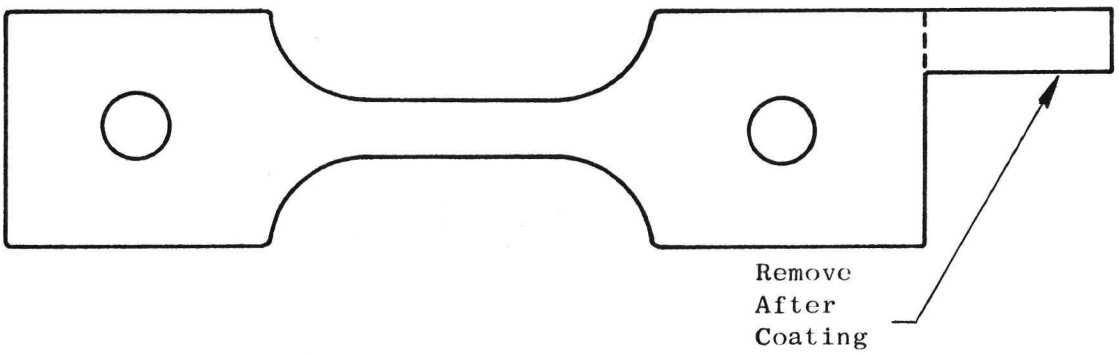

(b) Plasma Sprayed Barrier Layer Specimen

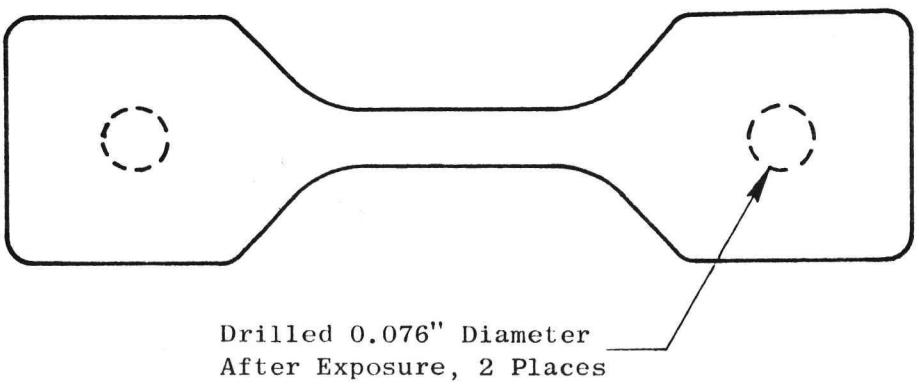

Figure 70 Tensile Test Specimen Configurations.

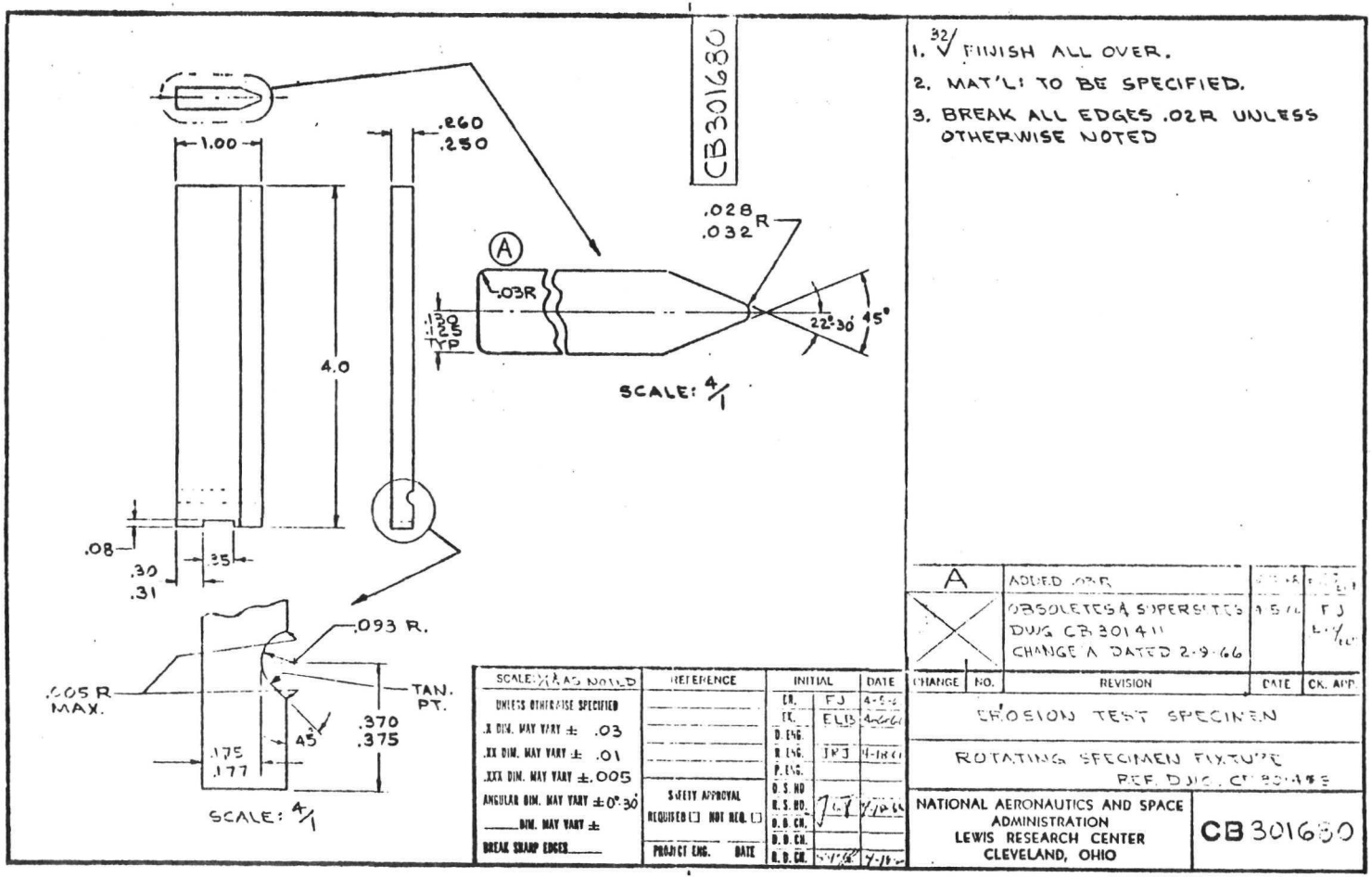

Figure 71 Erosion Test Specimen.

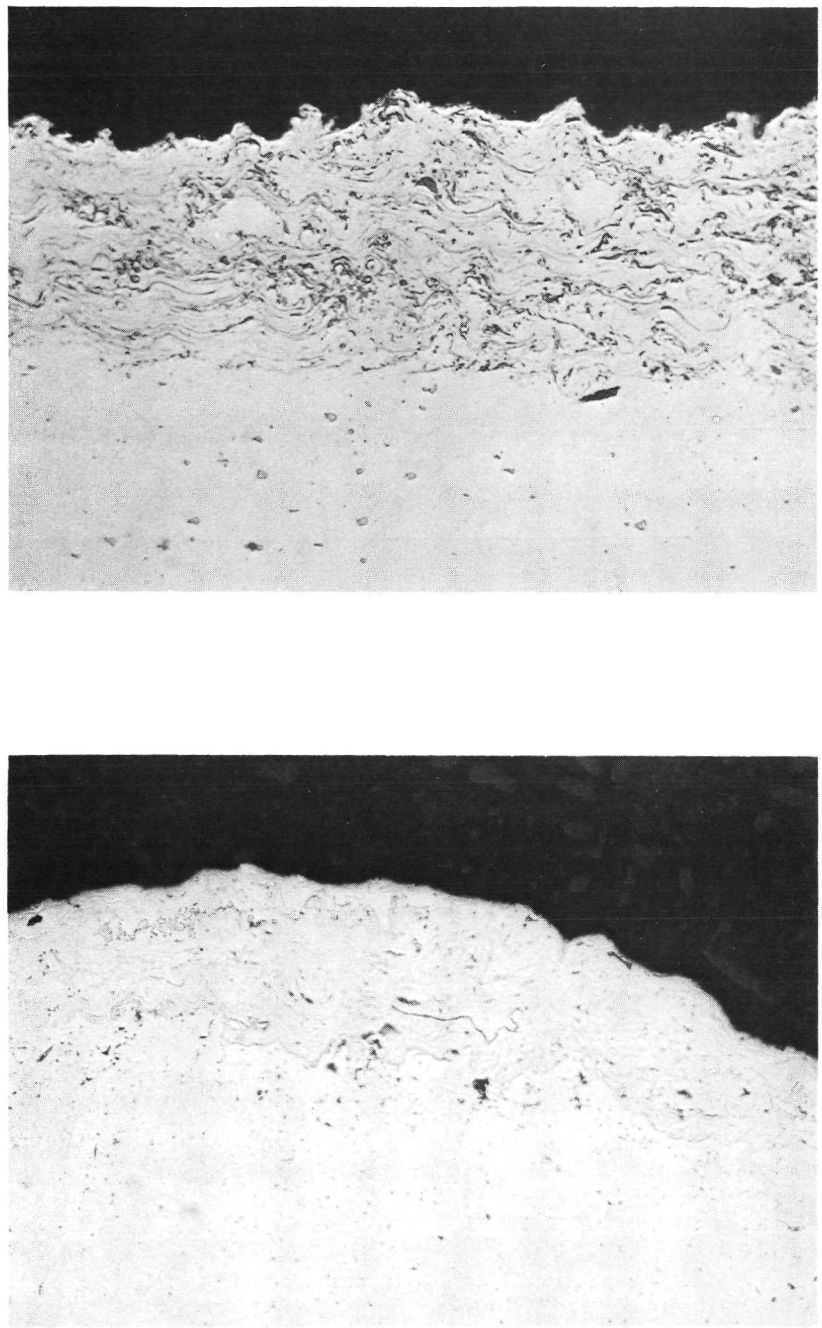

Figure 72 Thermal-Sprayed Barrier Layer Coatings, 250X, Unetched.
Top: Plasma-Sprayed Hastelloy C-1, High Velocity Nozzle
Bottom: Detonation-Gun-Sprayed X40

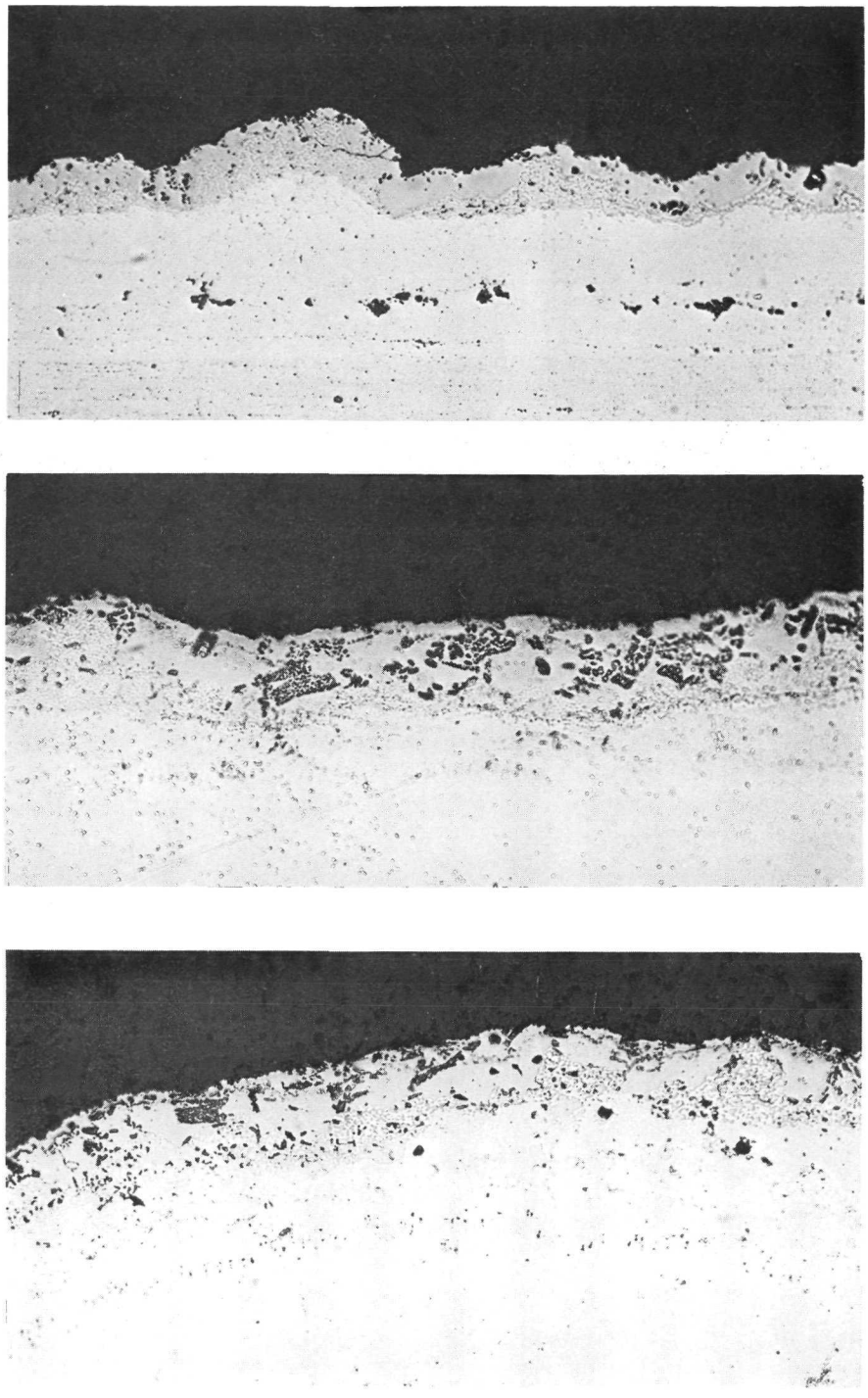

Figure 73. NC11A Coated Barrier Layer Coatings, 250X, Unetched
Top: X40 Barrier/TDNiCr
Center: Hastelloy C-1/TDNiCr
Bottom: Hastelloy C-1/TDNi

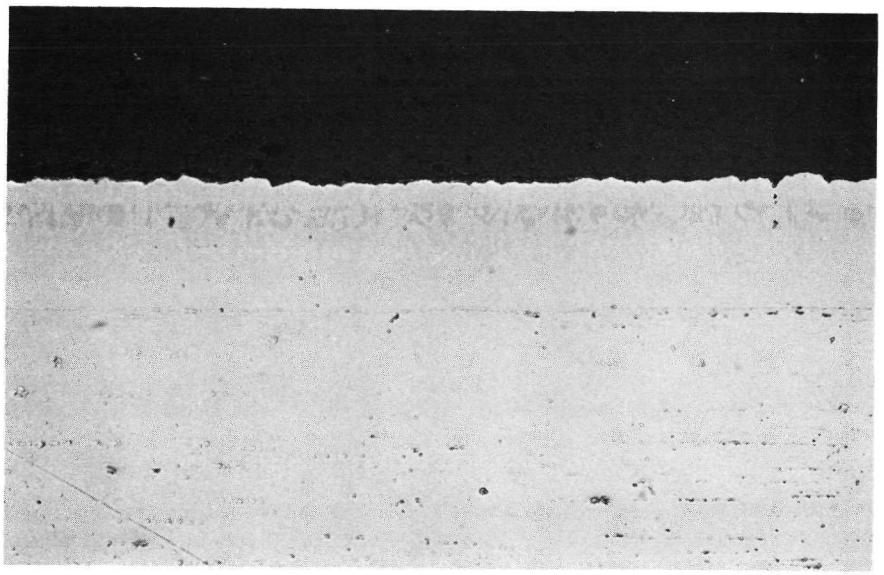

Figure 74. Vapor-Deposited NiCrAlY Coating, 250X, Untched.

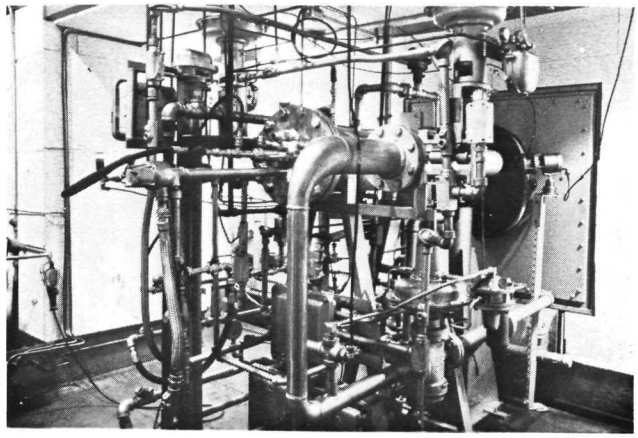

a.) Overall view of rig and portion of test cell.

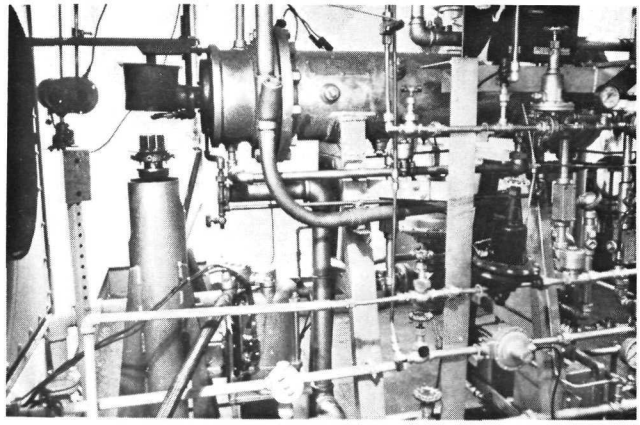

b.) Side view of rig exhibiting specimen holder with specimens in a "semi-down" position. To left is exhaust duct. Gun type instrument aimed at specimen "up" position is the Ircon controller.

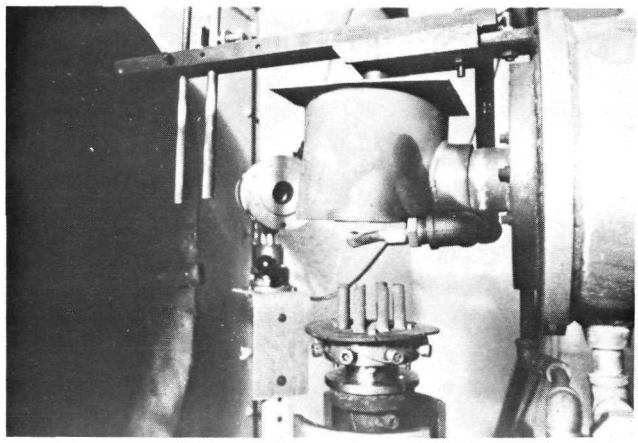

c.) Close-up of test fixture. Specimen "semi-down" position, note the Ircon. During test for hot gas exposure the fixture is in the "up" position, which is inside the cylindrical shield. When specimens are cycled they drop to low "down" position (bottom of photo) and are blasted with line air.

Figure 75. High Velocity Burner Rig

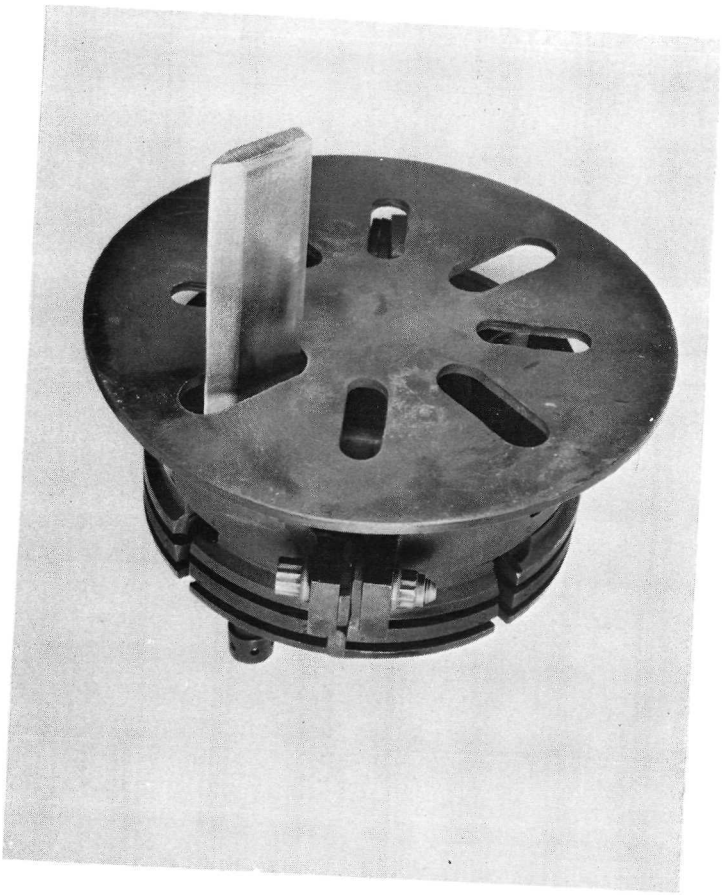

Figure 76. Oxidation/Erosion Test Specimen with Rotating Fixture

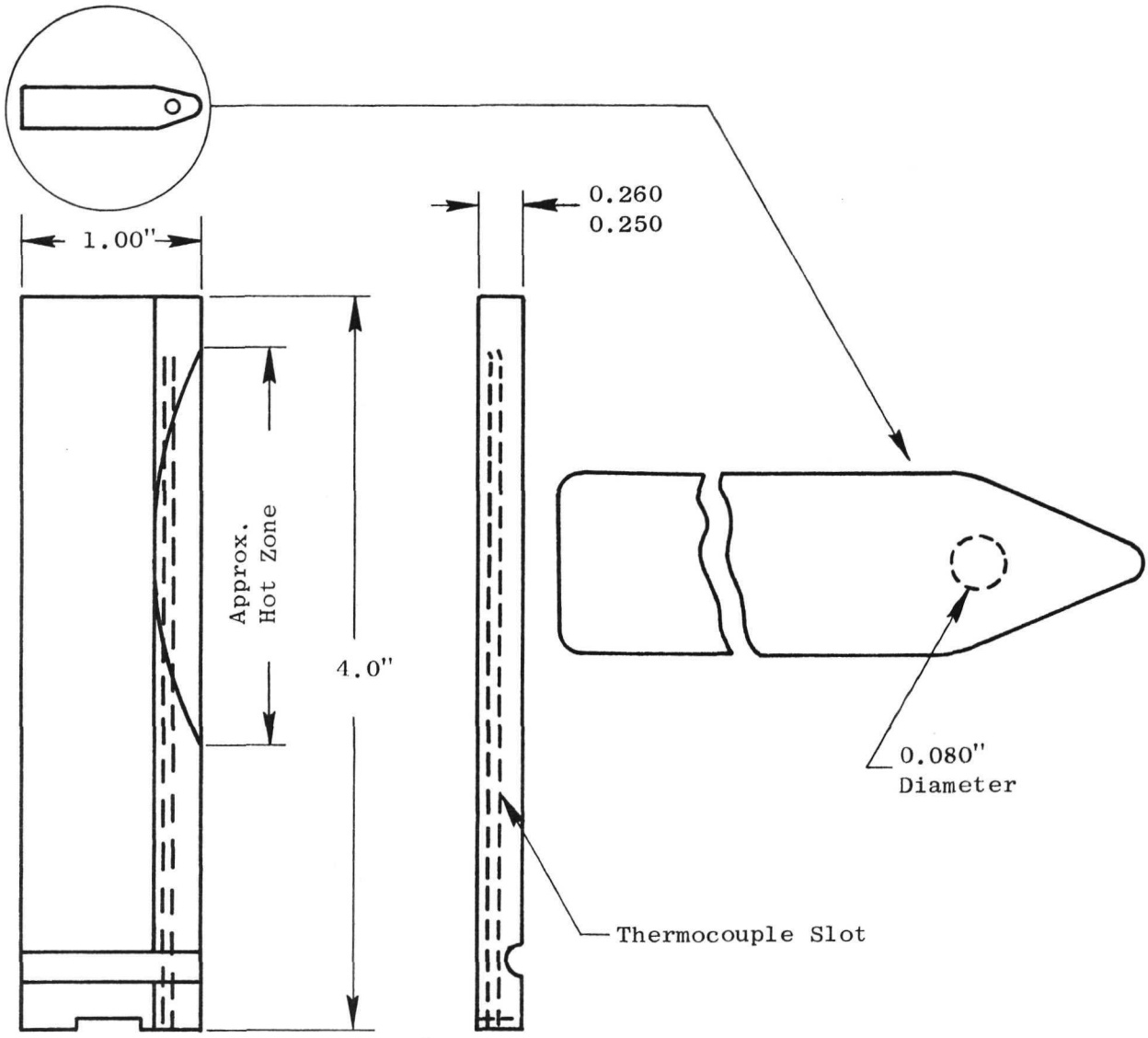

Figure 77 Instrumented Erosion Test Specimen.

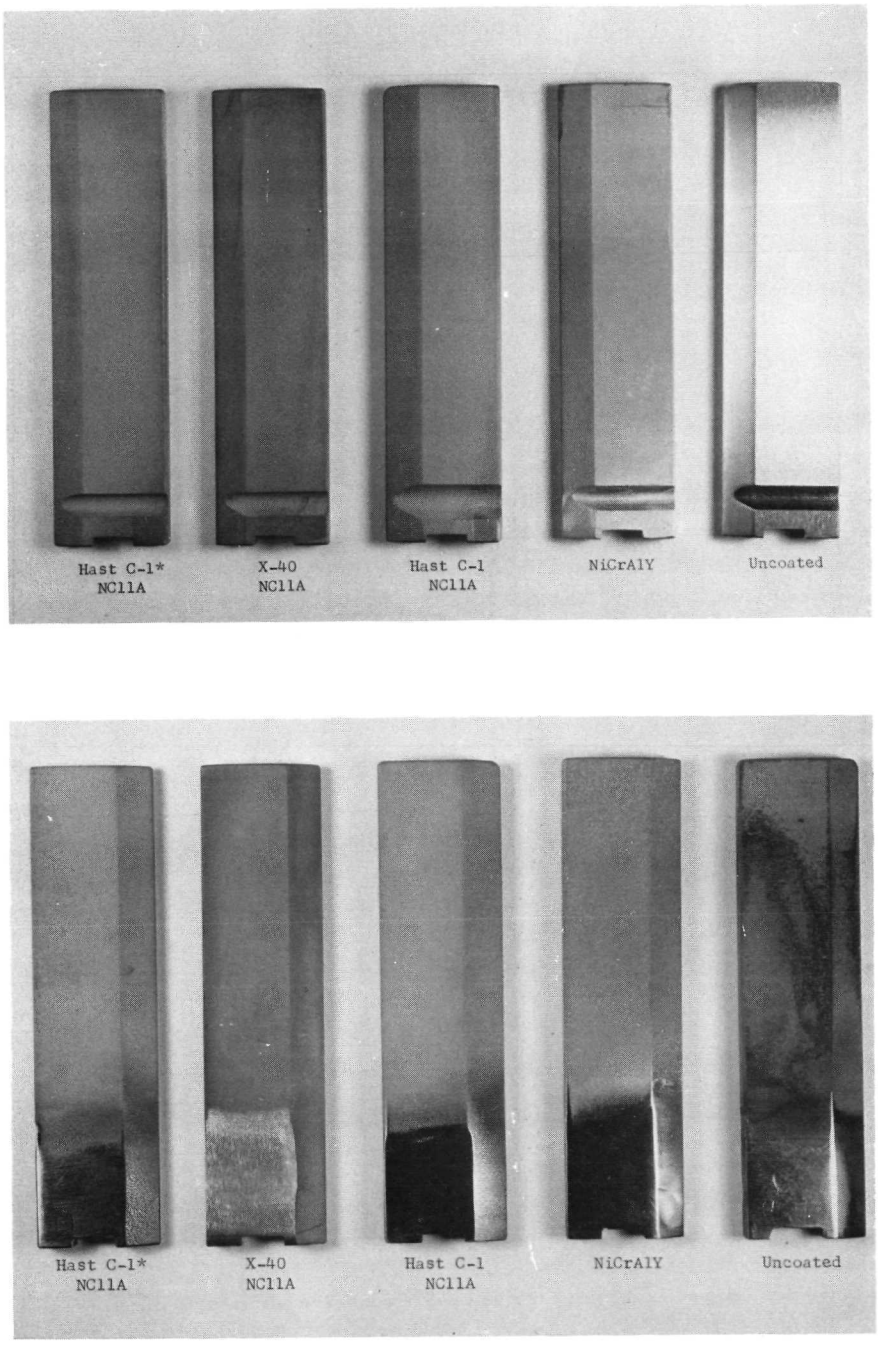

Figure 78. $1422^{o}K$ ($2100^{o}F$) Burner Rig Test Specimens.
Top: Prior to Test. Hastelloy C-1/TDNi Substrate
Bottom: After 46 Hours. X40/NC11A, Replacement for Fatigue-Failed Specimen.

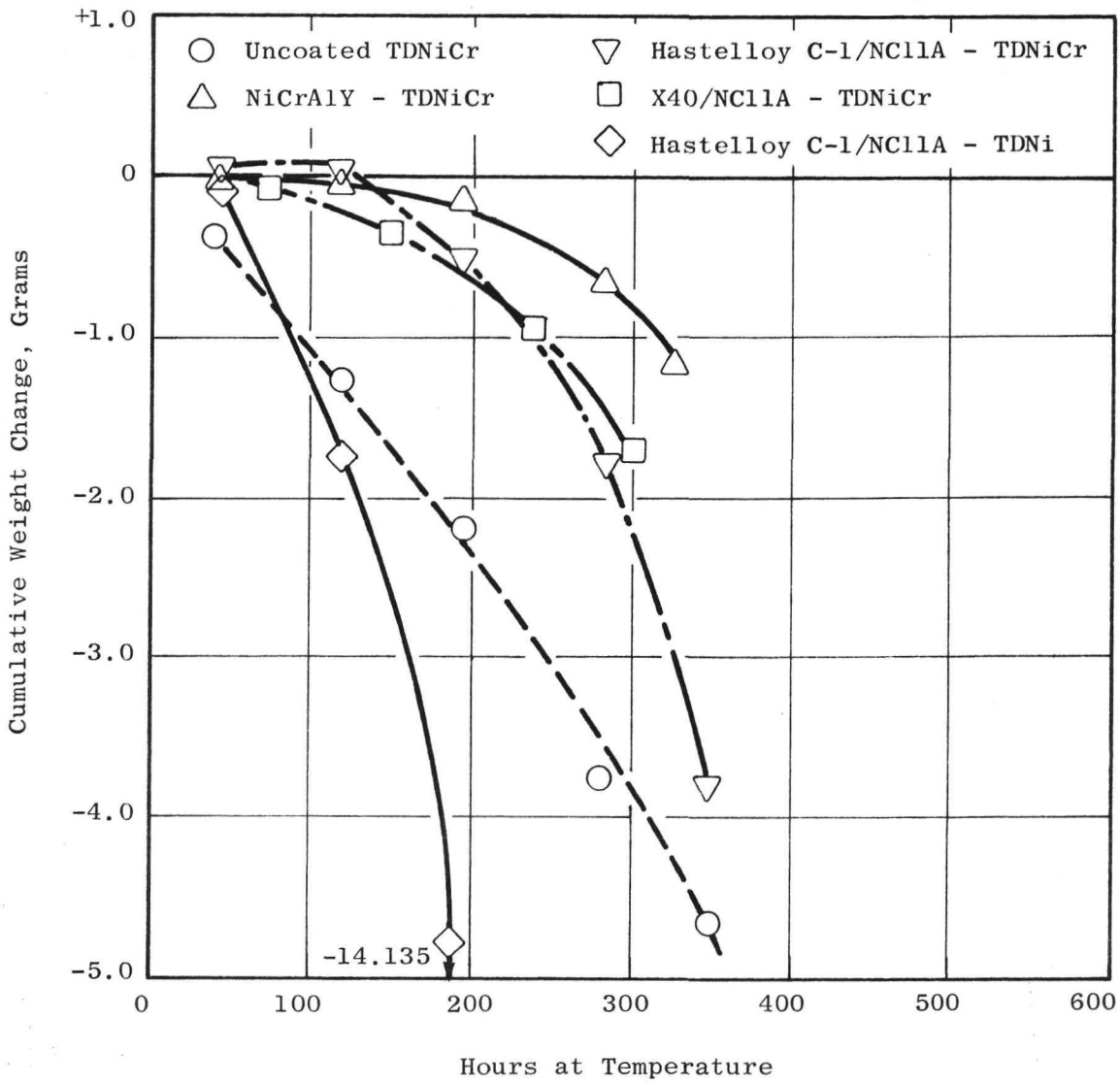

Figure 79. Cumulative Weight Change, 1422° K (2100° F) Mach 1 Burner Rig Test, 1 Hour Cycles.

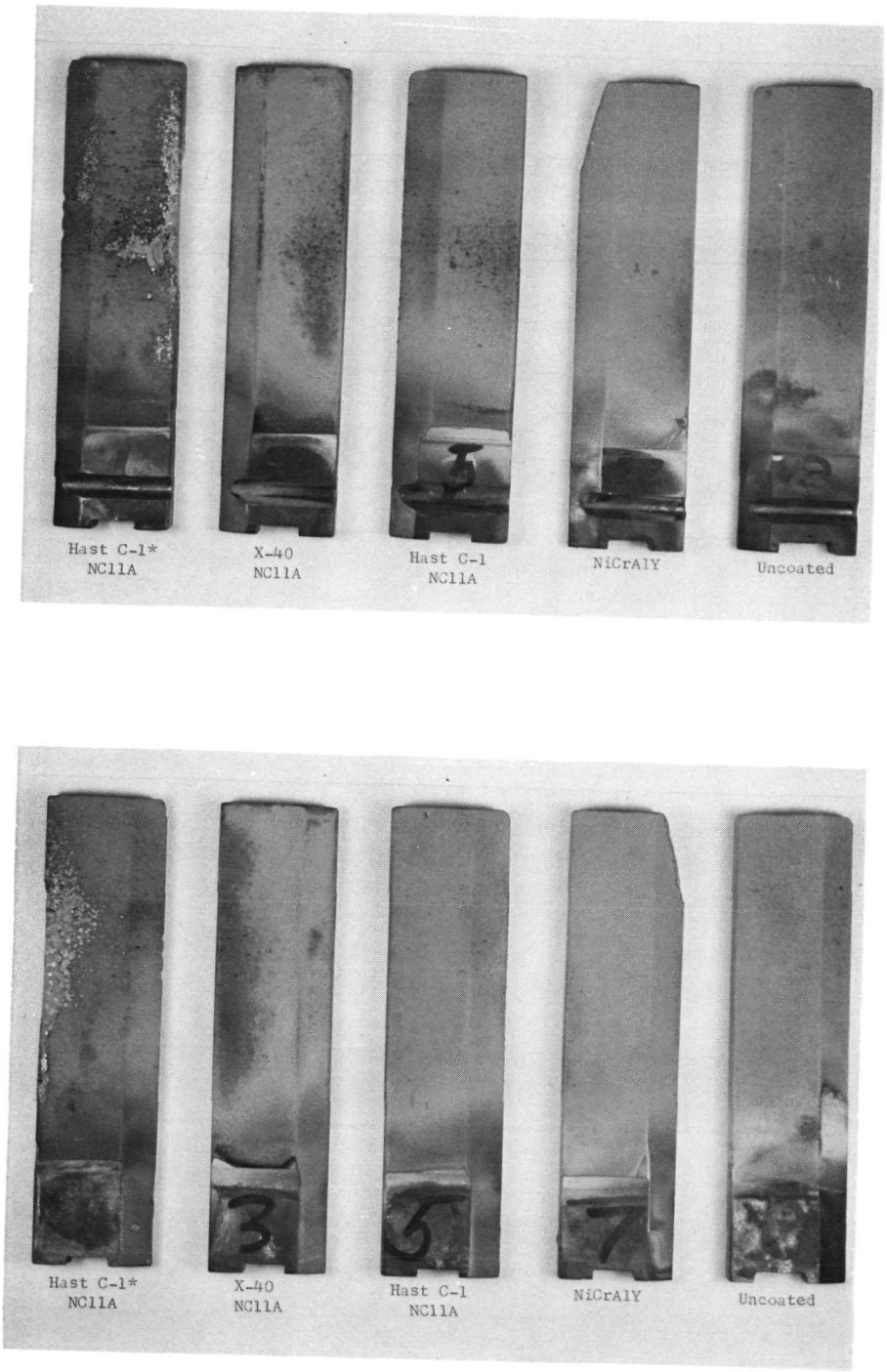

Figure 80. 1422°K (2100°F) Burner Rig Test Specimens After 118 Hours Exposure (X40/NC11A - 72 Hours), Two Views.

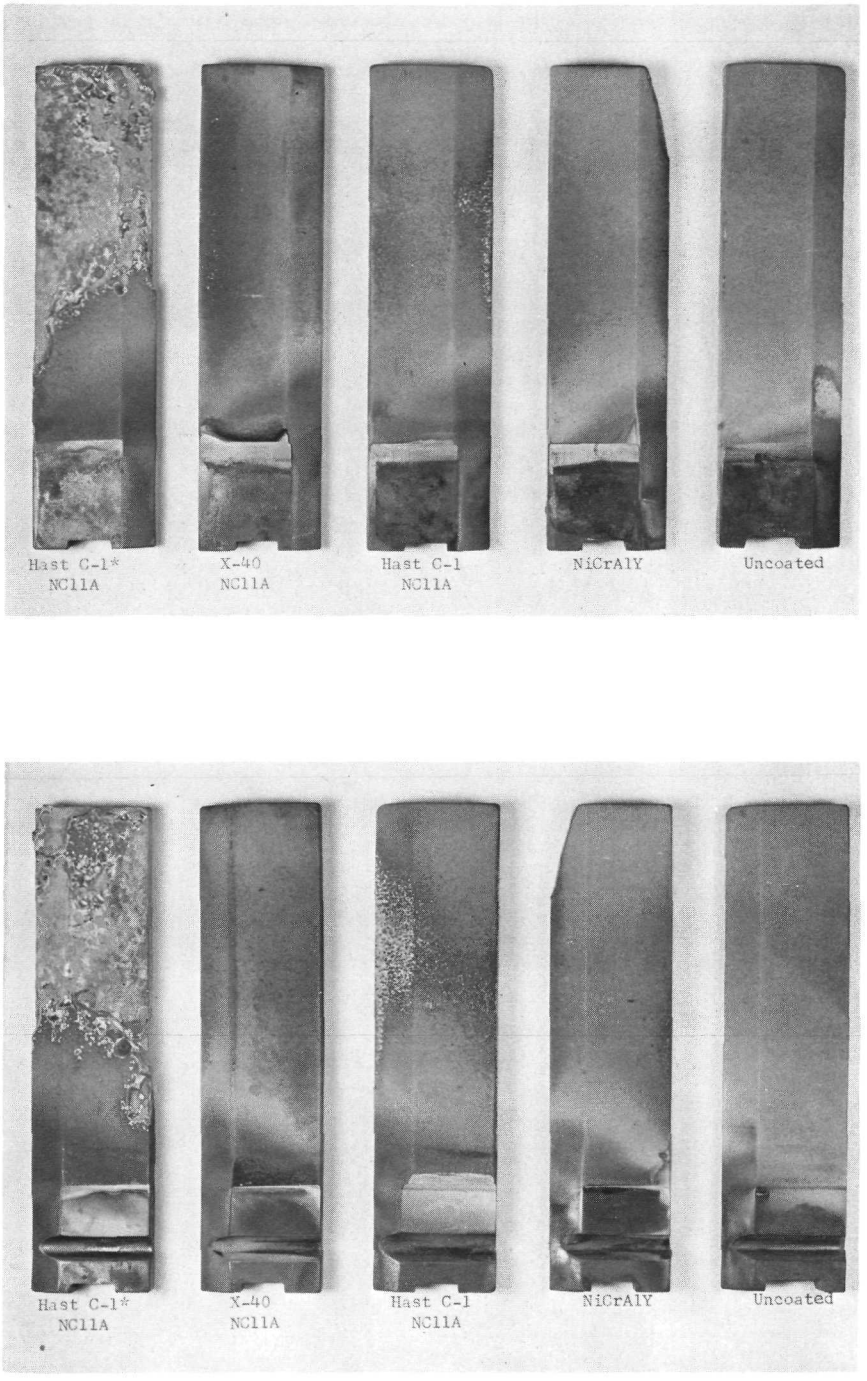

Figure 81. 1422°K (2100°F) Burner Rig Test Specimens After 196 Hours Exposure (X40/NC11A - 150 Hours), Two Views

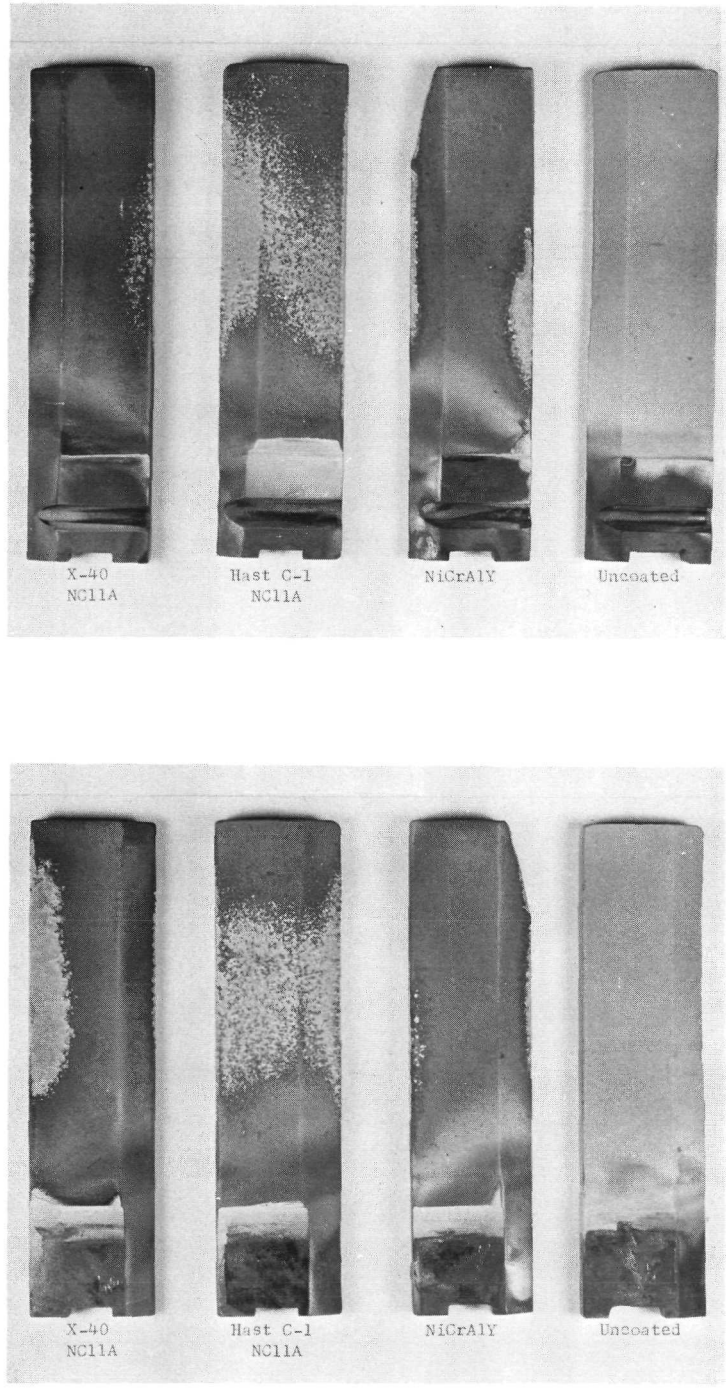

Figure 82. 1422°K (2100°F) Burner Rig Test Specimens After 284 Hours Exposure (X40/NC11A - 238 Hours), Two Views

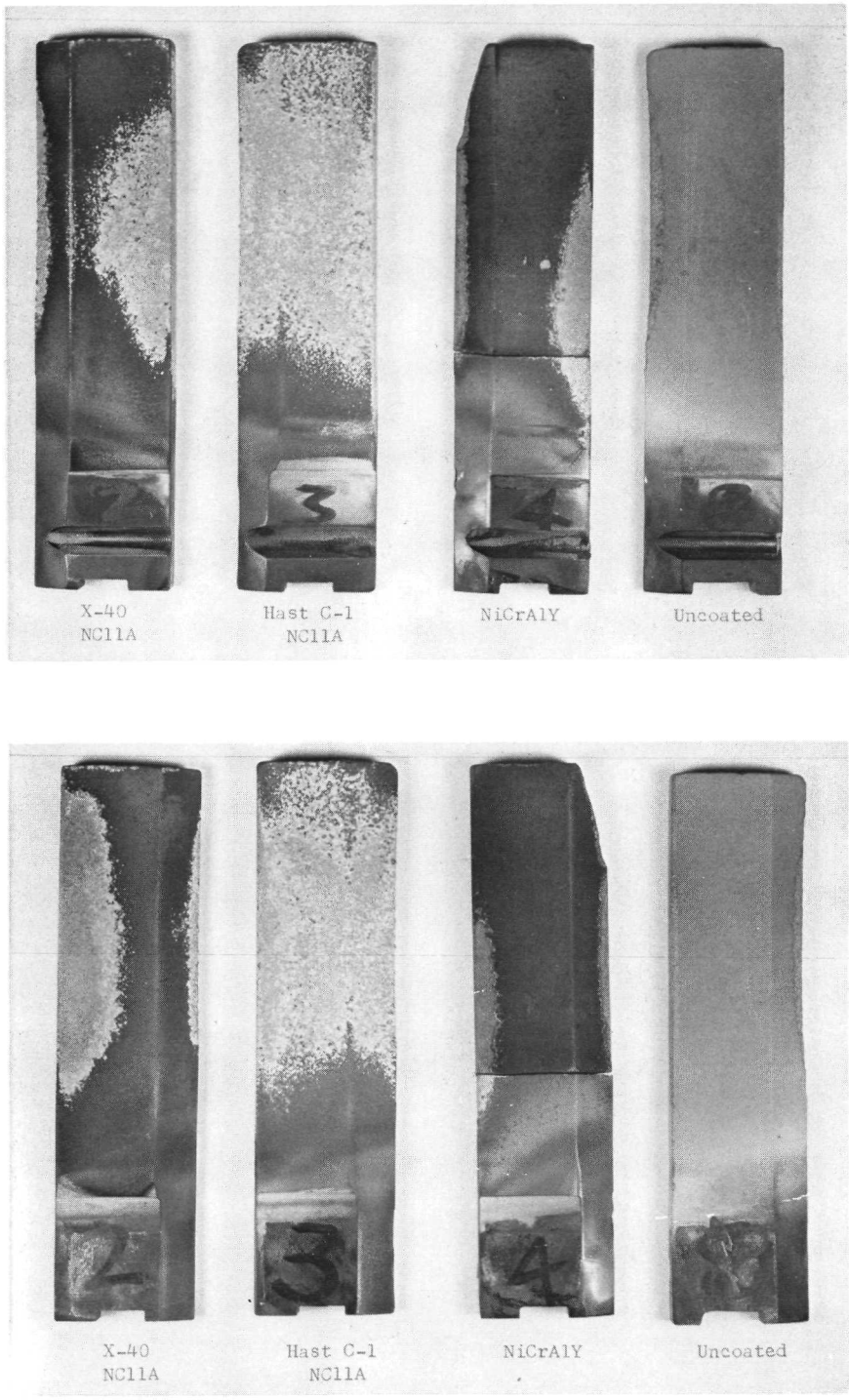

Figure 83. 1422°K (2100°F) Burner Rig Test Specimens After 350 Hours Exposure (X40/NC11A - 304 Hours, NiCrAlY Fatigue Failure - 326 Hours), Two Views

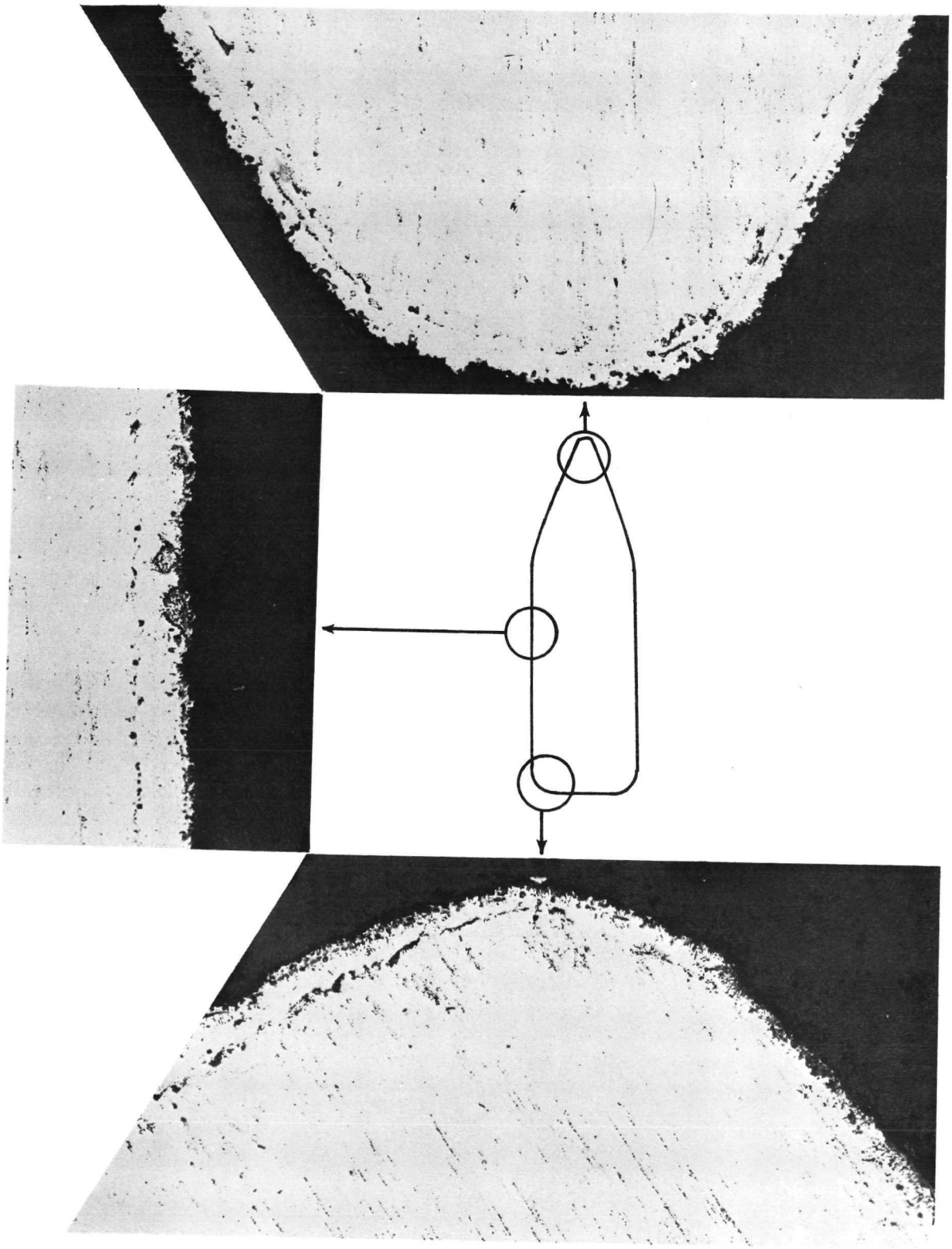

Figure 84. X40/NC11A Coated TDNiCr After 46 Hours in 1422°K (2100°F) Burner Rig Test, 100X, Unetched.

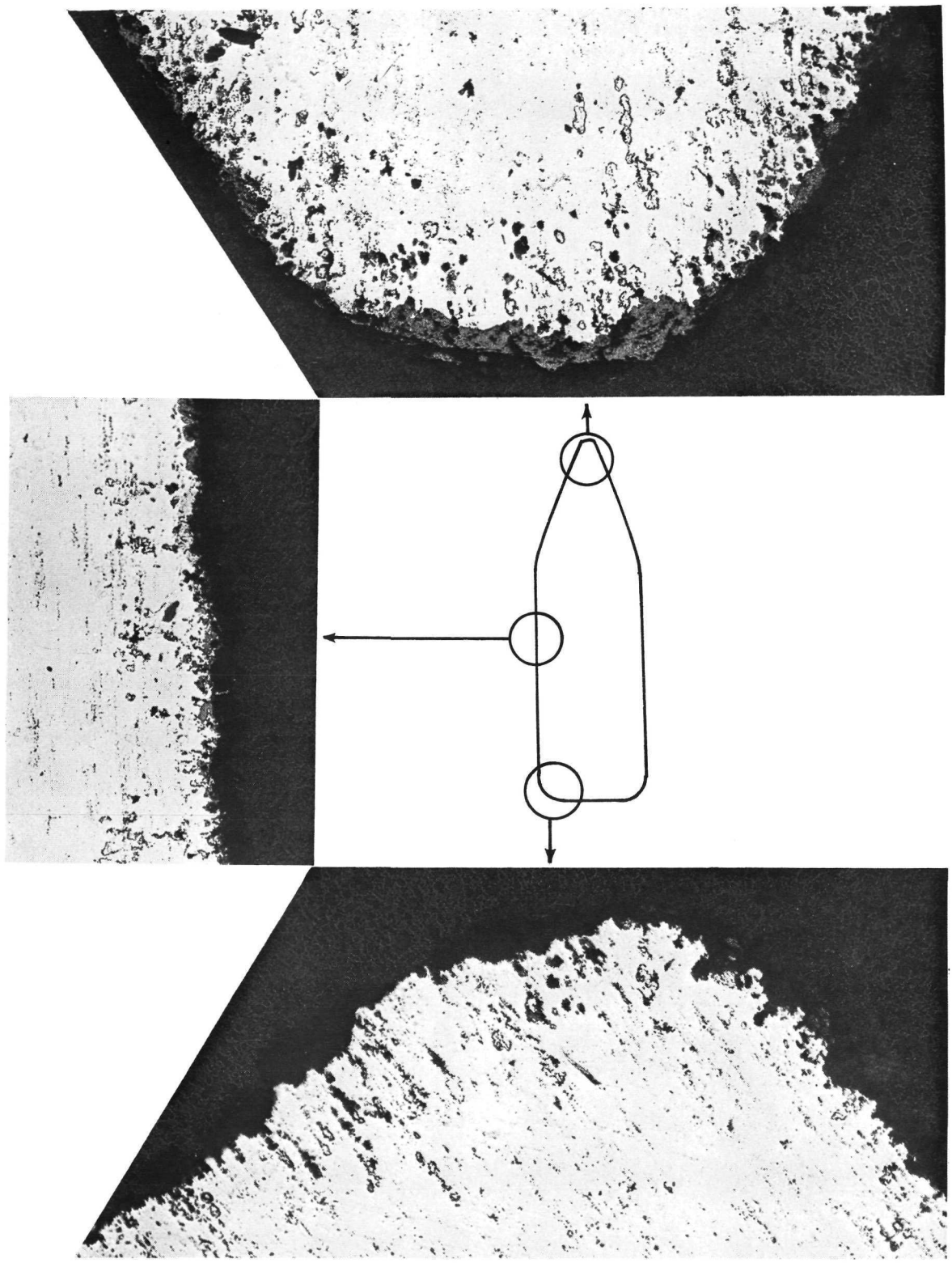

Figure 85. X40/NC11A Coated TDNiCr After 304 Hours in 1422°K (2100°F) Burner Rig Test, 100X, Unetched.

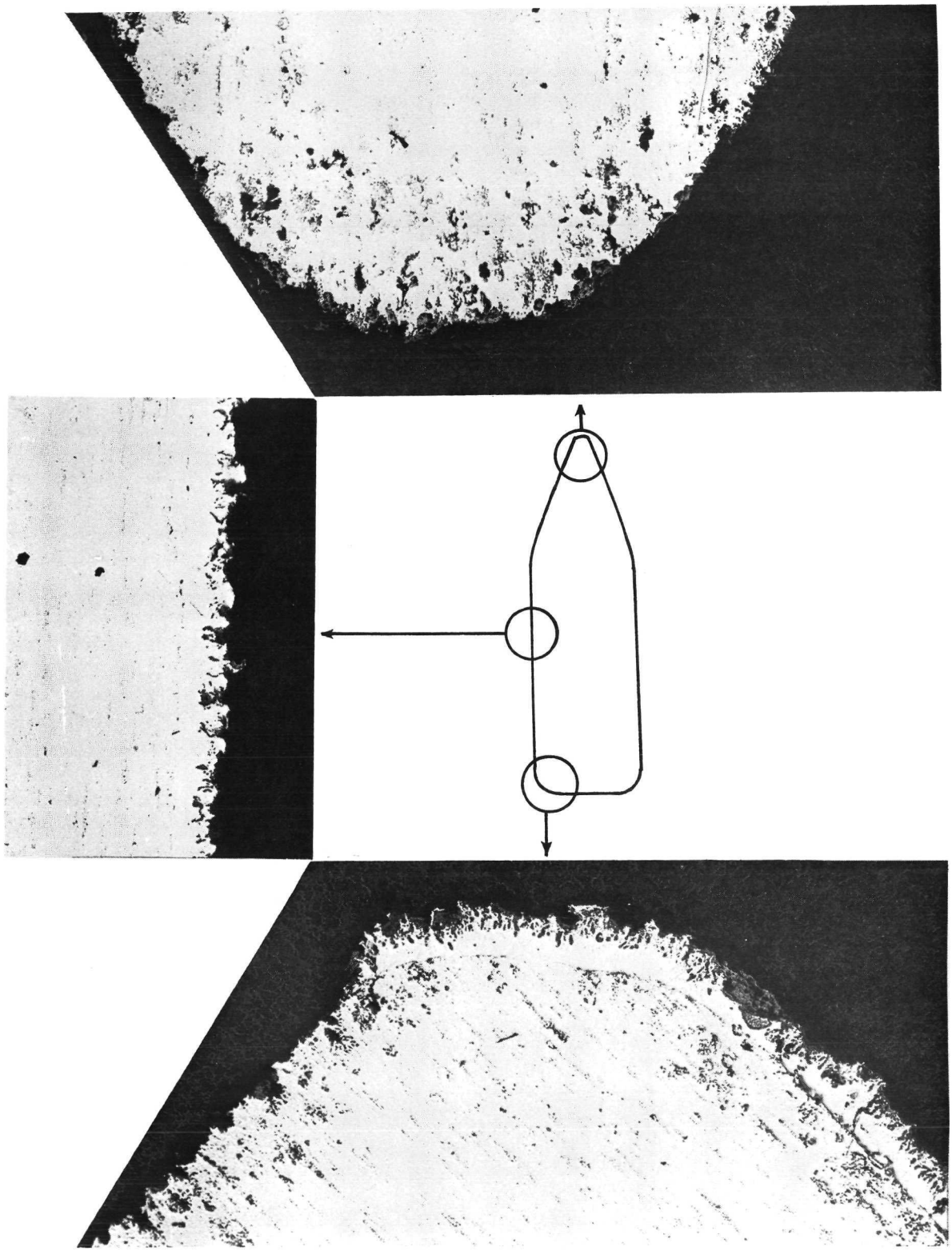

Figure 86. NiCrAlY Coated TDNiCr After 326 Hours in 1422°K (2100°F) Burner Rig Test, 100X, Unetched.

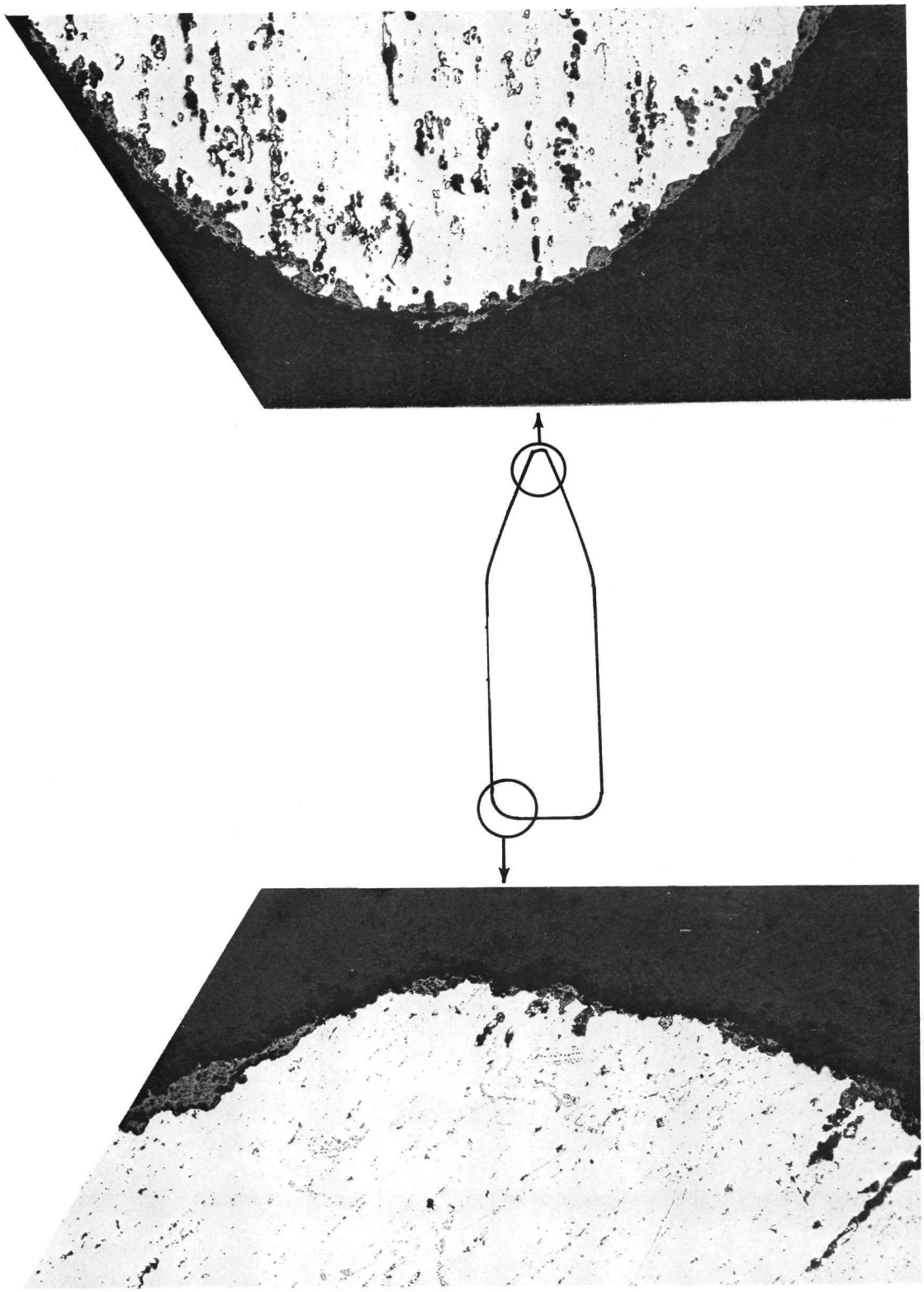

Figure 87. Uncoated TDNiCr After 350 Hours in 1422°K (2100°F) Burner Rig Test, 100X, Unetched.

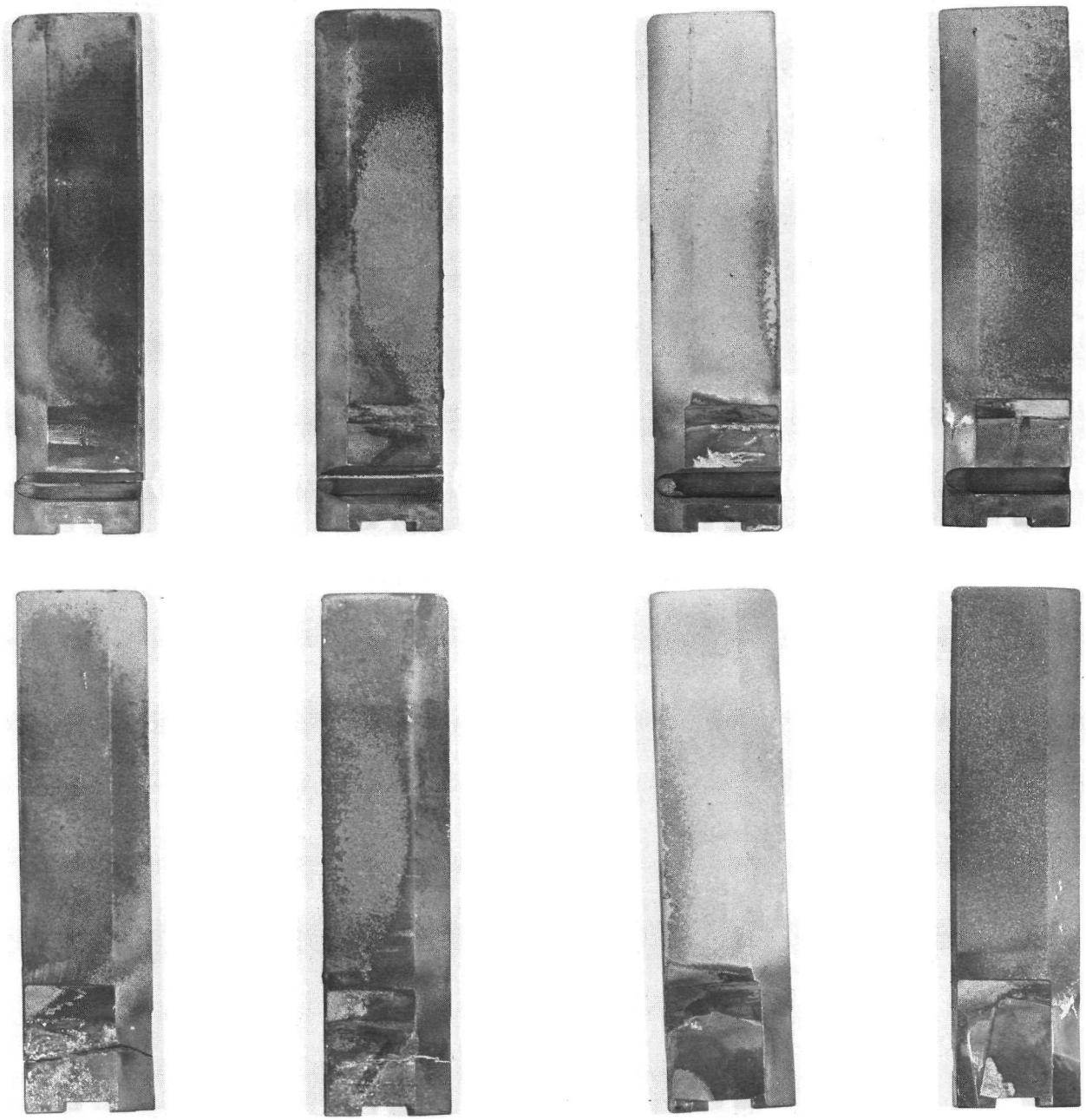

X40/NC11A
36 Hours
Fatigue Failure

X40/NC11A
38 Hours
Broke on Removal

Hast. C-1/NC11A
20 Hours
Local Attack

NiCrAlY
38 Hours
X40 Splatter

Figure 88. Coated TDNiCr From 1477°K (2200°F) Burner Rig Test Following Rotating Fixture Failure.

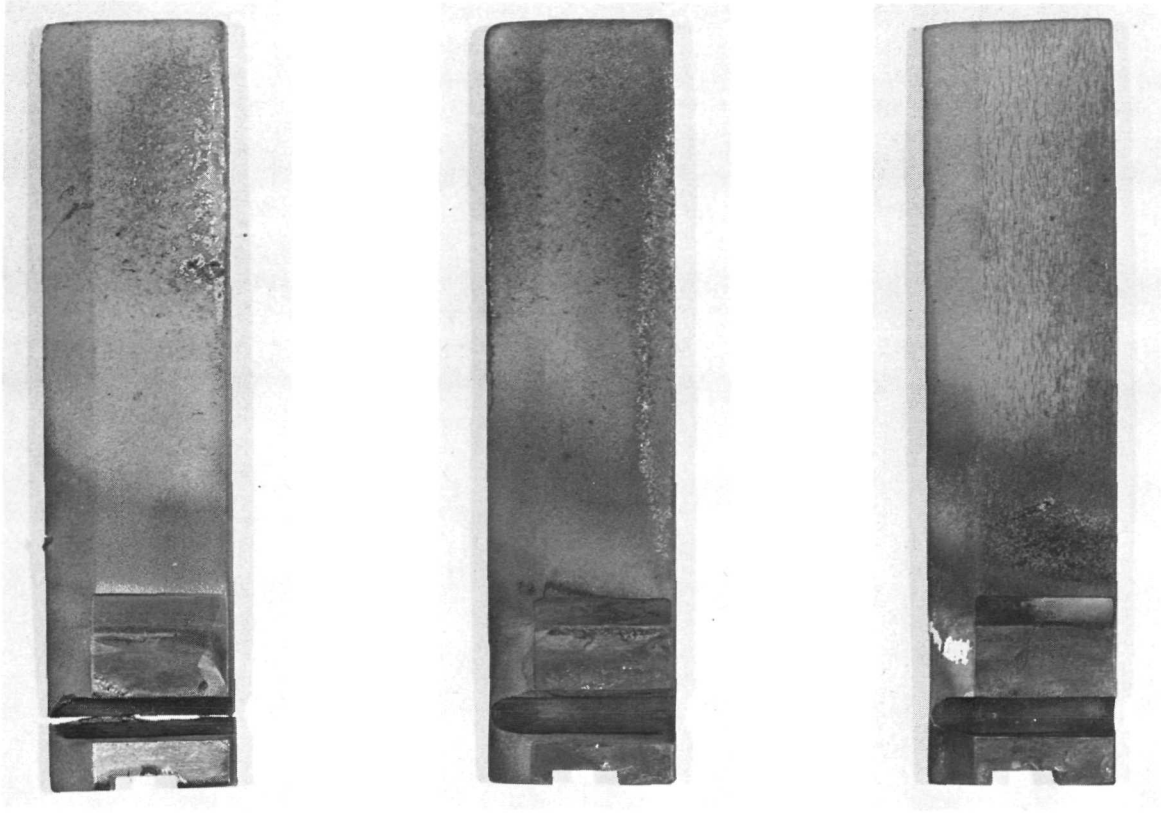

Hast. C-1/NC11A
TDNi
32 Hours

Hast. C-1/NC11A
TDNiCr
82 Hours

NiCrAlY
TDNiCr
100 Hours

Figure 89. Coated Test Specimens at Completion of 1477°K (2200°F)/ 100-Hour Burner Rig Test. Hastelloy C-1/NC11A/TDNi Failed in Fatigue.

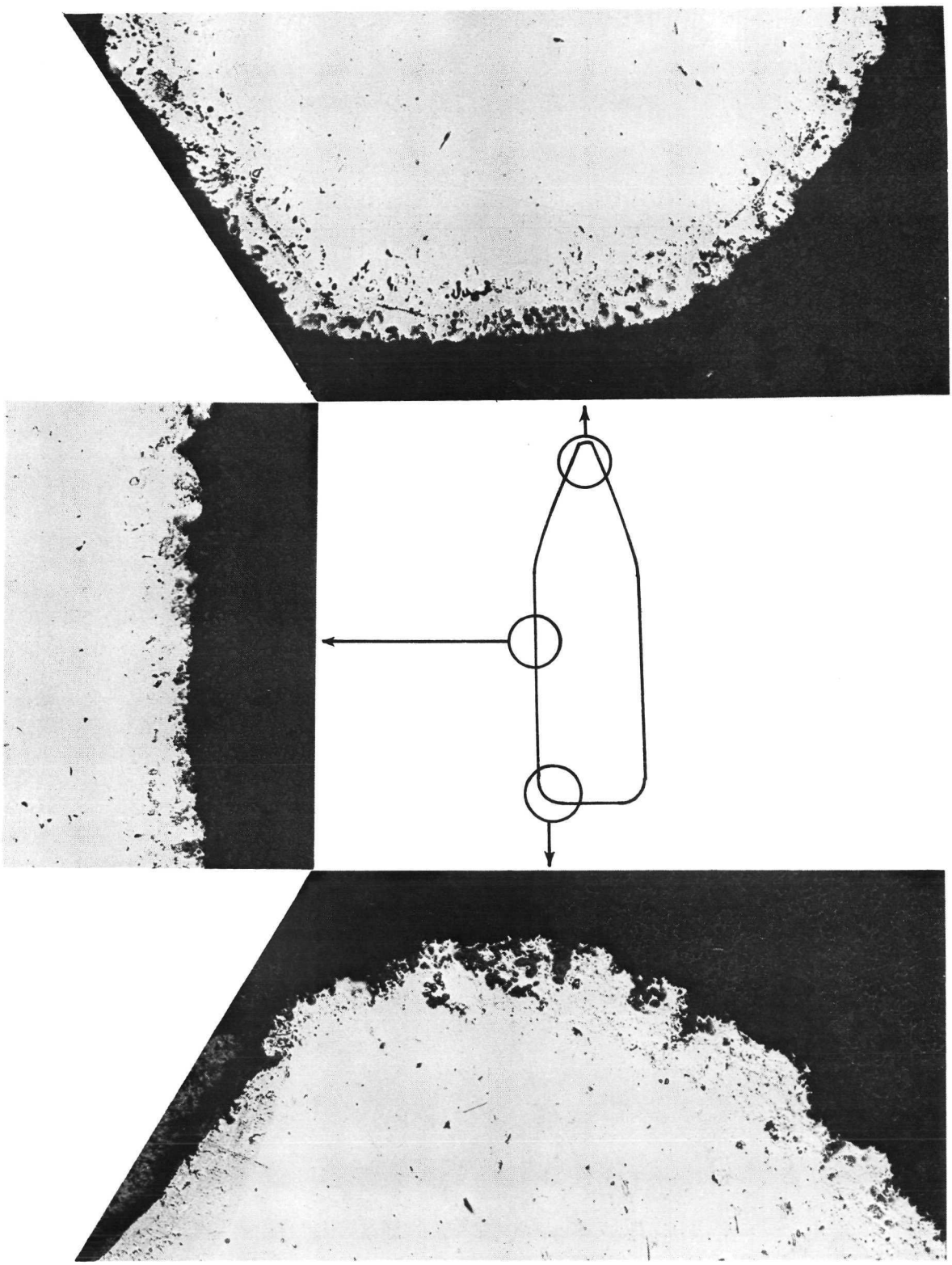

Figure 90. Hastelloy C-1/NC11A Coated TDNi Specimen After 32 Hours in 1477°K (2200°F) Burner Rig Test, 100X, Unetched.

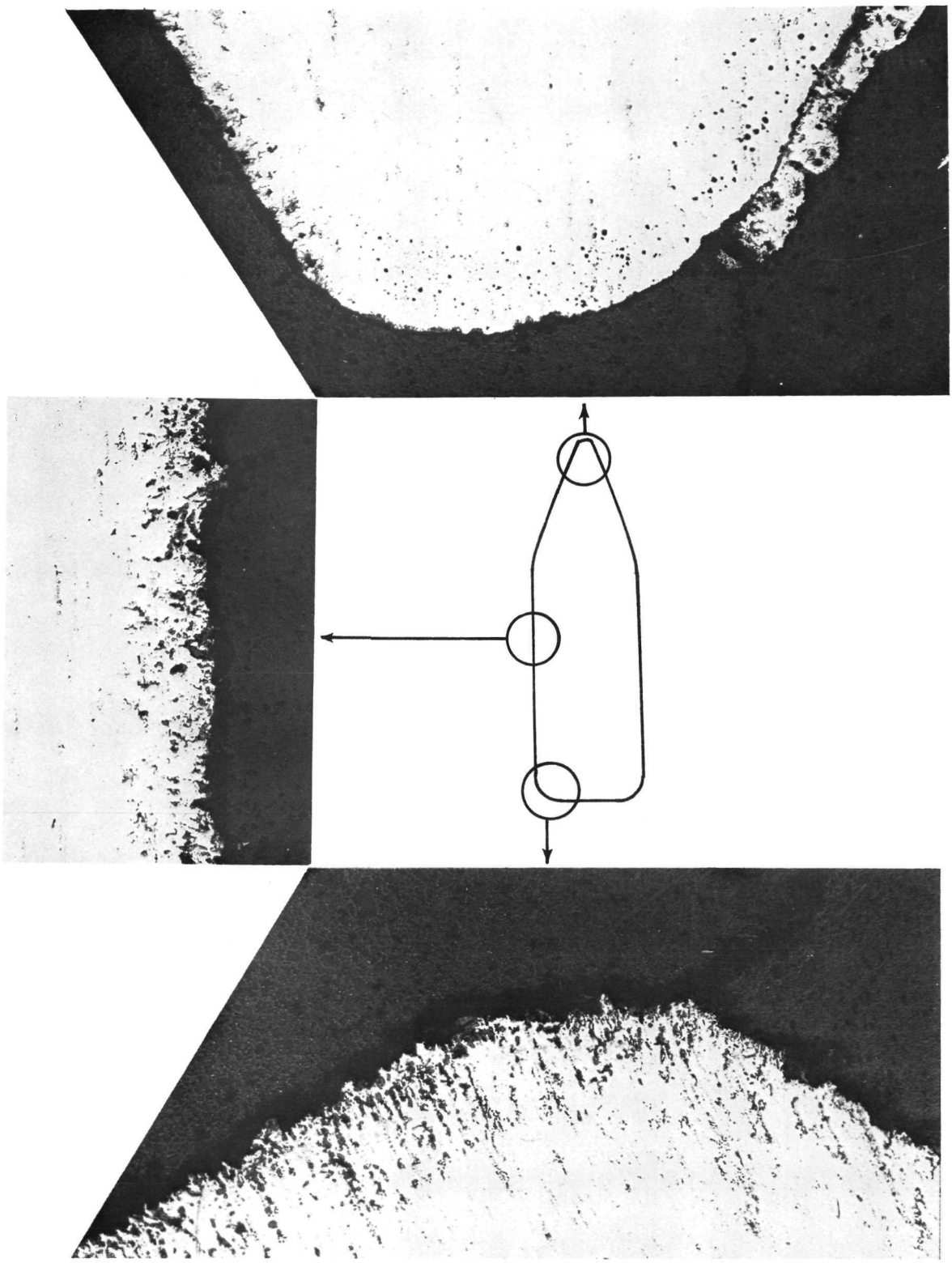

Figure 91. Hastelloy C-1/NC11A Coated TDNiCr Specimen After 32 Hours in 1477°K (2200°F) Burner Rig Test, 100X, Unetched.

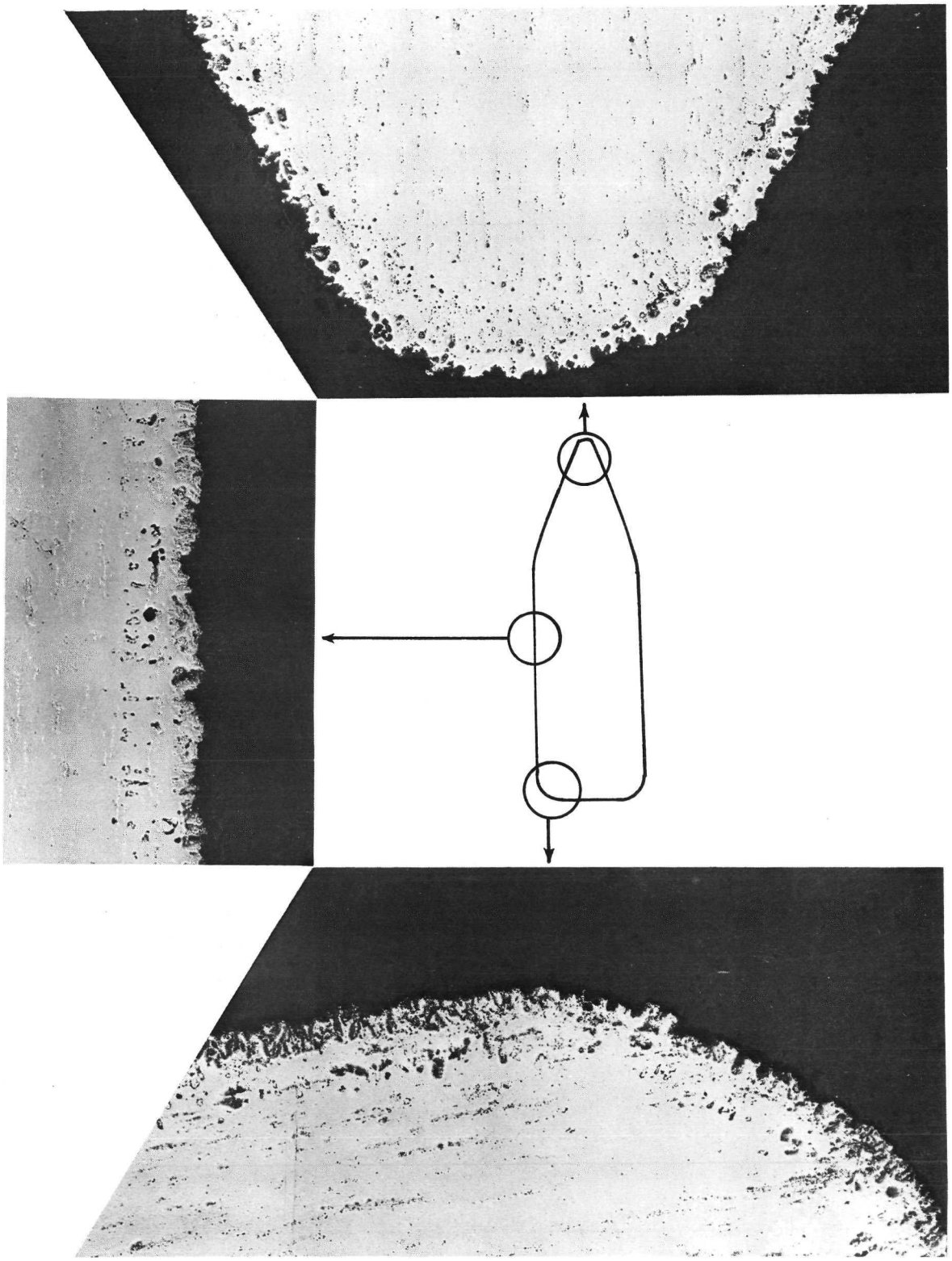

Figure 92. X40/NC11A Coated TDNiCr Specimen After 36 Hours in 1477°K (2200°F) Burner Rig Test, 100X, Unetched.

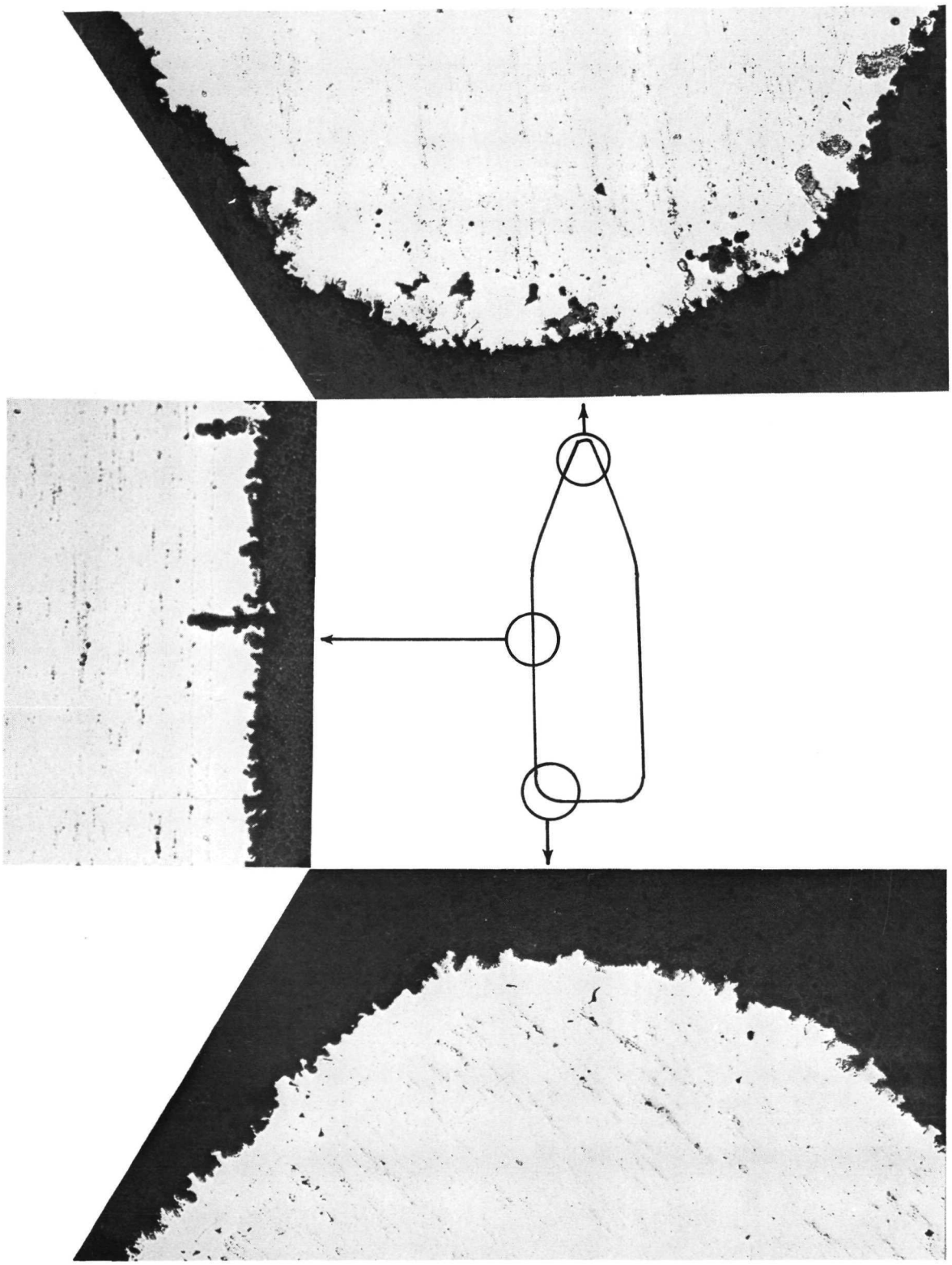

Figure 93. NiCrAlY Coated TDNiCr Specimen After 100 Hours in 1477°K (2200°F) Burner Rig Test, 100X, Unetched.

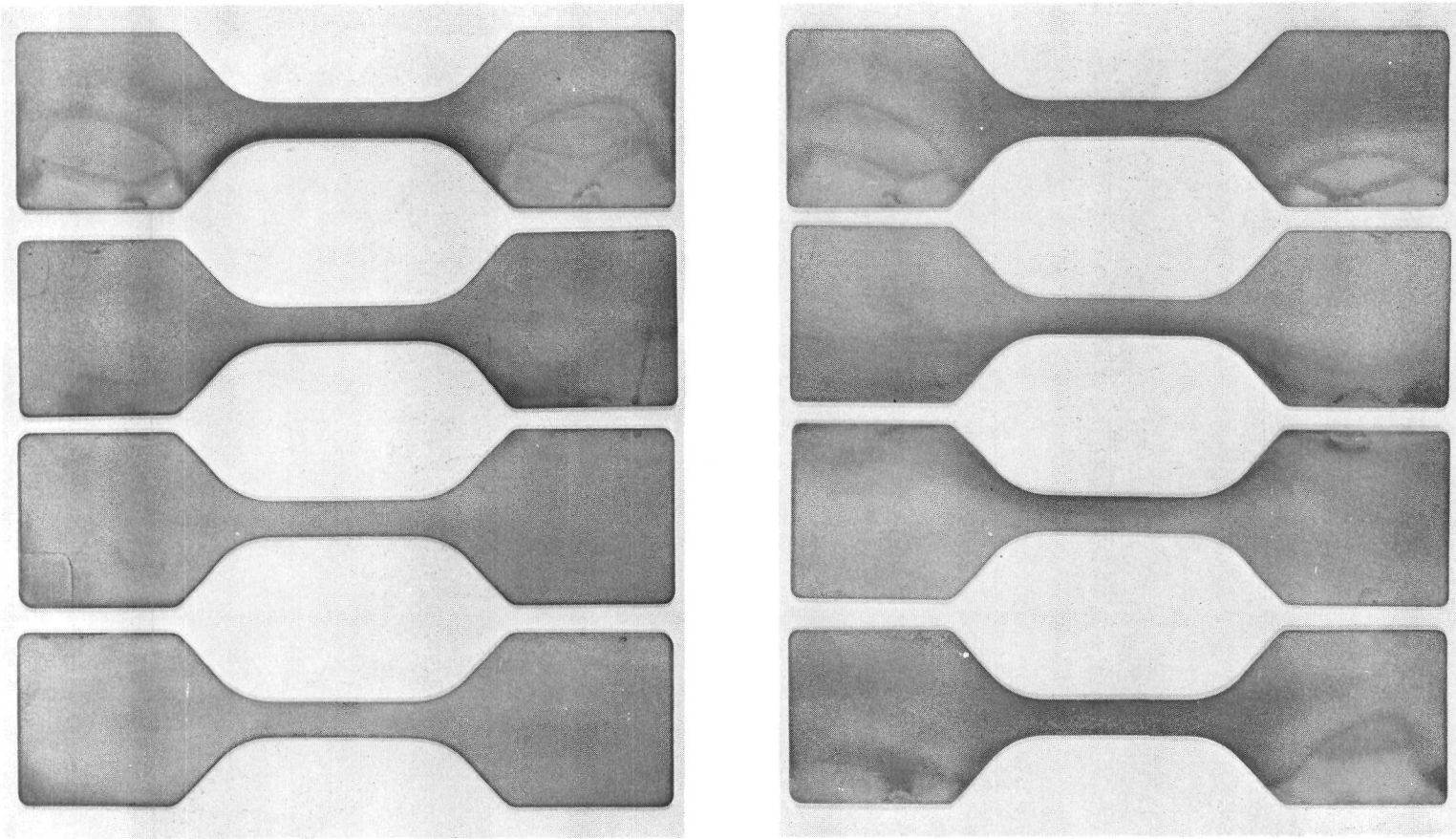

Hastelloy C-1/NC11A/TDNi

Hastelloy C-1/NC11A/TDNiCr

Figure 94. As-Processed Coated Tensile Specimens.

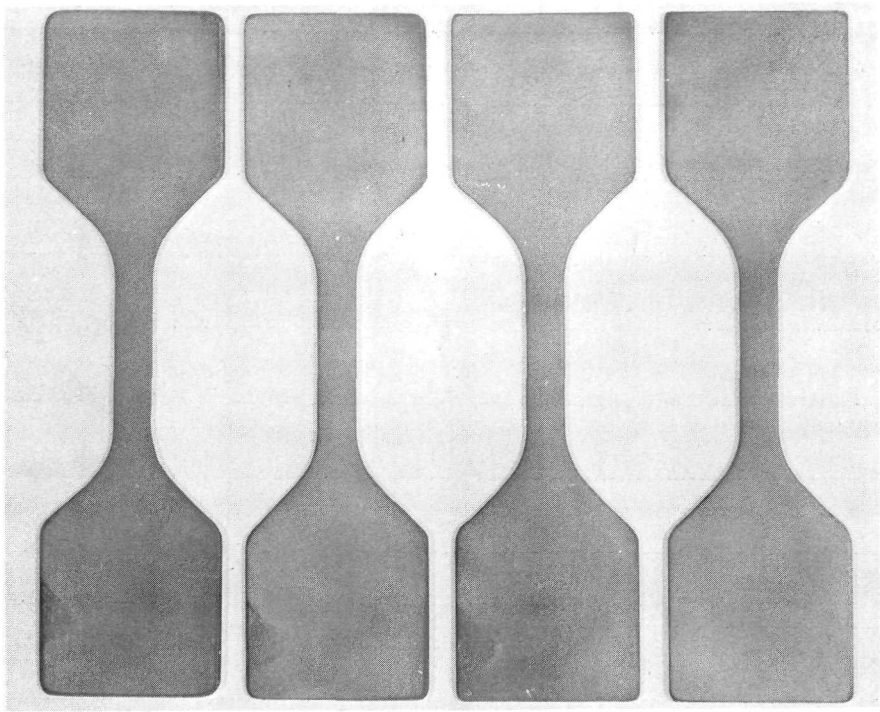

X40/NC11A/TDNiCr

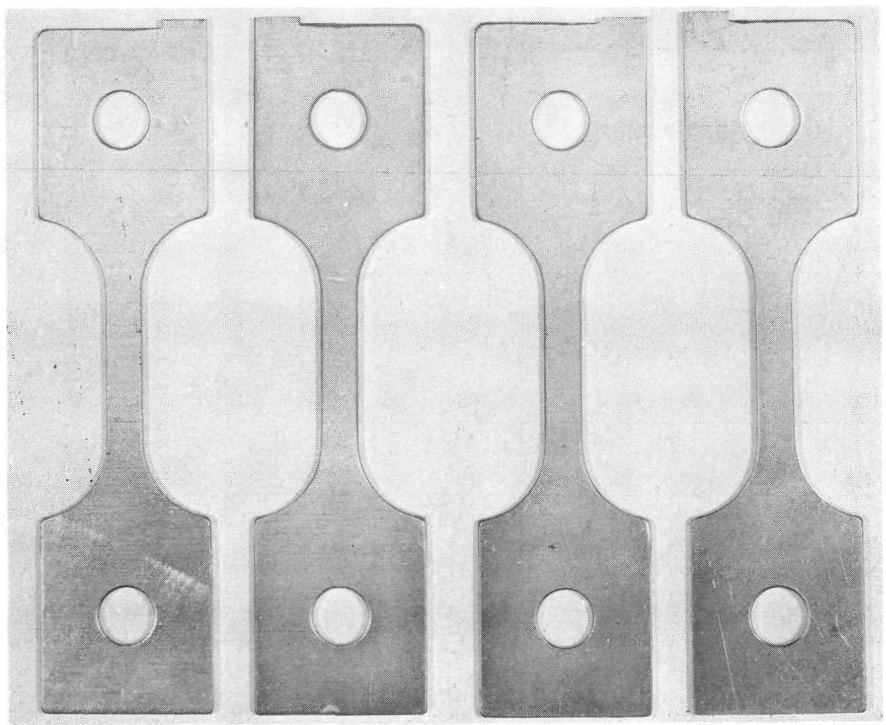

NiCrAlY/TDNiCr

Figure 95. As-Processed Coated Tensile Specimens.

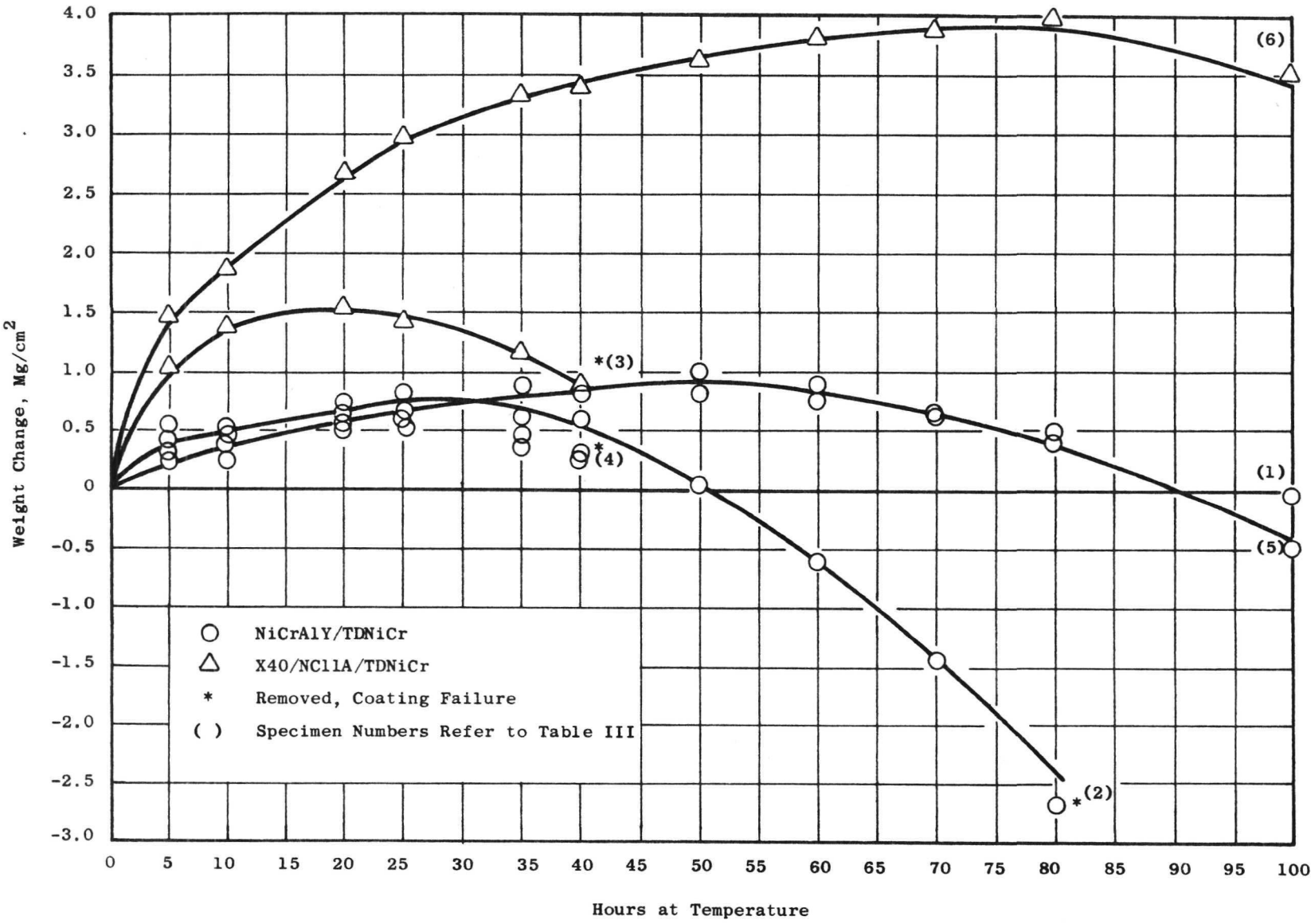

Figure 96. 1533° K (2300° F) Static Oxidation Test, Cumulative Weight Change for X4p/NC11A and NiCrAlY Coated TDNiCr.

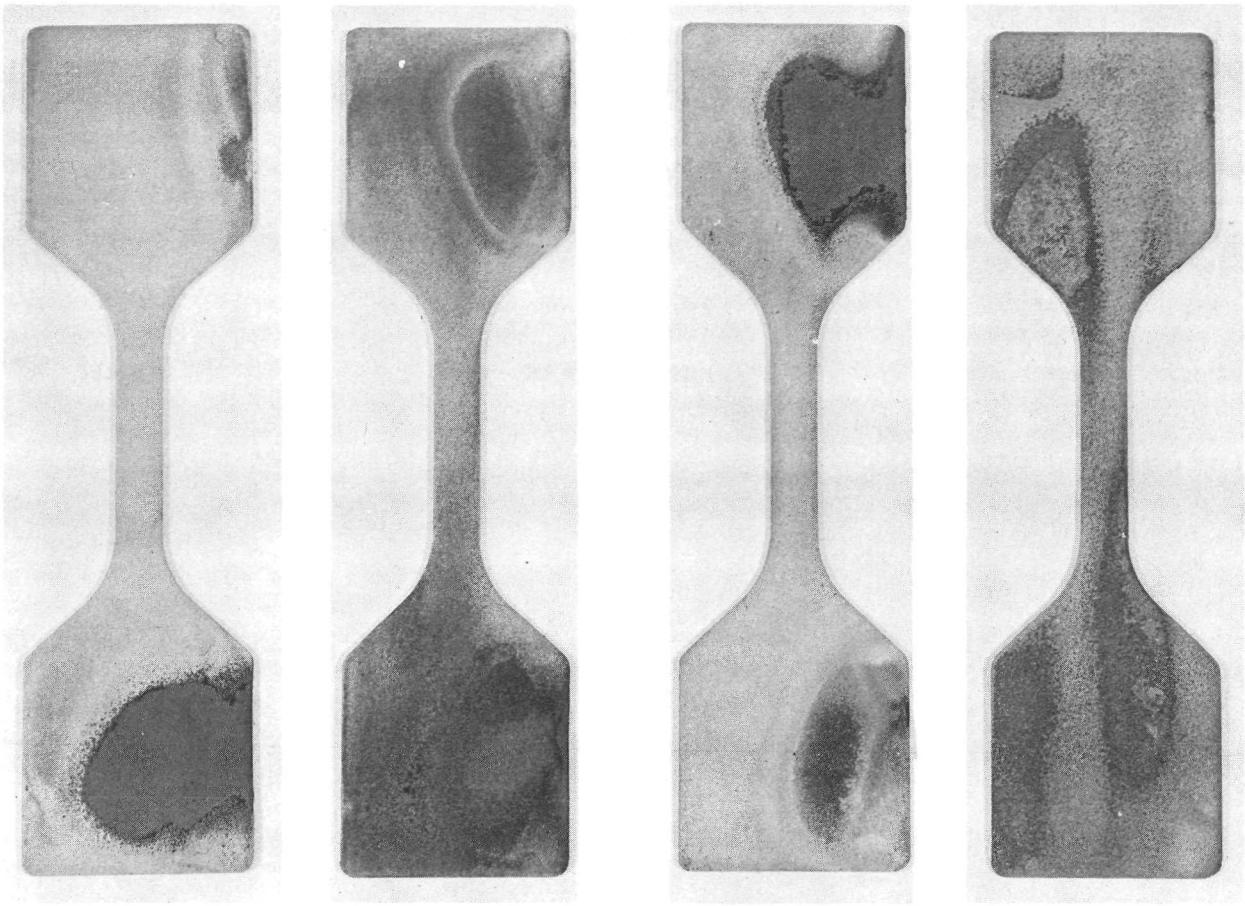

1 Hour
Hast. C-1/NC11A
TDNiCr

2 Hours
Hast. C-1/NÇ11A
TDNiCr

1 Hour
Hast. C-1/NC11A
TDNi

5 Hours
Hast. C-1/NC11A
TDNi

Figure 97. 1533°K (2300°F) Static Oxidation Test Specimens, Premature Failures.

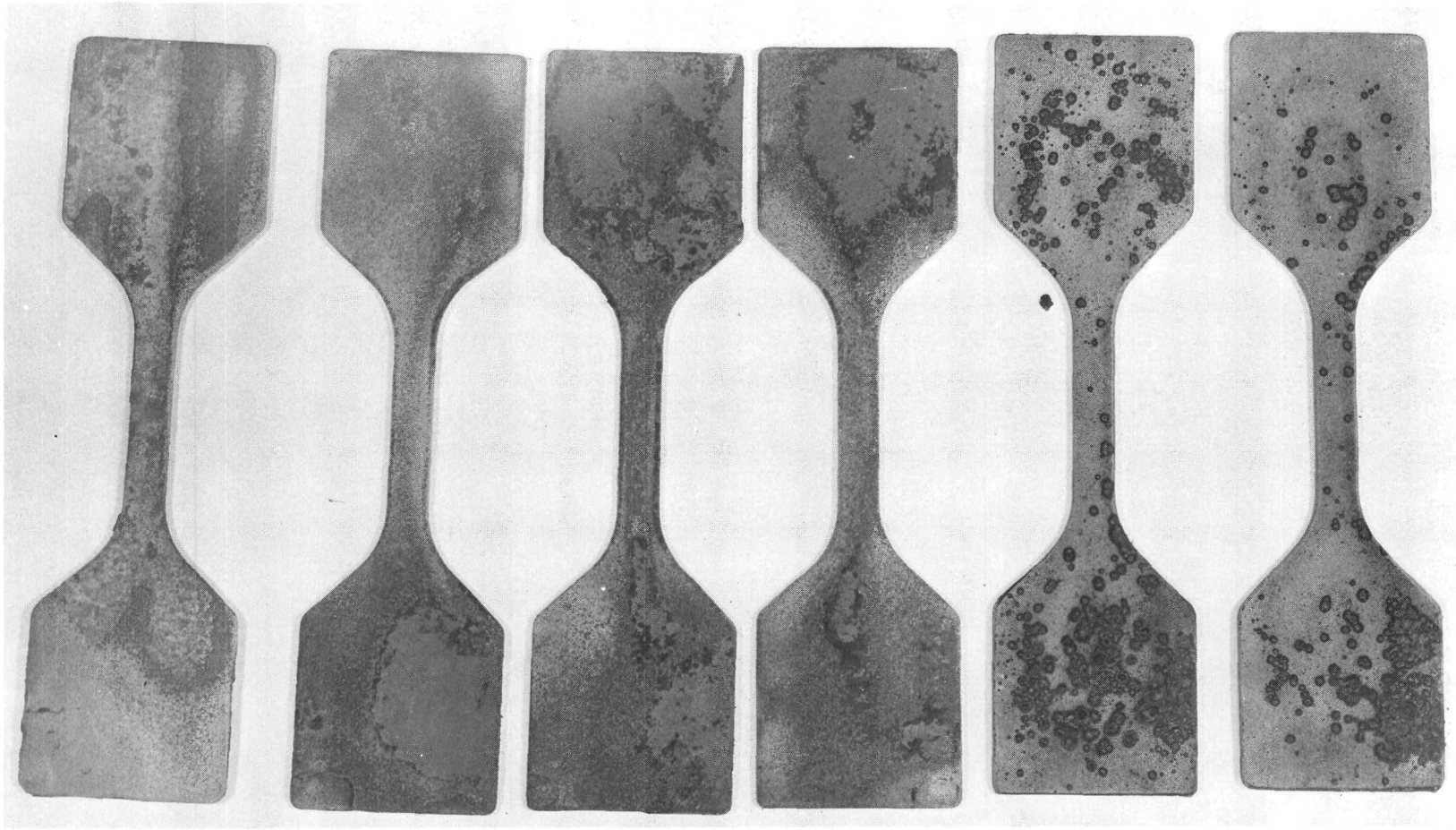

Hast. C-1/NC11A TDNi | Hast. C-1/NC11A TDNi | Hast. C-1/NC11A TDNiCr | Hast. C-1/NC11A TDNiCr | X40/NC11A TDNiCr | X40/NC11A TDNiCr

Figure 98. 1533°K (2300°F) Static Oxidation Test Specimens, Premature Failures.

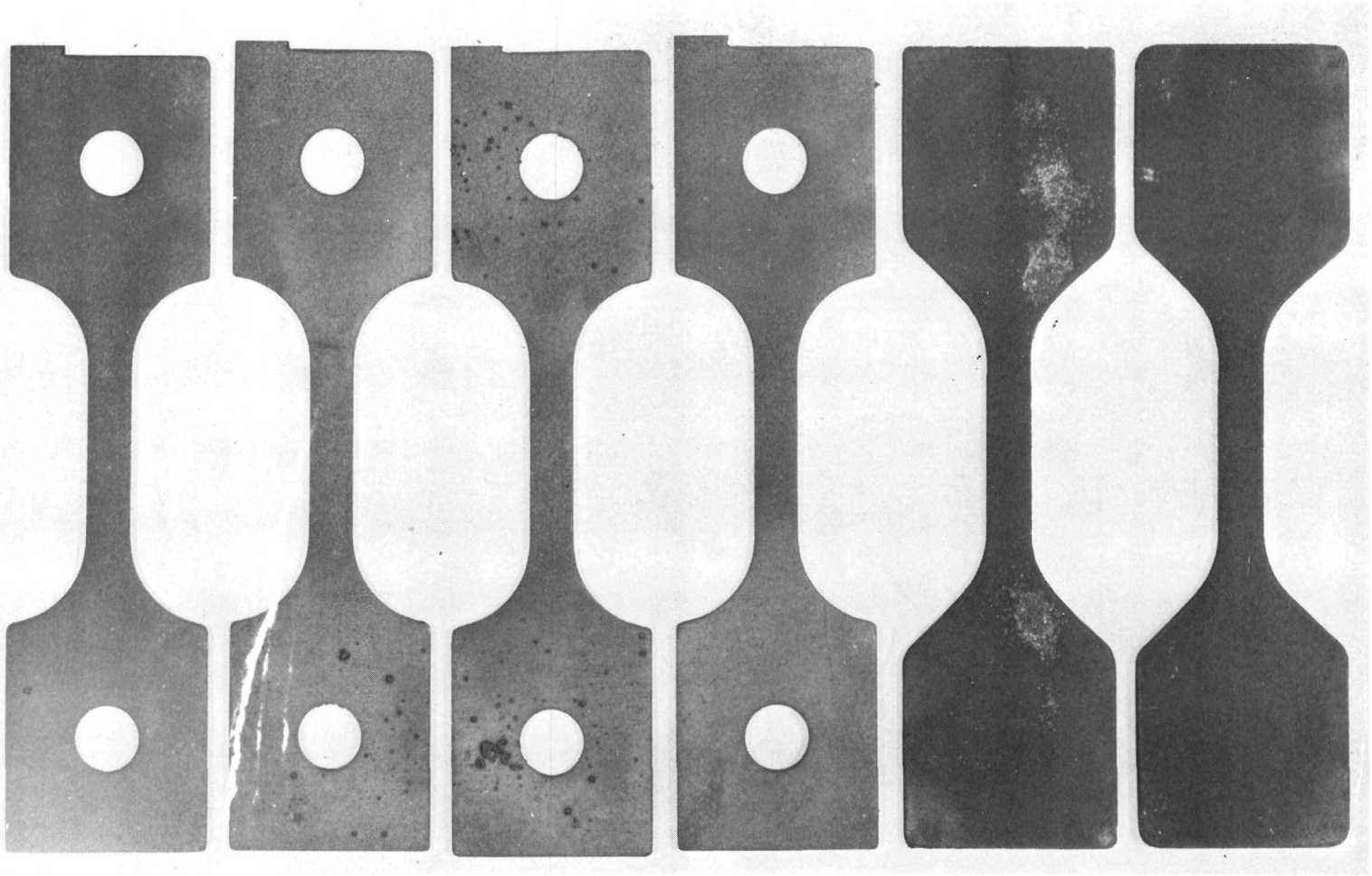

Figure 99. Four NiCrAlY and Two X40/NC11A Coated TDNiCr Tensile Specimens After 40 Hours 1533°K (2300°F) Static Oxidation Testing. NiCrAlY Specimen, Third from Left, and X40/NC11A Specimen, Second from Right, Failed.

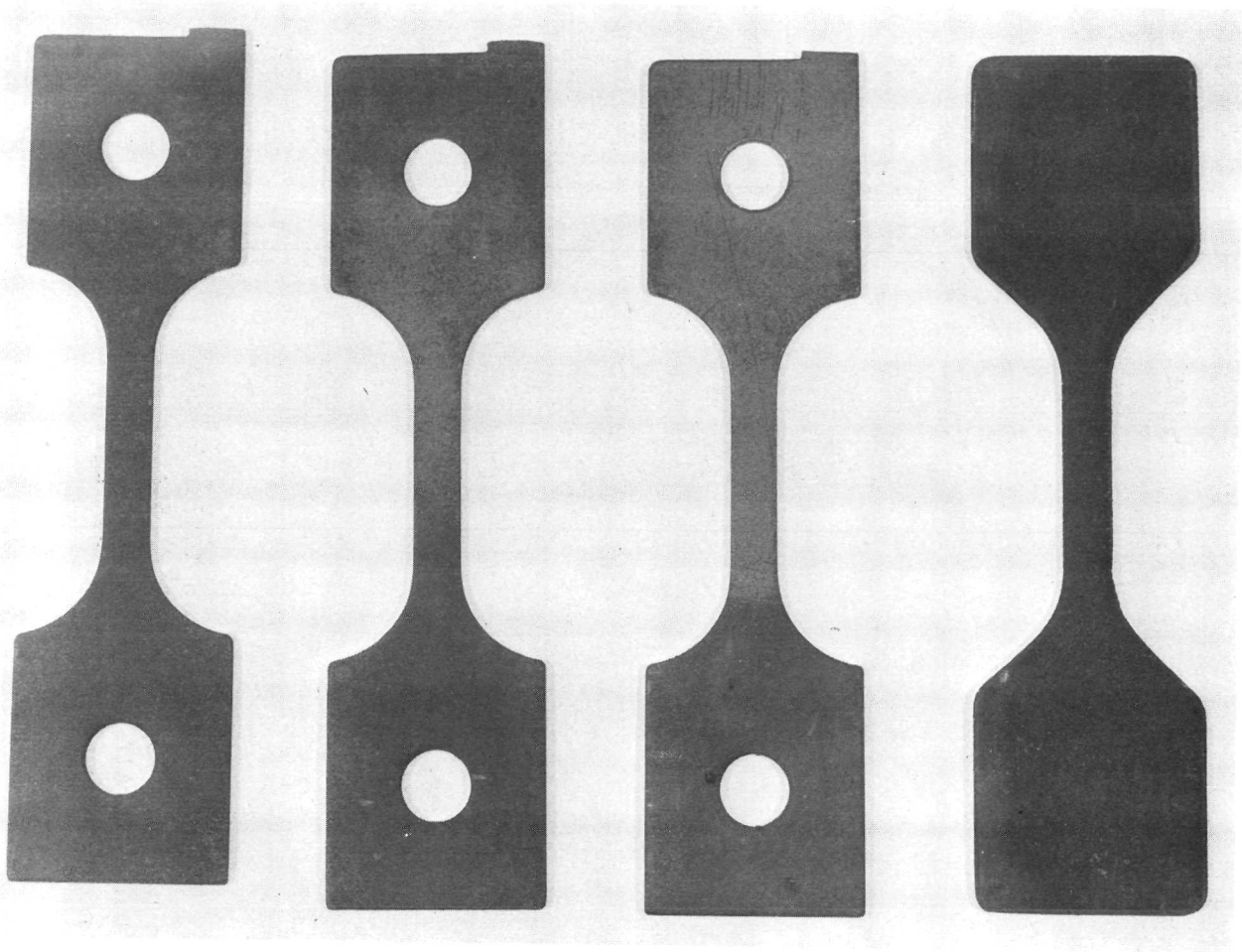

NiCrAlY
100 Hours

NiCrAlY
100 Hours

NiCrAlY
80 Hours

X40/NC11A
100 Hours

Figure 100. NiCrAlY and X40/NC11A Coated TDNiCr Tensile Specimens After 80 and 100 Hours 1533°K (2300°F) Static Oxidation Test. NiCrAlY Specimen, Third from Left Failed After 80 Hours.

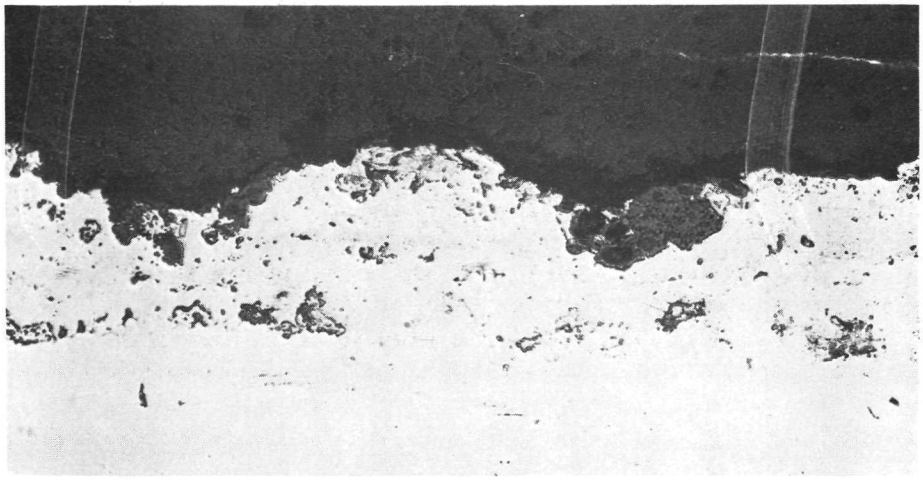

Hastelloy C-1/NC11A on TDNi After 5 Hours, Intact

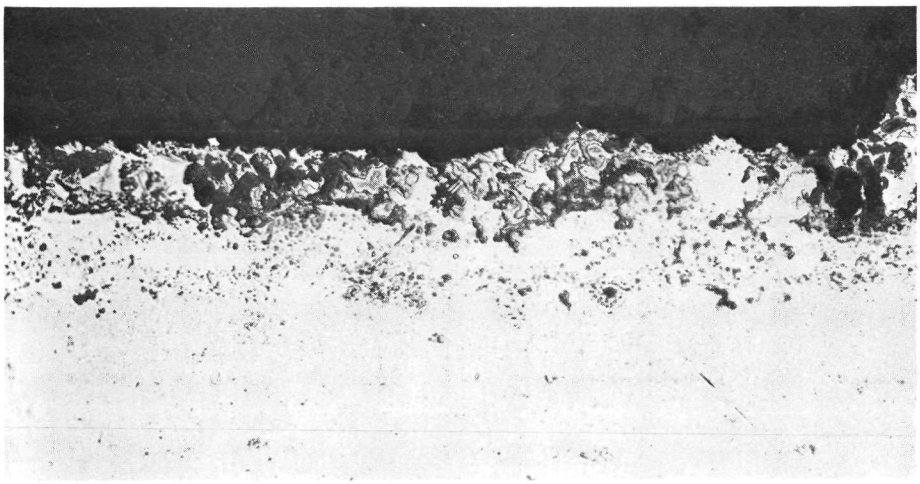

Hastelloy C-1/NC11A on TDNiCr After 4 Hours, Intact

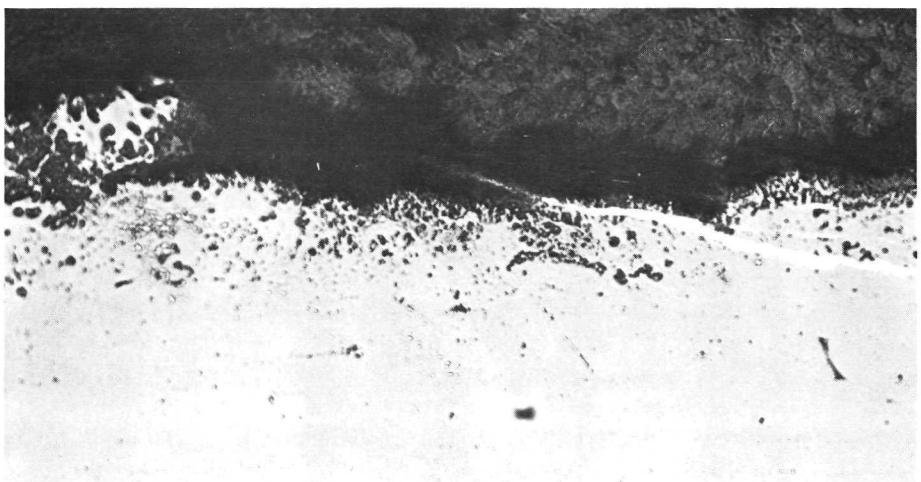

Hastelloy C-1/NC11A on TDNiCr After 4 Hours. Failed

Figure 101. Metallographic Sections of Coatings from 1533°K (2300°F) Static Oxidation Test, 250X, Unetched.

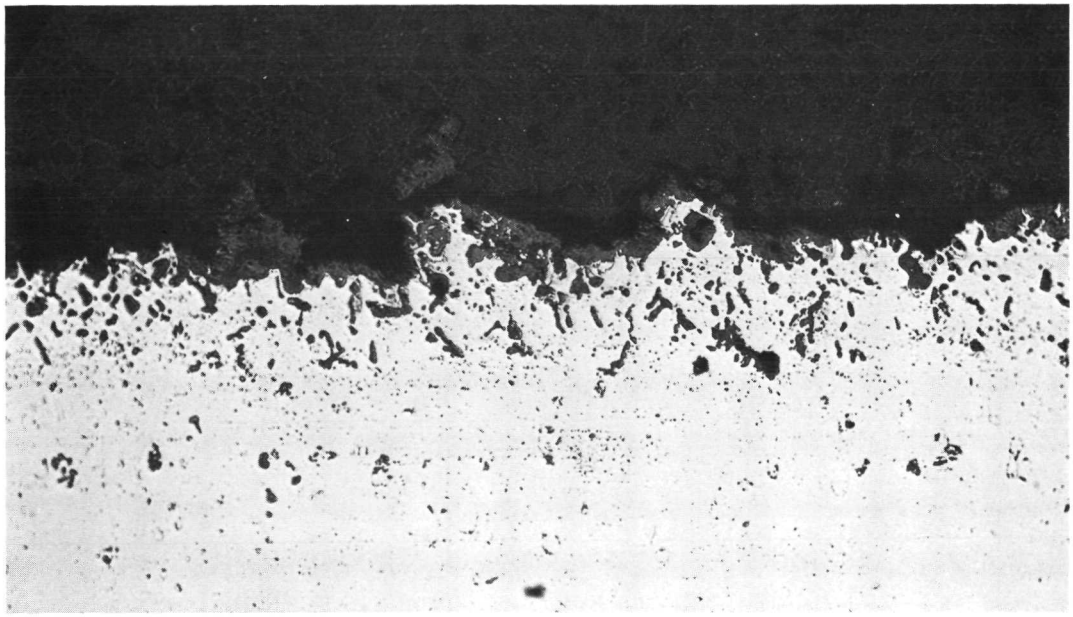

Intact Area

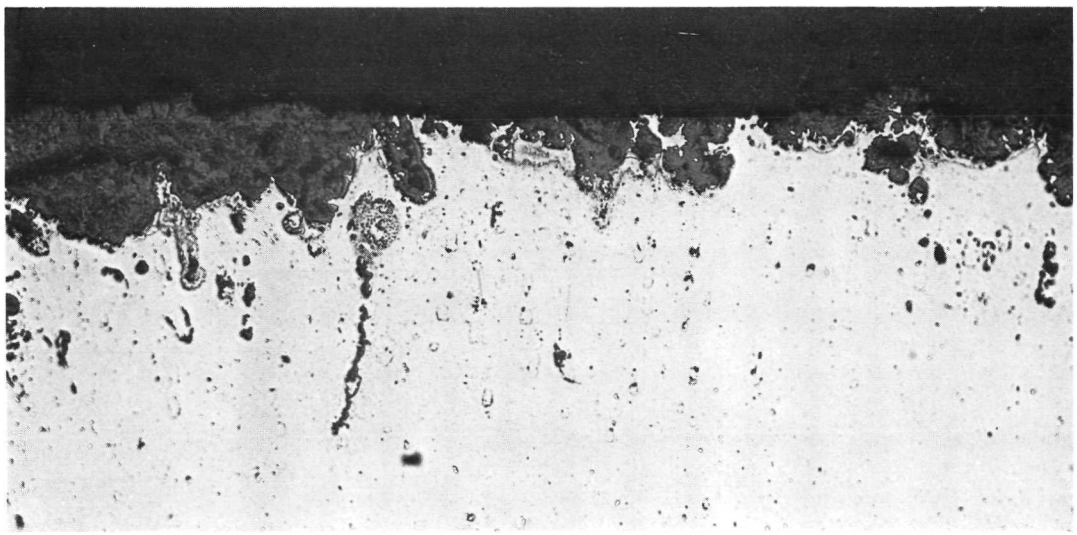

Failed Area

Figure 102 Metallographic Sections of X40/NC11A Coating on TDNiCr After 4 Hours at 1533°K (2300°F), 250X, Unetched.

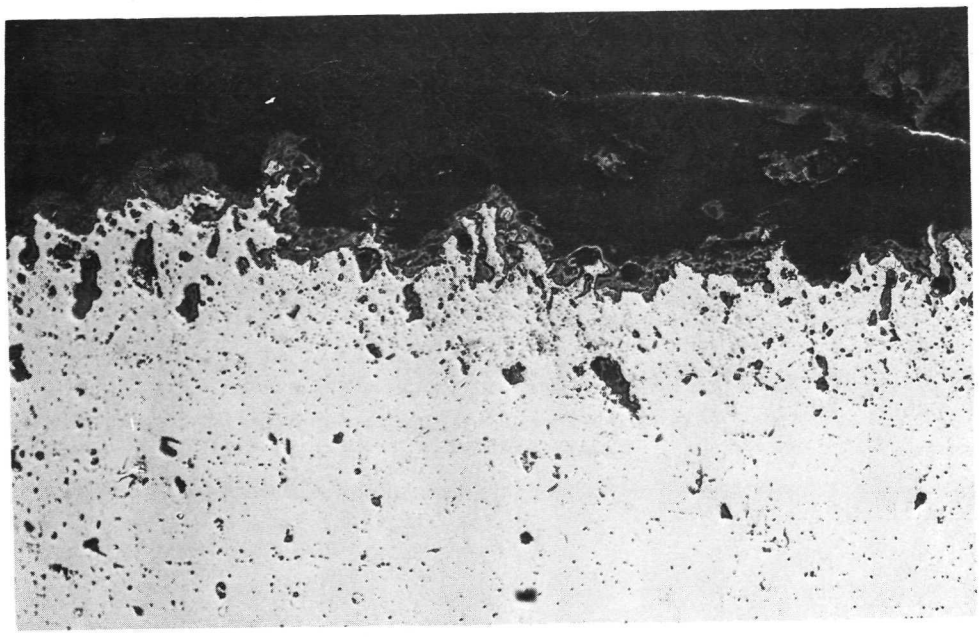

Intact Area

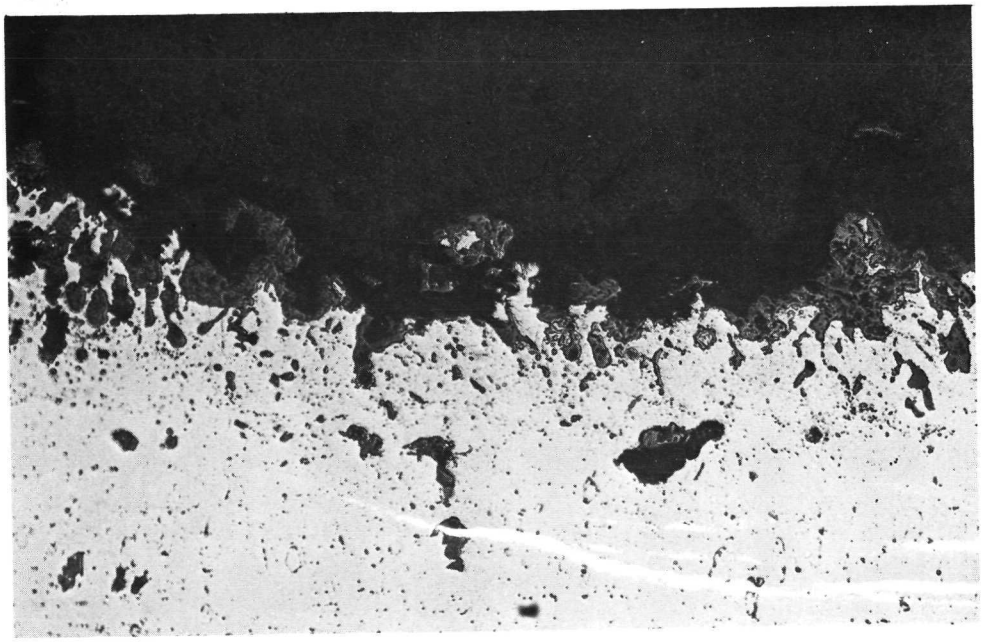

Failed Area.

Figure 103. Metallographic Sections of X40/NC11A Coating on TDNiCr After 100 Hours at 1533°K (2300°F), 250X, Unetched.

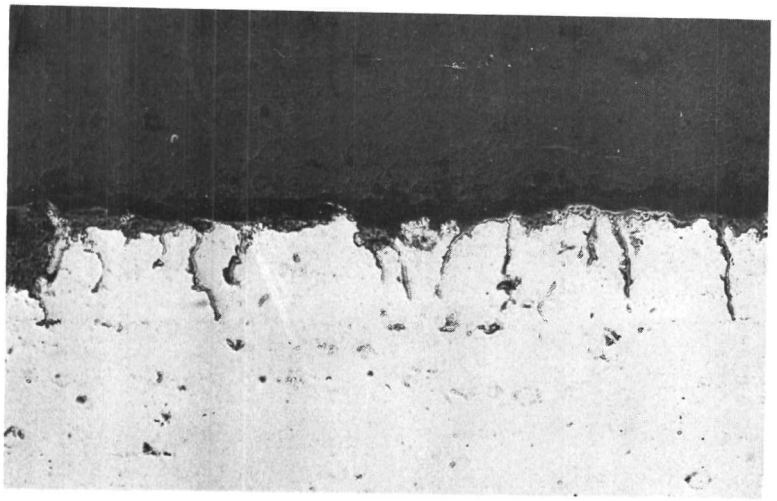

Grainboundry Oxide Attack

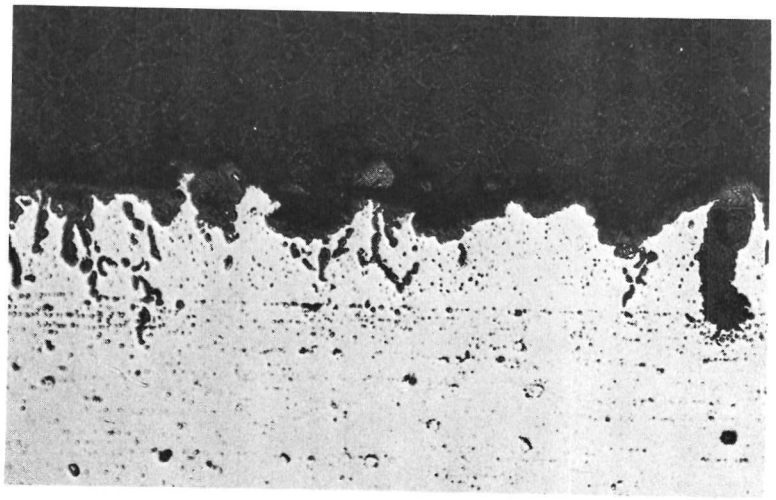

Coating Failure

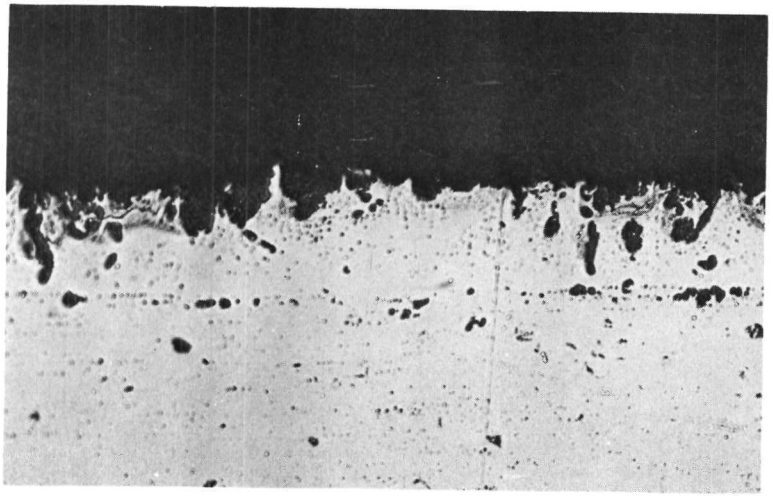

Intact Coating

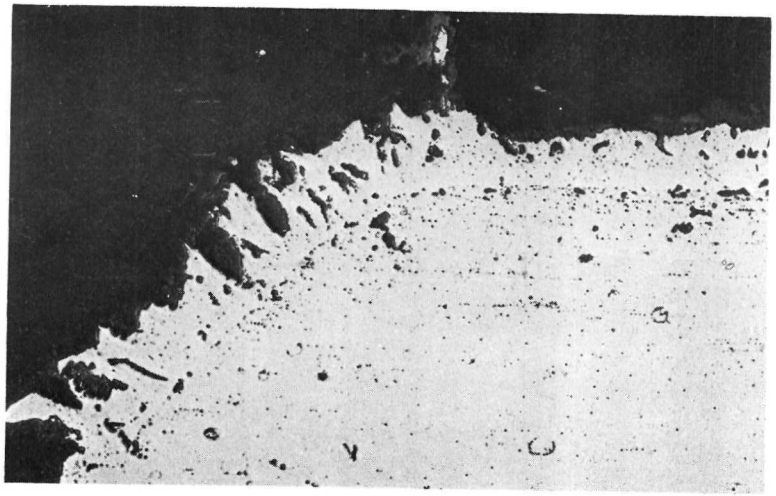

Intact Area

Figure 104. Metallographic Sections of NiCrAlY Coated TDNiCr After 80 Hours Left, and 100 Hours Right, at 1533°K (2300°F) 250X, Unetched.